Spring 5-22-2021

Targeting the MEK5, MEK1/2, and/or PI3K Pathways to Reverse Epithelial to Mesenchymal Transition and Enhance Chemotherapeutic Sensitivity in Breast And Brain Cancers

Akshita Bhatt

TARGETING THE MEK5, MEK1/2, AND/OR PI3K PATHWAYS REVERSES EPITHELIAL TO MESENCHYMAL TRANSITION AND ENHANCES CHEMOTHERAPEUTIC SENSITIVITY IN BREAST AND BRAIN CANCERS

A Dissertation

Submitted to the Graduate School of Pharmaceutical Sciences

Duquesne University

In partial fulfillment of the requirements for

the degree of Doctor of Philosophy

By

Akshita B. Bhatt

May 2021

TARGETING THE MEK5, MEK1/2, AND/OR PI3K PATHWAYS REVERSES EPITHELIAL TO MESENCHYMAL TRANSITION AND ENHANCES CHEMOTHERAPEUTIC SENSITIVITY IN BREAST AND BRAIN CANCERS

By

Akshita B. Bhatt

Approved March 4, 2021

_____ Dr. Jane E. Cavanaugh Associate Professor of Pharmacology (Committee Chair)	_____ Dr. Paula Witt-Enderby Professor of Pharmacology (Committee Member)
_____ Dr. Rehana Leak Associate Professor of Pharmacology (Committee Member)	_____ Dr. Kevin Tidgewell Associate Professor of Medicinal Chemistry (Committee Member)
_____ Dr. Patrick T. Flaherty Associate Professor of Medicinal Chemistry (Committee Member)	_____ Dr. James K. Drennen Dean, School of Pharmacy Professor of Pharmaceutics
_____ Dr. Carl Anderson Chair, Pharmacy Professor of Pharmaceutics	

ABSTRACT

TARGETING THE MEK5, MEK1/2, AND/OR PI3K PATHWAYS TO REVERSE EPITHELIAL TO MESENCHYMAL TRANSITION AND ENHANCE CHEMOTHERAPEUTIC SENSITIVITY IN BREAST AND BRAIN CANCERS

By

Akshita B. Bhatt

May 2021

Dissertation supervised by Dr. Jane E. Cavanaugh

Triple-negative breast cancer (TNBC) is the most aggressive form of breast cancer and accounts for 10-15% of breast cancer cases. Due to absence of estrogen, progesterone, and human epidermal growth factor receptors, there is lack of targeted therapies and chemotherapy remains the mainstay treatment. Moreover, drug resistance is a major problem associated specifically with TNBC. Similarly, while estrogen receptor positive (ER+) breast cancer can be treated with targeted therapies such as tamoxifen, 40% of patients develop resistance and resulting in recurrence of the disease.

There is a dire need for identifying novel targets and developing therapeutics to target triple-negative and tamoxifen-resistant (TAMR) breast cancers. Activation of one of the newest members of mitogen-activated protein kinase (MAPK) family, extracellular-regulated kinase

(ERK) 5 is known to increase cell viability, proliferation, and migration in different cancers and its overexpression correlates with poor patient survival. In breast cancer, activation of mitogen activated protein kinase kinase (MEK) 5, the upstream kinase of ERK5, and/or ERK5 promotes drug resistance, the epithelial to mesenchymal transition (EMT), and hormone independence. Once the cancer cells undergo an EMT, they are harder to target and contain, leading to metastases. Therefore, there is an urgent need to understand the pathways that drive proliferation and the EMT and develop novel therapies that target these pathways.

TNBCs are heterogeneous in their mutational profile and reliance on specific signaling pathways. Therefore, in addition to the ERK5 pathway, the ERK1/2 and phosphoinositol-3-kinase (PI3K)-AKT pathways have been shown to have overlapping and distinct functions as the ERK5 pathway to regulate tumorigenesis in TNBC and TAMR breast cancers. Interestingly, inhibition of one of these signaling pathways often leads to a compensatory increased activation of the other signaling cascades, including the PI3K-AKT pathway. Emerging evidence suggests that the MAPK and PI3K pathways play an important role in the progression and metastases of other aggressive cancers such as glioblastoma multiforme.

The main goals of this project are 1) to target the ERK1/2 and ERK5 pathways and develop strategies to reverse the EMT using novel and known pharmacological inhibitors and molecular tools and 2) determine the effect of novel and known kinase inhibitors on chemotherapeutic sensitivity and 3) determine the effect of novel compounds that target the ERK1/2 and ERK5 pathways in combination with the AKT inhibitor ipatasertib on spheroid viability, migration, and proliferation in TNBCs. The results from this study will aid in the

design of innovative therapeutic strategies that target cancer metastases and reduce therapeutic resistance.

DEDICATION

To my parents Babaraju Bhatt and Smita Bhatt and my grandparents Kanaiyalal Pandya and Savitri Pandya for their unconditional love. Thank you for always encouraging my dreams and being my strength during tough times.

ACKNOWLEDGEMENT

I am enormously grateful to my advisor Dr. Jane E. Cavanaugh for giving me the opportunity to pursue PhD in her laboratory. It has been a true blessing to be mentored by you. Thank you for setting an example of excellence as a mentor, leader, scientist, and researcher. I have really enjoyed live and energetic discussions with you during our meetings. I will take your lessons with me, every day. I am very grateful to my committee members for their encouragement. I could not have asked for a better committee. Your enthusiasm and love for teaching is contagious. Dr. Paula Witt-Enderby has provided brilliant suggestions and feedback during my graduate study that helped me grow as a scientist and teacher. Dr. Rehana Leak has been very helpful in providing suggestions for my research several times during my graduate school career. Your help with several writing assignments during seminar class has helped me grow as a writer.

I was very interested in both Pharmacology and Medicinal Chemistry during my undergraduate study. I feel that these research disciplines are inseparable from one another. I am very grateful that I got the opportunity to pursue both the subjects for my research, and this would not have been possible without the wonderful support of Dr. Patrick Flaherty and Dr. Kevin Tidgewell. I am grateful to Dr. Kevin Tidgewell for your wonderful collaboration. Your critical and attentive feedback has been very helpful for my project. Dr. Patrick Flaherty has been very helpful in strengthening my medicinal chemistry knowledge over the years. I would like to thank Dr. Carl Anderson who has been very kind and supportive throughout my career at Duquesne University.

I am very grateful to Dr. James Drennen for his enthusiastic support in my academic and research endeavors at Duquesne University. I would like to thank our collaborators Dr. Matthew Burow, Dr. Nathanael Gray, Dr. Zhengui Xia, and Dr. Lucio Miele. Insightful discussions with you at AACR meetings and conference calls have been very beneficial in enhancing my understanding of the tumor biology. Thank you for sharing reagents and biological materials from your lab(s), which has greatly helped enhance the understanding of ERK5 biology in cancer research. I am very grateful to Dr. David Johnson, Dr. Wilson Meng, and Dr. Lauren O'Donnell for their wonderful teaching over the years. I would like to thank my former college professor Dr. Parloop Bhatt who inspired the love for research in me.

I would like to thank all the members of the Cavanaugh Lab. I am very grateful to Dr. Thomas Wright for initially training me in the lab and providing meaningful suggestions for my project. I would like to thank Dr. Sneha Potdar and Asef Faruk for their friendship. I could not have asked for better lab-mates. I would like to thank the PharmD students and summer students who contributed to this research. Katie Anna, Erin Lexner, Jordan Martin, Seraina Schottland, Emily Tran, and Peter Goralski have been a great team. I am very grateful to the Duquesne University AAPS student chapter, especially Dr. Ira Buckner, Women in STEM Committee, and Center for Teaching Excellence for advancing my professional and academic careers. I would like to thank the administrative team at Duquesne University for their kind help with everything. I am very grateful to my family, all professors at Duquesne University, and my fellow graduate students. Thank you!

TABLE OF CONTENTS

LIST OF FIGURES

Page

LIST OF ABBREVIATIONS

BRD4: bromo-domain-containing protein 4

CDK: cyclin-dependent kinase

E-cadherin: epithelial cadherin

ERK: extracellular signal-regulated kinase

EMT: epithelial to mesenchymal transition

GBM: glioblastoma multiforme

GFP: green fluorescent protein

MEK: mitogen-activated protein kinase kinase

MET: mesenchymal to epithelial transition

PI3K**:** phosphoinositol (PI) 3-Kinase

PDX: patient-derived xenograft

PTEN: phosphatase and tensin homolog

RAF: rapidly accelerated fibrosarcoma

RAS: rat sarcoma

Rb: retinoblastoma

RSK: ribosomal s6 kinase

TAMR: tamoxifen-resistant

TNBC: triple-negative breast cancer

ZEB: zinc-finger E-box binding homeobox

Chapter 1: Literature Review

1.1 Introduction

1.1 .1 Breast Cancer

Cancer is the second leading cause of death in the United States with 1.8 million new cancer cases and 0.6 million deaths estimated for 2020.[1] Among these cases are 0.28 million new breast cancer cases with 42,000 anticipated deaths anticipated for the year 2020. Metastases accounts for 90% of deaths due to cancer. Cancers display phenotypes[2-3] of increased self-sufficiency in growth signaling, an insensitivity to anti-growth signals, increased tissue invasion and metastasis, limitless replication potential, sustained angiogenesis, and evasion of apoptotic cell death. Breast cancer accounts for 30% of all cancers occurring in women and triple-negative breast cancer (TNBC), which constitutes about 10-15% of total breast cancer cases is among the most difficult to treat forms of cancer.

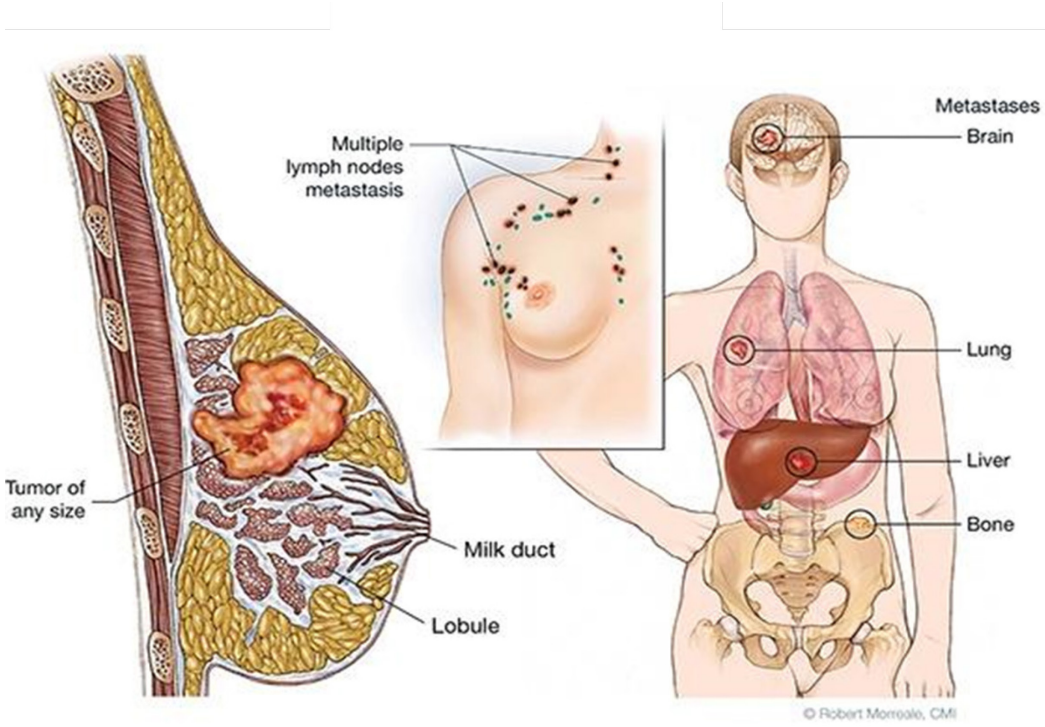

Figure 1.1: Metastatic breast cancer. Metastatic breast cancer is challenging to treat due to its aggressive nature and lack of well-defined therapeutic targets (Image source: https://www.cancersupportcommunity.org/metastatic-breast-cancer). Courtesy of Bob Morreale.

The normal mammary lobule consists of aggregate of acini embedded in the surrounding stroma. The acini drain into a terminal ductule and a few lobules and ductules drain together to form terminal duct lobular unit. The inner lining of the ducts and lobules comprises of an inner epithelial layer, which stains positive for the transmembrane adhesion molecule E-cadherin encoded by the CDH1 gene. Growth and differentiation of normal breast tissue is regulated by estrogen and progesterone via estrogen and progesterone receptors, respectively.

Breast carcinomas are comprised of transformed epithelial cells. Breast cancers progress from regions of cellular atypia into clinically evident premalignant or malignant lesions with further progression to metastatic spread and therapeutic resistance.[4] Breast

cancer is very heterogeneous in terms of histology, response to therapy, metastatic patterns, and patient outcomes. Breast cancers can be classified based on the different molecular subtypes, stage of disease, and grade (Figure 1.2). Global gene expression analyses and high-throughput sequencing have helped characterize breast cancer as Luminal A, Luminal B, HER2-enriched, claudin-low, and basal-like.

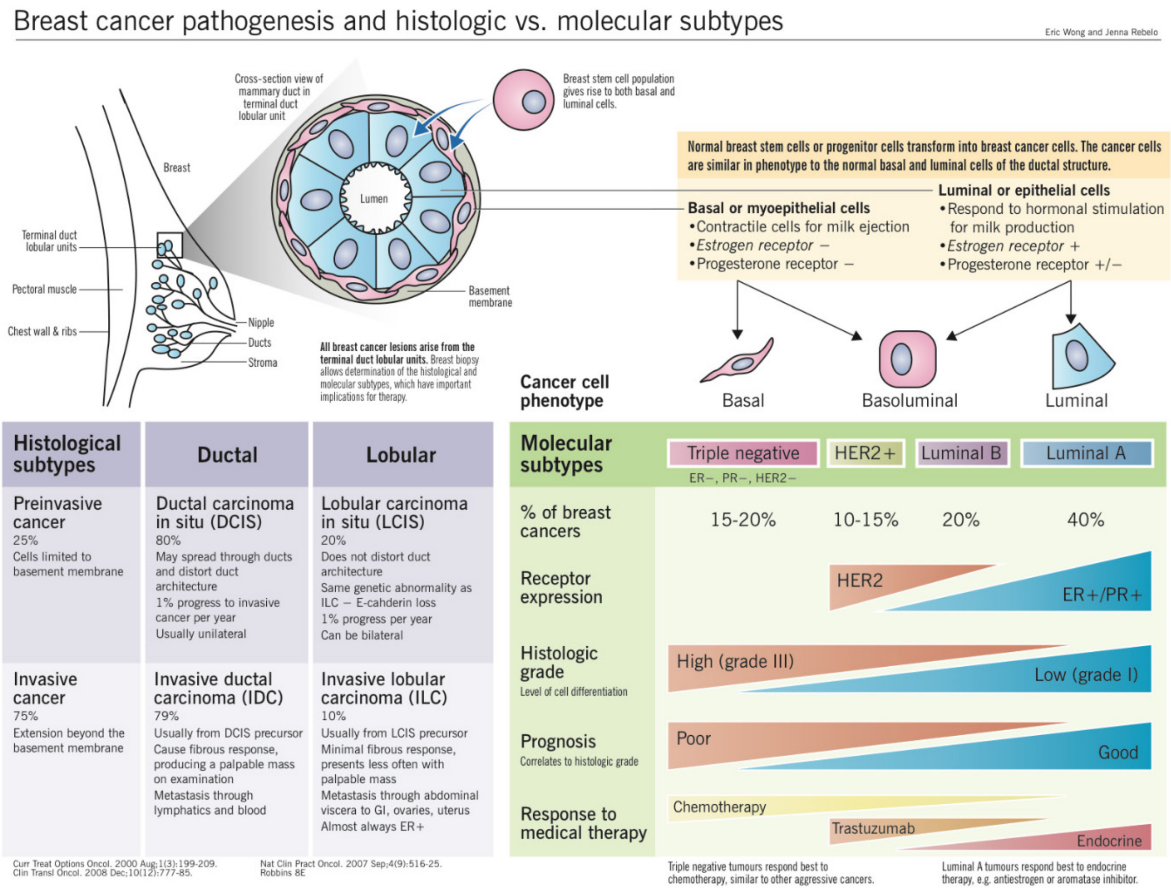

Figure 1.2: Histologic and molecular subtypes of breast cancer. Breast cancer can be classified based on the origin, stage, and molecular subtypes (Image source: http://www.pathophys.org/breast-cancer/). Courtesy of Eric Wong and Sultan Chaudhry.

1.1.2 Triple-negative breast cancer

TNBCs lack HER2, ER, and PR receptor expression, yet retain the growth normally expected from activation of these receptors. It has been proposed that the pathways display increased activity decoupled from receptor occupancy. Most TNBCs and drug-resistant cancers adapt to develop a mesenchymal phenotype over time. Epithelial to mesenchymal transition is the first step of metastases, which accounts for ~90% of cancer-associated deaths in humans. EMT is a cascade of cellular events including the loss of epithelial marker E-cadherin and gain of mesenchymal markers ZEB1, snail, and vimentin. Loss of E-cadherin expression is a crucial event in the metastases and recurrence of aggressive lobular breast cancer.[5-6]

1.1.3 Epithelial to mesenchymal transition and cancer metastases

The epithelial to mesenchymal transition (EMT), one of the first steps in cancer metastases, is a continuum of morphologic transitions from cobblestone-like epithelial state to a spindle-like mesenchymal state (Figure 1.3). The complex process of metastases involves EMT, intravasation in the blood vessels, survival in blood stream, extravasation at the secondary site, mesenchymal to epithelial transition (MET), and secondary tumor growth.[7] Cells can also exist in an epithelial/mesenchymal stage, where they co-express epithelial and mesenchymal markers. This intermediate EMT state is often associated with greater metastatic potential and poor patient outcome. Cancer metastases requires high cellular plasticity and adaptability to survive in diverse physiological environments. It is important to identify therapies to target different stages

of metastases. Upregulation of EMT transcription factors via growth factors, epigenetic plasticity, and downregulation of tumor suppressor microRNAs (miRs) are a few mechanisms that drive EMT in cancer.[8]

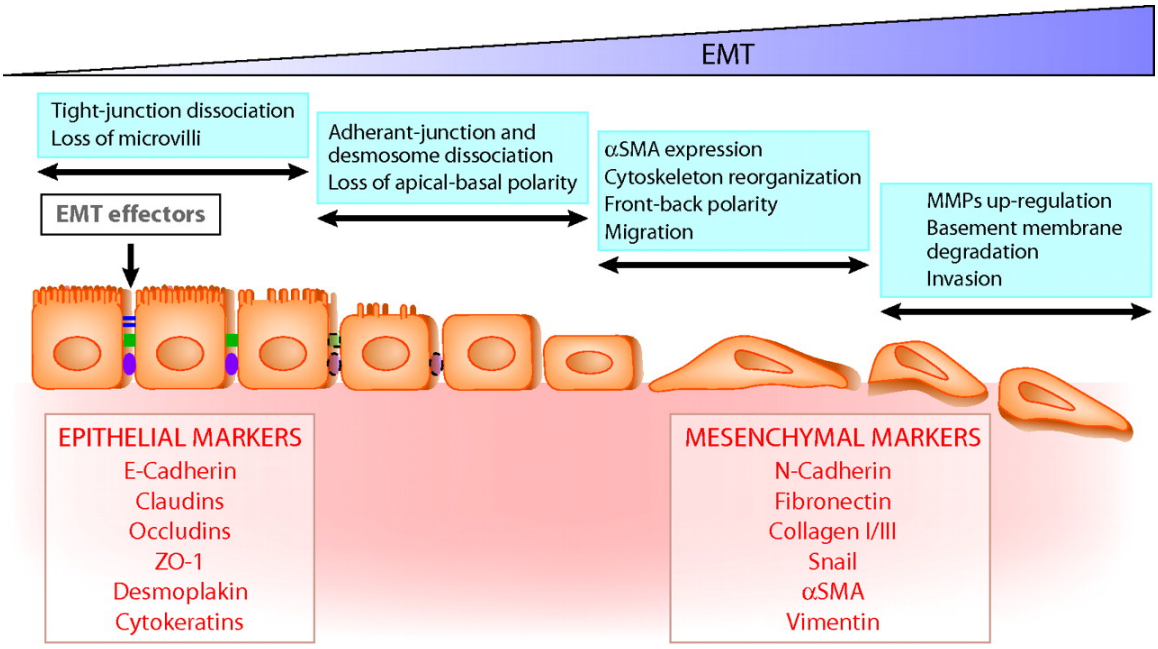

Figure 1.3: Events involved in epithelial to mesenchymal transition.[9]

Tumor heterogeneity in terms of difference in driver mutations within the same cancer subtype and complexity of the tumor microenvironment have made the application of oncology therapeutics extremely challenging. The extracellular signaling factors and epigenetic effectors cooperate to initiate the EMT program and ultimately lead to metastases. One of the cellular adaptations during EMT involves increased capabilities of cancer cells to preferentially interact with the extracellular matrix, rather than the adjacent epithelial and stromal cells. Integrins are known to activate Src and focal

adhesion kinases (FAK), which results in an increase in secretion of matrix metalloproteinases, loss of E-cadherin, and disruption of the adherens junctions (AJs).[10]

Tumor-associated chronic inflammation could initiate EMT via crosstalk between the inflammatory and tumor cells.[11] The tumor is infiltrated by diverse inflammatory and immune mediators. For example, 50% of the tumor is infiltrated with inflammatory macrophages. These infiltrated activated macrophages and proinflammatory T-cells can release cytokines, including transforming growth factor-β (TGF- β), tumor necrosis factor α (TNF- α), and interleukin-6, which are potent EMT inducers.[12] Expression of immune checkpoint proteins such as PD-L1 mediates escape of cancer cells from NK cell-mediated cytotoxicity. In the given feedforward mechanism, EMT increases in PD-L1 expression via the microRNA-200-ZEB1 axis, which results in immune suppression and metastases.[13] Several mechanisms that regulate EMT are summarized in Figure 1.4.

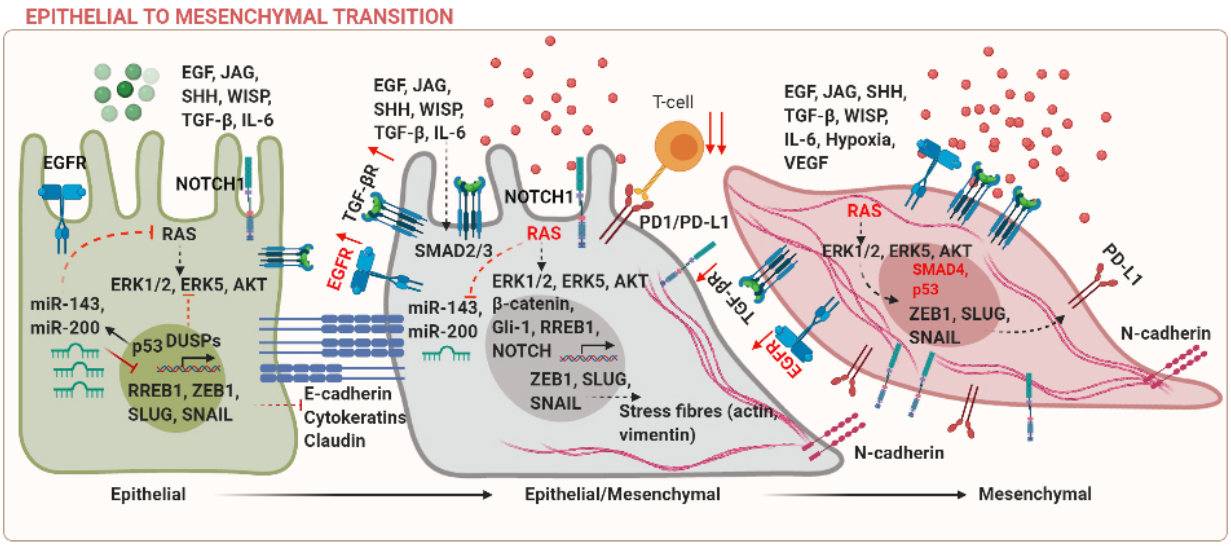

Figure 1.4: Mechanisms that drive EMT in cancer. EMT in gradual progression from a cobblestone-like morphology to spindle-like morphology, initiated by growth factors, activation of MAPK pathway, and upregulation of transcription factors involved in EMT. Original figure created in Biorender.com.

Another feature that the cancer cells adopt as they transition to a mesenchymal state and enter the blood circulation for metastases is their ability to activate and bind platelets. At this stage, the cancer cells are termed as circulating tumor cells. Many studies argue that the cells are in an intermediate epithelio-mesenchymal state at this stage. There are coagulation-dependent mechanisms modulated via fibrin, which help the cancer cells to bind platelets and gain protection against loss of anchorage-triggering anoikis, immune attack, and shear stress.[14] Drug resistant stem cells at the primary and metastatic sites are also known to possess EMT characteristics.[15]

1.1.4 The Mitogen-Activated Protein Kinase Pathway in cancer

MAPK pathway is activated in response to growth factors, cytokines, stress, and hormones and leads to alteration of cell division, proliferation, and differentiation. Mutations in BRAF, KRAS, EGFR, and receptor tyrosine kinase (RTK) pathways can lead to constitutive activation of MAPK pathway, characterized by phosphorylation of downstream targets MAPK/ERK Kinase Kinase 2 (MEKK2)/3, ERK1/2, ERK5, RSK, and FRA-1. Figure 1.5 summarizes the intracellular signaling pathways, which are involved in cell viability, proliferation, epithelial to mesenchymal transition, and migration.

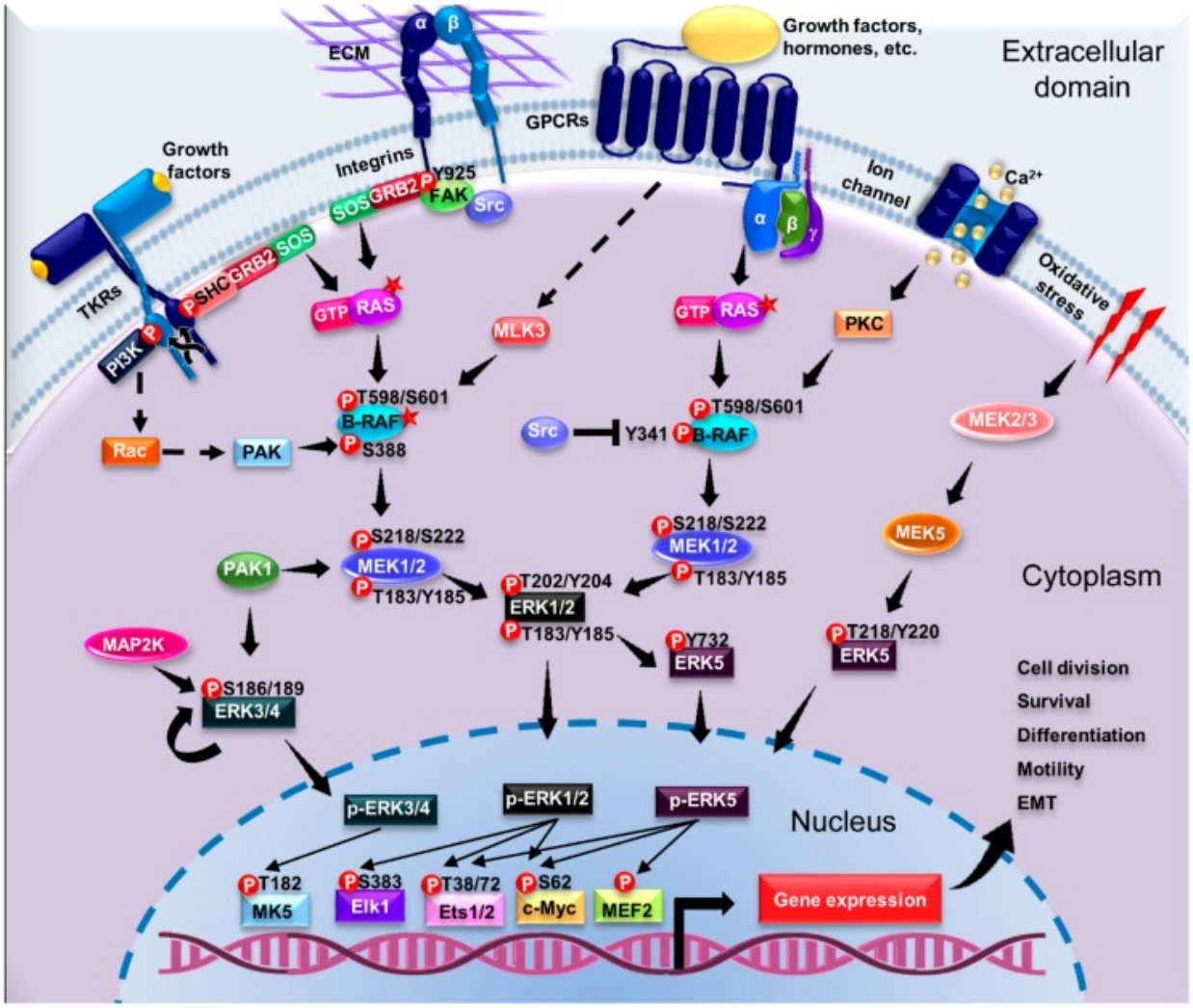

Figure 1.5: Pathways driving ERK activation and cellular process regulated by the kinase.[16]

Activation of MAPK can increase EMT, migration, invasion, and stemness in several cancers. Extracellular-regulated kinase (ERK)1/2 is one of the most well-characterized members of the MAPK pathway. ERK1/2 activation can be a result of tyrosine kinase dimerization, RAS, or RAF mutation. RTKs serve as binding sites for the Src homology and collagen (SHC) adapter protein and growth factor receptor-bound protein (GRB2). These adapter proteins have phosphotyrosine-binding (PTB) and SH2

domains. GRB2 then interacts with Son of Sevenless (SOS) through its SH3 domain, leading to the activation of MEK1/2 and MEK5.

1.1.4.1 ERK1/2 pathway in cancer

Extracellular signal-regulated kinase (ERK)1 and ERK2 isoforms share 85% sequence homology and can be activated by phosphorylation at the TEY motif (Thr202 and Tyr204).[17] The ERK1/2 pathway is one of the most well characterized MAPK pathways in cancer (Figure 1.6). The MAPK cascade and subsequent ERK1/2 is initiated when an extracellular signal activates the corresponding receptor and causes conformational changes and activation of the small GTPase RAS at the plasma membrane. RAS activates Raf-MEK-ERK by phosphorylation of serine residues. This pathway is activated in 85% of all cancers due to mutations in RAS, RAF, MEK or epidermal growth factor receptor (EGFR). ERK1/2 activation leads to subsequent activation of downstream effectors and gene transcription. These signals are amplified at each stage. ERK1/2 is known to induce fos and jun, Activator protein 1 (AP-1), Erythroblast Transformation Specific ETS-1 genes. Moreover, ETS-1 has been found to upregulate ZEB1 expression and regulate EMT in breast cancer.[18]

Connexin 43 (inhibitor of gap junction communication) and regulator of cell migration myosin light chain kinase (MCLK) are plasma membrane proteins activated by ERK1/2.[19] ERK1/2 activation leads to association of paxillin to Src.[20] Ribosomal S6 kinase (RSK), mitogen and stress-activated protein kinase (MSK), and MAPK-interacting kinase (MNK) are the main cytoplasmic substrates of ERK.[21] RSK family are known to be exclusively activated by ERK1/2 but we have found that ERK5 can also modulate RSK activity. The activity of transcription factors cAMP response element binding (CREB),

serum response factor (SRF), estrogen receptor (ER) is modulated by RSK activation. RSK also regulates pro-apoptotic protein Bcl-2-associated death promoter (BAD). Direct and indirect regulators of ERK1/2 signaling cascade and downstream effectors are summarized in figure 1.5. While ERK1/2 pathway in cancer is well-understood, the details about ERK5 pathway in cancer are only being recently explored.

RAS is an important regulator of ERK1/2 pathway. RAS mutation can promote cancer growth via influencing several hallmarks of cancer described by Weinberg et. al.: Sustained growth and proliferation, evasion of immune system, invasion, inhibition of apoptotic signaling, EMT, and alteration of cell metabolism. Reasons why RAS is undruggable include: (i) binding of RAS to GTP (covalent interaction) results in the closing of GTP-binding domain on RAS, thus making the binding pocket inaccessible for RAS inhibitors. (ii) Unique C-terminal domain: C-terminal domain of RAS can undergo post-translational modifications, including palmitoylation and farnesylation. Several approaches were developed to target these post-translational modifications. However, RAS mutant cancer cells adapted to develop an alternative PTM mechanism known as GGTase (geranylgeranyl isoprenoid), preventing RAS from turning off. Therefore, targeting the downstream effector of RAS signaling including the MEK1/2-ERK1/2 and MEK5-ERK5 signaling pathways is a relevant strategy to target RAS-mutant cancers.

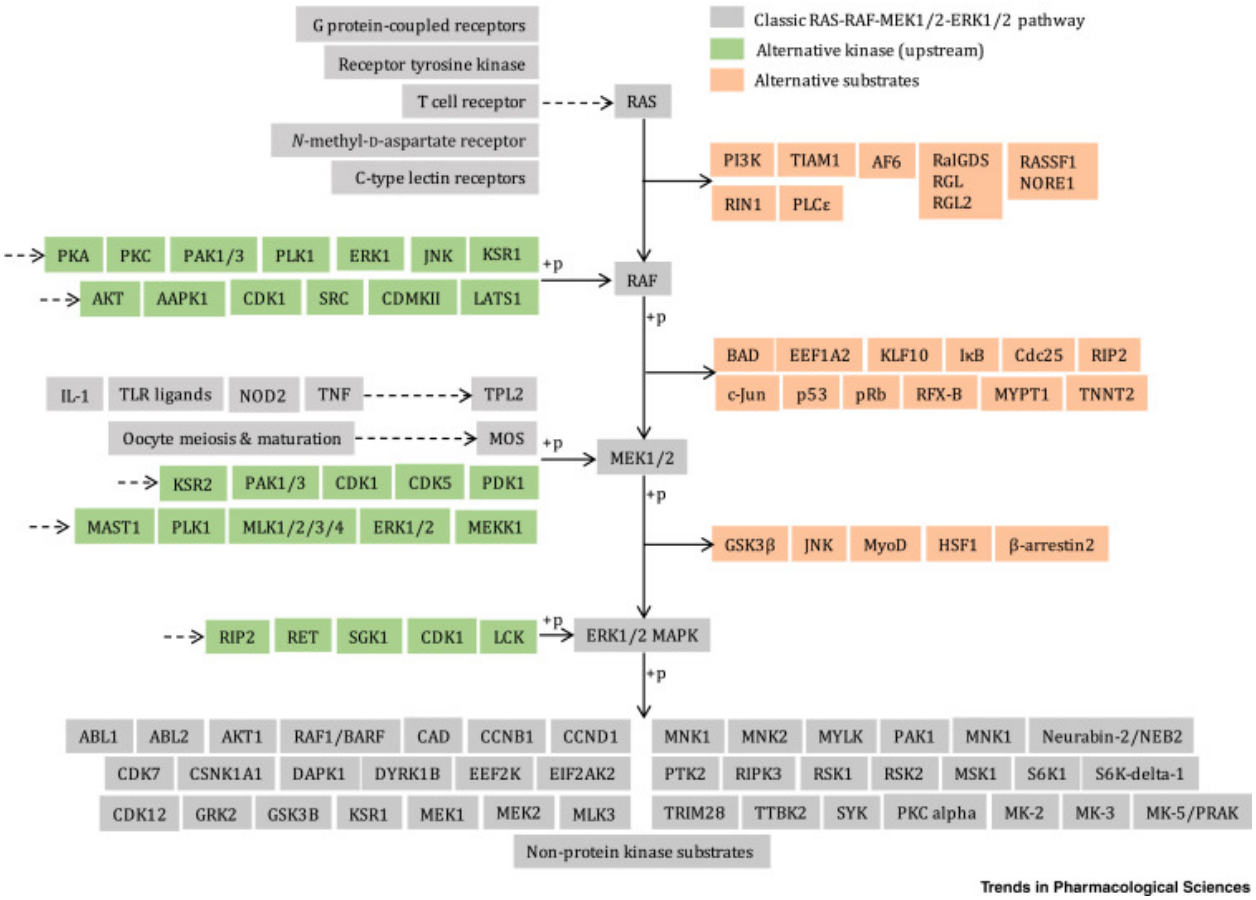

Figure 1.6: Upstream and downstream regulators of the ERK1/2 pathway[22]

1.1.4.2 ERK5 pathway in cancer

ERK5, the newest member of the mitogen-activated protein kinase family (MAPK), is a marker for poor prognosis in cancer patients.[23] ERK5 is one of the members of the 4 MAPK signaling cascades, including ERK1 and ERK2, c-JUN N-terminal kinase (JNK) 1, and p38-MAPK. These cascades are regulated by 3 to 5 tiers of phosphorylation events, which are initiated by receptor tyrosine kinases and subsequent components of the MAPK family. While these pathways are under strict regulation by feedforward activation and feedback inhibition loops in healthy cells, these do not operate similarly in cancer cells.

Although ERK1/2 and ERK5 pathways share greater than 50% sequence homology at the N-terminal domain, ERK1/2 and ERK5 have been shown to mediate differential responses to growth factors, hypoxia, and pharmacological targeting with BRAF and MEK1/2 inhibitors. ERK1/2 and ERK5 pathways regulate hypoxia-related genes via distinct mechanisms in normoxic versus hypoxic condition.[24] These differences could be attributed to the unique C-terminal domain of ERK5, which contains two proline-rich regions and a nuclear localization sequence and facilitates transcriptional activation of oncogenes.[25] We have most recently studied the overlapping and distinct functions of ERK1/2 and ERK5 signaling in regulating EMT in triple negative and tamoxifen-resistant breast cancer.[26]

High ERK5 expression correlated with EMT, drug resistance, and poor patient survival in several cancers.[27-30] Whole-genome microarray analysis revealed that overexpression of cyclin-dependent kinase 5 (CDK5), an important prognostic marker for development of malignant CRC in human samples, could directly activate ERK5 and promote progression of colorectal cancer via AP-1.[31] ERK5 negatively correlated with miR-143 expression and regulated proliferation, migration, and invasion in osteosarcoma.[32-33] DNA damage initiates apoptotic signaling cascade via activation of ataxia-telangiectasia mutated (ATM) kinase, which is a cell cycle regulator and mediates phosphorylation of DNA damage and repair marker H2AX. Loss-of-function mutation in ATM is one of the causes of cancer and ERK5 deletion in ATM-/- mice has been shown to delay tumorigenesis and increase response to DNA-targeting agents via H2AX phosphorylation in thymic lymphoma.[34] This was one of the few studies to identify the role of ERK5 in relation to tumor suppressors.

1.1.4.3 Mechanisms for dysregulated ERK5 signaling in cancer

Activating mutations in genes such as BRAF (70% melanoma, 59% thyroid, 10% colon, and 6.7% lung cancer)[35] and KRAS (90% pancreatic, 50% thyroid, 30% lung, 15% ovarian, breast, liver, kidney cancer, and leukemias) have a major influence on MAPK signaling in several cancers. Most of these cancers have FDA-approved therapies as a line of treatment, but it becomes really challenging to treat these cancers once they metastasize. BRAF mutations in particular are known to mediate the EMT and metastases via hyperactivation of the MAPK, nuclear factor kappa B (NF-kB), and phosphatidyl inositol-3-kinase (PI3K)/AKT pathways.[36]

ERK5 and AKT pathways are known to transactivate each other and regulate cell survival via phosphorylation and cytosolic sequestration of the pro-apoptotic protein Bad in triple negative breast cancer (TNBC).[37] Moreover, PI3K/AKT pathway is also known to mediate MEK5-ERK5 activation in malignant mesothelioma and neuroblastoma.[38-39] Hepatocyte growth factor (HGF) and its receptor c-met are also known to activate ERK5 and upregulate one of the downstream targets fos-related antigen-1 (FRA-1) via PI3K-AKT signaling in malignant mesotheliomas (MMs).[38] HGF also induced ERK5 and protein tyrosine kinase (PTK) 6 activation and cell migration in breast cancer cells.[40] Platelet-derived growth factor (PDGF) BB increased bone morphogenetic protein (BMP) signaling in fibroblasts via PI3K-MEK1/2-MEK5-ERK5 activation.[41] Interleukin-6 is known to promote ERK5 activation and proliferation in multiple myeloma.[42]

Hyperactivation of ERK5 could be a result of downregulation of tumor suppressor proteins, microRNAs, or phosphatases/ proteases that inhibit ERK5 via a negative feedback loop. microRNAs (miRs) are a class of short non-protein-coding single-stranded

RNAs and their function is to silence protein expression post-transcriptionally. These bind with the 3'-untranslated region (UTR) of the target mRNAs, leading to their translational repression or destabilization. Loss of tumor suppressor miRs is an important mechanism responsible for the overexpression of oncoproteins. Some studies suggest that ERK5 is negatively regulated by tumor suppressor miRNAs miR-143 and miR-200 in breast cancer and glioblastoma, respectively.[43-44]

Downregulation of transcription factor special AT-rich sequence-binding protein 2 (SATB2) via miR-31, miR-34, or TGF-b signaling has been indicated to be associated with cancer progression.[45] High SATB2 expression correlates with favorable prognosis and enhanced chemosensitivity in colorectal cancer (CRC).[45-46] Overexpression of SATB2 increased the epithelial marker E-cadherin, decreased mesenchymal markers vimentin, N-cadherin in CRC cell lines *in vitro*, and suppressed metastases *in vivo*.[47] SATB2 was identified to inhibit ERK5 activity and decrease CRC cell migration, invasion, and colony formation *in vitro* and tumor progression *in vivo*.[48] However, the total ERK5 expression was unaffected, indicating that SATB2 may not transcriptionally regulate ERK5. Finally, ERK5 degradation is mediated by the tumor suppressor von Hippel-Lindau (VHL) through prolyl hydroxylation-dependent ubiquitination and subsequent proteasomal degradation.[49] VHL gene is often mutated in clear cell renal cell carcinoma (CCRCC). Hypoxia-inducible factor-1α (HIF-1α), one of the major targets of VHL-mediated degradation, mediates the survival of cancer cells under low oxygen conditions.[50] Disease-specific survival was greater with high ERK5 and HIF-1α expression and low VHL expression in CCRCC patients, indicating ERK5 as an essential target in CCRCC. Molecular mechanisms regulating ERK5 are summarized in figure 1.7.

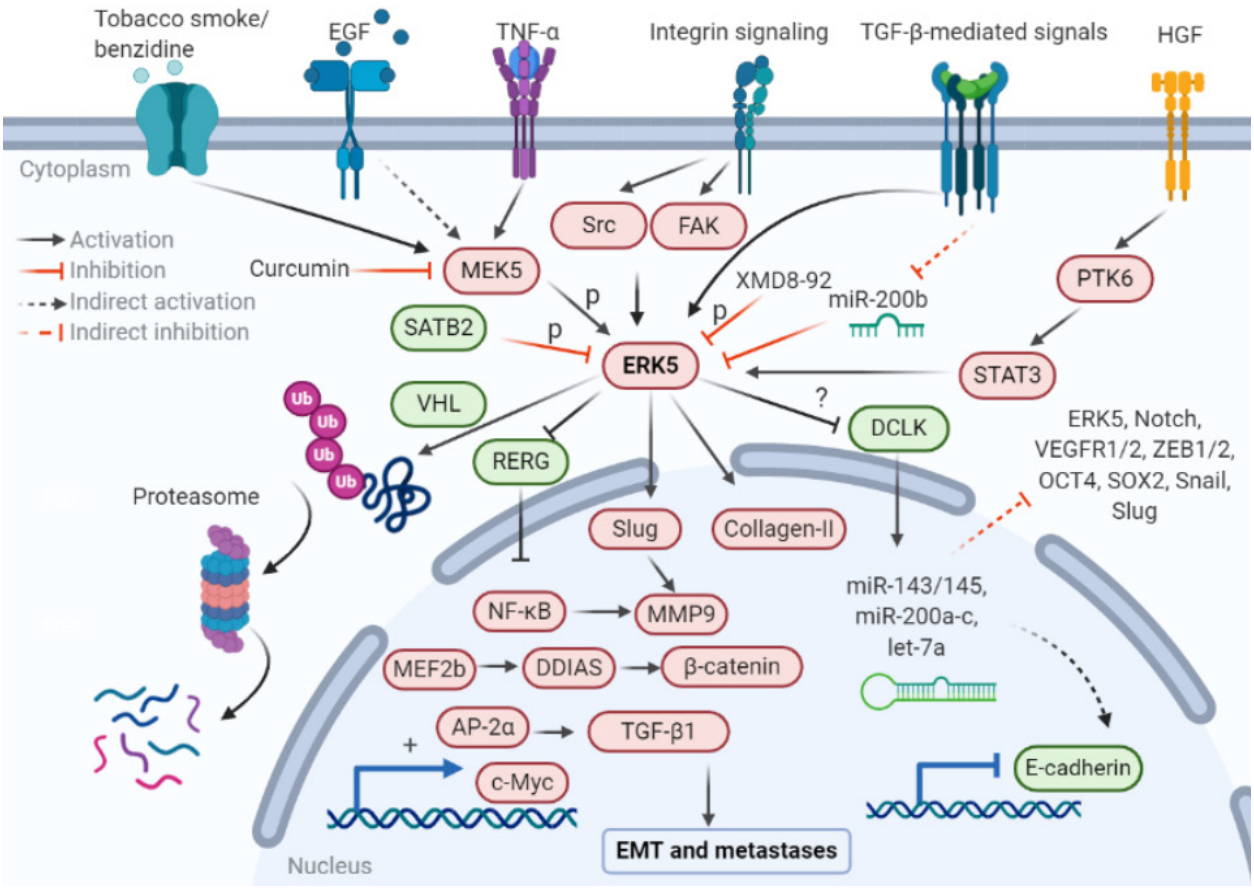

Figure 1.7: Upstream and downstream regulators of EMT mediated via ERK5. Original figure created in Biorender.com.

1.1.4.4 Crosstalk between the ERK1/2 and ERK5 pathways

Crosstalk among the different members of the MAPK family, including ERK1/2 and ERK5, has been noted. ERK1/2 and ERK5 are known to commonly regulate downstream targets such as RSK, c-Fos, and CD-1. We have shown that novel inhibitors of MEK1/2 and MEK5 pathways reverse the mesenchymal phenotype of MDA-MB-231 TNBC cells to epithelial and increase E-cadherin protein expression.[51] Some studies revealed that targeting the ERK1/2 pathway can lead to a compensatory increase in ERK5 activation via upregulation of c-MYC or IGFR.[52-55] ERK5 can compensate for targeting ERK1/2 to inhibit upregulation of macrophage colony stimulating factor receptor (M-CSFR)-

mediated macrophage differentiation in acute myeloid leukemia cells.[56] Inhibition of both ERK1/2 and ERK5 has been found to be necessary for efficient targeting of NRAS and BRAF-mutant melanomas.[52, 54-55, 57] On the contrary, ERK5 has been found to be downstream of the BRAF-MEK1/2-ERK1/2 signaling in melanoma and ERK1/2 is known to promote nuclear localization of ERK5 in HEK293 and PC12 cells via Thr732 phosphorylation (Figure 1.8).[58-59] Although the MEK1/2-ERK1/2 pathway is fairly understood in regulating EMT in cancer, the involvement of the MEK5-ERK5 pathway in EMT is overlooked (293 versus 22 results in Pubmed search). ERK1/2 and ERK5 were thought to have redundant roles, our research goals include examining distinct and overlapping roles of ERK1/2 and ERK5 pathways on MET in breast cancer. Roles of ERK1/2 and ERK5 pathways in regulating EMT are discussed in more detail in chapter four.

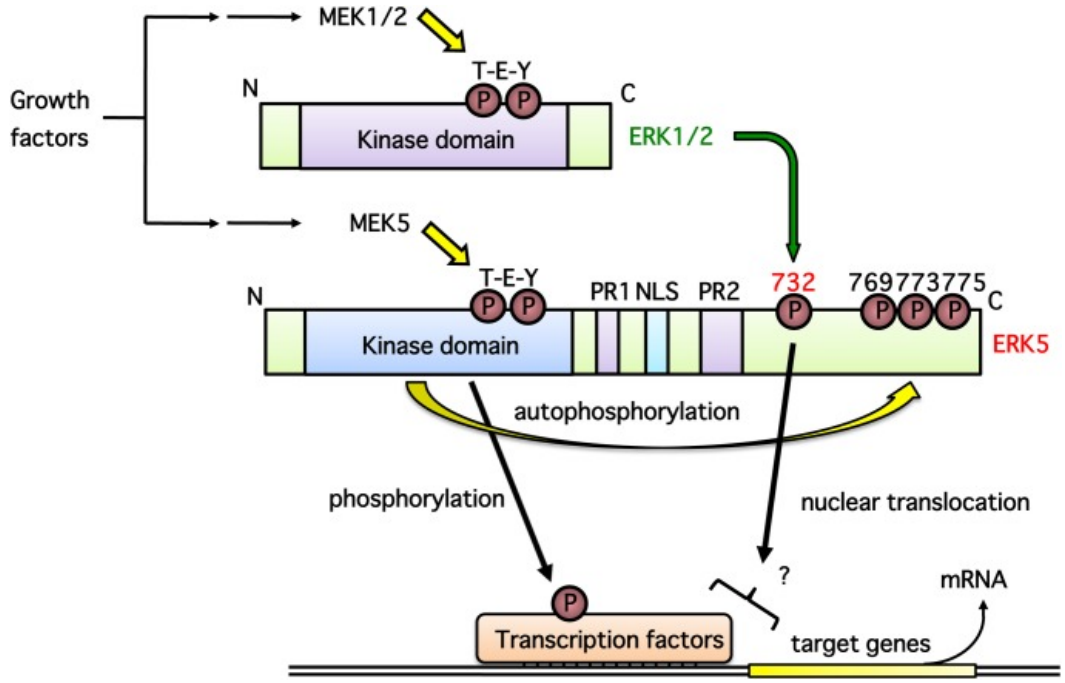

Figure 1.8: Putative crosstalk between the ERK1/2 and ERK5 pathways.[60]

1.1.5 PI3K/AKT pathway in cancer

The crosstalk between MAPK and PI3K pathways has been noted in cancer.[61] In our study, we propose dual inhibitors of MEK5 and PI3K pathways as a strategy to target cancer. Therefore, this section includes the details on the PI3K/AKT signaling pathway. The PI3K/AKT signaling pathway is involved in proliferation, cell survival, apoptosis, differentiation, vacuolar trafficking, and cytoskeletal rearrangement. Class I PI3K family of proteins are implicated in cancer, which is activated by receptor tyrosine kinase, G-protein coupled receptor, and various oncoproteins. The 110-kDa catalytic subunit (p110) of PI3K is associated with an 85-kDa adapter, non-catalytic subunit (p85). p85 subunit is encoded by various genes that code for multiple proteins with distinct function, most of the splice variants, and adapter subunits two Src-homology 2 (SH2) domains. A p110-binding domain is located between the two SH2 domains, which allows for the interaction and stabilization of p110 protein and inhibition of the PI3K kinase activity.[62] Phosphorylation of tyrosine at the growth factor receptor recruits p85 to the cell membrane, relieving its inhibition on p110. Subsequently, PI3K colocalizes with its regulatory molecules and substrate membrane phosphatidylinositols.[63] The PI3K-AKT pathway is illustrated in figure 1.9.

PI3K complex is recruited from the cytoplasm to the inner cell membrane when growth factor binds to the receptor tyrosine kinases. PI3K phosphorylates and converts its substrate phosphatidylinositol (4,5) bisphosphate (PIP2) at the 3-position of the inositol ring to form the secondary messenger phosphatidylinositol (3,4,5) triphosphate (PIP3). The reverse conversion is regulated by the action of the phosphatase and tensin homolog

(PTEN). The levels of PIP3 are controlled by SH2-containing inositol-5-phosphatase (SHIP).[64] PIP3 is an anchor for proteins such as AKT1, AKT2 and AKT3, which contain Pleckstrin Homology (PH) domain. These proteins are activated by 3-phosphoinositide dependent protein kinase-1 (PDK1) when localized to the membrane; further activation of downstream targets such as mTOR, Bad, Caspase 9, GSK3B, tuberin, and certain forkhead transcription factors is initiated.[65-67]

The major targets of the PI3K/AKT pathway include PI3Ks, PDK1, AKT, and mTOR. The most common research tools used to inhibit this pathway include LY294002 and wortmannin, which target the catalytic site of p110. LY294002 did not pass clinical trials because of its unfavorable pharmacokinetic profile and toxicity. New inhibitors of the class imidazopyridines, quinazolyne, pyridopyrimidines, thiazoles that target the catalytic ATP-binding pocket are in development.[68]

1.1.5.1 p110: the catalytic subunit:

The catalytic class I PI3K isoforms of p110: p110α, p110β, p110δ, and p110γ are known to preferentially govern cell signaling and tumor cell survival depending upon the malignancy and the genetic or epigenetic aberrations.[69] Simultaneous mutations are frequent in triple-negative breast cancer, endometrial, and prostate cancer. However, many cancers respond much better to single isoform inhibition when compared to pan-PI3K inhibition. The two distinct functions of p110 isoforms p110a and p110b have been recently studied, which provide a platform for targeting the pathway in the context of the oncogenic driver of AKT signaling: PIK3CA mutation or PTEN loss. Hence, isoform specific targeting could be a novel therapeutic targeting strategy.

PIK3CA mutation driven cancers are dependent on p110a signaling, however, p110b is the major isoform known to drive tumorigenesis in PTEN deficient cancers. PIK3CA mutant cell lines exhibit greater sensitivity to pan-PI3K inhibitors compared to PTEN deficient cancers. Similar response has been observed in the clinic.[70] This might be the case because pan-PI3K inhibitors are more potent against p110a isoform versus the p110b isoform.

The importance of developing isoform specific inhibitors is to target specific mutations in the PI3K pathway and avoid cumulative toxicity of inhibiting irrelevant targets. Most cancers characterized by PI3KCA mutation or amplification are more sensitive to p110a inhibitors such as INK1402, which led to 80-100% growth inhibition versus about 50% growth inhibition in the PTEN mutant cancers, which exhibited resistance.

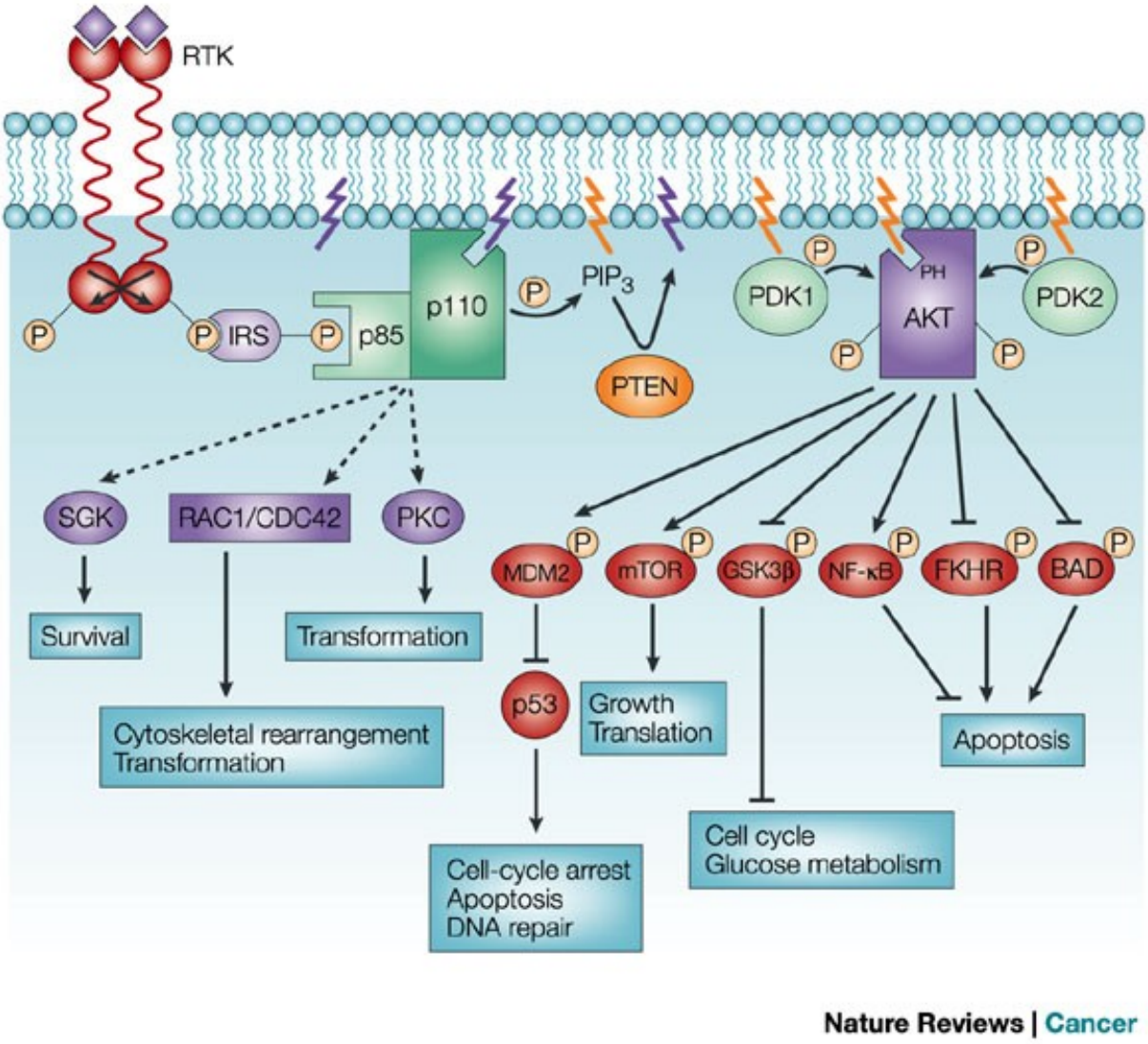

Figure 1.9: The PI3K-AKT pathway in human cancer.[71]

1.1.5.2 Targeting specific p110 isoforms:

The development of isoform specific inhibitors helped to delineate the functional role of p110α and p110β. The p110α knockout mice were embryonic lethal at day 9.5-10.5, and the embryos showed proliferative defects and impaired insulin signaling.[72] The p110a-null embryos and MEFs with kinase-dead p110 knock-in mice showed impaired

growth and insulin signaling with homozygous and heterozygous kinase-dead p110a knock-in, respectively, indicating a kinase dependent function of the p110a isoform.[73] p110β knockout also leads to early embryonic lethality and impaired cell proliferation. However, p110b-null MEFs reconstituted with a p110b kinase-dead allele survive normally, suggesting a kinase independent function of the p110b isoform, and its role as an important scaffold.[74-75]

A panel of breast cancer cells MCF7, BT474, BT20, and BT47D with mutant p110a are sensitive to p110a isoform-specific inhibitors.[76] Targeting p110a isoform inhibits tumor cell proliferation, chemoresistance, and mig[77]ration in medulloblastoma cells that over-express p110a. p110a inhibition is effective also in tumors that harbor mutant Ras and PTEN deficiency, which exacerbate the oncogenic transformation. Although the rates of activating mutations in PIK3CA gene are high, loss of PTEN is the most common mechanism for oncogenic PI3K signaling in most cancers. It was misconstrued in the past that frequent activation of p110a was the major oncogenic driver and the loss negative PI3K regulation by PTEN mutation contributed to the aberrant signaling. However, p110a ablation in PTEN mutant cancers did not significantly affect tumorigenesis.[78]

In contrast, p110b targeting sufficiently inhibits downstream AKT activation and tumor formation in PTEN deficient prostate cancer.[78] It is important to consider that PTEN loss could be an amplifier of PI3K signaling coupled to an initial weak signal driven by either PIK3CA, GPCR or p110a mutation, which has an influence on the type of response to specific isoform inhibition. Cell lines with PTEN loss and coexisting PIK3CA or Ras mutation were sensitive to p110a and dual p110a/mTOR inhibition, but not p110b

inhibition.[79] However, if the signals are initiated from a GPCR, then p110b inhibition would be a more relevant strategy to reduce tumor formation.

1.2 Statement of the Problem

Reversing epithelial to mesenchymal transition (EMT) is an emerging strategy to target the invasive cancers that show poor sensitivity to chemotherapeutic agents. EMT is characterized by loss of cell polarity, disruption of intercellular junctions, reorganization of the cytoskeleton, downregulation of E-cadherin, and increased cell migration and invasion[80] Disruption of actin skeleton via ras and src mediated activation of extracellular regulated kinase 1/2 (ERK1/2) and ERK5 is reported, indicating their role in oncogenic transformation[81]. Most invasive cancers, including triple negative (TNBC) and tamoxifen resistant (TAMR) breast cancers have a mesenchymal phenotype. There are no current studies that have explored the role of MAPK inhibitors as inducers of mesenchymal to epithelial transition (MET), the reverse process of EMT, in breast cancer.

Activation of mitogen activated protein kinase (MAPK) pathways, including ERK1/2 and ERK5 signaling cascades can activate downstream targets such as Fos-related antigen (Fra-1), zinc finger E-box binding protein ZEB1, and Slug, which lead to EMT[82]. Several MEK5 independent mechanisms for ERK5 activation and nuclear localization, mediated via phosphoinositol-3-kinase (PI3K)/AKT and MEK1/2 pathways, respectively have been reported[39, 60]. A crosstalk between AKT and ERK5 pathways has been suggested as a mode of chemoresistance in breast cancer cells. The goal of this research is to examine the independent and converging roles of MEK1/2 and MEK5 in regulating

EMT, crosstalk with the AKT pathway, and chemoresistance in mesenchymal breast cancer cells.

1.2.1 Research Objectives

1.2.2 Hypothesis and Specific Aims:

Hypothesis: MEK5 and MEK1/2 or PI3K pathway inhibition will reverse epithelial to mesenchymal transition and enhance chemotherapeutic drug sensitivity in breast and brain cancers.

Specific Aim 1: To elucidate the structure-activity relationship of novel diphenylamine analogs that induce mesenchymal to epithelial transition in breast cancer.

Specific Aim 2: To elucidate the effect of targeting the ERK1/2 and ERK5 pathways using pharmacological inhibitors and molecular tools on MET in breast cancer.

Specific Aim 3: To examine the effect of ERK1/2, AKT, and ERK5 pathway inhibitors on chemosensitivity in triple negative and tamoxifen resistant breast cancer cells.

Specific Aim 4: To examine the effect of dual ERK5 and ERK1/2 or AKT inhibition on MET, proliferation, migration, and colony formation in glioblastoma multiforme.

Chapter 2: Methods

2.1 Cell Culture and Reagents

MDA-MB-231, MDA-MB-231 VIM RFP, BT-549, MCF-7, and U87MG cell lines were obtained from American Type Culture Collection (ATCC). MDA-MB-231 cells were maintained in Dulbecco's Modified Eagle Medium and Ham F-12 (1:1), BT-549 and MCF-7 cells were maintained in RPMI- 1640 medium, and U87MG cells were cultured in MEM medium supplemented with 5% FBS (Gibco) and 0.5% Pen Strep (Gibco) in a humified atmosphere containing 5% CO2 at 37◦C. To generate a tamoxifen resistant cell line, MCF-7 cells were cultured in phenol red-free RPMI-1640 media, supplemented with 5% charcoal-stripped FBS in the presence of DMSO or 0.1μM (Z)-4-Hydroxytamoxifen (4-OHT) (Sigma-Aldrich Cat. No. H7904) for 6 months. Charcoal-stripped FBS was used to remove endogenously expressed protein growth factors present in the media (TAMR MCF-7 cell line was generated by Dr. Thomas Wright).

2.2 Inhibitor treatment and EGF stimulation

To examine the specificity of the kinase inhibitors, cells (500,000 cells/well) were cultured in a 6-well plate for 24 hours. To examine kinase activity or inhibition, the cells were serum-starved for 18-24 hours. The inhibitors XMD8-92 (Tocris, Minneapolis, MN), Trametinib (Selleckchem, Houston, TX), and VX-11e (Cayman chemical, Ann Arbor, MI) were added for 30 minutes prior to EGF (100ng/ml) stimulation for 15 minutes as described previously.[83] Cell lysates were examined for kinase activation using standard western blot procedure.

2.3 Lentivirus treatment

Since pharmacological inhibitors may have off-target effects, molecular tools were utilized in our study to examine the kinase pathway and EMT/ MET. Lentivirus vectors were a generous gift from Dr. Zhengui Xia (University of Seattle, Washington). MDA-MB-231, MDA-MB-231 VIM RFP, and BT-549 cells were cultured in a 12-well plate (150,000 cells/ well). The volume of lentivirus (µL) required per well was calculated as [(# of cells/well x desired multiplicity of infection (MOI)/viral titer (IU/µL)]. This volume of lentivirus was diluted in fresh media. 50% of media was replaced with the lentivirus-containing media. The transfection efficiency was about 50% after 24 hours of infection at MOI=1, as calculated by microscopic observation of the percentage of GFP-positive cells. The cells were infected with lentivirus at the MOI =1 for 96 hours. Western blotting was performed to examine cell E-cadherin and ZEB1 protein expression or ERK1/2 and ERK5 activation, respectively and immunocytochemistry was performed to examine cell morphology.

Lentivirus Vector	Titer (IU/ml)	Cryobaby color
GFP	$3.35x10^8$	Green
caMEK5	$4x10^7$	Yellow
dnMEK5	$5x10^6$	Yellow
wtERK5	10^7	Red

dnERK5	$3.2x10^7$	Yellow
caMKK1	$1.85x10^7$	Orange
dnMKK1	$3.10x10^7$	Blue

Table 2.1 Lentivirus titer

2.4 Nuclear/Cytosolic fractionation

Cells were cultured in 6-well plates (500,000 cells/well) for 24 hours. After 24 hours, cells were treated with the kinase inhibitors for 72 hours. The nuclear/ cytosolic fractionation was performed using standard manufacturer's instructions (Cell Biolabs, San Diego, CA). In brief, the medium was aspirated, and cells were washed with pre-chilled 1X PBS. DTT and Protease inhibitor cocktail was added to Cytosol Extraction Buffer (CEB). 100 µL CEB was added to cells for 10 minutes. Cells were scraped and collected in 1.5 mL pre-chilled microcentrifuge tubes. Cell lysis buffer was added for 5-15 minutes and the lysates were vortexed for 10 seconds. The lysates were centrifuged at 10,000 rpm for 10 minutes at 4°C. The supernatant (cytosolic fraction) was collected and stored at -80°C. The pellet was resuspended in CEB and lysis buffer was added for 10 minutes. The suspension was vortexed and centrifuged at 10,000 rpm for 10 minutes at 4°C. The supernatant was discarded, this step was performed to ensure clean separation. The pellet was resuspended in 40 µL nuclear extraction buffer (NEB) with DTT and protease inhibitors. The solution was incubated on ice for 30 minutes with occasional vortexing. The samples were centrifuged at 14,000 rpm for 30 minutes at 4°C. The supernatant (nuclear fraction) was stored at -80 °C.

2.5 Western Blot Analysis

Cells were lysed at experimental endpoint in 1X cell lysis buffer (Cell Signaling Technology) and 0.1M PMSF. The proteins were resolved using 8% SDS polyacrylamide gel electrophoresis and transferred to nitrocellulose membranes (LI-COR Biosciences; Lincoln, NE). The membranes were blocked for 1 h at room temperature and incubated at 4°C overnight with respective primary antibodies (Appendix B) diluted in casein blocking buffer (LI-COR Biosciences). The membranes were washed three times with wash buffer (PBS 1X, Tween 0.02%) at 10-minute intervals. The membranes were incubated with goat anti-mouse (1:10000, Invitrogen) and goat anti-rabbit (1:10000, Invitrogen) secondary antibodies for 1 h. Membranes were washed three times at 10-minute intervals with PBS-tween wash buffer and scanned on an LI-COR's Odyssey CLx Imager at 700 nm (goat anti-rabbit) and 800 nm (goat anti-mouse). The blots were quantified with LI-COR Image Studio Software.

2.6 Crystal Violet Staining

Crystal violet staining was performed to examine cell morphology. Cells (50,000 cells/well) were seeded in a 12-well plate for 24 hours and treated with 1μM concentration of compounds for 5 days. After 5 days, media was aspirated, and cells were gently washed with 1X PBS. Cells were fixed with 50 μl 4% paraformaldehyde per well for 15 minutes. Cells were washed once with 1X PBS and stained with 50 μl crystal violet per well for 15 minutes. Cells were washed with 100 μl PBS three times and imaged using EVOS^{TM} FL inverted microscope (Life Technologies) under 10X magnification.

2.7 Spindle Index Calculation

Spindle index calculation was performed to quantify cell shape and validate the structure-activity relationship of the novel diphenylamines. Spindle indices (SI) of individual cells were calculated from at least 200 cells per treatment from at least three images as the ratio of length (l) to width (w); SI = l/w of each cell. Cells with SI < 3 were considered as epithelial.[84] % cells with SI<3 were calculated as the ratio of the number of cells with spindle index < 3 to the total number of cells per image. The method was adopted from reference 82. Length and width of cells were measured using the Image J software, U. S. National Institutes of Health, Bethesda, Maryland, USA.

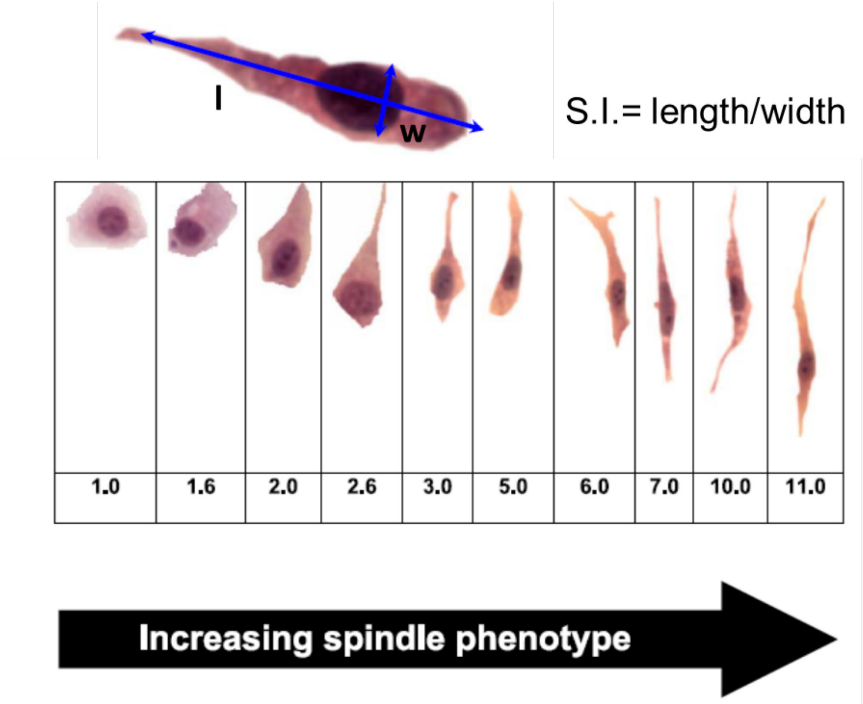

Figure 2.1: Calculating the spindle index[85]

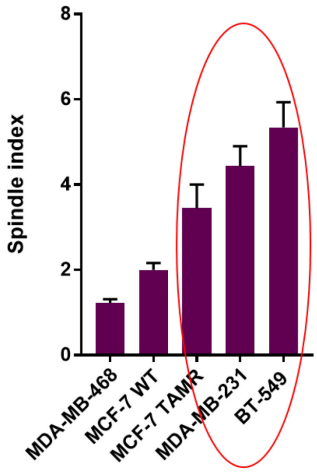

Mesenchymal phenotype: MDA-MB-231, BT-549, MCF-7 TAMR
Epithelial phenotype: MCF-7 WT, MDA-MB-468

Figure 2.2: Validating spindle index calculation using panel of breast cancer cell lines: Cells with mesenchymal phenotype correspond have SI value > 3.

2.8 Colony Formation Assay

Colony formation assay was performed to examine the growth of cells in 3-D extracellular matrix-based conditions. Colony formation assay was performed using a Soft Agar Colony Formation assay (Cell Biolabs; CBA-130). Briefly, base agar layer was added first. MDA-MB-231 cells (5,000 cells/well) were cultured in 5% FBS growth media and 1.2% agar solution in a 96-well plate. DMSO or compound **1** (0.1, 1, and 10 μM) diluted in media was added on the top of cell layer. The colonies were allowed to grow for 7 days. The agar layer was solubilized, the colonies were lysed and stained with CyQuant dye. Florescence at 485 nm was measured on VICTOR3 1420 Perkin Elmer multi-label counter.

2.9 Spheroid Culture

Spheroid culture was performed to examine the effect on cells that have gained the ability to survive in anchorage-independent conditions. Cells (5,000 cells/ well) were cultured in 96-well low attachment plates (Corning Cat. No. 4520). DMSO or inhibitors were added after 24 h of plating. Pictures were taken using the EVOSTM FL inverted microscope (Life Technologies) under 4X magnification at the time of treatment and after 7 days from treatment. 10 µl of Reliablue viability reagent (ATCCR 30-1014TM) was added to each well after 7 days from treatment. The plates were incubated in the incubator at 37◦C for 3 h. The fluorescence was measured at ex570/ em590 on a Synergy microplate reader (Biotek, Winooski, VT). Data is represented as spheroid viability normalized to DMSO control ±SEM of triplicate experiments.

2.10 Immunofluorescence Assay

Immunofluorescence assay was performed to examine number of proliferating cells, cell morphology, and EMT marker ZEB1 after treatment with kinase inhibitors. Cells were plated at a density of 5,000 cells/well in a 96-well plate for 24 hours. After 72 hours of treatment, cells were fixed with 4% paraformaldehyde for 15min and washed with 1X PBS. Cells were blocked for 1 h with 0.3% Triton-X solution in Casein blocking buffer and 1X PBS. The Primary antibodies α-actinin, α-tubulin, and Ki67 (Cell Signaling Technology) were added at a dilution of 1:750 and plate was incubated overnight at 4°C. The cells were subsequently washed three times at 5-minute intervals, incubated for 1 h with goat anti-mouse Alexa Flour 488 nm and goat anti-Rabbit Alexa Flour 555 nm (1:1000, Invitrogen), and counterstained with Hoechst (Fisher) to visualize the nucleus.

The cells were washed with 1X PBS three times at 5-minute intervals. The plate was imaged with the EVOS^{TM} FL inverted microscope (Life Technologies). The proliferative index was calculated as the ratio of number of Ki67^{+} cells to the number of Hoechst^{+} cells.

2.11 Scratch Assay

Cell migration was assessed using a scratch assay after treatment with DMSO or inhibitors for 72 hours. Cells were seeded at a seeding density of 50,000 cells/ well in a 12-well plate in 1ml full media in the presence of 5% FBS. Scratches were made after 48 h of the treatment (0 hr). The underside of the plate was marked to denote the location of the initial wound. Cells were washed gently with 1x PBS to remove detached cells and debris. Images were taken at the time of scratch and after 24 h from the time of scratch. Cell migration was calculated as wound closure = (border width at 24 h-border width at 0 h)/ (border width at 0 h) X 100. Results are represented as cell migration normalized to DMSO control ± SEM of experiments repeated three times. The principle behind cell migration is illustrated in figure 2.4.

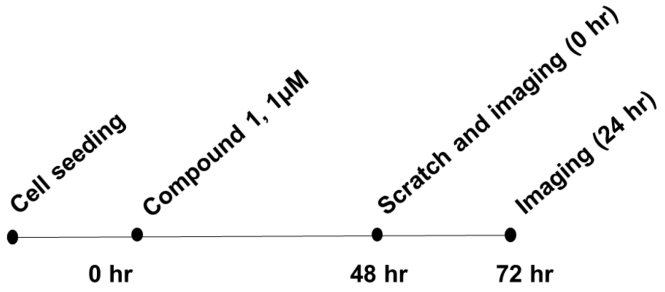

Figure 2.3 Treatment scheme for scratch assay

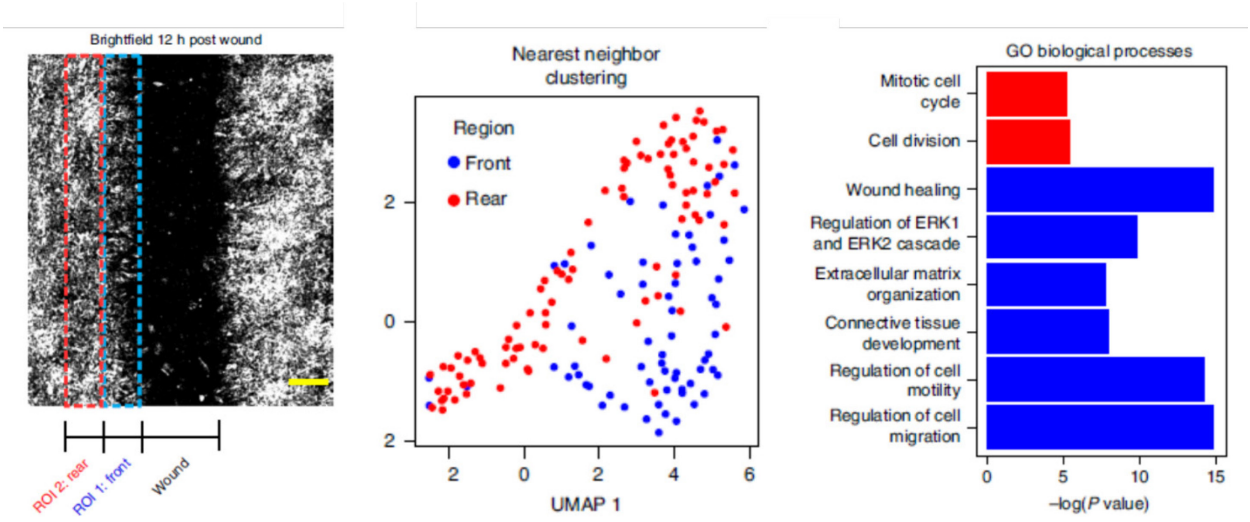

Figure 2.4 Principle behind cell migration assay. Cells in the front end of the scratch differentially express genes involved in cell motility, migration, and wound healing (figure reproduced with permission).[86]

2.12 Cell Viability Assay

Cell viability was evaluated using MTT (3-(4,5-dimethylthiazol-2-yl)-2,5-diphenyltetrazolium bromide) assay. Cells were seeded at a density of 5,000 per well in 96-well plates containing 90 µl of full media for 24 h. Cells were then treated inhibitors for 72 hours. After 72 hours, 10 µL of MTT (Acros, Cat. No. 298-93-1) solution (5 mg/ml in phosphate-buffered saline, PBS) was added to each well. The plate was incubated at 37°C and 5% CO_2 for 3 hours. After removal of the MTT solution via aspiration, 100 µl of DMSO was added to the wells for 10 minutes under agitation to dissolve the formazan crystals. Absorbance was measured at a wavelength of 570 nm using Wallac 1420 software on a Perkin Elmer 1640 multilabel counter. Results are represented as cell viability normalized to DMSO control ± SEM of triplicate experiments repeated three times.

2.13 Synergy Calculation

Data from combination experiments were analyzed using the CompuSyn (v1.4) synergy software. Individual concentration response graphs of SC-1-151 in combination with JQ-1 or LBH-549 were compared to 1:1 combination ratio. Combination indices (CI) < 1 and fraction affected (Fa) > 50% were considered synergistic.

2.14 Statistical Analyses

Two-tailed Student's unpaired t-test was used in to analyze data that involved a comparison between treated (diphenylamine derivatives) and control (DMSO) groups (fold change, E-cadherin and spindle index). If p-values were below 0.05, differences were considered significant. Data represent ± SEM of at least three independent experiments. One-way analysis of variance (ANOVA) with Bonferroni post-hoc correction was used to examine concentration-dependent effect of the inhibitors on cell viability, proliferation, spheroid viability, and cell migration. Two-tailed Pearson correlation analysis and linear regression was used for correlation experiment. Statistical analyses were performed using GraphPad Prism version 8 for Windows, GraphPad Software, La Jolla California USA.

Chapter 3: Novel diphenylamine analogs inhibit MEK1/2 and MEK5 pathways, induce a mesenchymal to epithelial transition, and decrease spheroid formation, cell migration, and proliferation in triple-negative and tamoxifen-resistant breast cancer cells

3.1 Introduction

Triple negative breast cancers (TNBC) account for about 13-15% of total breast cancer cases.[87] TNBCs are associated with poor prognoses and patient outcomes, and a high frequency of relapse. About 70% of breast cancer patients are diagnosed with ER-positive breast cancer. These patients can be treated with ER-antagonists, such as 4-Hydroxytamoxifen (4-OHT). However, the incidence of developing tamoxifen-resistance (TAMR) is high.[88] Tamoxifen-resistance is also associated with gain of a mesenchymal phenotype due to β-catenin phosphorylation.[89] TNBCs and TAMR cancers have a mesenchymal phenotype. Mesenchymal cells are migratory and invasive, which leads to secondary tumor formation or metastasis. Metastasis is the leading cause of death in cancer, and there are currently no treatments that effectively inhibit metastasis. Therefore, there is a dire need of targeted therapy for TNBCs and TAMR cancers.

Mitogen Activated Protein Kinase (MAPK) pathways are important regulators of cell cycle and differentiation and the MEK1/2 and MEK5 MAPK signaling pathways are emerging targets for drug discovery. The MEK5-ERK5 pathway is an important therapeutic target in many cancers as it has been shown to regulate tumor growth and metastasis.[90] Moreover, activation of the MEK5-ERK5 pathway, in response to inhibition of the MEK1/2-ERK1/2 cascade, may mediate resistance to MEK1/2-ERK1/2 pathway

inhibitors.[91] MEK1/2 inhibitors trametinib and cobimetinib are FDA-approved for the treatment of NSCLC and melanomas; however, MEK5/ERK5 pathway inhibitors are only currently used as experimental tools. Our research interests include the development of selective novel pharmacological inhibitors of the MEK5-ERK5 pathway.

Activation of MAPK results in phosphorylation of downstream targets ERK1/2 and ERK5, which can activate gene transcription of epithelial to mesenchymal transition (EMT) regulators such as ZEB1, Snail, and Vimentin.[90, 92] EMTs play an instrumental role in cancer metastases.[93-94] Therefore, inhibition of EMT is emerging as a target to attenuate the aggressive characteristics of cancer cells. Induction of the mesenchymal to epithelial transition (MET), the reverse of EMT, by small molecules, represents a practical and viable approach for treating the cancers which have a mesenchymal phenotype. While small-molecule kinase inhibitors mostly target the ATP-binding pocket, several novel diphenylamine derivatives were synthesized to target an allosteric site of MEK5 (Figure 3.1 A).[83] Allosteric inhibition of kinases may offer reduced resistance and greater kinase selectivity.[95]

While the kinase domain of ERK1/2 and ERK5 proteins share about 60% sequence homology, ERK5 differs from ERK1/2 in its N-terminal domain, which harbors the nuclear localization sequence, and a unique allosteric binding pocket (Figure 3.1 A-B). Novel MEK5 pathway inhibitors were synthesized by making structural modifications of the lead MEK1/2 inhibitor, PD325901. Compound 1, a dual MEK1/2 and MEK5 inhibitor, was identified to target the EMT axis in MDA-MB-231 cells (Figure 3.2). The highly invasive MDA-MB-231 cell line (TNBC) was selected, as it consists of more than

90% of high CD44+/CD24−/low stem cells,[96] and has high expression of mesenchymal markers including vimentin, SNAIL, SLUG, and ZEB1.

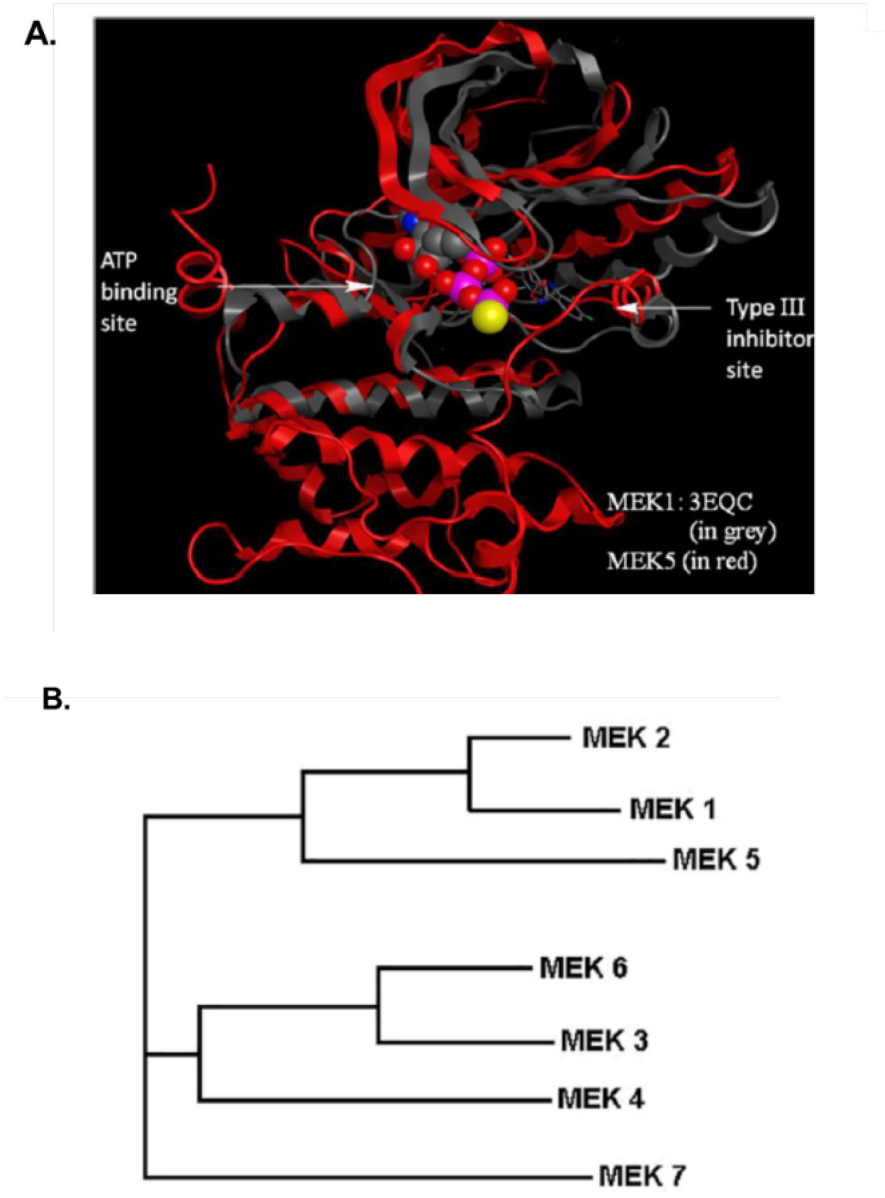

Figure 3.1: Drug discovery. A. ATP and Type III binding sites of the MEK1 crystal structure (PDB ID:3EQC) superimposed on a homology model of MEK5. ATP is shown as space filling and compound 1 is shown as a stick representation in the proposed type III binding site. **B.** Phylogram analysis of MEK isoforms; MEK5 is most closely related to MEK1 and MEK2.[83]

Structural variants of compound **1** were synthesized to identify the functional groups responsible for induction of MET. We examined two experimental endpoints to quantify the activity of diphenylamine derivatives for a inducing mesenchymal to epithelial transition in MDA-MB-231 cells after treatment with structural analogs of compound **1**: (i) upregulation of the epithelial marker E-cadherin examined via western blotting and (ii) phenotypic switch from mesenchymal to epithelial as indicated by a decrease in spindle index (SI) and an increase in % cells with SI<3. The lead molecule, compound **1**, was found to decrease spheroid formation, cell migration, and cell proliferation in TNBC (MDA-MB-231 and BT-549) and tamoxifen-resistant (TAMR) MCF-7 breast cancer cells. Compound **1** also decreased ZEB1, Snail, SOX2, and Vimentin (mesenchymal and stem cell markers) in MDA-MB-231 cells.

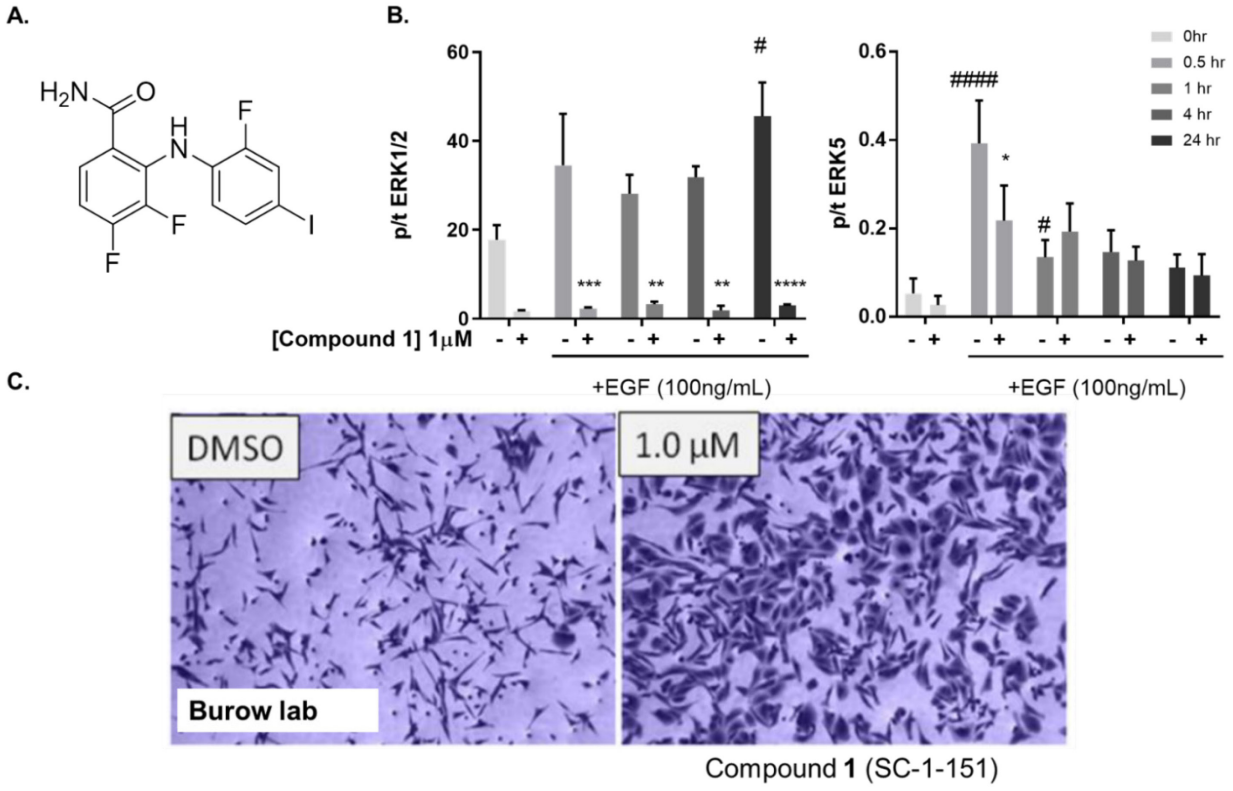

Figure 3.2. Compound 1 (SC-1-151), a dual ERK1/2 and ERK5 inhibitor induces a phenotypic switch in MDA-MB-231 cells. (A.) Structure of Compound **1**. **(B.)** Compound **1** inhibits ERK1/2 and ERK5 phosphorylation in MDA-MB-231 cells. Data represent the +/- SEM of three different experiments determined by two-way ANOVA with the Bonferroni post hoc test. *p<0.05; **P<0.01; ***P<0.001; ****P<0.0001; vs untreated respective control group determined; #P<0.001, ####P<0.0001; vs untreated control at 0 hour determined by two-way ANOVA with the Bonferroni post hoc test. **(C.)** Compound 1 was serendipitously identified to induce a phenotypic switch from mesenchymal to epithelial in MDA-MB-231 cells.

3.2 Hypothesis: Novel diphenylamine analogs will induce MET and decrease spheroid formation, cell migration, and proliferation in triple-negative and TAMR breast cancer cells.

3.3 Results:

3.3.2 Structure-activity relationship of novel diphenylamine analogs for MET induction:

MDA-MB-231 cells were treated with the diphenylamine structural variants (Figure 3.3) at a concentration of 1 μM for 5 days. Increase in E-cadherin protein expression and change in morphology from mesenchymal to epithelial were the primary endpoints to study the effect on MET. E-cadherin expression order for amide variations at R1 (Figure 3.3) was NHCH3 (**2**) > NH2 (**1**) > 4-Boc-piperazine (**16**) > piperazine (**15**) > N(CH3)2 (**5**) > N(C2H5)2 (**4**) > NHC2H5 (**3**) > N(CH3)C2H4N(CH3)2 (**17**) > 4-methylpiperazine (**13**; **Table 3.1**) at R1. Compounds **1**, **2**, **15,** and **16** caused a >9-fold increase compared to DMSO. The 4-methyl piperazinyl analog **13** was 3-fold less active compared to compound **1.** Removal of the 4-methyl group led to a 3-fold improvement in E-cadherin induction (compound **13** vs. **15**). The 4-Boc protected derivative **16** was 3-fold more active than **13**.

Compounds **15** and **16** were equally effective as compound **1**. The acid (**7**) was 2-fold less active, and ester **6** was about 5-fold less potent compared to **1**. Both basic side chain amides (**15**) and neutral amides (**1-5**, **16**) were active in inducing MET consistent with significant functional group tolerance attached to the amide group.

Replacement of the R2 and R3 fluoro atoms with hydrogen atoms led to a >3-fold decrease in the E-cadherin expression (**1** vs. **8**). Similarly, replacing the R4 hydrogen with a methyl group led to a >3-fold reduction in the E-cadherin expression (**1** vs. **9**). Substituting the iodo atom (**11**) at R6 or the fluoro atom (**12**) at R5 with hydrogen results in a 3-fold decrease in E-cadherin expression as compared to **1**. Removal of both the groups (**10**) did not increase E-cadherin expression. These data indicate that the fluorine atom at R5 and the iodine atom at R6 are essential for MET induction. The derivatives with substitutions at the R7 position were found to be inactive (**19**–**21**). The structural variations on the diphenylamine core, increase in E-cadherin expression, SI values, and % cells with SI<3 are summarized in table 3.1.

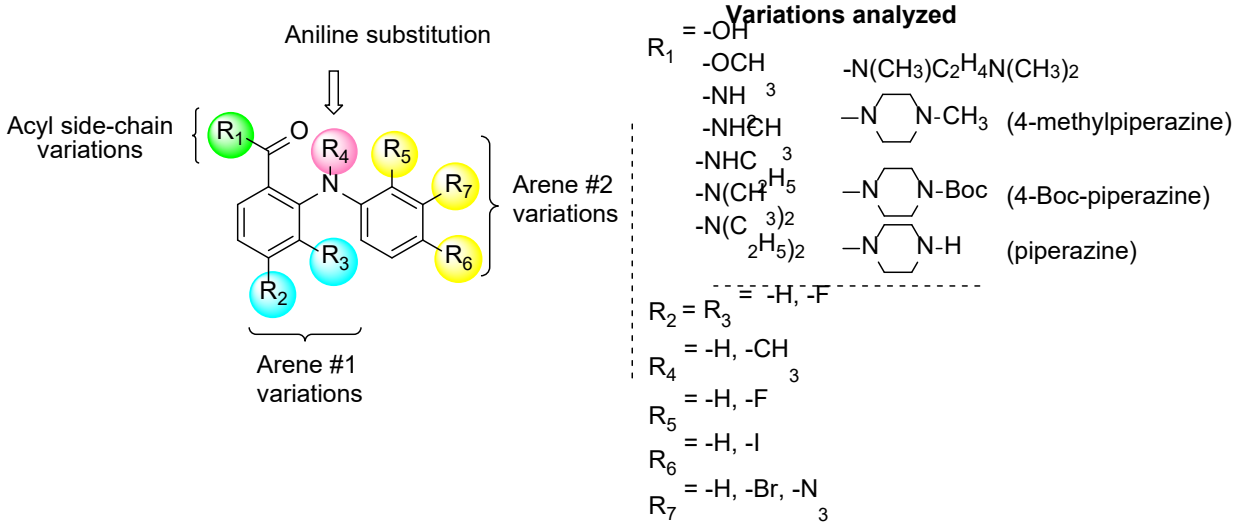

Figure 3.3. Diphenylamine structural variants.

#	Side chain R_1	Arene #1		R_4	Arene #2			E-cadherin (Fold change ± S.E.M.)[a]	p-value	S.I. ± S.E.M.	% cells with SI<3 ± S.E.M.
		R_2	R_3		R_5	R_6	R7				
1	**$-NH_2$**	**-F**	**-F**	**-H**	**-F**	**-I**	**-H**	**10.5 ± 3.5**	**0.012**	**2.2 ± 0.1**	**85.9 ± 3.4**
2	-NHMe	-F	-F	-H	-F	-I	-H	12 ± 4.6	0.002	2.7 ± 0.2	64.6 ± 0.4
3	-NHEt	-F	-F	-H	-F	-I	-H	4.9 ± 1.9	0.001	2.5 ± 0.4	81.9 ± 7.8
4	$-N(C_2H_5)_2$	-F	-F	-H	-F	-I	-H	6.1 ± 2.1	<0.0001	2.6 ± 0.2	67.5 ± 6.2
5	$-N(CH_3)_2$	-F	-F	-H	-F	-I	-H	7.6 ± 0.5	<0.0001	2.6 ± 0.2	73.1 ± 5.5
6	-OMe	-F	-F	-H	-F	-I	-H	2.3 ± 0.7	0.015	2.9 ± 0.1	62.2 ± 2.4
7	-OH	-F	-F	-H	-F	-I	-H	4.5 ± 2.05	0.009	2.8 ± 0.1	66.1 ± 6.4
8	$-NH_2$	-H	-H	-H	-F	-I	-H	2.9 ± 1.4	0.062	3.3 ± 0.2	61.5 ± 5.1
9	$-NH_2$	-F	-F	$-CH_3$	-F	-I	-H	2.8 ± 1.1	0.008	3.3 ± 0.4	52.4 ± 12
10	$-NH_2$	-F	-F	-H	-H	-H	-H	1.3 ± 0.1	0.002	3.9 ± 0.3	29.7 ± 1.1
11	$-NH_2$	-F	-F	-H	-F	-H	-H	4.3 ± 1.5	0.004	3.6 ± 0.1	44.9 ± 0.3
12	$-NH_2$	-F	-F	-H	-H	-I	-H	3.1 ± 0.6	<0.0001	2.4 ± 0.1	83.1 ± 1.8
13	4-methylpiperazine	-F	-F	-H	-F	-I	-H	3.4 ± 0.8	<0.0001	2.8 ± 0.1	70.7 ± 2.1
14	4-methylpiperazine	-F	-F	-H	-F	-H	-H	1.1 ± 0.2	0.550	3.5 ± 0.1	41.3 ± 4.7
15	-piperazine	-F	-F	-H	-F	-I	-H	9.1 ± 2.2	<0.0001	1.9 ± 0.2	86.3 ± 7.7
16	4-Boc-piperazine	-F	-F	-H	-F	-I	-H	9.9 ± 4.1	<0.0005	2.8 ± 0.1	68.3 ± 4.7
17	$-N(CH_3)C_2H_4N(CH_3)_2$	-F	-F	-H	-F	-I	-H	4.3 ± 3.3	0.048	3 ± 0.2	59.3 ± 6.1
18	4-methylpiperazine	-F	-F	-H	-H	-H	-H	1.7 ± 0.47	0.0009	3.6 ± 0.1	55.8 ± 5.2
19	4-methylpiperazine	-F	-F	-H	-H	-H	$-N_3$	1.6 ± 0.90	0.2786	3.5 ± 0.2	47.4 ±2.9
20	-NHEt	-F	-F	-H	-H	-H	$-N_3$	0.77 ± 0.01	<0.0001	3.4 ± 0.2	47.1 ± 6.7
21	4-methylpiperazine	-F	-F	-H	-H	-H	-Br	1.6 ± 0.88	0.2394	3.8 ± 0.2	37.6 ± 5.5
	DMSO							1		4.2 ± 0.4	30.5 ± 4.8

Table 3.1: Effect of diphenylamine analogs on E-cadherin expression, spindle index, and % cells with S.I.<3 in MDA-MB-231 cells. MDA-MB-231 cells were treated with compounds 1-20 at 1μM concentration for 5 days. Data represent mean ± SEM. E-Cadherin was normalized to a-tubulin, and fold change is compared to DMSO. One-way ANOVA with Bonferroni post-hoc comparison analysis was performed where the compounds were compared to the DMSO control and to each other; compounds 1 and 2 were found to be statistically significant compared to the DMSO control group ($P < 0.05$). We missed significance across groups because there was large difference between the minimum and the maximum effect produced by the different compounds. Therefore, we switched to performing t-test and compared each compound individually to the DMSO control group. [a]Data represent the ± SEM of three different experiments determined by unpaired two-tailed Student's t-test (n = 3).

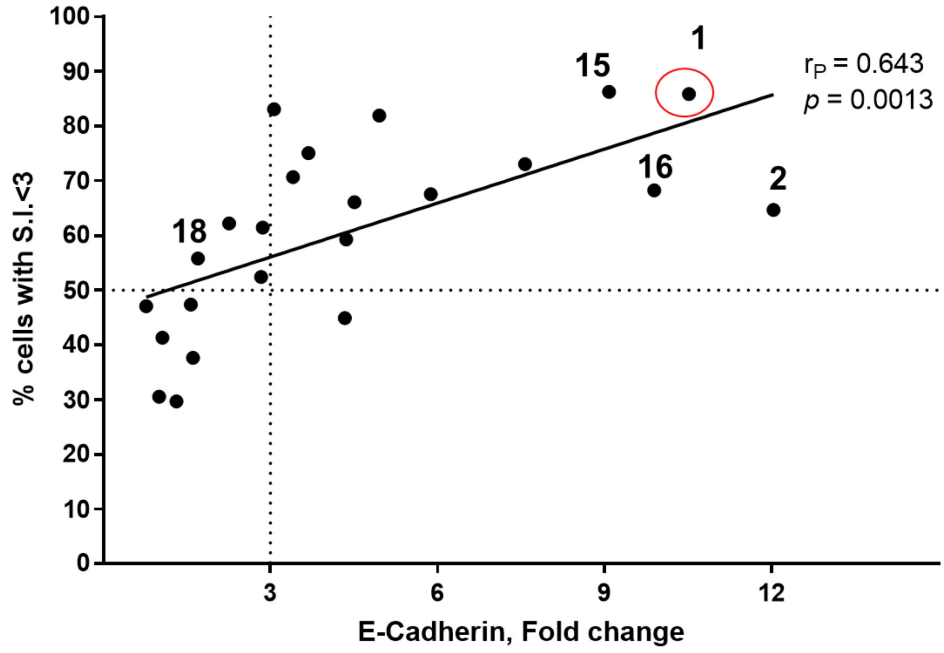

Figure 3.4. Increase in E-cadherin expression significantly correlates with the percentage of cells with SI<3. A positive correlation between E-cadherin protein expression, compared to DMSO and an increase in percentage of cells with SI < 3 was observed. Data was analyzed by two-tailed Pearson correlation. The correlation coefficient (rP) and significance (*p*-value) are indicated on the scatter plot.

3.3.3 Increase in E-cadherin positively correlates with an increase in % cells with SI<3

MET is characterized by a morphological switch from a spindle-like phenotype to a cobblestone-like phenotype. To determine cell morphology, crystal violet staining was performed after 5 days of treatment with the diphenylamine analogs. To quantitate the phenotypic transition, spindle index (SI) was determined as the length to width ratio of each cell. Cells with a SI < 3 were considered epithelial.[84] The compounds that led to an increase in E-cadherin protein expression also altered the morphology of MDA-MB-231 cells from mesenchymal to epithelial, as measured by a reduction in the spindle index value. The compounds that increased E-cadherin expression by at least 3-fold and that displayed >50% of the cells with a SI < 3 were described as MET activators (Figure 3.4).

The most potent MET activators from this series were analogs **1**, **2**, **15**, and **16** (Table 3.1, and Figure 3.4) inducing >9-fold increase in E-cadherin compared to DMSO (vehicle) and increasing % cells with SI < 3 by greater than 50%. Based on the primary endpoints of E-cadherin induction and spindle index, analogs **1** and **15** showed the best profile in increasing E-cadherin (10.5 and 9.1 fold increase, respectively vs. **1** with DMSO), percentage of cells with SI < 3 (85.9 and 86.3%, respectively vs. 30.5% with DMSO), and decreasing SI (2.2 and 1.9 fold, respectively vs. 4.2 with DMSO). Similar to diphenylamine analogs, tolfenamic acid and thyroid hormones contain two aromatic rings connected by a single heteroatom. Therefore, these compounds were evaluated for E-cadherin expression and cell morphology. There was no increase in E-cadherin after treatment with NSAIDS or decrease in cell viability (Figure 3.5). The morphology of cells after treatment with the diphenylamine analogs is shown in Figure 3.6.

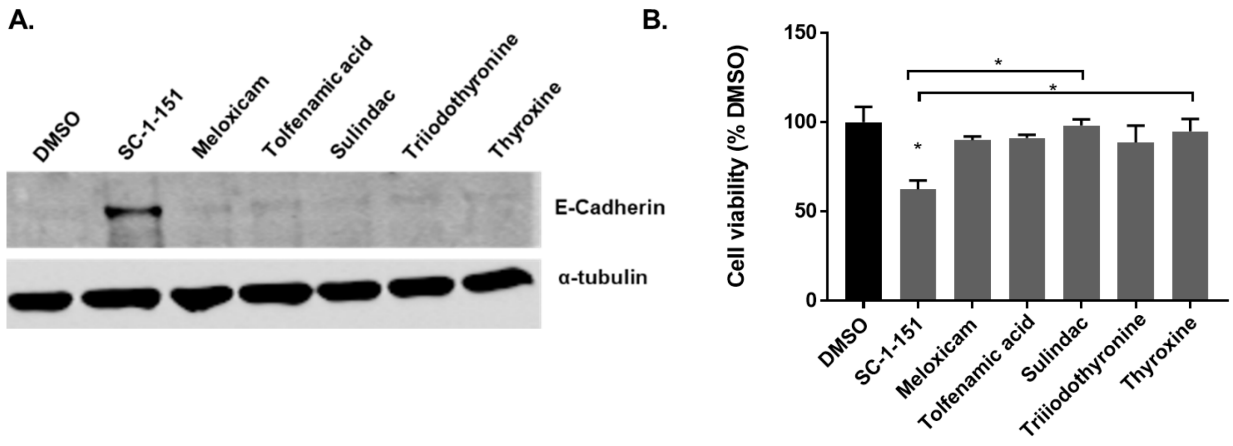

Figure 3.5 NSAIDS and thyroid hormones do not induce MET in MDA-MB-231 cells **(A)** E-Cadherin expression did not increase after treatment with NSAIDS. The compounds were treated for 5 days at 1μM concentration. **(B.)** NSAIDS did not inhibit cell viability. Data represent the ± SEM of three different experiments. *P<0.05 vs control group determined by one-way ANOVA with the Bonferroni post hoc test.

Analogs 1, 2, 15 and 16 were further tested in spheroid viability assays. Analog **18** was included as a negative control. EMT can cause resistance to anchorage-independent death "anoikis," and increase in spheroid-forming ability.[97] To evaluate the effect of diphenylamines on spheroid formation, MDA-MB-231 cells were grown in ultra-low-attachment plates (Figure 3.7A). Compound **1** significantly decreased spheroid viability compared to DMSO, compound **15,** and compound **18** (Figure 3.7A and B). Therefore, we concluded that compound **1** was the best in-series and the effects of compound **1** were evaluated on cell migration and proliferation.

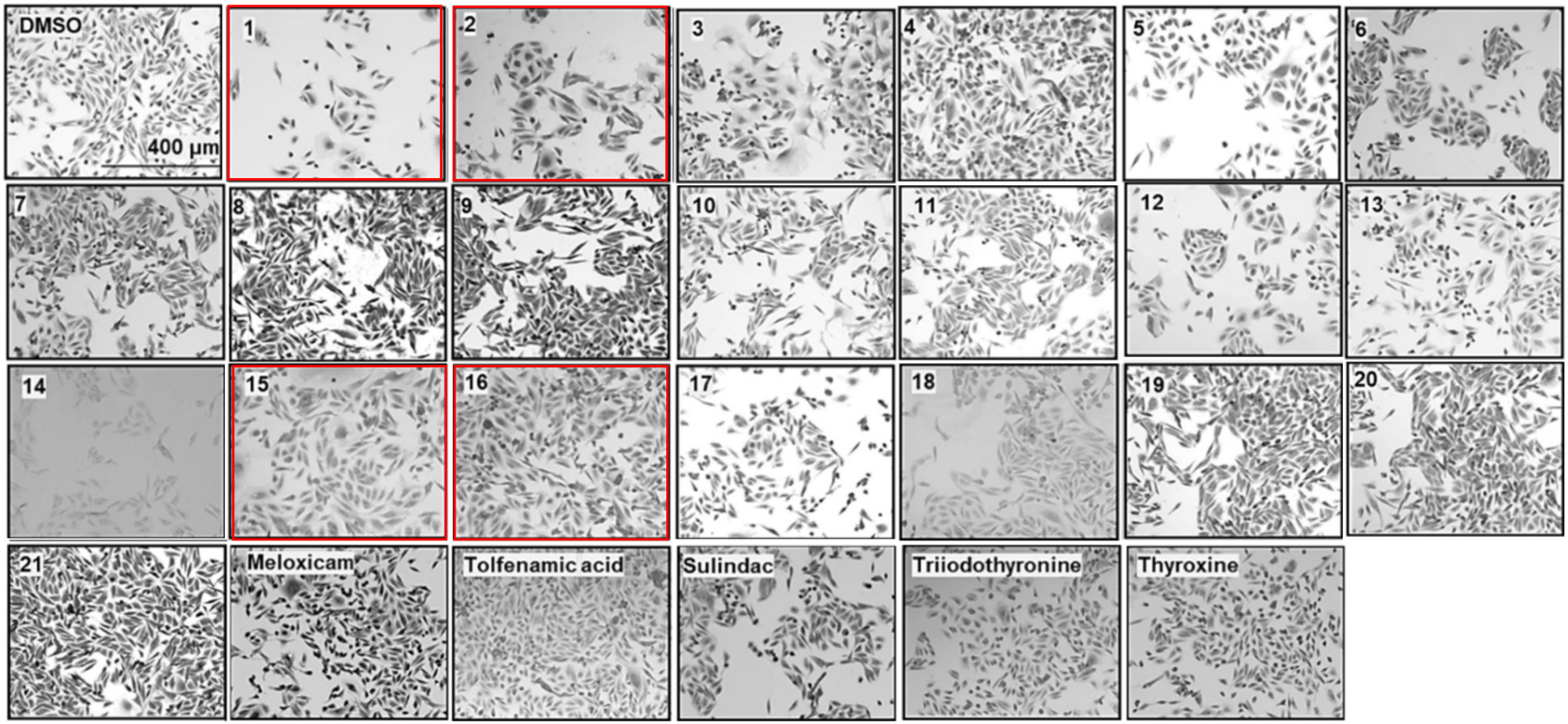

Figure 3.6. MDA-MB-231 cell morphology after treatment with diphenylamine analogs. MDA-MB-231 cells were treated with 1 µM compound or vehicle for 5 days. Crystal violet staining was performed. Images were taken to examine cell morphology.

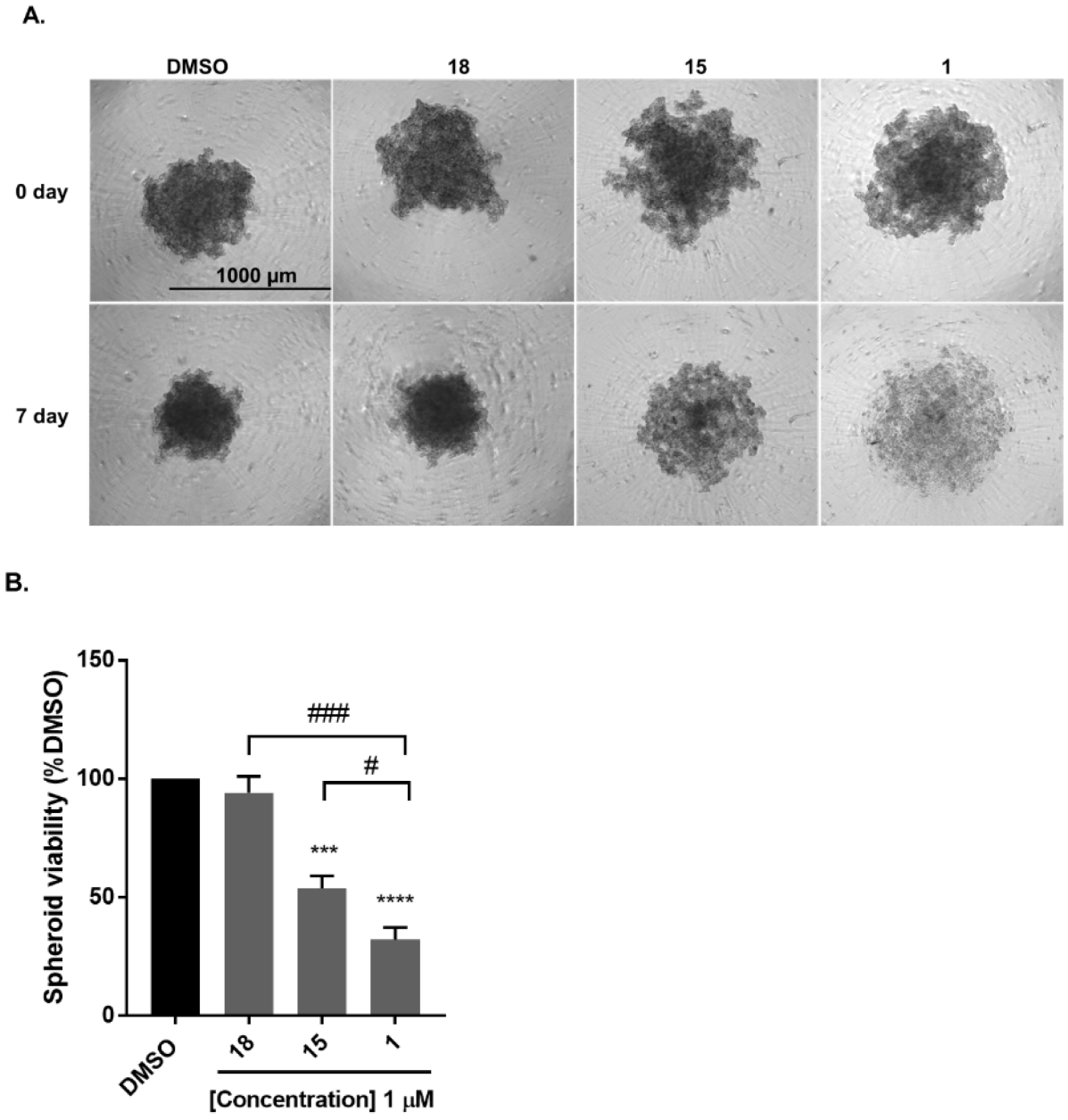

Figure 3.7. Compounds 1 and 15 decrease spheroid viability in MDA-MB-231 cells. (A) Spheroid formation in MDA-MB-231 cells after treatment with DMSO or compounds 18, 15, and 1 for 7 days of treatment. (B) Quantification of the spheroid viability in MDA-MB-231 cells, values indicate ± SEM of three experiments run in triplicate. ***$p < 0.001$, ****$p < 0.0001$ vs. control group, ###$p < 0.001$ compound 1 vs. compound 18 #$p < 0.05$ compound 1 vs. compound 15 determined by one-way ANOVA with the Bonferroni *post hoc* test in MDA-MB-231 cells.

3.3.4 Compound 1 increases E-cadherin and decreases mesenchymal markers in TNBC and TAMR cells

Next, we wanted to examine the effect of the lead compound on more EMT markers, models, and in functional assays. We included another TNBC cell line BT-549 and TAMR MCF-7 cells with a mesenchymal phenotype. When compared to the epithelial phenotype of parental MCF-7 cells, TAMR MCF-7 cells do not express E-cadherin (Figure 3.8). These observations were consistent with previous studies, which have shown that tamoxifen resistance leads to EMT in MCF-7 cells.[98-99] MDA-MB-231, BT-549, and TAMR MCF-7 cells were treated with compound 1 (Figure 3.9) for 5 days and the lysates were collected for western blotting. EMT markers, including the epithelial marker E-cadherin, a downstream target of ERK5, fos-related antigen (FRA-1), and mesenchymal markers ZEB1, vimentin, and snail were evaluated in TNBC and TAMR MCF-7 cells. Compound **1** attenuated the expression of vimentin and stemness marker SOX2 in cells that underwent MET (Figure 3.9B-C).

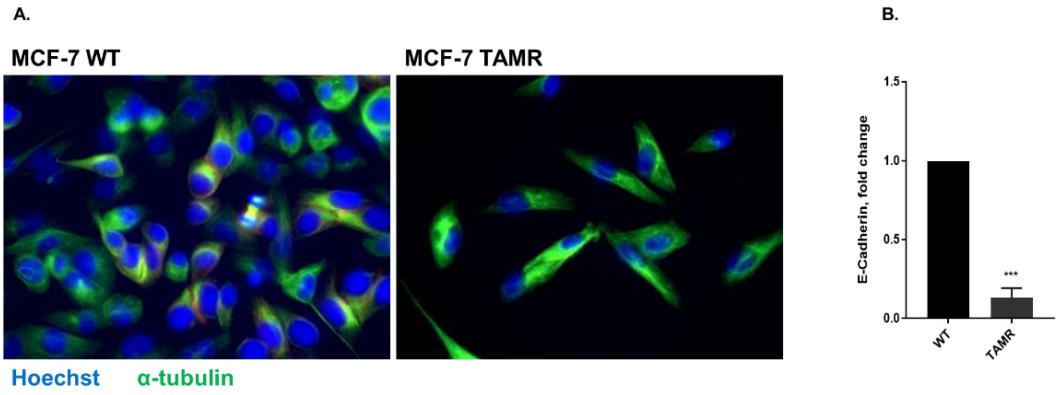

Figure 3.8. Tamoxifen resistance is associated with EMT in ER+ MCF-7 cells. (A) Cell morphology of WT and TAMR MCF-7 cells. (B) E-cadherin expression in TAMR MCF-7 is significantly decreased compared to WT MCF-7 cells.

Compound **1** increased E-cadherin expression, decreased ZEB1, Snail, and FRA-1 activation in MDA-MB-231, BT-549, and TAMR MCF-7 cells (Figure 3.9A). Compound 1 decreased vimentin expression in MDA-MB-231 and TAMR MCF-7 cells, but not in BT-549 cells.

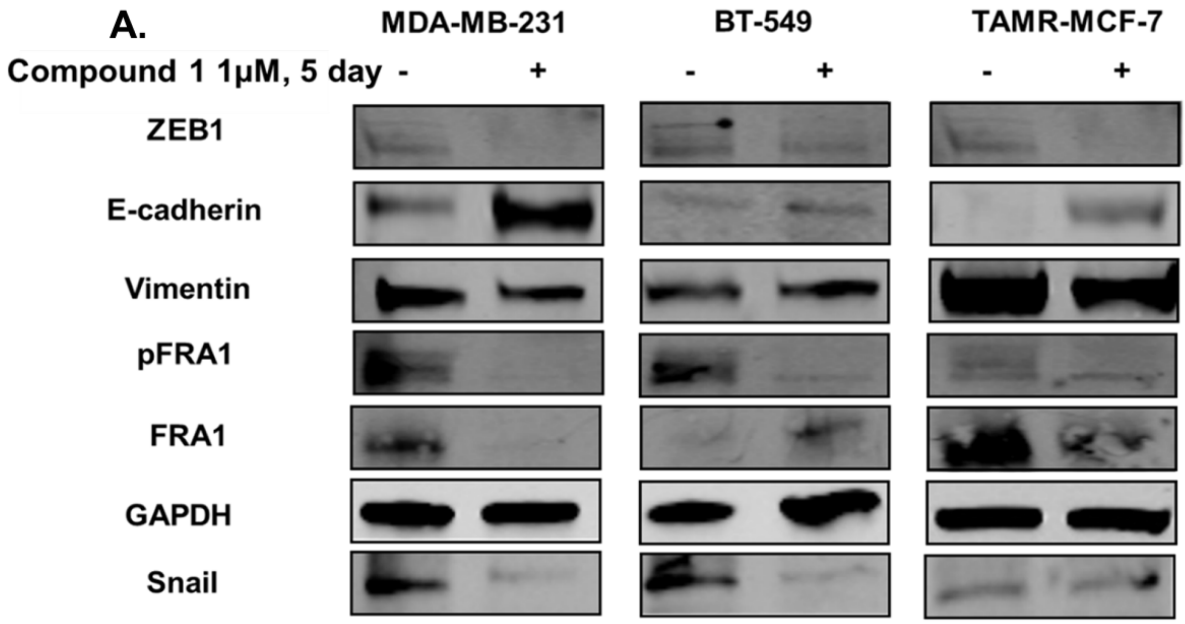

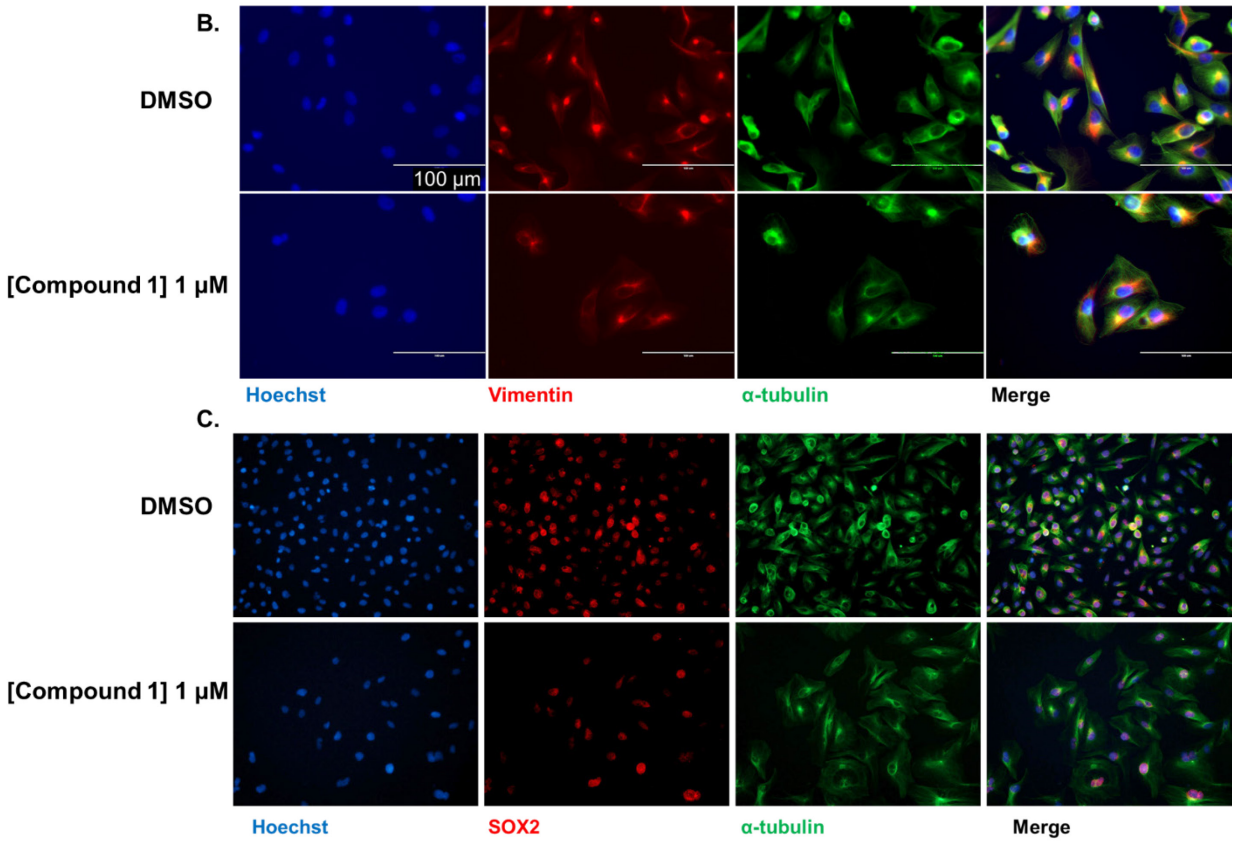

Figure 3.9. Compound 1 decreases mesenchymal markers and increases E-cadherin expression in breast cancer cells (A) Compound 1 decreases EMT markers, FRA-1 activation, and induces E-cadherin in TNBC and TAMR MCF-7 cells. **(B)** Compound **1** attenuates vimentin expression in MDA-MB-231 cells. **(C)** Compound **1** attenuates SOX2 expression in MDA-MB-231 cells.

3.3.5 Lead compound 1 decreases cell migration, colony formation, and cell proliferation in MDA-MB-231 cells.

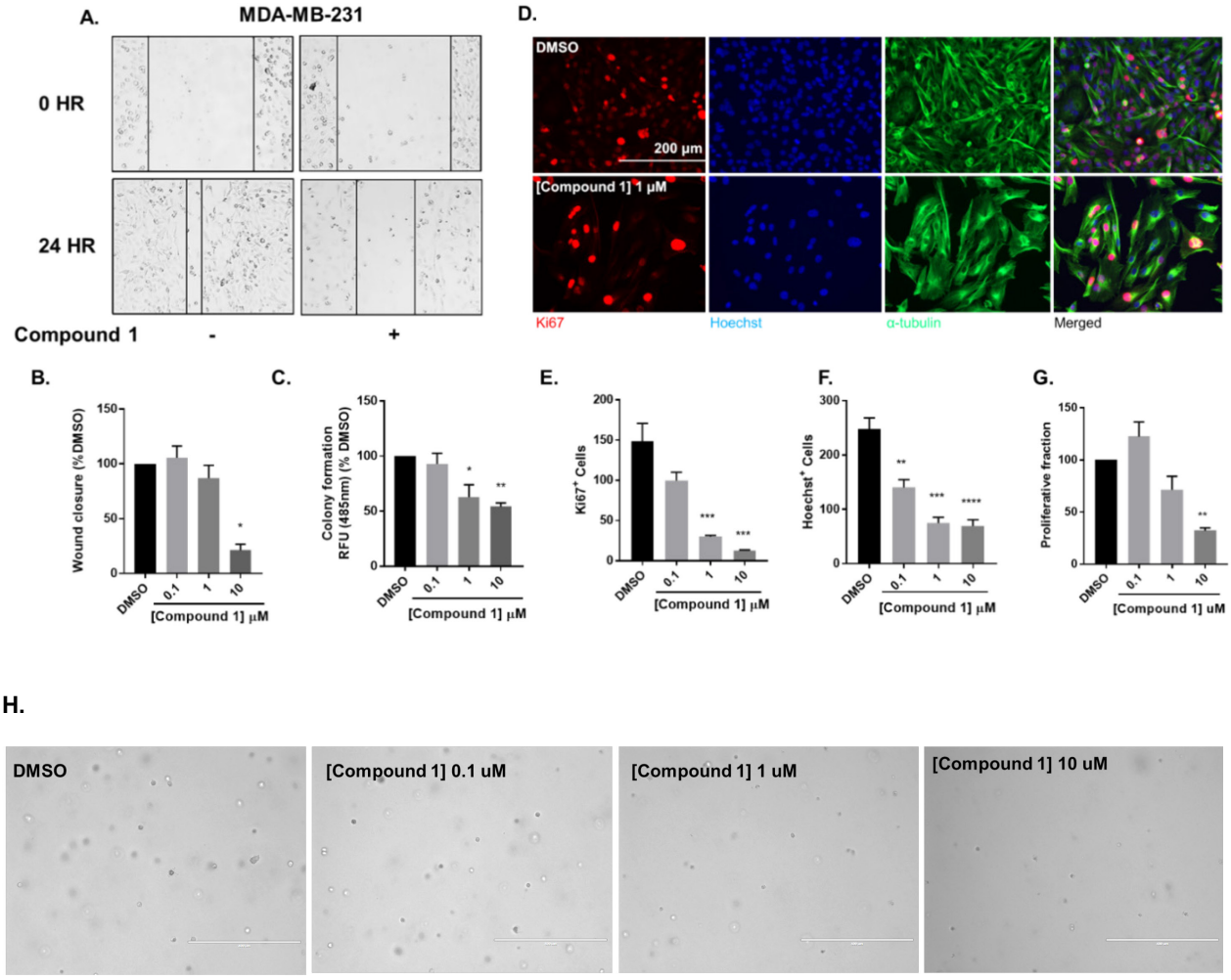

Figure 3.10. Compound 1 decreases cell migration, colony formation, and cell proliferation in MDA-MB-231 cells. (A, B) Wound closure was measured as a percentage of untreated DMSO control group. *p < 0.05 vs. DMSO control group determined by one-way ANOVA with the Bonferroni *post hoc* test. (C) Compound **1** inhibited MDA-MB-231 colony formation after 14 days of treatment in a concentration-dependent manner. Data represent ± SEM of experiments run in triplicate, *p < 0.05; **p < 0.01 vs. DMSO control group determined by one-way ANOVA with the Bonferroni *post hoc* test. (D) Immunofluorescence staining of Ki67, Hoechst, and a-tubulin in MDA-MB-231 cells treated with DMSO or compound 1 (1µM), for 72 hours, scale bar 200µm. (E) Ki67+ cells decreased with increasing concentrations of compound 1. (F) Decrease in Hoechst+ cells with increasing concentrations (0.1, 1, 10µM) of compound 1. (G) The proliferative fraction calculated as the ratio of Ki67+ cells to Hoechst+ cells at increasing concentration. Data represent ± SEM of three different experiments. **p < 0.01; ***p < 0.001 vs. control group determined by one-way ANOVA with the Bonferroni *post hoc* test. (H) Pictures of colonies after treatment with DMSO or Compound **1.**

Treatment with compound **1** produced a concentration-dependent reduction in cell migration (Figure 3.10A-B), and colony formation (Figure 3.10C) in MDA-MB-231 cells. Immunofluorescence staining for Ki67 and Hoechst was performed to evaluate cell proliferation in MDA-MB-231 cells. Compound **1** significantly decreased the number of Ki67+ and Hoechst+ cells (Figure 3.10D-E) and the proliferative fraction determined as the number of Ki67+/ number of Hoechst+ cells (Figure 3.10F). The effects of compound **1** were also evaluated on spheroid formation, cell migration, and proliferation in BT-549 TNBC cells and TAMR MCF-7 ER+ breast cancer cells.

3.3.6 Compound 1 inhibits spheroid formation, cell migration, and proliferation in BT-549 and TAMR-MCF-7 cells.

BT-549 and TAMR-MCF-7 cells were treated with 0.1, 1, and 10 μM concentrations of compound **1**. Compound 1 produced a concentration-dependent decrease in spheroid viability after 7 days in BT-549 cells (Figure 3.11A-B) and TAMR MCF-7 cells (Figures 3.11C-D). At 1 μM concentration, compound 1 decreased spheroid viability by 51.55 and 72.91% in BT-549 and TAMR MCF-7 cells, respectively. Compound **1** produced a concentration-dependent decrease in cell migration and proliferation in BT-549 cells (Figures 3.12A and C). There was a 67.9% reduction in cell proliferation at 10μM concentration in BT-549 cells.

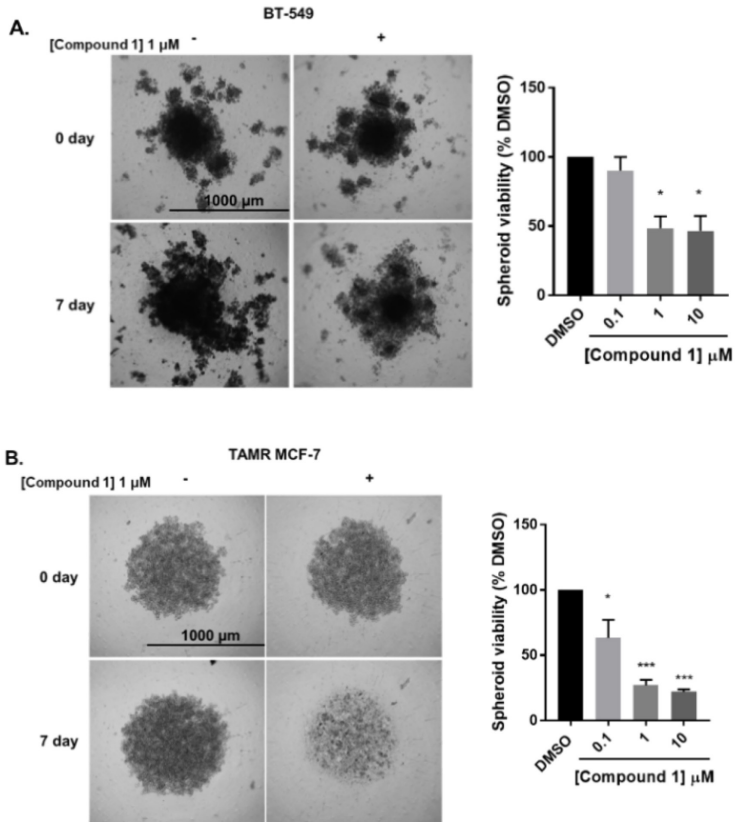

Figure 3.11. Compound 1 inhibits spheroid viability in BT-549 and TAMR MCF-7 cells. (A) Spheroid formation in BT-549 cells after treatment with DMSO or compound 1 at 1µM concentration for 7 days, scale bar 1,000µm. (B) Quantification of the spheroid viability in BT-549 cells after treatment with compound 1 at increasing concentrations (0.1, 1, 10 µM) after 7 days of treatment, data represents ± SEM $*p < 0.05$; $***p < 0.001$ vs. control group determined by one-way ANOVA with the Bonferroni *post hoc* test in BT-549 cells. (C) Spheroid formation in TAMR MCF-7 after treatment with DMSO or compound 1 at 1µM concentration for 7 days, cells scale bar 1,000µm. (D) Quantification of the spheroid viability after treatment with compound 1 at increasing concentrations (0.1, 1, 10 µM) after 7 days of treatment in TAMR MCF-7 cells, values indicate ± SEM of three experiments run in triplicate. $*p < 0.05$; ***p < 0.001 vs. control group determined by one-way ANOVA with the Bonferroni *post hoc* test.

In TAMR MCF-7 cells, compound **1** produced a concentration-dependent decrease in cell migration (Figure 3.13A-B). Additionally, treatment with compound 1 significantly decreased the number of Ki67+ (Figure 3.13D) and Hoechst+ (Figure 3.13E) cells. There was 79.7% decrease in the proliferative fraction at 1 µM (Figure 3.13F).

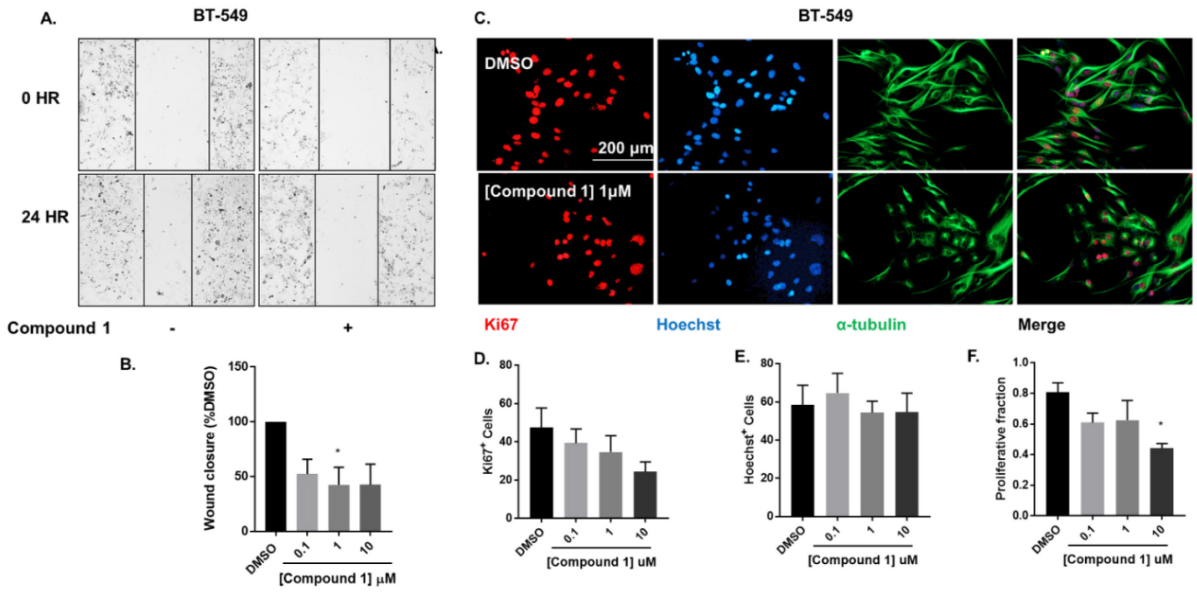

Figure 3.12. Compound 1 inhibits cell migration and proliferation in BT-549 cells. (A) Wound closure was measured after treatment with increasing concentrations (0.1, 1, 10μM) of compound 1. The data is presented as a percentage of untreated DMSO control group. *p < 0.05 vs. control group determined by one-way ANOVA with the Bonferroni *post hoc* test (BT-549 cells). Compound 1 inhibits cell proliferation in BT-549. (C) Immunofluorescence staining of Ki67, Hoechst, and a-tubulin in BT-549 cells treated with DMSO or compound 1 (1μM), for 72 hours, scale bar 200μm. (B) Ki67+ cells decreased with increasing concentrations (0.1, 1, 10μM) of compound 1. (C) Decrease in Hoechst+ cells with increasing concentrations (0.1, 1, 10μM) of compound 1. (D-F) The proliferative fraction calculated as the ratio of Ki67+ cells to Hoechst+ cells at increasing concentrations (0.1, 1, 10μM) of compound 1. Data represent ± SEM of three different experiments. *p < 0.05 vs. control group determined by one-way ANOVA with the Bonferroni *post hoc* test.

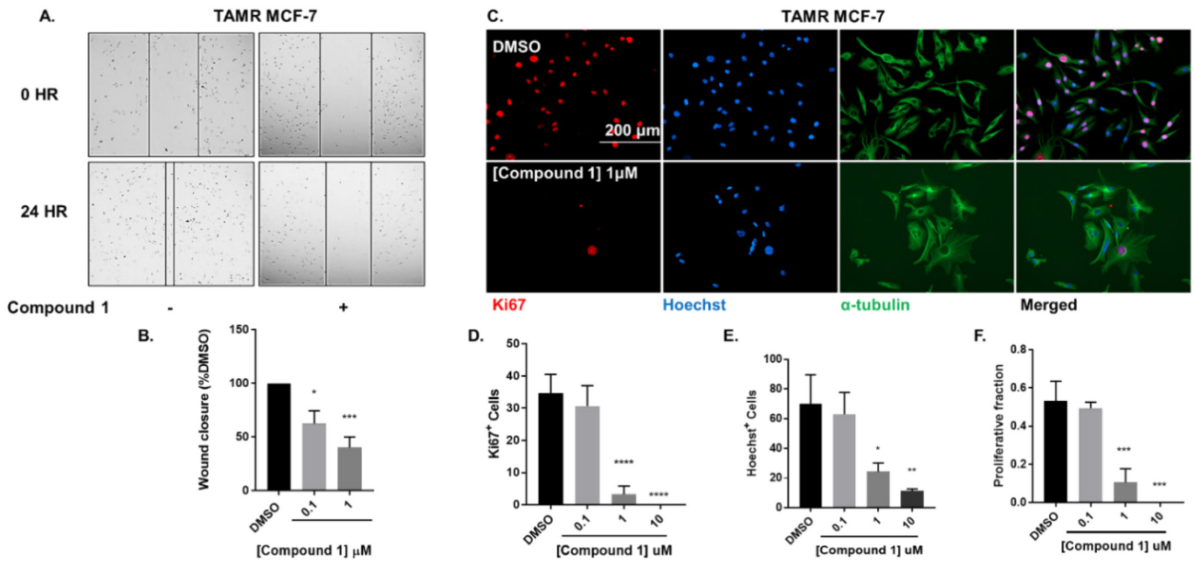

Figure 3.13. Compound 1 inhibits cell migration and proliferation in TAMR MCF-7 cells. (A) Wound closure was measured after treatment with increasing concentrations (0.1, 1, 10μM) of compound 1. The data is presented as a percentage of DMSO control group. *$p < 0.05$; ***$p < 0.001$ vs. control group determined by one-way ANOVA with the Bonferroni *post hoc* test (TAMR MCF-7 cells). Compound 1 inhibits cell proliferation in TAMR MCF-7 cells (C) Immunofluorescence staining of Ki67, Hoechst, and a-tubulin in TAMR MCF-7 cells treated with DMSO or compound 1 (1 μM), for 72 hours, scale bar 200 μm. (D) Ki67+ cells decreased with increasing concentrations (0.1, 1, 10 μM) of compound 1. (E) Decrease in Hoechst+ cells with increasing concentrations (0.1, 1, 10 μM) of compound 1. (TAMR MCF-7 cells) (F) The proliferative fraction calculated as the ratio of Ki67+ cells to Hoechst+ cells at increasing concentrations (0.1, 1, 10 μM) of compound 1 (TAMR MCF-7 cells). Data represent ± SEM of three different experiments. *$p < 0.05$; **$p < 0.01$; ***$p < 0.001$; ****$p < 0.0001$ vs. control group determined by one-way ANOVA with the Bonferroni *post hoc* test.

3.4 Discussion

Our findings suggest that at the R1 position the diphenylamine core, amides (primary, secondary, and tertiary) induced E-cadherin to a greater fold compared to ester (**6**) or acid (**7**). The R1 position showed tolerance toward steric bulk and charge. At R2 and R3, the removal of both fluoro groups reduced the E-cadherin expression by 3.5 fold (**8** vs. **1**). We speculate that the electron-withdrawing fluorine atoms either polarize the arene 1 ring, potentiating its interactions with its biological target (p- p stacking

interactions and/or ion-dipole interactions) or the fluorine atom may act as hydrogen bond acceptor (HBA) (32). At R4 position, the replacement of the hydrogen atom (**1**) with a methyl group (**9**), led to a 4-fold reduction in E-cadherin expression. These data suggest that the R4 hydrogen participates in an intramolecular hydrogen bond with the carbonyl group attached to R1, forming a conformation favoring MET. The N-methyl group of analog **9** may disrupt the intramolecular hydrogen bond, leading to the corresponding decrease in E-cadherin expression.

By substituting the fluorine at R5 and iodine at R6 with hydrogen atoms, there was no increase in E-cadherin expression (analog **10** vs. **1**). We speculate that the fluoro group at R5 may: a) decrease the pKa of the R4 hydrogen making it a better hydrogen bond donor to facilitate MET induction, and/or b) increase the lipophilicity of the molecule; improving hydrophobic interactions with the biological target(s) (33, 34).

The iodo group at R6 is a large group, which can undergo hydrophobic interactions and/or can form a halogen bond. At R7 position all the three analogs (**19- 21**) were inactive in inducing MET. An important contributing factor could be that these compounds do not have any substitutions at R5 and R6 positions. Moreover, they did not possess a free NH2 group at R1, which may contribute to their inability to induce MET. Overall, our initial structure-activity study suggests that different substitutions at R1 are tolerated and this position can be exploited toward improving potency or deducing the molecular target of diphenylamines. Removal/change of substituents at R2-R7 positions are not tolerated. Therefore, they may represent the minimum pharmacophore required for MET activity. There was a positive correlation between increase in E-cadherin expression and the percentage of cells with SI < 3, which strengthens the structure-activity relationship. This

also suggests that spindle index measurement could be a reliable quantitative analysis for cells that undergo morphological transitions.

NSAIDS (tolfenamic acid, sulindac, and meloxicam) and thyroid hormones (triiodothyronine and thyroxine) bear structural similarity to the diphenylamine compounds, but they did not induce MET in MDA-MB-231 cells (Figure 3.5). One reason could be both NSAIDs and thyroid hormones do not have the minimum pharmacophore required for inducing MET. Also, the in-house diphenylamines inhibit MEK1/2 and MEK5; since the biological targets of the two drug classes under study are different, this may explain why NSAIDS and thyroid hormones did not induce MET.

MDA-MB-231 cells cultured in low-attachment plates were examined to determine the effect of compounds **1**, **15**, and **18** on spheroid formation. The selection of compounds was made based on their ability to induce MET: low (compound **18)**—high (compounds **1** and **15)** and differences in their structures (primary vs. tertiary amides at R1). Two-way ANOVA with Bonferroni post-hoc test revealed that compound **1** was the most effective in inhibiting spheroid growth. One of the reasons why compound **1** was more effective is because compound **1** is a dual MEK1/2 and MEK5 inhibitor, but compounds **15** and **18** inhibit MEK1/2 and MEK5, respectively.[83] Therefore, the effects of compound **1** were examined on cell migration and proliferation. Moreover, the effect of compound **1** was characterized in two additional breast cancer cell models, which have a mesenchymal phenotype: TNBC cell line BT-549 and tamoxifen-resistant MCF-7 cell line.

Since EMT triggers cell migration and motility, the scratch assay/ wound closure assay was performed to examine cell migration. Cells at the border of the wound are known to be enriched in pathways involved in cell migration and not proliferation.[86] Cells

that undergo MET may re-acquire the proliferative potential to promote metastatic colonization.[100] Therefore, we examined the effect of compound **1** on cell proliferation. Compound **1** significantly decreased cell migration and proliferation in diverse breast cancer models. Compound **1** also decreased spheroid formation in MDA-MB-231, BT-549 TNBC, and TAMR MCF-7 cells including spheroid formation, cell migration, and cell proliferation. In summary, to our knowledge, this is the first time that novel inhibitors of MEK1/2 and/or MEK5 pathways were examined to influence EMT reversal in triple-negative and tamoxifen resistant breast cancers. Compound 1, a novel dual MEK1/2 and MEK5 inhibitor was effective in inducing MET in diverse breast cancer subtypes, decreasing proliferation, migration, and spheroid formation.

In conclusion, EMT is a crucial process for cancer progression and metastases. Therefore, a reversal of the EMT to induce an MET may decrease metastases to allow targeting of the less aggressive epithelial cancer cells in situ. Through analog-based drug design, analogs that potentiate MET were discovered. Compound **1** was identified as the lead, as treatment with this compound increased E-cadherin expression and caused morphological change from mesenchymal to epithelial phenotype. Moreover, compound **1** attenuated the migratory and proliferative properties of TN and TAMR breast cancer cells. In the next chapters, we will discuss about independent and overlapping functions of ERK1/2 and ERK5 pathways on EMT/MET, nuclear localization of ERK, and migration, proliferation, and spheroid formation. Moreover, several combination strategies of compound **1** with AKT or epigenetic inhibitors will be discussed.

Chapter 4: Targeting the ERK5 and/or ERK1/2 pathways reverses EMT, decreases proliferation, migration, and spheroid formation in triple-negative and tamoxifen-resistant breast cancer cells

4.1 Introduction

Metastases account for ~90% of cancer related human deaths.[101] An increasing body of evidence suggests that activation of ERK1/2 and ERK5 signaling is a marker for node metastases and a predictor of poor responses to hormone therapy such as 4-OHT.[102-104] Moreover, activation of intracellular signaling pathways, such as the ERK MAPK pathways, has been shown to mediate tumorigenesis in TNBCs and tamoxifen resistant breast cancers.[105-106] For example, ERK1/2 activation is known to mediate EMT in several cancer models[18, 92, 107-108], and overexpression of the newest member of the MAPK family, ERK5, induces EMT and hormone-independent growth of breast cancer.[104] Although activation of the ERK1/2 and ERK5 pathways have been shown to mediate EMT, the effect of ERK1/2 and ERK5 inhibition on inducing MET, the reverse of EMT, is poorly understood in cancer.

To identify the link between MAPK pathways and EMT, MAPK3 (ERK1), MAPK1(ERK2), and MAPK7 (ERK5) gene expression was correlated with EMT markers CDH1, ZEB1, or VIM in tumors derived from TNBC patients using publicly available datasets. Additionally, overall survival in patients with inflammatory breast cancer was plotted against ERK1, ERK2, or ERK5 gene expression using publicly available datasets. TNBCs account for about 40% of all inflammatory breast cancers.[109]

We hypothesize that inhibition of the ERK1/2 and ERK5 pathways is a relevant strategy to induce a MET in TNBCs. To test this hypothesis, we examined the effects the

ERK1/2 and ERK5 pathways on the MET using pharmacological inhibitors of MEK1/2 and ERK5, trametinib and XMD8-92, respectively. Since the location-specific roles of ERK1/2 and ERK5 with respect to EMT are less well-understood, we examined the effect of XMD8-92 and trametinib on nuclear localization of ERK1/2 and ERK5. To validate the inhibitor data, the effect of lentivirus-mediated activation or inhibition of ERK1/2 and ERK5 pathway components on the MET was examined. Cell morphology and protein expression of epithelial and mesenchymal markers, E-cadherin and ZEB1 were examined and activation of ERK1/2, ERK5, and RSK, a downstream target of MAPK signaling, were evaluated. The effects of XMD8-92 and trametinib were evaluated on cell migration and cell proliferation in MDA-MB-231, BT-549 TNBC cells, and tamoxifen-resistant (TAMR) MCF-7 breast cancer cells. Moreover, TU-BcX-4IC patient-derived primary TNBC cells were included to enhance the translational relevance of our study.

4.2 Hypothesis

Inhibition of ERK1/2 and/or ERK5 pathways will induce MET and decrease cell migration, proliferation, and spheroid formation in TNBC and TAMR breast cancer cells.

4.3 Results

4.3.1 ERK1, ERK2, and ERK5 expression correlates with EMT markers and is associated with poor patient survival in breast cancer

Since the effect of ERK1/2 and ERK5 pathways on EMT is less well-understood in TNBCs, we first used publicly available datasets from Purrington, K. S. and colleagues[110] to correlate MAPK3 (ERK1), MAPK1 (ERK2), or MAPK7 (ERK5) gene expression with EMT markers CDH1 (E-cadherin), ZEB1, or vimentin in primary, invasive tumors derived

from African-American TNBC patients (Figure 4.1). There was a moderate to strong correlation between MAPK3, MAPK1, and MAPK7 with mesenchymal markers ZEB1 and vimentin. Using Kaplan-Meier survival analysis to examine the relationship between ERK1/2/5 expression and patient survival in inflammatory breast cancer (public datasets from Bertucci et al.[109]), MAPK3, MAPK1, or MAPK7 gene expression were found to be associated with poor patient survival (Figure 4.2). Overall, these data suggest that ERK1, ERK2, and ERK5 may be important therapeutic targets in breast cancer.

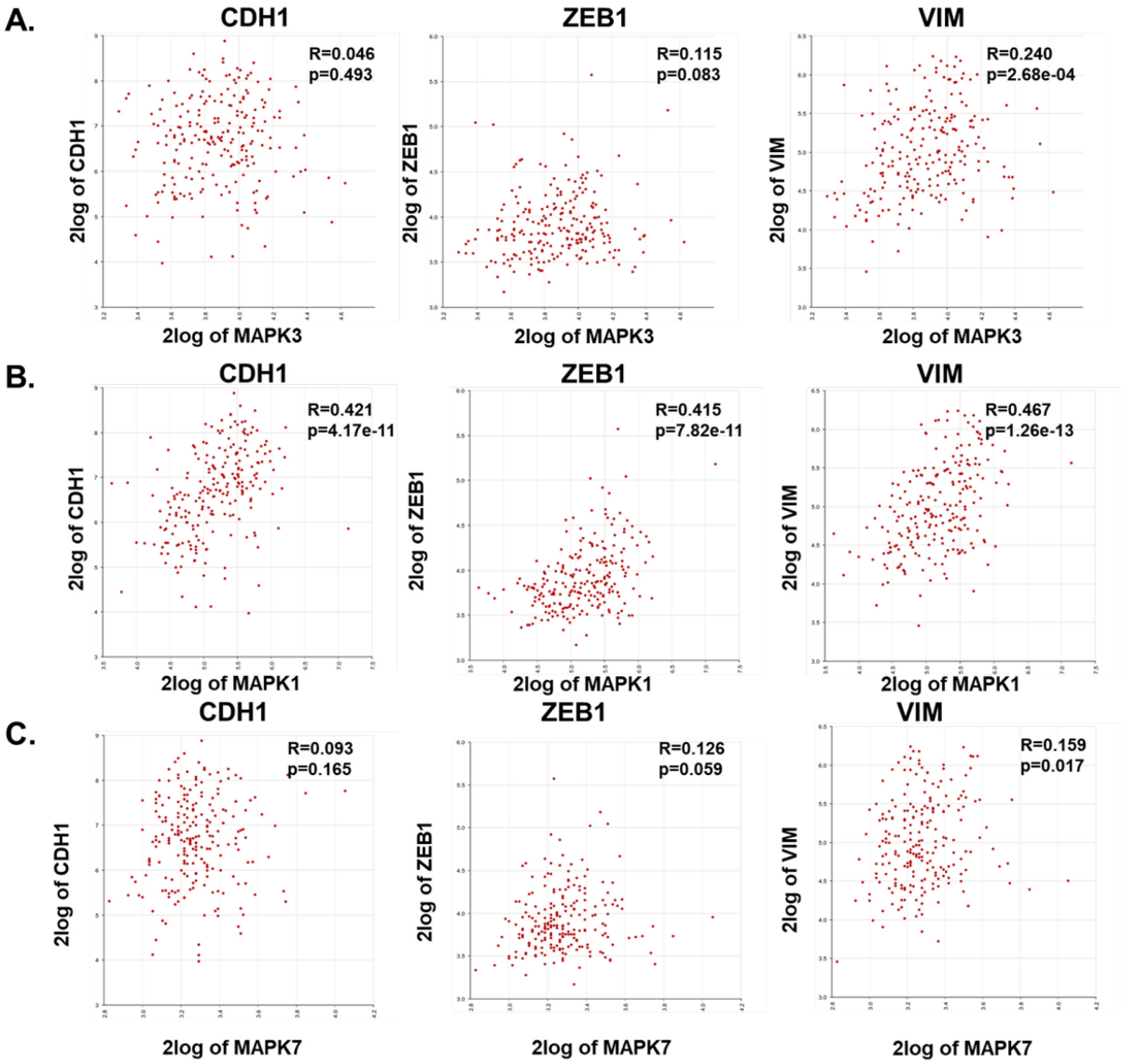

Figure 4.1 Correlation of ERK1, ERK2, or ERK5 with EMT markers in tumors derived from TNBC patients. Gene correlation between **(A)** MAPK3(ERK1), **(B)** MAPK1(ERK2), or **(C)** MAPK7 (ERK5) and EMT markers CDH1, ZEB1, or VIM was plotted using R2: Genomics analysis and visualization platform (https://hgserver1.amc.nl/cgi-bin/r2/main.cgi). Datasets were exported from Tumor Breast (triple negative) - Purrington - 226 - rma_sketch - hugene21t.

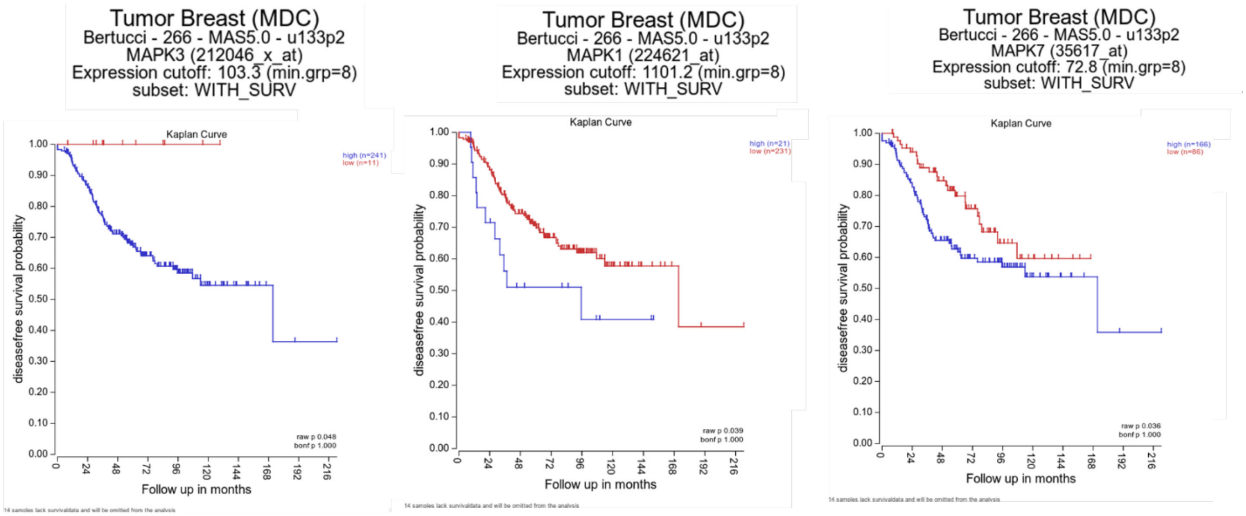

Figure 4.2 MAPK3, MAPK1, and MAPK7 expression correlates with poor patient survival in breast cancer. Disease free survival was analyzed using R2: Genomics analysis and visualization platform (https://hgserver1.amc.nl/cgi-bin/r2/main.cgi). Datasets were exported from Tumor Breast (MDC) Bertucci - 266 - MAS5.0 - u133p2.

4.3.2 Pharmacological inhibition of the ERK1/2 and/or ERK5 pathways induces MET in TNBC and TAMR breast cancer

Since ERK1, ERK2, and ERK5 were identified as important targets in breast cancer and their gene expression was found to correlate with EMT markers, pharmacological inhibitors of these pathways were utilized to examine their effect on MET, the reverse of EMT. MDA-MB-231, BT-549, TU-BcX-4IC TNBC, and TAMR cells were treated with increasing concentrations of XMD8-92, an ERK5 and BRD4 inhibitor, and trametinib, a MEK1/2 inhibitor, for 72 hours. Following treatment with the inhibitors,

the morphology of the breast cancer cells was examined. Trametinib induced a morphological switch from mesenchymal to epithelial in all the cell lines, while XMD8-92 only induced this morphological change in MDA-MB-231 cells (Figures 4.3).

To confirm the morphological switch, we examined the expression of the epithelial and mesenchymal markers, E-cadherin and ZEB-1, respectively. Trametinib increased E-cadherin expression in MDA-MB-231, BT-549, TU-BcX-4IC, and TAMR cells and decreased ZEB-1 expression in MDA-MB-231 and TU-BcX-4IC cells. XMD8-92 (10uM) decreased the expression of E-cadherin and ZEB1 only in MDA-MB-231 cells (Figure 4.3A). WT-MCF-7 epithelial cells were included as a control to study EMT. Treatment of the WT-MCF-7 cells with XMD8-92 or trametinib did not alter cell morphology or E-cadherin expression (Figure 4.4A, B). p-P90RSK, a downstream target of MAPK pathway was undetected in WT-MCF-7 cells, indicating that RSK activation may be a major event in regulating EMT associated with tamoxifen-resistance (Figure 4.4C). Cells that undergo EMT may exhibit a complete cadherin switch, which is characterized by a complete loss of E-cadherin; however, partial EMT state is characterized by co-expression of epithelial and mesenchymal markers.[111] The extent of MET induced by the inhibitors was determined by examining the correlation between E-cadherin and ZEB1 expression (Figure 4.5). A greater than 3-fold change in protein expression is indicative of a significant difference. Therefore, treatment that induced E-cadherin expression by greater than 3-fold and decreased ZEB1 by greater than 0.3-fold was determined to induce a full MET, whereas treatment that induced a 3-fold increase in E-cadherin expression or 0.3-fold was determined to induce a partial MET. Trametinib induced a full MET in MDA-MB-

231 and TAMR MCF-7 cells at low and high doses, whereas it induced a partial MET in BT-549 cells (Figure 4.5).

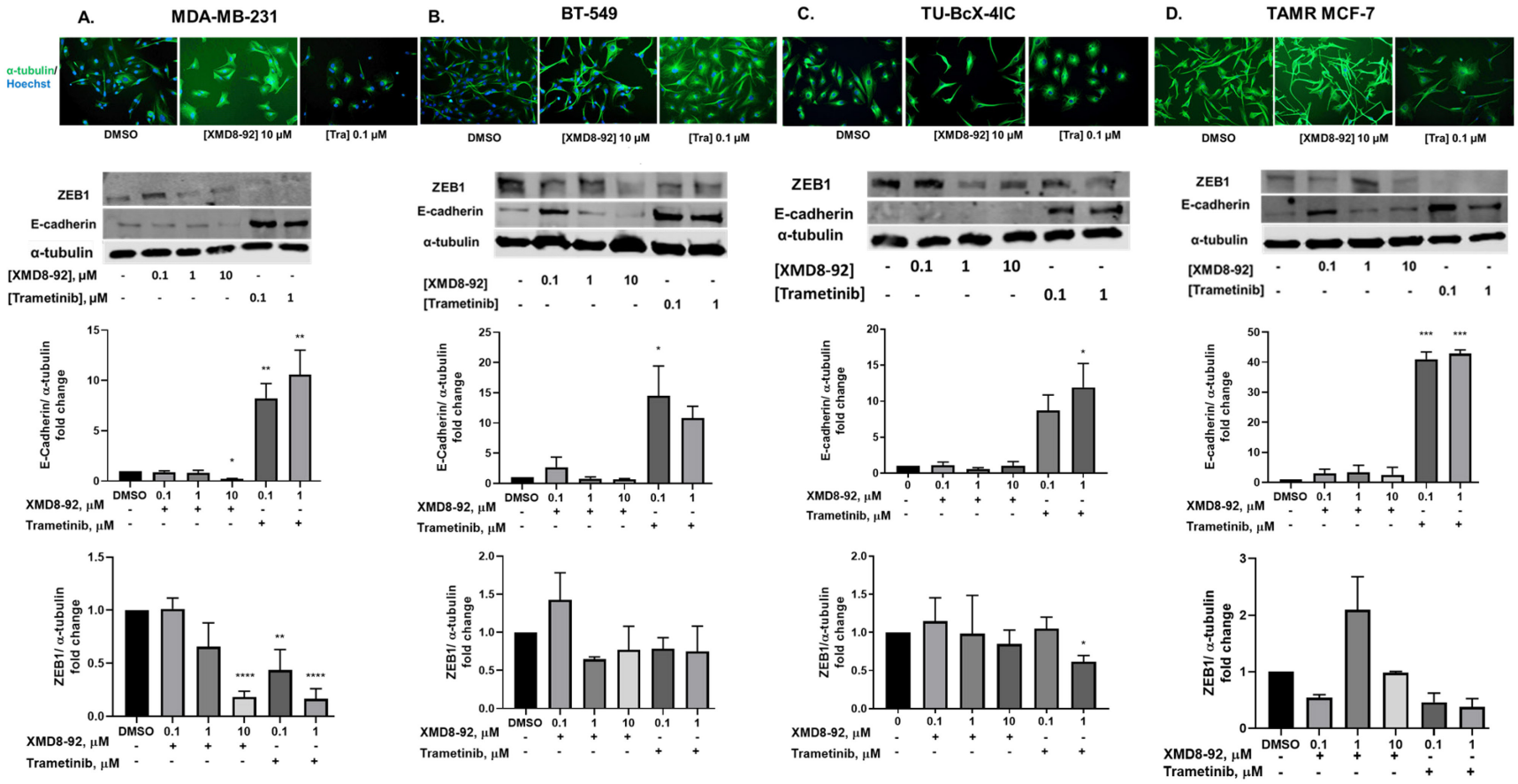

Figure 4.3 ERK1/2 and ERK5 pathway inhibition induces MET in TNBC and TAMR MCF-7 cells. Cells were treated with XMD8-92 and trametinib at increasing concentrations for 72 hours. Cell morphology (20X magnification) and EMT markers E-cadherin and ZEB1 were examined in **(A)** MDA-MB-231, **(B)** BT-549, **(C)** TU-BcX-4IC, and **(D)** TAMR MCF-7 cells. Data represent the ± SEM of three different experiments for each inhibitor compared to DMSO control. *p<0.05; **p<0.01; ***p<0.001; ****p<0.0001 *vs* DMSO control group determined by one-way ANOVA with the Bonferroni post hoc test.

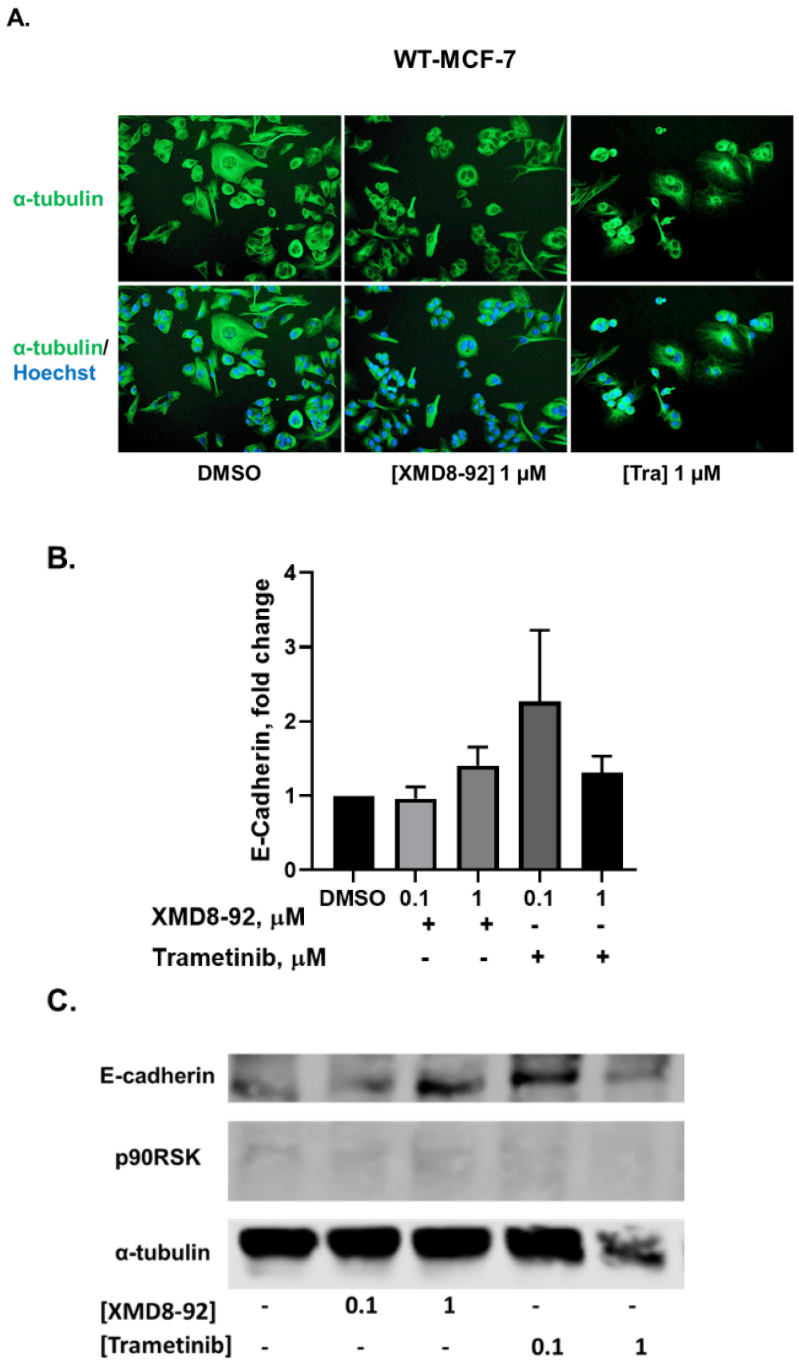

Figure 4.4 Evaluation of cell morphology, E-cadherin and p-P90RSK levels in WT-MCF-7 cells. (A) Kinase inhibitors do not alter the phenotype (20X magnification) or (B) E-cadherin expression in ER+ MCF-7 epithelial cells. (C) p-P90RSK was not detected in WT MCF-7 cells.

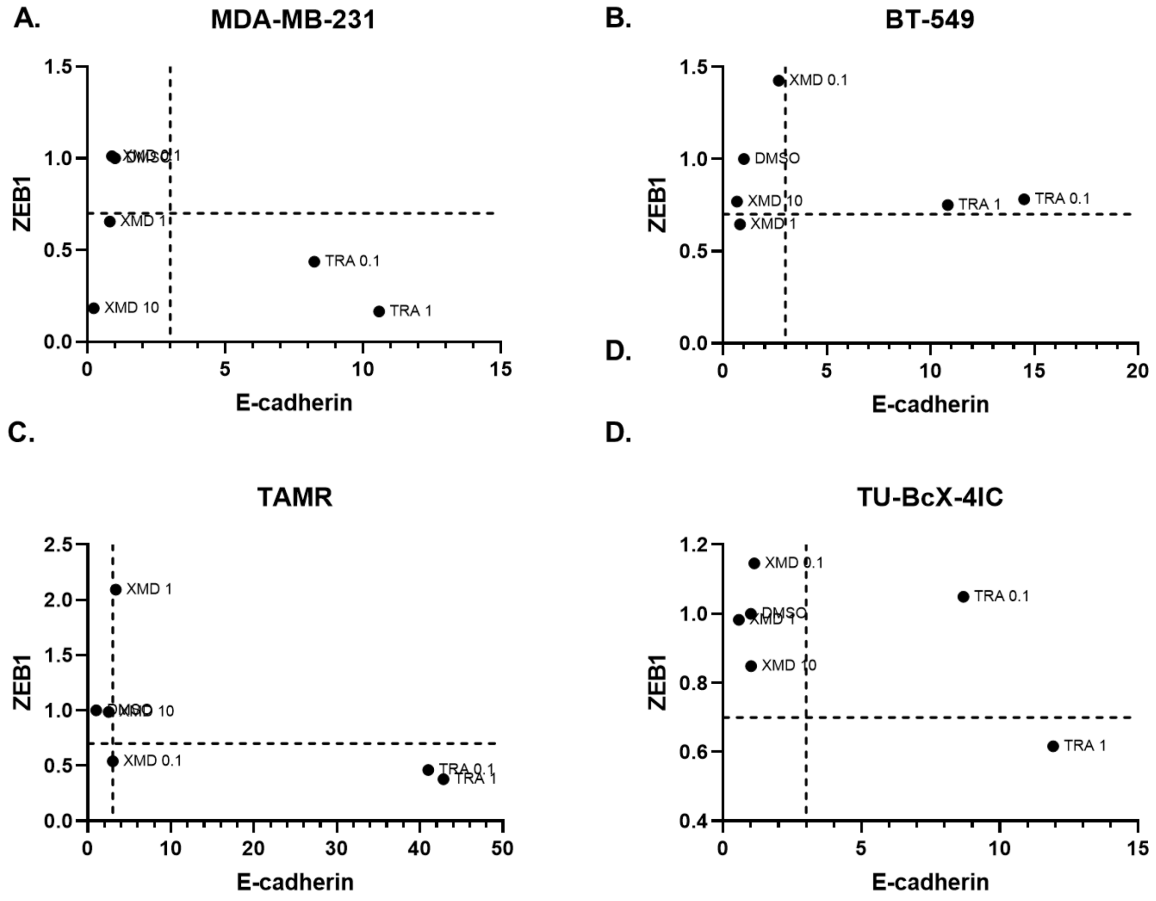

Figure 4.5 Correlation to determine extent of MET induced by trametinib or XMD8-92. (A) MDA-MB-231, **(B)** BT-549, **(C)** TU-BcX-4IC, and **(D)** TAMR MCF-7 cells.

4.3.3 Role of kinases in MET

ERK1/2 and ERK5 pathways are important regulators of EMT. To examine a role for the MAPK pathways in MET, ERK1/2, ERK5, and RSK activation in MDA-MB-231, BT-549, TU-BcX-4IC and TAMR MCF-7 cells were examined after 72 hours of treatment of trametinib or XMD. As expected, trametinib significantly decreased ERK1/2 and RSK phosphorylation in the panel of breast cancer cell lines. Interestingly, trametinib (0.1 μM) decreased ERK5 phosphorylation in MDA-MB-231 cells. XMD8-92 decreased ERK5 phosphorylation in MDA-MB-231 cells by 40% and 65% at 1 and 10 μM concentrations, respectively (Figure 4.6A). In contrast, XMD8-92 did not decrease ERK5 activation in

BT-549, TU-BcX-4IC, and TAMR cells, (Figure 4.6 B, C, D). XMD8-92 decreased RSK phosphorylation by ~ 40% at all concentrations in MDA-MB-231 cells and at the lowest concentration in BT-549 cells. Overall, these findings that ERK1/2 and ERK5 activities are differentially modulated by kinase inhibitors, indicating involvement of crosstalk mechanisms between these pathways in diverse breast cancer models.

Cells were also treated with trametinib and XMD8-92 for shorter time points to determine the effect of the inhibitors on EGF-mediated stimulation of the MAPK pathways. This is a relevant assay to examine specificity of kinase inhibitors. Following serum starvation for 18-24 hours, cells were treated with an inhibitor for 30 minutes, and then with epidermal growth factor (EGF) for 15 minutes. XMD8-92 significantly decreased ERK5 phosphorylation, as compared to DMSO+EGF treatment control in MDA-MB-231 and TAMR MCF-7 cells. Interestingly, in MDA-MB-231 and TAMR-MCF-7 cells, XMD8-92 had the opposite effect on ERK1/2 phosphorylation, such that ERK1/2 phosphorylation was increased in BT-549 cells and decreased in TAMR-MCF-7 cells. In BT-549 and TU-BcX-4IC cells, XMD8-92 did not significantly alter ERK5, ERK1/2, or RSK phosphorylation induced by EGF. As expected, trametinib, a MEK1/2 inhibitor significantly decreased activation of downstream targets of MEK1/2: ERK1/2 and RSK, in a dose-dependent in response to EGF stimulation in BT-549, TU-BcX-4IC, and TAMR MCF-7 cells (Figure 4.7). However, trametinib significantly decreased EGF-mediated ERK1/2, ERK5, and RSK phosphorylation in a dose-dependent manner in MDA-MB-231 cells (Figure 4.7). These data indicate that trametinib is a dual inhibitor of ERK1/2 and ERK5 pathways in MDA-MB-231 cells, but not in BT-549, TU-BcX-4IC, and TAMR MCF-7 cells. These data also suggest that MEK1/2 may be upstream of ERK5 in MDA-MB-231 cells.

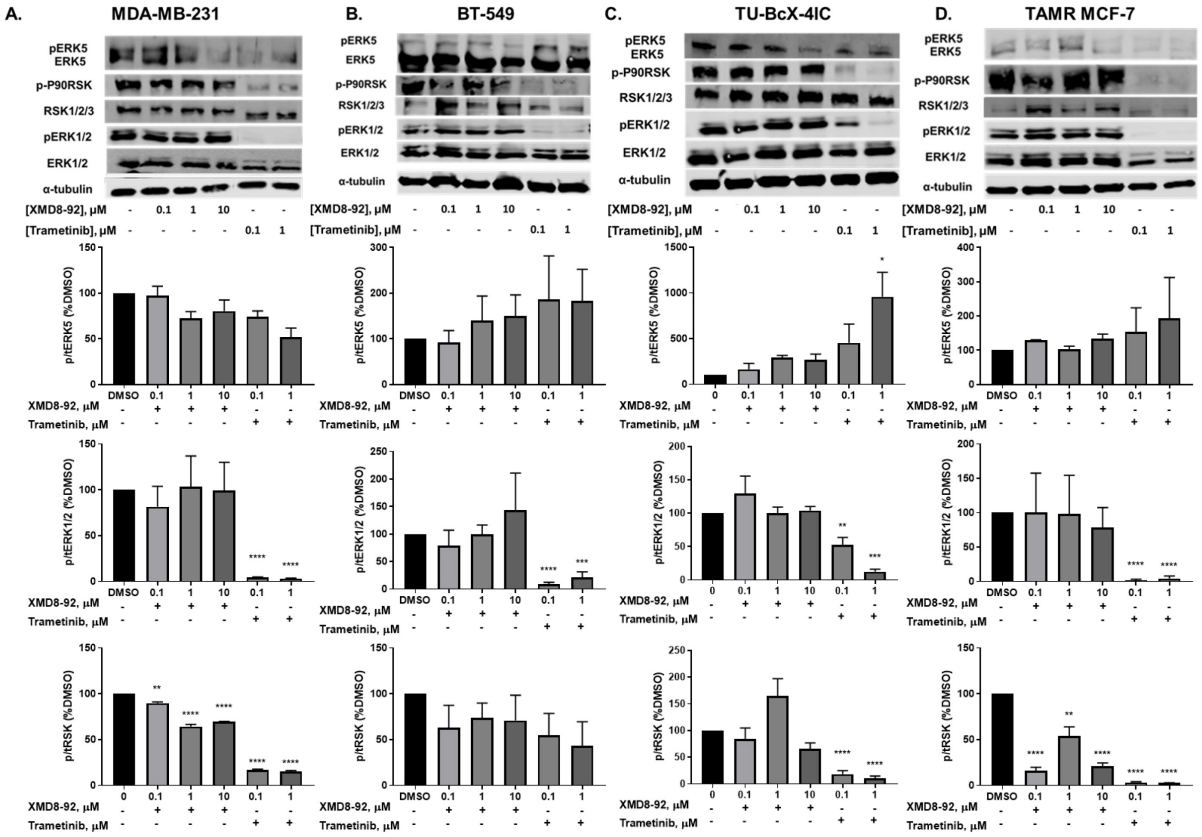

Figure 4.6 Western blot analysis of MAPK downstream targets pERK5, pERK1/2, and p-P90RSK in TNBC cells. (A) MDA-MB-231, **(B)** BT-549, **(C)** TU-BcX-4IC, and **(D)** TAMR MCF-7 cells. Data represent the ± SEM of three different experiments for each inhibitor compared to DMSO control. *p<0.05; **p<0.01; ***p<0.001; ****p<0.0001 *vs* DMSO control group determined by one-way ANOVA with the Bonferroni post hoc test.

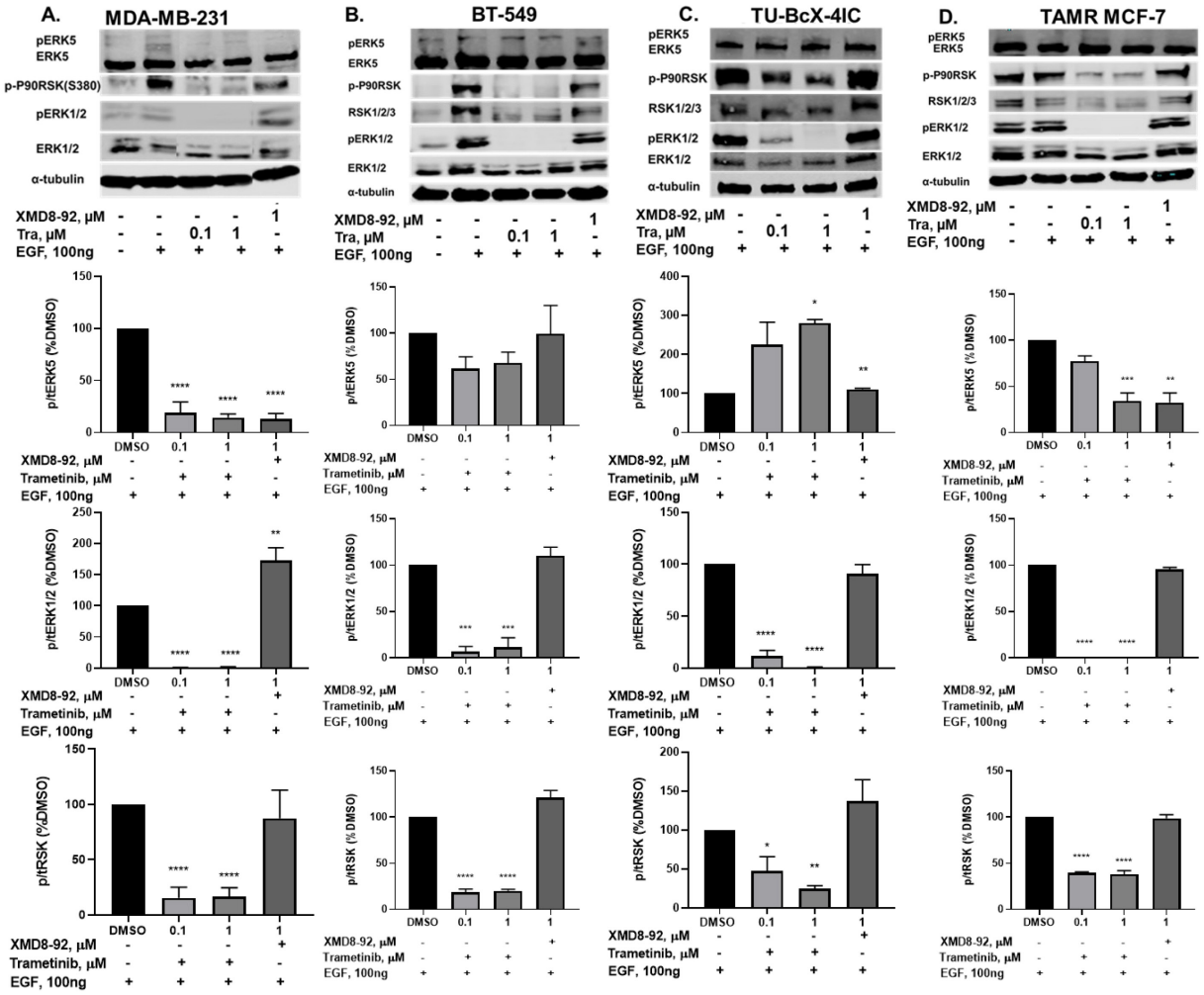

Figure 4.7 Evaluation of kinase inhibition under EGF stimulation. Cells were serum starved for 18-24 hours and treated with the respective inhibitors for 30 minutes. EGF was added at a 100ng concentration for 15 minutes and western blot was performed on the lysates collected for analysis of ERK5, ERK1/2, and P90RSK activation in **(A)** MDA-MB-231, **(B)** BT-549, **(C)** TU-BcX-4IC, and **(D)** TAMR MCF-7 cells. Data represent the ± SEM of three different experiments for each inhibitor compared to DMSO control. *p<0.05; **p<0.01; ****p<0.0001 *vs* DMSO control group determined by one-way ANOVA with the Bonferroni post hoc test.

4.3.4 Effects of XMD8-92 and trametinib on cell migration and proliferation in breast cancer

EMT is known to promote cell migration via downregulation of cell-cell adhesion molecule E-cadherin.[97, 112] To examine cell migration, a wound was introduced to the cell

plates using a pipette tip. Wound closure was measured after treatment with DMSO or inhibitors to determine the efficacy of MAPK inhibitors on cell migration. XMD8-92 decreased cell migration in MDA-MB-231 and TU-BcX-4IC cells at 10 μM concentration (Figure 4.8A and C). Trametinib significantly decreased cell migration in MDA-MB-231, BT-549, TU-BcX-4IC, and TAMR breast cancer cells (Figure 4.8A-D).

Cancer cells have high proliferation rates. To determine this proliferative fraction, cells were stained with Ki67, a marker of proliferation. Proliferative fraction was calculated as the ratio of number of $Ki67^{+}$ cells to $Hoechst^{+}$ cells. XMD8-92 produced a significant decrease in proliferative fraction of MDA-MB-231, TU-BcX-4IC, and TAMR-MCF-7 cells (Figure 4.8E, G-H), but not in BT-549 cells (Figure 4.8F). Trametinib had no effect on the proliferative fraction in any of the cell lines.

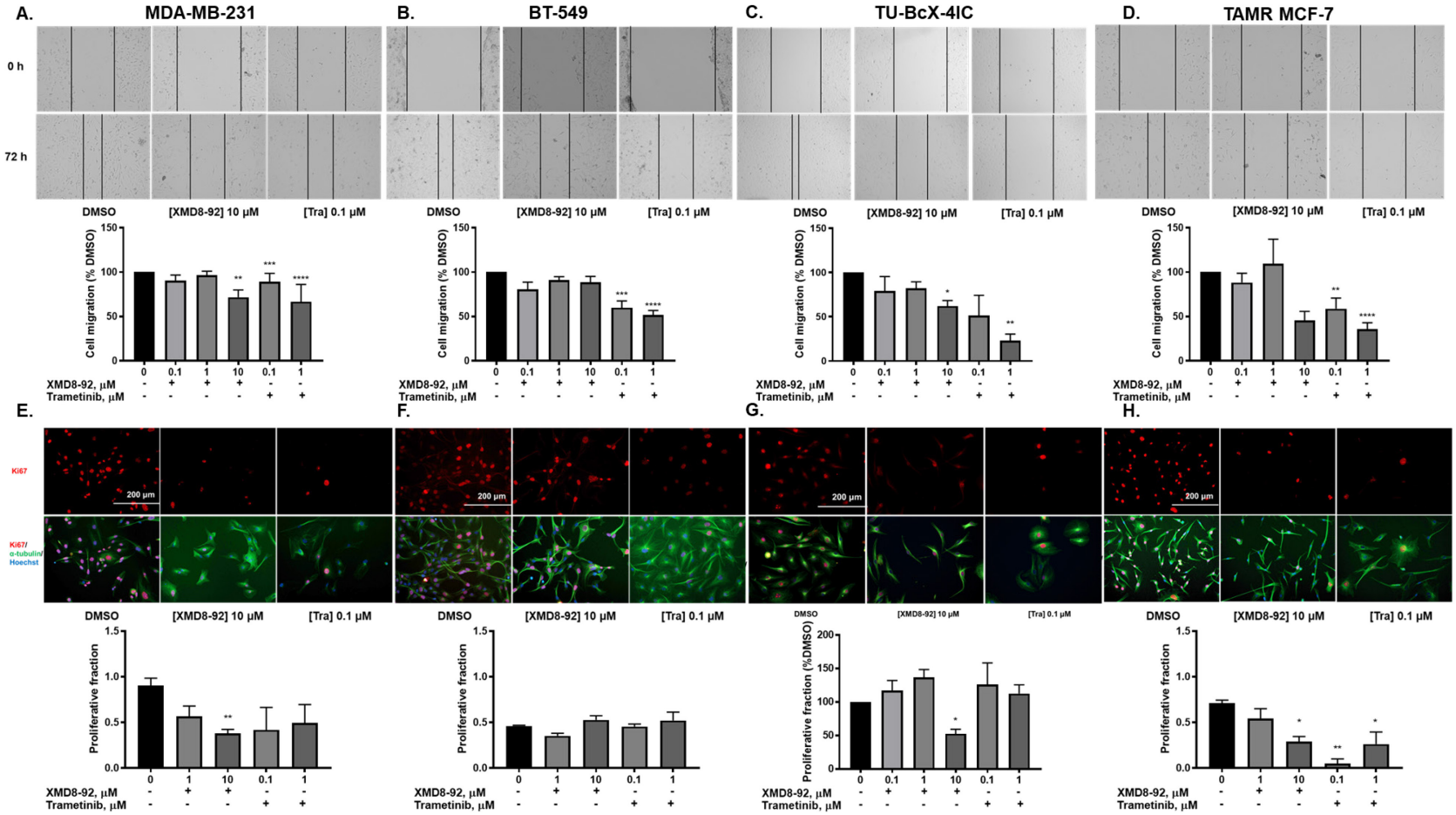

Figure 4.8. XMD8-92 and trametinib differentially decrease cell migration and proliferation in diverse breast cancer subtypes. **A)** MDA-MB-231, **(B)** BT-549 cells, **(C)** TU-BcX-4IC, and **(D)** TAMR MCF-7 cells were treated with the kinase inhibitors and scratch assay was performed (20X magnification). Cell migration was measured as a percentage of DMSO control group. Cell proliferation assay was performed **(E)** MDA-MB-231, **(F)** BT-549, **(G)** TU-BcX-4IC and **(H)** TAMR MCF-7 (20X magnification). Data represent the ± SEM of three different experiments. *p<0.05; **p<0.01; ***p<0.001; ****p<0.0001 *vs.* DMSO control group determined by one-way ANOVA with the Bonferroni post hoc test.

4.3.5 Trametinib decreases nuclear ERK5 in MDA-MB-231, but not in BT-549 cells

ERK5 has a large C-terminal domain, which can facilitate its nuclear localization in response to growth factors or via autophosphorylation.[113] ERK5 nuclear localization has been linked with increase in cell proliferation.[114] However, there are no studies that relate the role of ERK5 localization to EMT. To examine the localization of ERK5 in TNBC with distinct kinase mutation profiles, we selected two cell lines from our previously studied cells: MDA-MB-231 are driven by a mutation in RAF leading to aberrant activation of the MEK1/2-ERK1/2 and MEK5-ERK5 pathways, and BT-549 cells are driven by a loss of function mutation in tumor suppressor phosphatase, PTEN, leading to subsequent activation of the PI3K-AKT pathway.

MDA-MB-231 and BT-549 cells were treated with DMSO, 1 μM XMD, or 0.1 μM trametinib for 72 hours. ERK5 was found to be localized in the nucleus and cytosol, but active only in the nucleus of untreated MDA-MB-231 and BT-549 TNBC cells (Figure 4.9). While ERK1/2 were found in both the nucleus and cytosol, ERK1/2 expression was higher in the cytosol of the TNBC cells. In contrast to ERK5, ERK1/2 phosphorylation was noted only in the cytosol of untreated MDA-MB-231 and BT-549 cells. Surprisingly, XMD8-92 did not decrease ERK5 activation in the nucleus of either cells. Trametinib decreased total and phosphorylated ERK5 in the nucleus of MDA-MB-231 cells (Figure 4.9A, B), but inhibited ERK5 only in the cytosol in BT-549 cells (Figure 4.9D). Trametinib significantly decreased ERK1/2 activation in the cytosol in MDA-MB-231 and BT-549 cells. Total ERK1/2 expression was not altered with either treatment in the cytosol of either cell line. These findings indicate that decrease in total ERK5 expression in the nucleus may

contribute to the MET-inducing potential of trametinib in MDA-MB-231 cells. Future studies will be performed to examine the effect of ERK5 degradation on MET.

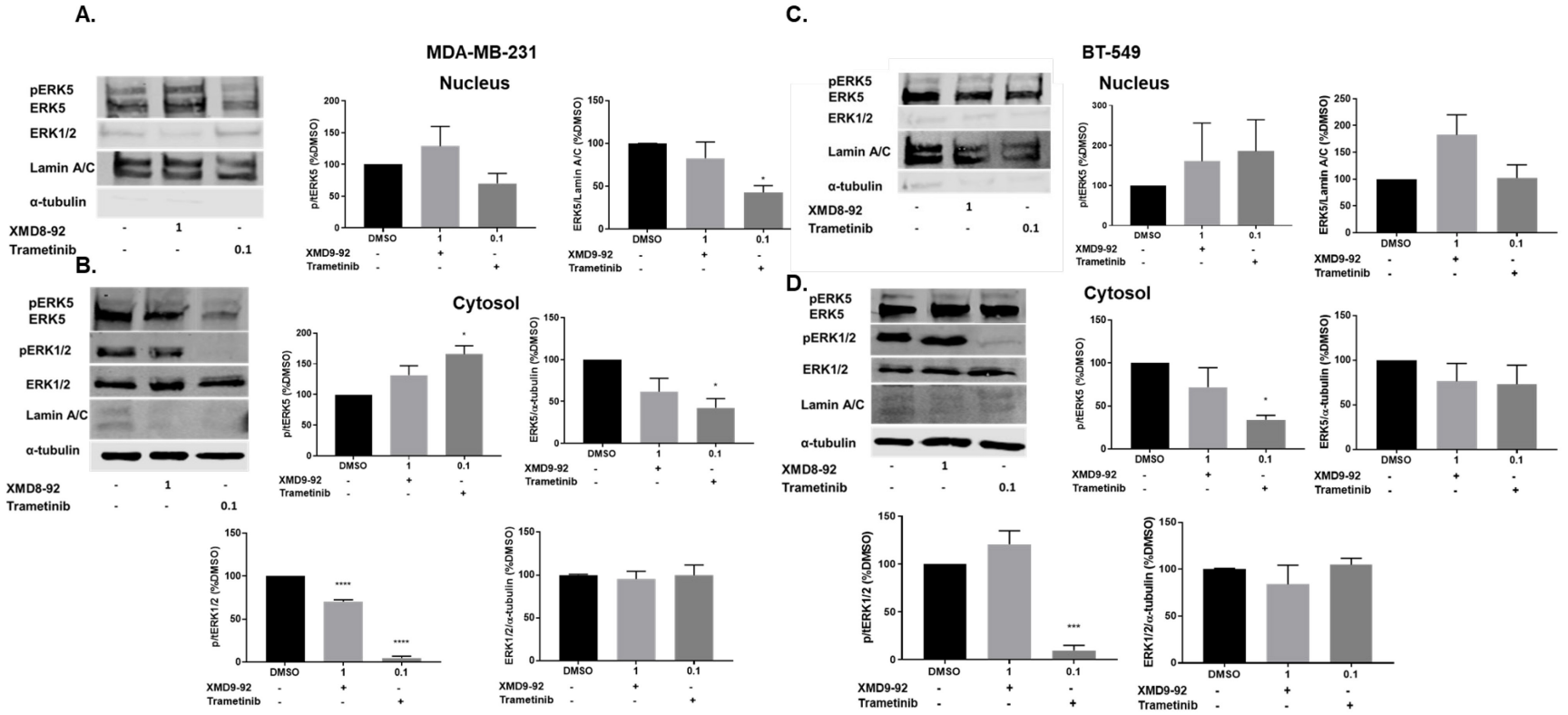

Figure 4.9 Effect of XMD8-92 and trametinib on ERK5 and ERK1/2 activation in the nucleus and cytoplasm. (A) MDA-MB-231 nuclear fraction **(B)** MDA-MB-231 cytosolic fraction **(C)** BT-549 nuclear fraction **(D)** BT-549 cytosolic fraction. *p<0.05; ***p<0.001 *vs* control group determined by one-way ANOVA with the Bonferroni post hoc test.

4.3.6 Diverse and converging roles of MEK1 and MEK5 on EMT and kinase activation in TNBC cells

To further examine the roles of the ERK1/2 and ERK5 pathways on MET, MDA-MB-231 and BT-549 cells were treated with dominant negative (dn) and constitutively active (ca) lentivirus vectors of MEK1 and MEK5 (generous gift from Dr. Zhengui Xia). The cells were transiently co-infected with GFP tagged dnMEK1, dnMEK5, caMEK1, and/or caMEK5 lentivirus vectors, as indicated, for 96 hours. The morphology of infected cells was assessed via immunostaining for the cytoskeletal protein α-actinin (Figure 4.10A). Cells that were infected with dnMEK1 or dnMEK5 alone and in combination displayed a phenotypic shift from mesenchymal to epithelial. Transfection with caMEK1 or caMEK5 alone and in combination increased the mesenchymalization of MDA-MB-231 and BT-549 cells (Figure 4.10A, C). Infection with dnMEK5 decreased ERK5 phosphorylation by ~25% and transfection with caMEK1+caMEK5 significantly increased ERK5 activation in MDA-MB-231 cells (Figure 4.10B). There were no significant changes in ERK1/2 phosphorylation in MDA-MB-231 cells. In BT-549 cells, infection with dnMEK1 and dnMEK5 did not significantly decrease ERK5 or ERK1/2 phosphorylation; however, transfection with caMEK1 or caMEK1+caMEK5 significantly increased ERK1/2 activation in BT-549 (Figure 4.10D).

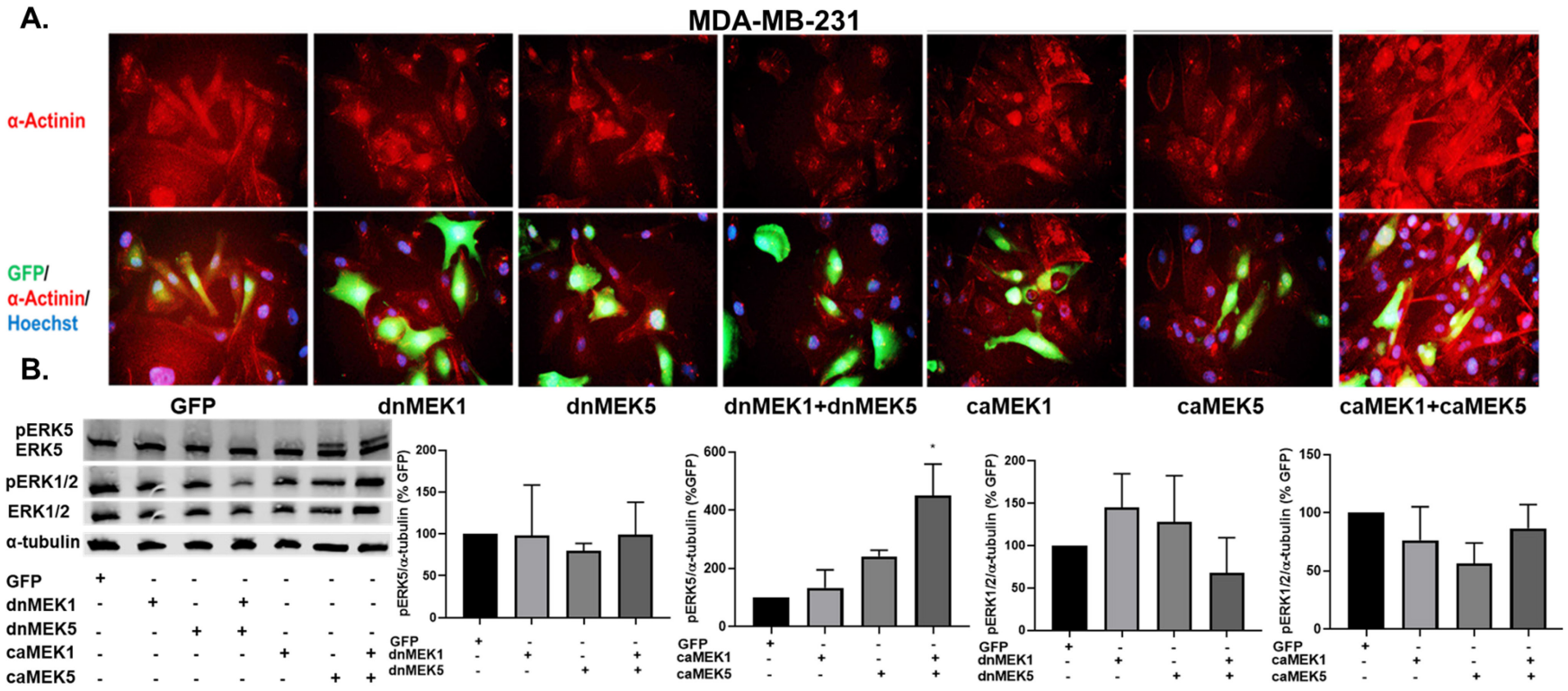
A.
MDA-MB-231
α-Actinin
GFP/
α-Actinin/
Hoechst
B.
GFP
dnMEK1
dnMEK5
dnMEK1+dnMEK5
caMEK1
caMEK5
caMEK1+caMEK5
pERK5
ERK5
pERK1/2
ERK1/2
α-tubulin
GFP
dnMEK1
dnMEK5
caMEK1
caMEK5
pERK5/α-tubulin (% GFP)
pERK5/α-tubulin (%GFP)
pERK1/2/α-tubulin (% GFP)
pERK1/2/α-tubulin (% GFP)

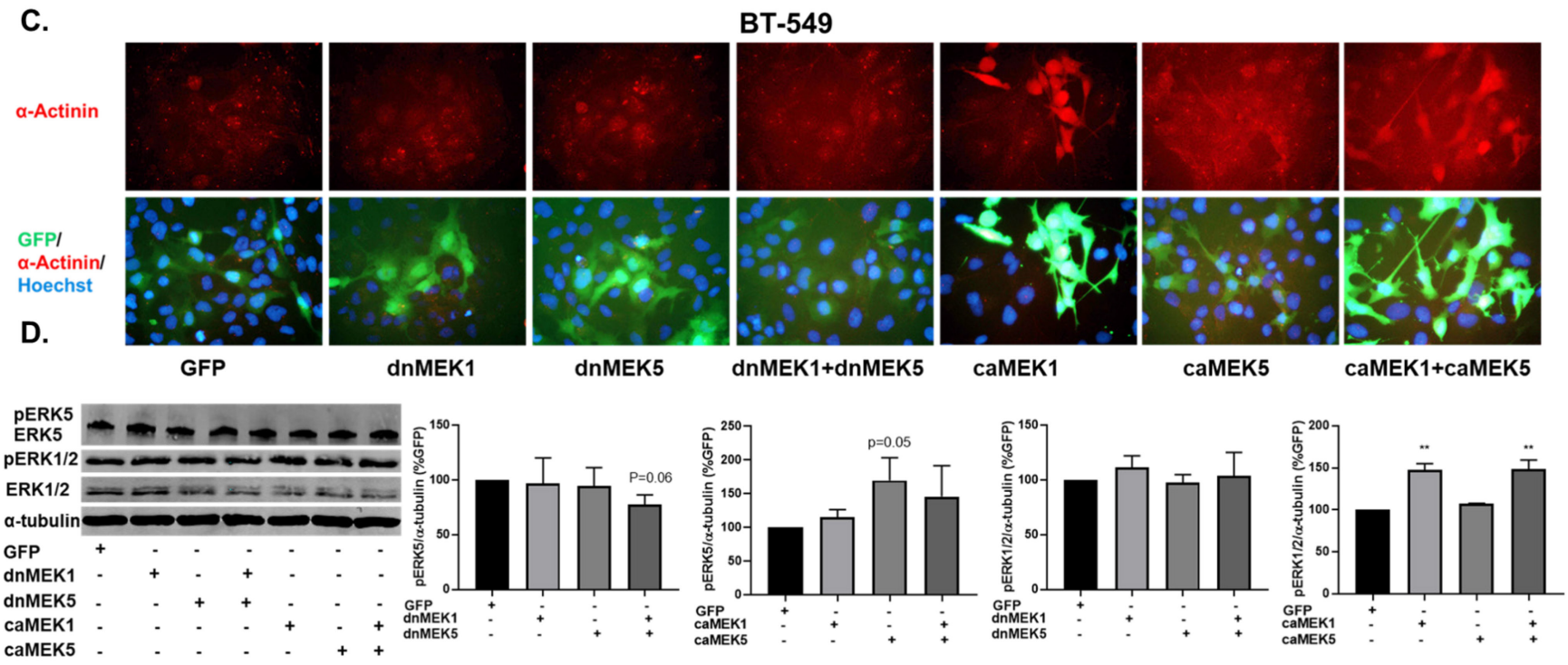

Figure 4.10. MEK1 and MEK5 activation mediates EMT in TNBC cells. (A, B) MDA-MB-231 and **(C, D)** BT-549 cells were treated with dnMEK5, dnMEK1, caMEK5, and caMEK1 alone and in combination as represented in the figure. The cells were incubated for 96 hours. Immunofluorescence staining for α-actinin was performed to assess the morphology (40X magnification). The effect on ERK1/2 and ERK5 activation was evaluated via western blotting. *p<0.05; **p<0.01 *vs* GFP control group determined by one-way ANOVA with the Bonferroni post hoc test.

4.3.7 MEK1 and MEK5 pathways regulate ZEB1 expression in TNBC cells

To further understand the role MAPK pathways in the induction of MET, cell-specific responses to lentivirus-mediated MEK1/2 and MEK5 pathway inhibition and activation on ZEB-1, a marker of mesenchymal cells, was examined. MDA-MB-231 and BT-549 cells infected with dnMEK1, dnMEK5, caMEK1, or caMEK5 lentivirus vectors alone and in combination were assessed for ZEB1 expression by immunofluorescence. MDA-MB-231 cells that were infected with dnMEK1, dnMEK5, and dnMEK1+dnMEK5 vectors (GFP+ cells) had an epithelial phenotype and attenuated ZEB1 expression (Figure 4.11A). Conversely, while cells infected with caMEK1, caMEK5, and caMEK1+caMEK5 groups had a more pronounced mesenchymal morphology compared to GFP control, ZEB1 expression was not increased (Figure 4.11A). BT-549 cells that were infected with dnMEK1, dnMEK5, or dnMEK1+dnMEK5 appeared epithelial but had no reduction in ZEB1 expression (Figure 4.11B). caMEK1, caMEK5, or caMEK1+caMEK5-infected BT-549 cells had a more pronounced mesenchymal morphology and showed an increase in ZEB1 expression (Figure 4.11B).

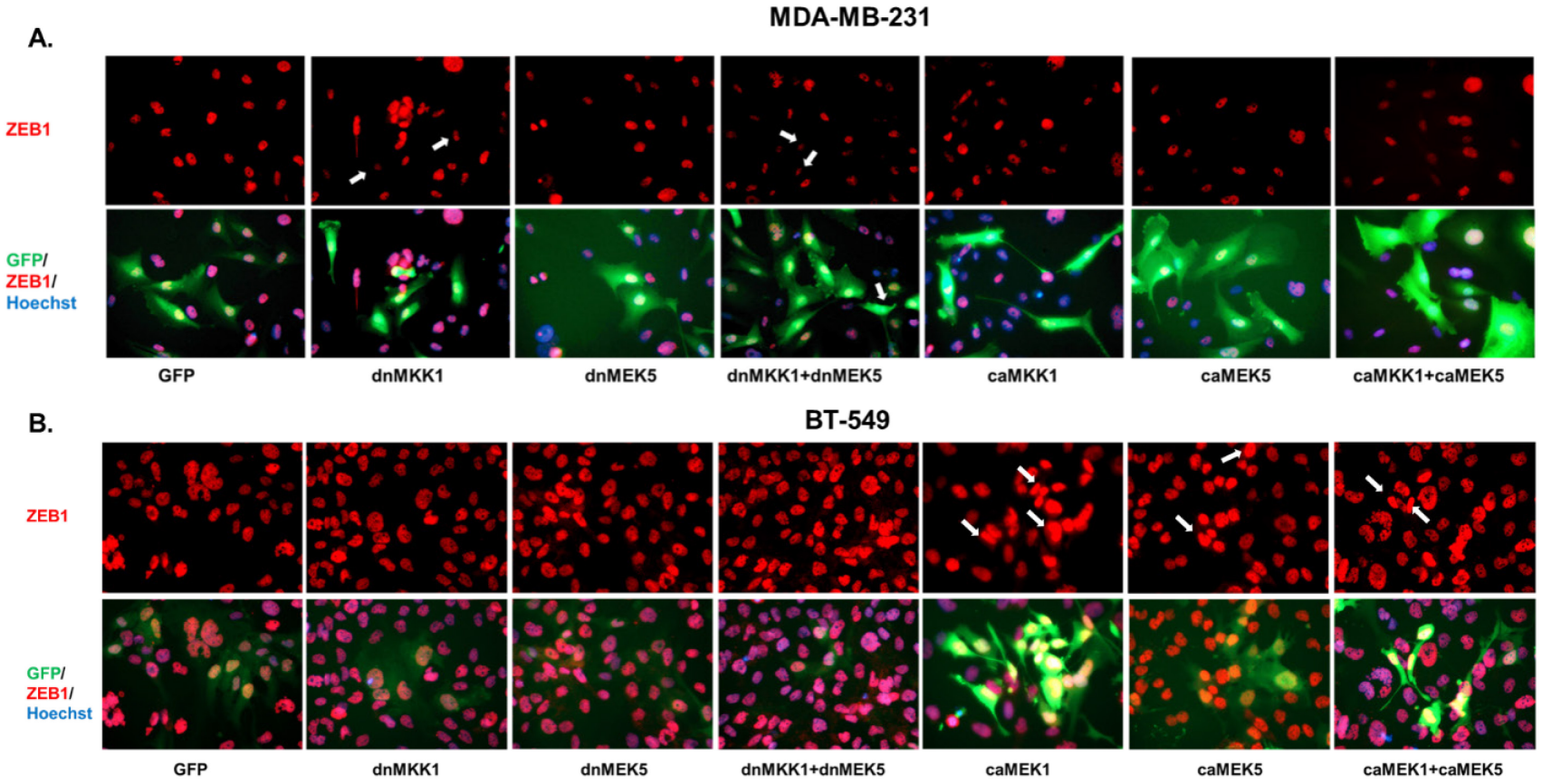

Figure 4.11 MEK1 and MEK5 activation mediates ZEB1 expression in TNBC cells. (A) MDA-MB-231 and **(B)** BT-549 cells were transfected with dnMEK5, dnMEK1, caMEK5, and caMEK1 alone and in combination as represented in the figure. The cells were incubated for 96 hours. Immunofluorescence staining for ZEB1 was performed (40X magnification).

Next, we determined if pharmacological inhibition of the MAPK pathways with trametinib could restore the epithelial phenotype and decrease mesenchymal cell markers following caMEK5 transfection in MDA-MB-231 and BT-549 cells. Cells were treated with 0.1 μM trametinib in the presence of GFP or caMEK5 lentivirus to examine the effects on cell morphology, E-cadherin, and ZEB1 expression. MDA-MB-231 cells treated with trametinib transitioned to an epithelial phenotype and had a reduction in ZEB1 expression (Figure 4.12) This reduction in ZEB1 was inhibited in cells that were infected with caMEK5 (Figure 4.12).

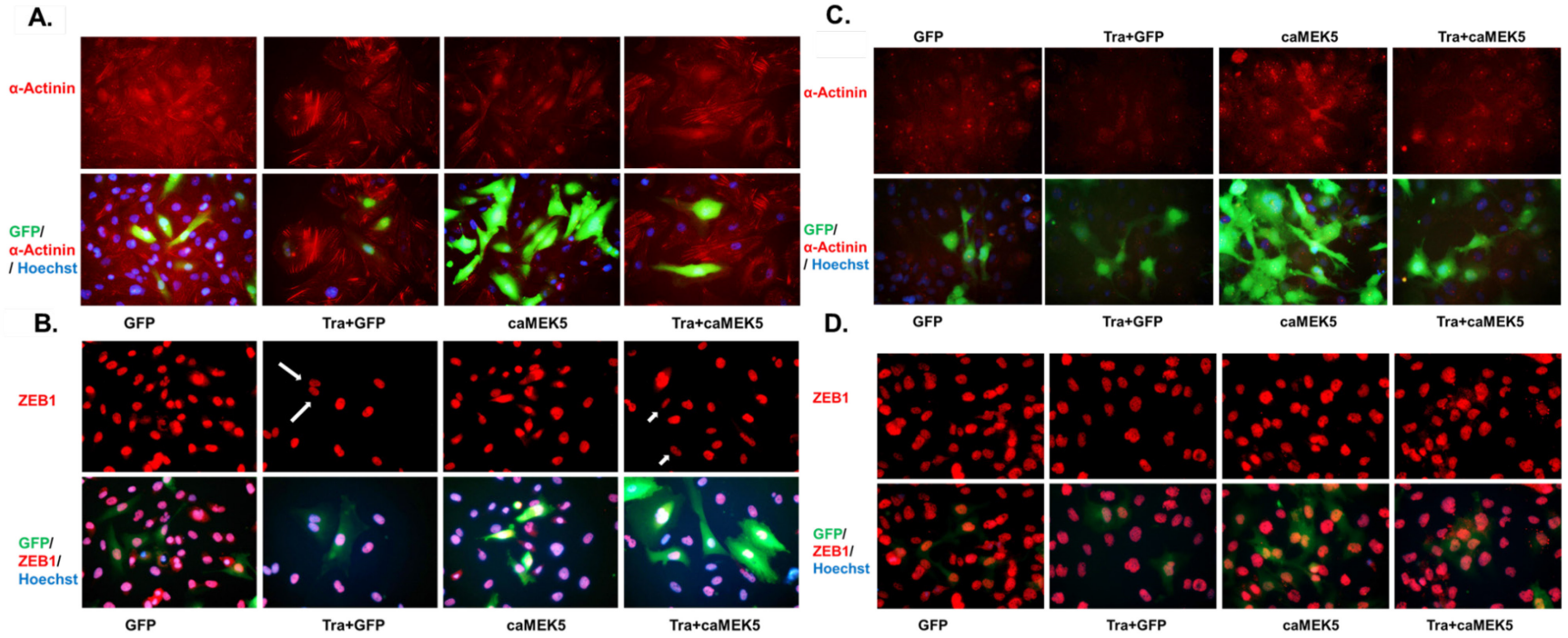

Figure 4.12 Effect of trametinib+caMEK5 on TNBC cell morphology and ZEB1 expression. (A, B) MDA-MB-231 and **(C, D)** BT-549 cells were treated with GFP, Tra+GFP, caMEK5, and Tra+caMEK5 for 96 hours. Immunofluorescence staining for α-actinin or ZEB1 was performed to assess MET (40X magnification).

Similar to the immunocytochemical data, caMEK5 inhibited the trametinib-mediated decrease in ZEB1 expression as determined by western blotting in MDA-MB-231 cells (Figure 4.13), but not in BT-549 cells (Figure 4.13). Interestingly, caMEK5 transfection did not increase the trametinib-mediated increases in E-cadherin expression in either TNBC cell line (Figure 4.13). Together our data suggest that targeting both ERK12 and ERK5 pathways induces MET in MDA-MB-231 cells but targeting ERK1/2 pathway alone induces MET in BT-549 cells as outlined in figure 4.13.

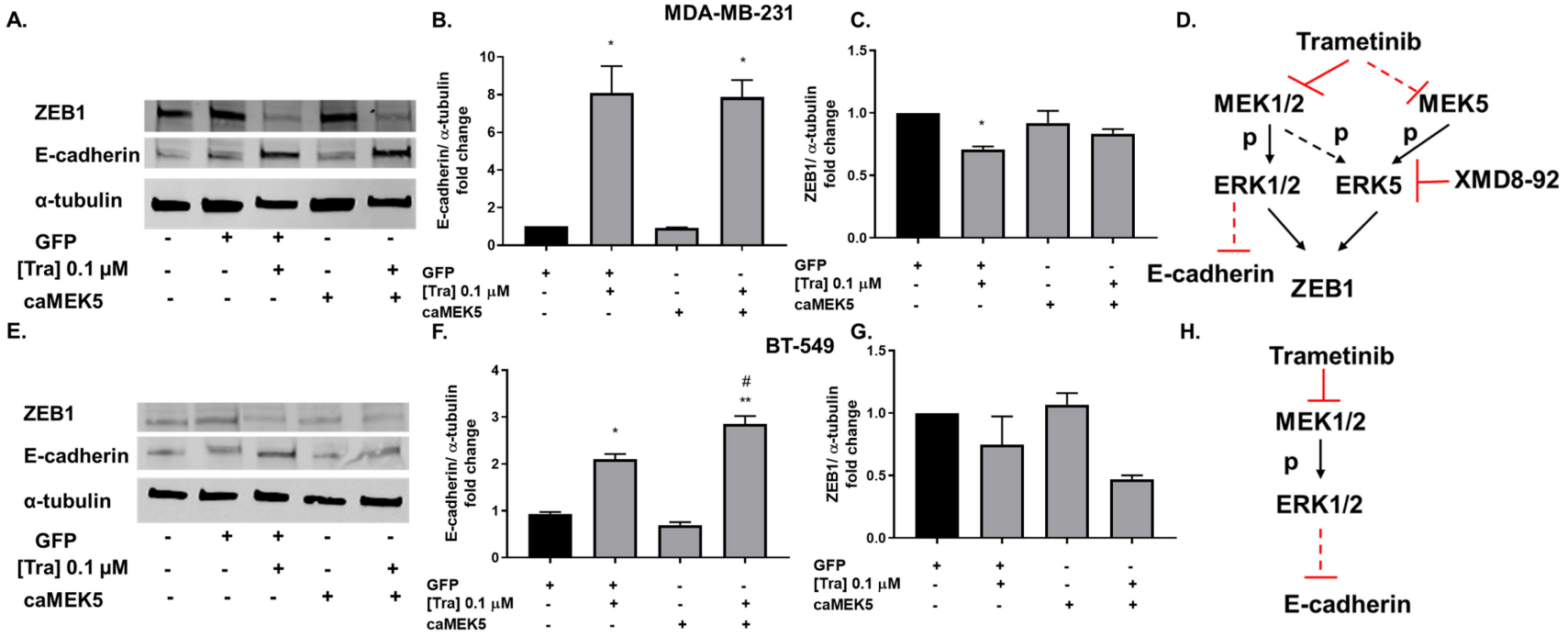

Figure 4.13 Effect of trametinib+caMEK5 on E-cadherin and ZEB1 expression in TNBC cells. (A-D) MDA-MB-231 and **(E-H)** BT-549 cells were treated/infected with GFP, Tra+GFP, caMEK5, and Tra+caMEK5 for 96 hours. Western blotting for E-cadherin and ZEB1 expression was performed to assess MET.

4.3.8 MEK1 and/or MEK5 activation reduces the ability of trametinib to decrease vimentin expression in MDA-MB-231 VIM RFP 2D and spheroid cell cultures.

The effect of dual ERK1/2 and ERK5 pathway inhibition on MET was found to be most promising in MDA-MB-231 cells. Therefore, to strengthen the functional contribution of inhibiting the ERK1/2 and ERK5 pathways in MET, MDA-MB-231 VIM RFP cells, a new model for MET research, were infected with caMEK1 and/or caMEK5 in the presence of DMSO, trametinib, or XMD8-92. These cells have been transformed to constitutively express vimentin, a mesenchymal marker, via CRISPR-knock-in system and serve as a good model to study MET (ATCC). Vimentin expression was examined in 2D and spheroid cultures following treatment with caMEK isoforms in the presence or absence of the MAPK inhibitors. While treatment with XMD8-92 alone did not reduce vimentin expression in 2D cultures, treatment with trametinib moderately decreased vimentin expression, specifically in cells that underwent a MET as determined by examining morphology of GFP+ cells via microscopy (Figure 4.14). Treatment with caMEK1, caMEK5, or caMEK1+caMEK5 increased vimentin expression and reduced the ability of trametinib to decrease vimentin expression (Figure 4.14). In spheroid culture, trametinib, but not XMD8-92, treatment reduced expression of vimentin at 96 hours, which was rescued by transfection of caMEK1, caMEK5, or caMEK1+caMEK5 (Figure 4.14).

Spheroid viability was assessed after 7 days of treatment with inhibitors or caMEKs (Figure 4.15). There was no baseline difference in spheroid viability after treatment with caMEK1, caMEK5, or caMEK1+caMEK5 groups. This may indicate that the spheroid-forming ability of MDA-MB-231 VIM RFP cells is at its maximum and cannot be further

increased. XMD8-92 significantly decreased spheroid viability at 1 and 10 μM concentrations. As expected, the reduction in spheroid viability at 1μM XMD8-92 concentration was rescued by co-treatment with caMEK5 or caMEK1+caMEK5. This effect of caMEK5 or caMEK1+caMEK5 transfection was reversed in the presence of a higher XMD8-92 concentration (10μM). While trametinib significantly decreased spheroid viability at 0.1μM concentration, this decrease in viability was not reversed in the presence of caMEK1, caMEK5, or caMEK1+caMEK5 (Figure 4.15). Pictures of vimentin-expressing spheroids at day 0, day 7, and evidence of lentivirus infection measured by examining GFP expression in spheroids are included in Figure 4.16.

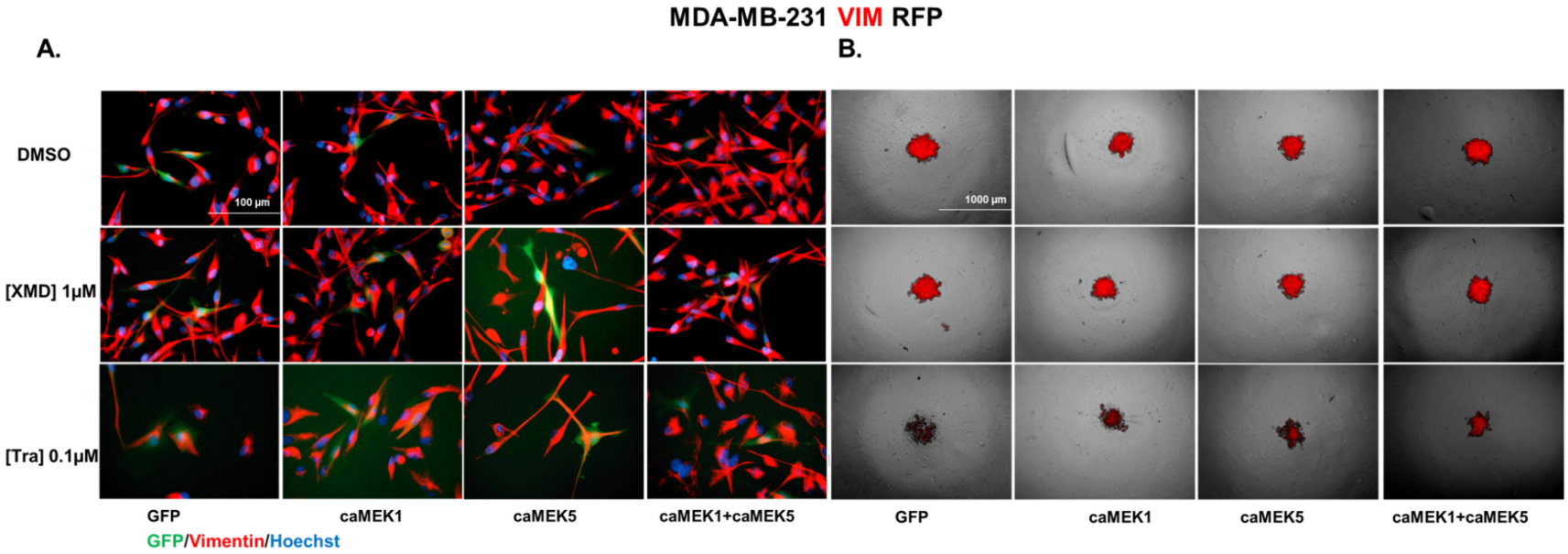

Figure 4.14. MEK1 and/or MEK5 activation reduces the ability of XMD8-92 or trametinib to decrease vimentin expression in MDA-MB-231 VIM RFP cells. (A) MDA-MB-231 VIM RFP cells were treated with constitutively active MEK1, MEK5, and MEK1+MEK5 in the presence of DMSO, XMD8-92, or trametinib for 72 hours. The cells were fixed and stained with Hoechst. Images of Vimentin-, GFP-, and Hoechst-expressing cells were captured under 40X magnification using EVOS microscope (n=3, most representative image shown). **(B)** MDA-MB-231 VIM RFP cells were treated with constitutively active MEK1, MEK5, and MEK1+MEK5 in the presence of DMSO, XMD8-92, or trametinib for 96 hours. Images of spheroids under transmitted light and RFP channel were captured under 4X magnification using EVOS microscope (n=3, most representative image shown).

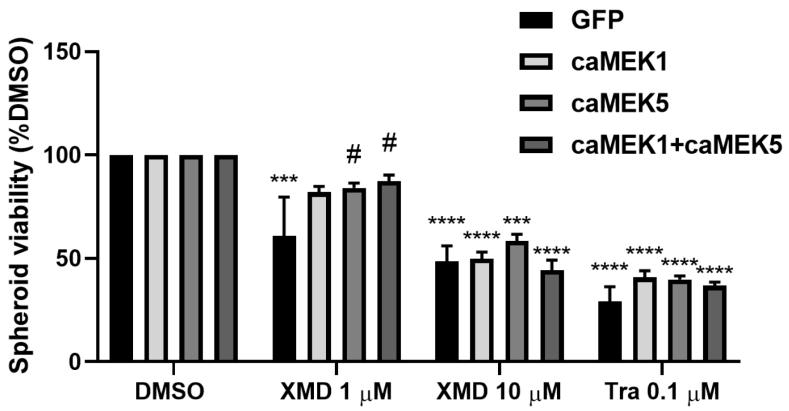

Figure 4.15: MEK1 and/or MEK5 activation reduces the ability of XMD8-92 or trametinib to decrease spheroid viability in MDA-MB-231 VIM RFP cells. Spheroid viability was assessed after 7 days of treatment with the same groups. Data indicate ± SEM of experiments run in triplicate. ***p<0.001; ****p<0.0001 *vs* DMSO control group, #p<0.05; *vs* individual drug+GFP determined by two-way ANOVA with the Bonferroni post hoc test.

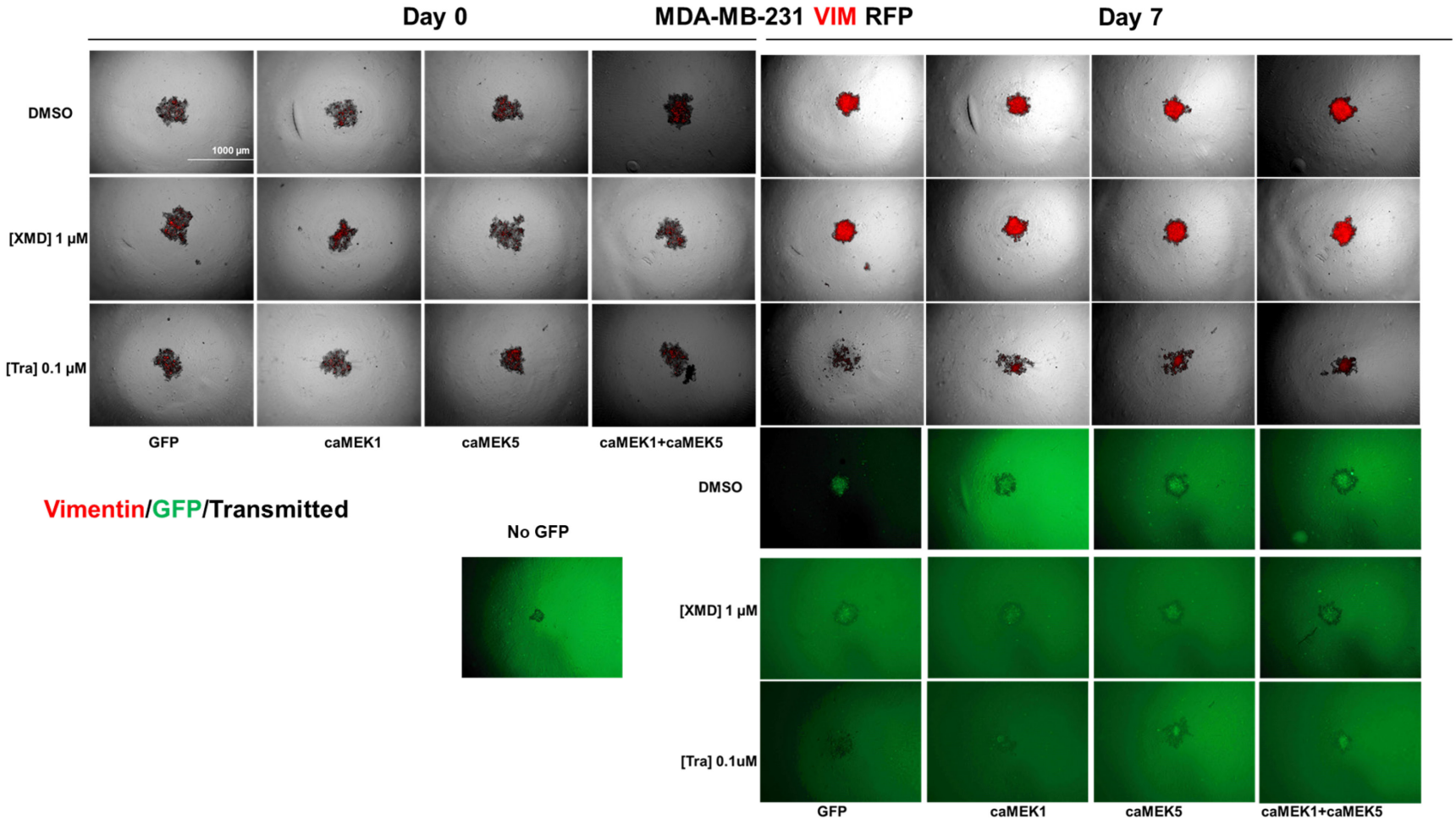

Figure 4.16 Tra or XMD in the presence of constitutively active MEK1 and/or MEK5 affect spheroid viability in MDA-MB-231 VIM RFP model. (A) Pictures of MDA-MB-231 VIM RFP spheroids before treatment. **(B)** Pictures of spheroids after 7 days of treatment. **(C)** GFP expression in GFP, caMEK1, and/or caMEK5-treated spheroids.

4.3.9 Effect of dual ERK1/2 and ERK5 pathway inhibition on cell viability and spheroid formation in breast cancer

We wanted to further characterize the effect of pharmacological inhibition of the ERK1/2 and ERK5 pathways on cell viability and spheroid formation. Breast cancer cells were treated with increasing concentrations of XMD8-92 and trametinib (0.1, 0.3, 1, 3 and 10 μM) alone and in combination for 72 hours (Figure 4.17). MTT assay was performed to evaluate cell viability. While trametinib and XMD8-92 alone decreased cell viability in MDA-MB-231 and TU-BcX-4IC cells, there was no synergy in combination groups. In BT-549 cells, there was a reduction in cell viability after treatment with XMD8-92, but not trametinib. In TAMR MCF-7 cells, the combination of XMD8-92 and trametinib synergistically reduced cell viability.

EMT is known to promote anchorage-independent growth.[97, 112] We found that trametinib alone significantly decreased cell viability and/or spheroid viability in all breast cancer models and its effects were most pronounced in MDA-MB-231 cells (Figure 4.18) At the 10uM concentration, XMD8-92 decreased spheroid viability in MDA-MB-231 and TU-BcX-4IC cells, but not BT-549 or TAMR cells. The reduction in spheroid viability in response to trametinib was greater in MDA-MB-231 cells (~90%) compared to BT-549 (~40%), TU-BcX-4IC (~35%), or TAMR-MCF-7 cells (~40%). These data suggest that while ERK1/2 and ERK5 inhibition is sufficient to target MDA-MB-231 and TAMR MCF-7 cells, alternative pathways may be important to further reduce spheroid viability in BT-549 and TU-BcX-4IC cells. The combination of Tra+XMD at the 0.1 and 1uM concentrations, synergistically inhibited spheroid viability in TAMR MCF-7 cells, but not the TNBC cells. (Figure 4.18). Overall, these findings suggest that dual ERK1/2 and ERK5

inhibition is a relevant strategy to target tamoxifen-resistant breast cancer cells. Additional alternative pathways that may mediate survival in TNBC cells will be discussed in chapter 5.

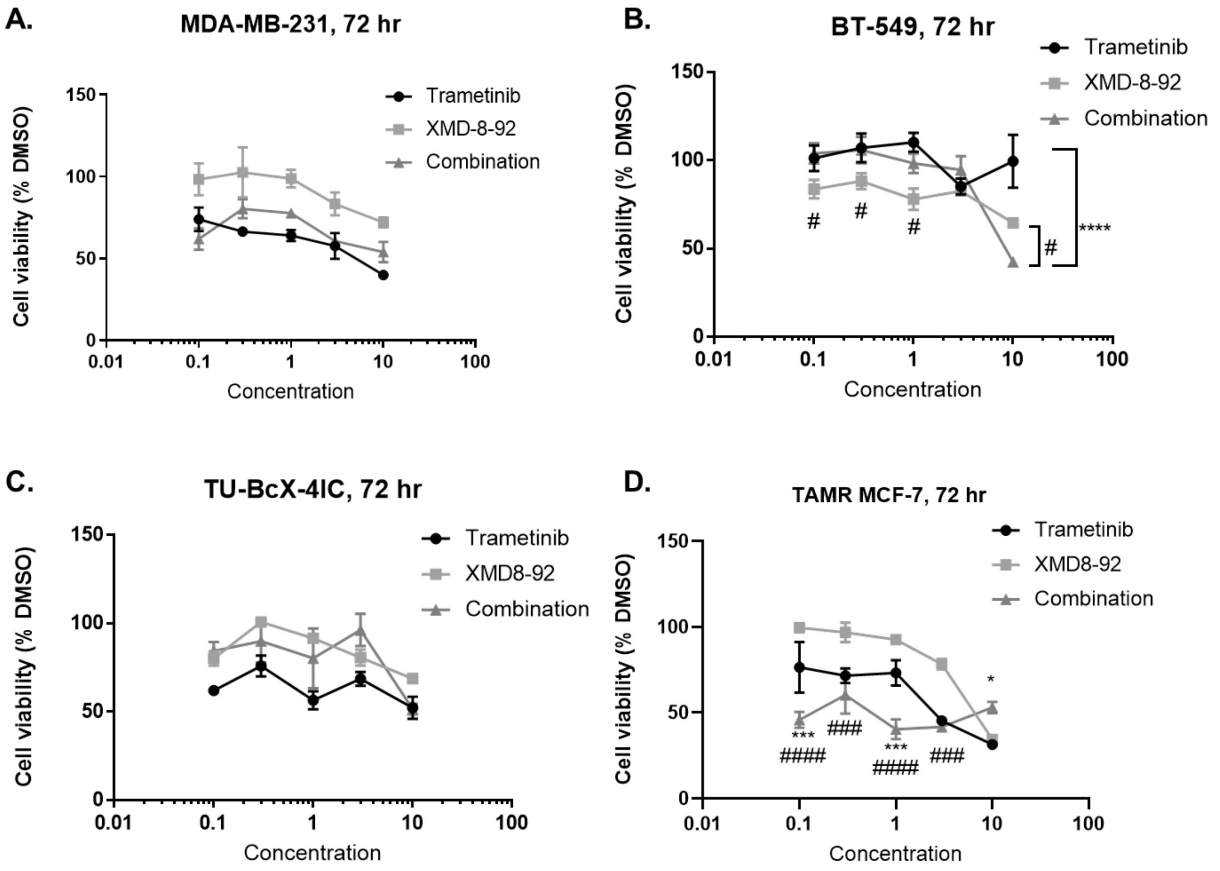

Figure 4.17: Effect of XMD8-92 and trametinib alone and in combination on breast cancer cell viability. Effect of simultaneous treatment with XMD8-92 and trametinib was evaluated compared to XMD and trametinib alone. *p<0.05; **p<0.01; ***p<0.001; ****p<0.0001 *vs* trametinib; ##p<0.01; ###p<0.001; ####p<0.0001 *vs* XMD8-92 as determined by two-way ANOVA with the Bonferroni post hoc test.

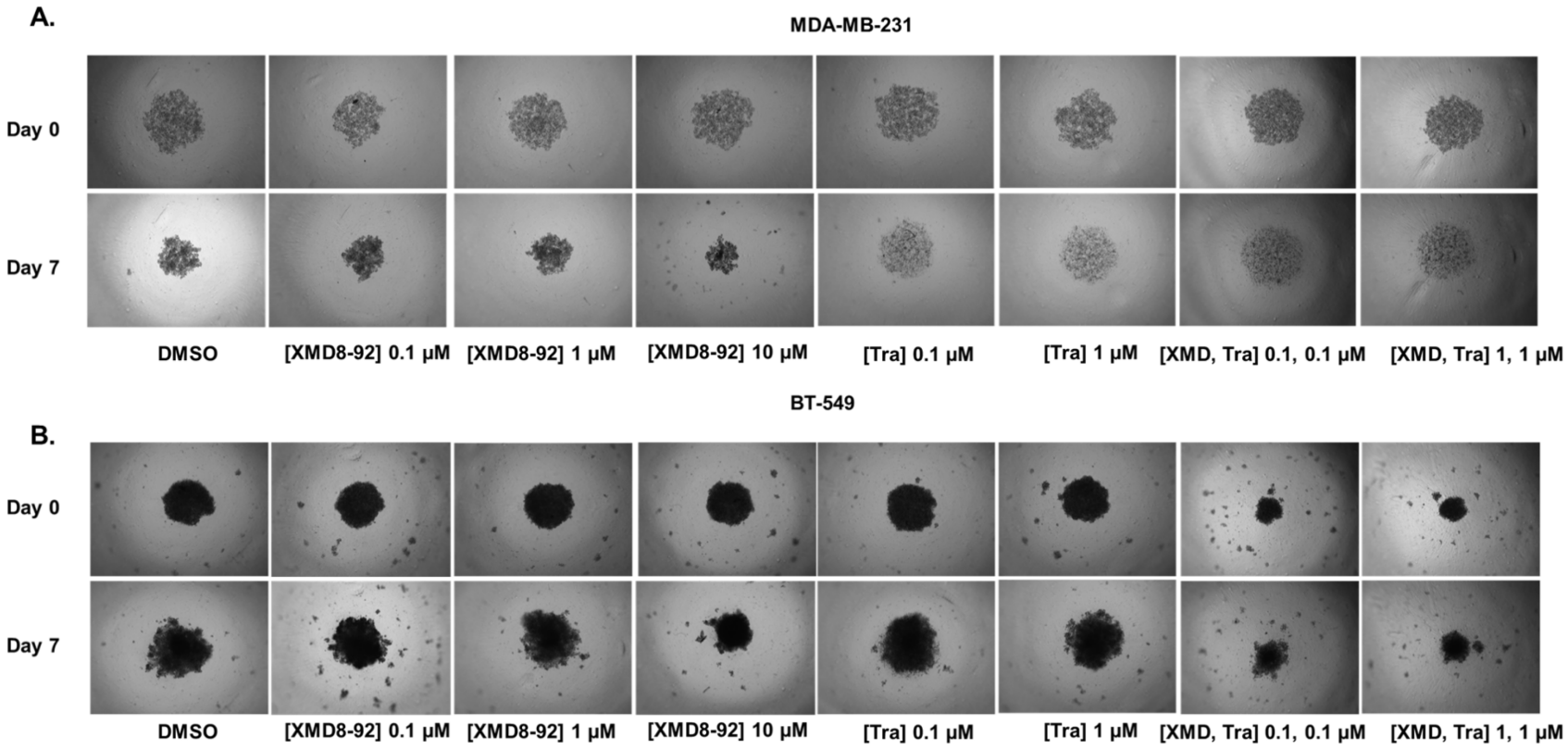
A.
MDA-MB-231
Day 0
Day 7
DMSO
[XMD8-92] 0.1 μM
[XMD8-92] 1 μM
[XMD8-92] 10 μM
[Tra] 0.1 μM
[Tra] 1 μM
[XMD, Tra] 0.1, 0.1 μM
[XMD, Tra] 1, 1 μM
BT-549
B.
Day 0
Day 7
DMSO
[XMD8-92] 0.1 μM
[XMD8-92] 1 μM
[XMD8-92] 10 μM
[Tra] 0.1 μM
[Tra] 1 μM
[XMD, Tra] 0.1, 0.1 μM
[XMD, Tra] 1, 1 μM

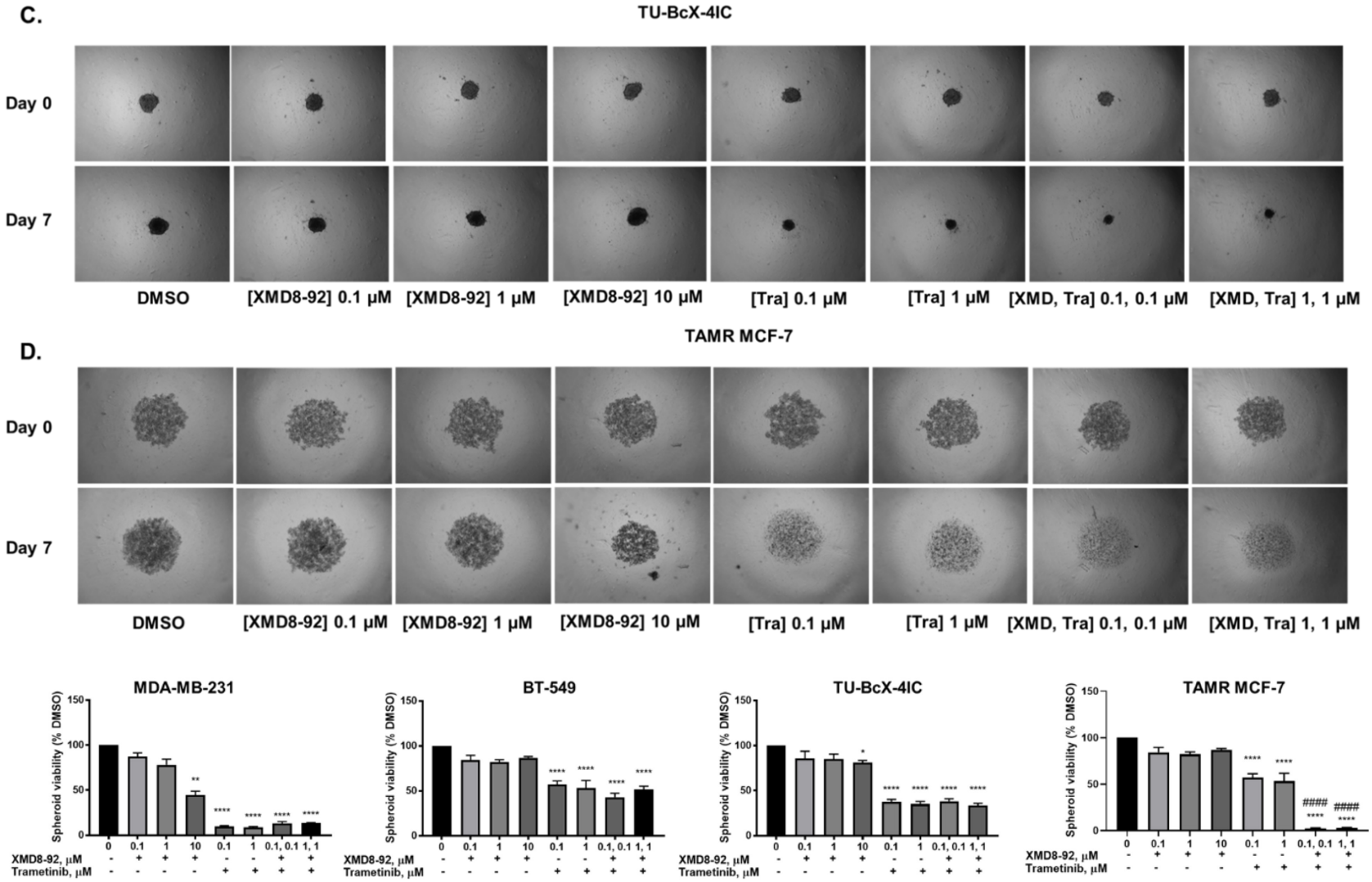
C.
TU-BcX-4IC
Day 0
Day 7
DMSO
[XMD8-92] 0.1 μM
[XMD8-92] 1 μM
[XMD8-92] 10 μM
[Tra] 0.1 μM
[Tra] 1 μM
[XMD, Tra] 0.1, 0.1 μM
[XMD, Tra] 1, 1 μM
D.
TAMR MCF-7
Day 0
Day 7
DMSO
[XMD8-92] 0.1 μM
[XMD8-92] 1 μM
[XMD8-92] 10 μM
[Tra] 0.1 μM
[Tra] 1 μM
[XMD, Tra] 0.1, 0.1 μM
[XMD, Tra] 1, 1 μM
MDA-MB-231
BT-549
TU-BcX-4IC
TAMR MCF-7
Spheroid viability (% DMSO)
XMD8-92, μM
Trametinib, μM

Figure 4.18. Effect of ERK1/2 and ERK5 inhibition alone and together on spheroid viability in diverse breast cancer subtypes. The cells were treated with increasing concentrations of XMD8-92 and/or trametinib for 7 days. Pictures of spheroids were obtained before treatment and 7 days after treatment (4X magnification) **(A)** MDA-MB-231, **(B)** BT-549, and **(C)** TU-BcX-4IC, and **(D)** TAMR MCF-7 cells. Data indicate ± SEM of experiments run in triplicate *p<0.05; **p<0.01; ***p<0.001; ****p<0.0001 *vs* DMSO control group, ####p<0.0001 *vs* individual drug determined by one-way ANOVA with the Bonferroni post hoc test.

4.4 Discussion

Mesenchymal cancer cells are migratory and invasive, leading to metastases. There are currently no effective treatments for metastasis. Interestingly, activation of the ERK1/2 and ERK5 signaling pathways leads to an epithelial to mesenchymal transition (EMT) and poor patient survival in several cancers, including TNBC and endocrine-resistant breast cancers.[16, 23, 30, 102-104, 115-117] Genomics data from our research indicate that MAPK3 (ERK2) and MAPK7 (ERK5) gene expression significantly correlated with the mesenchymal markers VIM or ZEB1, but not with the epithelial marker CDH1 (Figure 4.1A and C). MAPK1 (ERK1) positively correlated with mesenchymal markers VIM and ZEB1 and epithelial marker CDH1 (E-cadherin), indicating that MAPK1 may mediate an intermediate epithelial/mesenchymal state where both epithelial and mesenchymal markers are co-expressed (Figure 4.1B). These data support a role for ERK1/2 and ERK5 signaling in EMT in TNBC. However, the relative roles of these pathways in inducing MET, a reversal of the EMT, in these cancers is unknown. Understanding of EMT and response to therapy is further complicated due to crosstalk between the ERK1/2 and ERK5 pathways and different functions of ERK5 in the nucleus versus the cytosol. To our knowledge, this is the first study to examine the independent and overlapping roles of the ERK1/2 and ERK5 signaling cascades on MET, nuclear localization of ERK5, cell migration, proliferation, and spheroid formation in TNBC and TAMR breast cancer.

In the current study, trametinib, a clinically relevant MEK1/2 inhibitor, and XMD8-92, an ERK5 inhibitor, induced a MET in MDA-MB-231 TNBC cells as shown by morphological characteristics, increased expression of E-cadherin, and/or decreased

expression of ZEB1 (Figure 4.3A). In MDA-MB-231, BT-549, TU-BcX-4IC, and TAMR MCF-7 cells, treatment with trametinib resulted in an epithelial-like morphology (Figure 4.3B-D). However, the morphological changes induced by trametinib in BT-549 cells were less pronounced than those in MDA-MB-231 cells. This could be due to inhibition of both ERK1/2 and ERK5 pathways, a subsequent increase in E-cadherin, and decrease in ZEB1 expression by trametinib in MDA-MB-231 cells, but not in BT-549 cells. XMD8-92 treatment only induced an epithelial morphology MDA-MB-231 cells. Interestingly, the morphological changes induced by trametinib in the MDA-MB-231 cells were more pronounced than those induced by XMD8-92. Again, this may be because trametinib inhibited both ERK pathways and altered expression of cell markers in favor of an epithelial phenotype (increased E-cadherin; decreased ZEB1), while XMD8-92 only inhibited the ERK5 pathway and reduced only ZEB1 expression in MDA-MB-231 cells. Overall, these data suggest that inhibition of ERK1/2 or ERK5 activity is sufficient to induce an MET in MDA-MB-231 cells, while inhibition of both ERK1/2 and ERK5 pathways may be necessary to induce a full MET. Conversely, in BT-549, TU-BcX-4IC, and TAMR MCF-7 cells, inhibition of the ERK1/2 pathway may be sufficient to induce an MET. Additionally, as trametinib consistently increased E-cadherin in TNBC and TAMR breast cancer models, E-cadherin may be used as a potential biomarker to predict MET induced by trametinib treatment in metastatic cancers.

Consistent with the effect on MET, trametinib decreased cell migration in TNBC and TAMR MCF-7 cells, suggesting that ERK1/2 inhibition is sufficient to decrease cell migration in these cells. At 10 μM concentration, XMD8-92 decreased cell migration only

in MDA-MB-231 cells. Again, these data are consistent with the induction of MET following XMD8-92 treatment in MDA-MB-231 cells and suggest that ERK5 pathway inhibition is also sufficient to decrease cell migration in MDA-MB-231 cells.

ERK1/2 and ERK5 activation are known to mediate cell proliferation by mediating G1-S transition during the cell cycle via distinct effects on cyclinD1 expression and activation.[118] Trametinib decreased cell proliferation by 80% in TAMR MCF-7 cells. However, in MDA-MB-231 cells, trametinib only decreased cell proliferation by ~50%. These findings suggest that alternative pathways may mediate cell proliferation in these cells. The effect of XMD8-92 on cell proliferation was evident only at the highest dose (10 μM) in MDA-MB-231 and TAMR MCF-7 cells. We have previously shown that effects of a high XMD8-92 dose could be recapitulated by the addition of AX15836 (ERK5 inhibitor) and CPI203 (BRD4 inhibitor).[37] Therefore, at high doses, in addition to ERK5 inhibition, XMD8-92 may have off-target effects, including inhibition of bromodomain (BRD)4.[119] Trametinib or XMD8-92 did not decrease cell proliferation in BT-549 cells, which may indicate that alternative pathways mediate cell proliferation in these cells. XMD8-92 significantly decreased cell proliferation at 10 μM concentration, while trametinib did not decrease cell proliferation in TU-BcX-4IC cells. As indicated above, BT-549 cells are PTEN mutant cells and may rely more on the AKT pathway for survival and proliferation. Additionally, together with the data on cell migration, these data suggest that migration and proliferation may be controlled by distinct mechanism in TNBC cells.

We observed that MDA-MB-231 cells were the most responsive to the effects of XMD8-92 and trametinib on MET, whereas BT-549 cells were the least responsive, which

led us to characterize differences in cellular signaling between the two TNBC models. To explore these putative differences in the MAPK signaling pathways, we first examined the effects of trametinib and XMD8-92 on nuclear localization of ERK5. Our is the first study to examine nuclear localization of ERK5 in TNBC.

We found that the ERK5 inhibitor did not decrease nuclear ERK5 activation or total expression. This observation is consistent with a recent study, which has shown that ERK5 inhibitors that target the kinase domain were shown to activate the transcriptional activation domain (TAD) of ERK5, resulting in the nuclear localization and increased transcriptional activity of ERK5.[120] This may explain why our data with respect to the effect of ERK5 inhibition on E-cadherin conflicts with studies that have shown that inhibition of ERK5 via knockdown or knockout enhances E-cadherin expression in several cancer models.[121-122] Since trametinib decreased nuclear ERK5, ERK1/2 activation may be a putative mechanism for the translocation of ERK5 into the nucleus in MDA-MB-231 cells. ERK1/2 has been shown previously to promote ERK5 translocation to the nucleus in response to growth factor stimulation.[59] However, constitutively active RAF may be responsible for constitutive ERK1/2 activation and subsequent translocation of ERK5 in the nucleus of MDA-MB-231 cells under unstimulated condition. We are currently investigating mechanisms for ERK5 nuclear translocation in BT-549 cells.

To further explore hypothesis that inhibition of both the ERK1/2 and ERK5 pathways are necessary to induce the MET in TNBC, MDA-MB-231 and BT-549 cells were infected with dominant negative (dn) and constitutive active (ca) MEK1 and/or MEK5. Although phenotypic shifts were noted following infection of the ca or dn MEK,

the morphological transitions were more pronounced when both pathways were activated or inhibited in MDA-MB-231 and BT-549 cells. This was supported by decrease in ZEB1 expression in MDA-MB-231 cells following dnMEK1 and/or dnMEK5 infection and increase in ZEB1 expression in BT-549 cells following caMEK1 and/or caMEK5 infection (Figure 4.12). It is possible that ZEB1 expression is maximum in MDA-MB-231 cells and could not be induced further. Therefore, the more pronounced mesenchymal morphology following caMEK5 and caMEK1+caMEK5 infection may be a result of increase in vimentin expression (Figure 4.14) and/or ERK5 activation (Figure 4.10B) and its association with the actin cytoskeleton as previously described.[108] Moreover, ERK5 activation increased more significantly in caMEK1 + caMEK5 group vs GFP than in the caMEK5 group vs GFP (Figure 4.10B), indicating that ERK5 may be activated by both MEK1 and MEK5 signaling. This observation supports the data that show that trametinib, a known MEK1/2 inhibitor, decreased ERK5 activation in MDA-MB-231 cells. We speculate that the effect of trametinib on ERK5 inhibition was mediated via MEK1/2 inhibition and not by direct binding of trametinib to MEK5 or ERK5. Since ERK1/2 and ERK5 share 50% sequence homology at the N-terminal domain, it is possible that MEK1/2 may phosphorylate ERK5 by direct binding. It is also possible that ERK1/2 may phosphorylate ERK5 at its C-terminal by direct interaction, as reported previously.[59] These data further support the conclusion that inhibition or activation of both pathways is necessary for the MET or EMT, respectively. These data, together with the effect of trametinib and XMD8-92 on morphology, suggest that inhibition of both the ERK1/2 and ERK5 pathways is necessary to induce a full MET in TNBC cells.

The trametinib-mediated decrease in ZEB1 expression was partially reversed in MDA-MB-231 cells transfection with caMEK5. These data suggest that trametinib mediates its effect on MET in MDA-MB-231 cells, at least in part, via ERK5 inhibition and, most likely, via dual ERK1/2 and ERK5 inhibition. However, the trametinib-mediated increase in E-cadherin expression was not decreased by caMEK5, which may indicate that trametinib induces E-cadherin expression via ERK1/2 inhibition alone in these TNBC cells. This observation further supports the data that suggest there is no change in E-cadherin expression following XMD8-92 treatment in MDA-MB-231 cells.

While trametinib caused an overall decrease in ZEB1 expression in BT-549 cells, transfection with caMEK5 did not decrease its ability to induce MET as determined by examining cell morphology, E-cadherin, expression, and ZEB1 expression. This further supports our data that suggest that ERK1/2 inhibition, but not ERK5 inhibition, induces MET in BT-549 cells. We also observed that there was an overall reduction in ZEB1 expression in cells with an epithelial morphology following treatment with trametinib in both the TNBC cell lines and there was no cell population that had a complete loss of ZEB1. Such fine-tuning could be advantageous to avoid catastrophic side effects on healthy mesenchymal cells in the body, which depend on ZEB1 for their normal function.

The effect of ERK1/2 and ERK5 pathway inhibition or activation on vimentin expression were examined in 2D and spheroid cultures of MDA-MB-231 cells. Trametinib moderately decreased vimentin expression in MDA-MB-231 VIM RFP cells in 2D culture (Figure 4.14A), but completely inhibited vimentin expression in spheroid culture (Figure 4.14B), indicating that treatment with trametinib may be specifically important in targeting

mesenchymal and anoikis-resistant cells. Moreover, trametinib-mediated decrease in spheroid viability was not rescued by caMEK1, caMEK5, and caMEK1+caMEK5 groups at 7 day (Figure 4.15). This indicates that the reduction in vimentin expression in spheroids was not due to a decrease in spheroid viability. Since the reduction of vimentin by trametinib was partially reversed by co-treatment with constitutively active MEK1 and/or MEK5, trametinib-mediated decrease in vimentin may be due to inhibition of both ERK1/2 and ERK5 pathways in MDA-MB-231 cells. XMD8-92 significantly decreased the spheroid viability at 1μM concentration, which was rescued by caMEK5 and caMEK1+caMEK5 transfection indicating that ERK5 has a crucial role in regulating the survival of anoikis-resistant spheroids (Figure 4.15). Dysregulation of anoikis, a type of programmed cell death that occurs in cells when they detach from a cellular matrix, is an important step in tumor metastases. Together, these data suggest that ERK1/2 activation has a greater role in regulating the EMT in spheroids, while ERK5 activation regulates the survival of these anoikis-resistant spheroids.

As previously described, some single-agent inhibitors of MAPK pathway(s) led to an intermediate E/M state, which may be a predictor of metastases and poor prognosis. Therefore, combination strategy for MAPK inhibitors needs to be developed. We examined the effect of dual ERK1/2 and ERK5 pathway inhibition on spheroid viability, an assay representative of EMT. MAPK gene alterations are common in endocrine-resistant breast cancer.[123] This explains why Tra and XMD combination produced greater inhibition of spheroid and cell viability compared to either drug alone in TAMR MCF-7 cells (Figure 4.17-4.18). In conclusion, our data suggest crucial roles of ERK1/2 and

ERK5 pathways in mediating EMT and MET, cell migration, proliferation, and spheroid formation in TNBC and TAMR breast cancer. Since crosstalk may exist between the MAPK and PI3K or epigenetic pathways, in the next chapter, we will discuss some relevant combination strategies of MAPK pathway inhibitors with AKT or epigenetic inhibitors.

Chapter 5: Effect of Compound 1 (SC-1-151) alone and in combination with epigenetic inhibitors, CDK4/6 inhibitor Palbociclib, or AKT inhibitor ipatasertib on cell viability, proliferation, or spheroid formation in breast cancer

5.1 Introduction

The use of MEK1/2 inhibitors as cancer therapeutics has been clinically beneficial for treatment of previously incurable cancers, such as melanomas. However, the therapeutic use of MEK1/2 inhibitors is limited due to dose-dependent side effects and drug resistance. Therefore, several components, including activation mechanisms, kinase-substrate relationships, feedback mechanisms, and crosstalk with parallel pathways, need to be examined.

We have shown that the novel dual MEK1/2 and MEK5 inhibitor, compound 1 (SC-1-151; compound 1 will be referred to as SC-1-151 from here on) decreases cell proliferation, migration, and spheroid formation in the previous chapter. However, sustained inhibition of the MAPK pathway can result in the loss of negative feedback-mediated inactivation loops and paradoxical activation of ERK.[124] This could be mediated via a decreased expression of tumor suppressor dual specificity phosphatase (DUSP) 6, which is transcriptionally regulated by members of the Erythroblast Transformation Specific (ETS) family of transcription factors.[125] Reactivation of RNA polymerase-II-mediated parallel survival pathway transcription factors, such as ETS1, ETS2, and bromodomain 4 (BRD4), have been shown to compensate for the inhibition of the MAPK pathway, limiting the standalone targeting of MAPKs (Figure 5.1). In fact, BRD4 is known to promote breast cancer metastasis via Jagged1/Notch1 signaling.[126] Therefore, the

combination of MAPK inhibitors with transcription factor-targeted small molecule inhibitors, such as JQ-1 (pan-BRD inhibitor), is a relevant strategy for the treatment of breast cancer tumorigenesis. Histone deacetylases (HDACs) are another class of epigenetic regulators that are also known to mediate resistance to MAPK inhibitors in melanoma and prostate cancer.[127-128] Therefore, we hypothesized that SC-1-151+LBH-589 (HDAC inhibitor) will synergize to reduce cell viability in triple-negative and TAMR breast cancers.

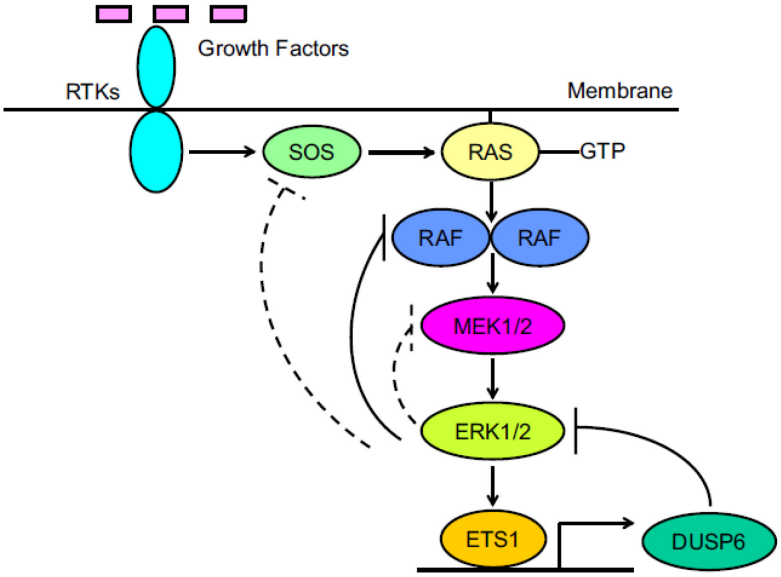

Figure 5.1: Negative feedback regulation of RAS/MAPK pathway.[129]

Dysregulation of the cell cycle often accompanies the dysregulation of the MAPK pathways, either as a direct consequence of aberrant MAPK activation (or vice versa) or as parallel pathways that promote tumorigenesis (Figure 5.2).[20, 130] Cyclin-dependent kinase 4/6 (CDK4/6) phosphorylates retinoblastoma (Rb) and promotes entry into the cell cycle by mediating transition into the synthesis (S) phase of the cell cycle. CDK4/6

inhibitors block Rb phosphorylation and lead to cell cycle arrest. Palbociclib, an oral and selective CDK4/6 inhibitor, is FDA approved for use in the first- and second-line settings for metastatic hormone-receptor positive breast cancer. Moreover, CDK4/6 inhibitors in combination with MAPK inhibitors decrease cell proliferation in melanoma, head and neck cancer, and colorectal cancer.[131] However, the effect of CDK4/6 inhibitors in combination with MAPK inhibitors at low concentration in tamoxifen-resistant breast cancer remains unknown. As crosstalk between the ERK and AKT signaling pathways has been noted in TNBC,[37] the AKT pathway may lead to reduced efficacy of MAPK inhibitors in TNBC. Therefore, the effect of MAPK pathway inhibition in combination with AKT inhibition was evaluated on spheroid viability in TNBC and TAMR MCF-7 cells.

In this chapter, we explore three strategies to improve the efficacy SC-1-151. First, we examine the effect of cotreatment with inhibitors of MAPK signaling and bromodomains or HDAC on cell viability in TNBC and TAMR cells using SC-1-151 in combination with JQ-1. Next, we evaluate the effect of SC-1-151 in combination with palbociclib on cell proliferation in TAMR breast cancer cells. Finally, SC-1-151 or the MEK5 inhibitor SC-1-181 was used in combination with the AKT inhibitor ipatasertib to evaluate the effect of combination on spheroid viability. Overall, these strategies may help decrease rate of recurrence due to drug resistance and prevent dose-limiting toxicities.

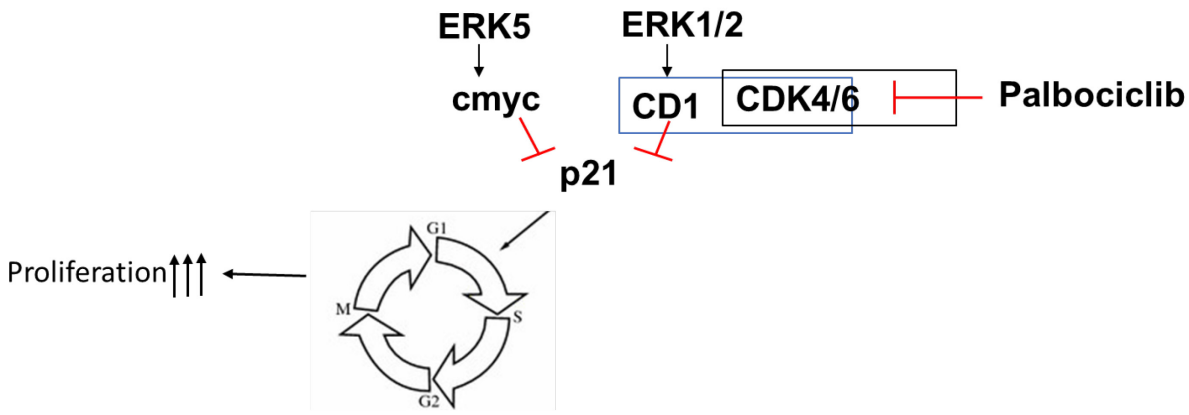

Figure 5.2: ERK5, ERK1/2, and CDK4/6 pathways and the cell cycle. ERK1/2 and ERK5 pathways may regulate the cell cycle and proliferation via CD1 and CDK4/6.

5.2 Hypothesis

SC-1-151 and epigenetic, CDK4/6, or AKT inhibitors will produce a synergistic decrease in cell viability in triple-negative and tamoxifen-resistant breast cancer cells.

5.3 Results

5.3.1 Effect of Compound 1 (SC-1-151) on cell viability in breast cancer.

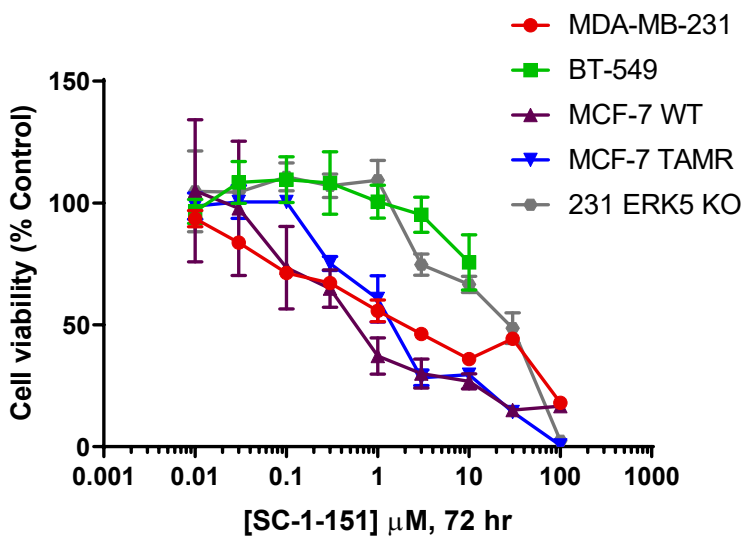

Figure 5.3: Effect of SC-1-151 on breast cancer cell viability. Cells were treated with SC-1-151 at increasing concentrations for 72 hours. MTT assay was performed to assess cell viability.

TNBC and TAMR breast cancer cell lines were treated with SC-1-151 at increasing concentrations (0.01, 0.03, 0.1, 0.3, 1, 3, 10 uM) for 72 hours. MTT assay was performed to assess cell viability. SC-1-151 decreased cell viability at 0.01 – 10uM concentrations in MDA-MB-231 cells, but not in BT-549 cells or in ERK5 knockout (KO) MDA-MB-231 cells. SC-1-151 was equally effective in reducing cell viability in wildtype and tamoxifen-resistant MCF-7 cells (Figure 5.3).

5.3.2 SC-1-151 synergistically inhibits cell viability in combination with JQ-1 in breast cancer

Since sustained MAPK inhibition may result in a loss of feedback mediated via DUSP6, it is important to investigate the effect of MEK inhibitors in combination with alternative therapies. Since alternative pathways, including BRD4 or HDAC signaling,

could promote cell survival in the absence of MEK1/2 signaling, we combined SC-1-151 with bromodomain inhibitor JQ-1 or HDAC inhibitor LBH589. SC-1-151 and JQ-1 were found to synergistically decrease cell viability in TNBC and TAMR cells at low concentrations. There was a greater that 50% reduction in cell viability after treatment of TNBC cells with 0.3 uM concentration of each inhibitor and TAMR cells with 0.1 uM of each inhibitor as indicated by the fraction affected (Figure 5.4, Table 5.1).

The crosstalk between RAS and PI3K pathways is well-defined in cancer.[132] Interestingly, we have noted an increase in AKT activation following treatment with SC-1-151. Others have reported that JQ-1 decreases AKT activation in endometrial cancer via upregulation of PTEN.[133] Therefore, to gain mechanistic insights behind the observed synergy between SC-1-151 and JQ-1, ERK1/2 and AKT activation was examined after 5 days of treatment with SC-1-151 or JQ-1 alone and in combination. SC-1-151, but not JQ-1, inhibited ERK1/2 phosphorylation, however, the combination of SC-1-151 and JQ-1 produced a greater inhibition of ERK1/2 phosphorylation than SC-1-151 alone. A compensatory increase in AKT phosphorylation was noted following SC-1-151 treatment. While JQ-1 did not decrease AKT activity alone, it inhibited the increase in AKT activation by SC-1-151 (Figure 5.5).

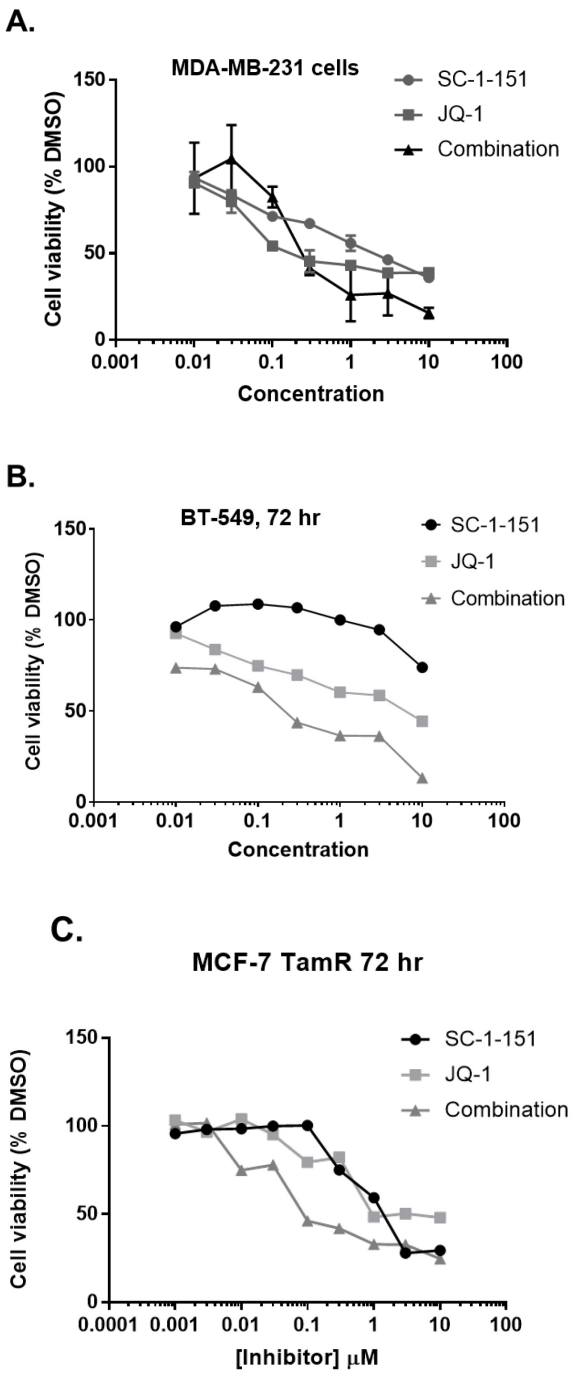

Figure 5.4: SC-1-151 + JQ-1 combination synergistically decreases cell viability in diverse breast cancer subtypes. (A) MDA-MB-231, **(B)** BT-549, **(C)** MCF-7 TAMR cells were treated with drugs alone and in combination for 72 hours. Cell viability was determined using MTT assay.

MDA-MB-231			
Combination (151+JQ-1)	**Fraction affected (Fa)**	**Combination index (CI)**	**Synergy designation**
0.01, 0.01	0.066	15.35	Antagonism
0.03, 0.03	0.066	46.04	Antagonism
0.1, 0.1	0.18	8.50	Antagonism
0.3, 0.3	0.59	0.22	Strong synergy
1, 1	0.74	0.13	Strong synergy
3, 3	0.73	0.45	Strong synergy
10, 10	0.844	0.27	Strong synergy

BT-549			
Combination (151+JQ-1)	**Fraction affected (Fa)**	**Combination index (CI)**	**Synergy designation**
0.01, 0.01	0.25081	0.04685	Strong synergy
0.03, 0.03	0.2634	0.11683	Strong synergy
0.1, 0.1	0.359	0.11069	Strong synergy
0.3, 0.3	0.5568	0.03447	Strong synergy
1, 1	0.63033	0.04880	Strong synergy
3, 3	0.63375	0.14049	Strong synergy
10, 10	0.85065	0.01659	Strong synergy

TAMR MCF-7			
Combination (151+JQ-1)	**Fraction affected (Fa)**	**Combination index (CI)**	**Synergy designation**
0.01, 0.01	0.2486	0.01694	Strong synergy
0.03, 0.03	0.2179	0.05750	Strong synergy
0.1, 0.1	0.536	0.06919	Strong synergy
0.3, 0.3	0.579	0.18330	Strong synergy
1, 1	0.671	0.46164	Strong synergy
3, 3	0.673	1.37601	Strong synergy
10, 10	0.75007	3.50970	Strong synergy

Table 5.1: Effect of SC-1-151 and JQ-1 combination on fraction affected and combination index. The fraction affected was calculated and synergy was determined by Chou-Talalay Method using CompuSyn Software.

5.3.3 Effect of SC-1-151 and JQ-1 alone and in combination on ERK1/2 and AKT activation.

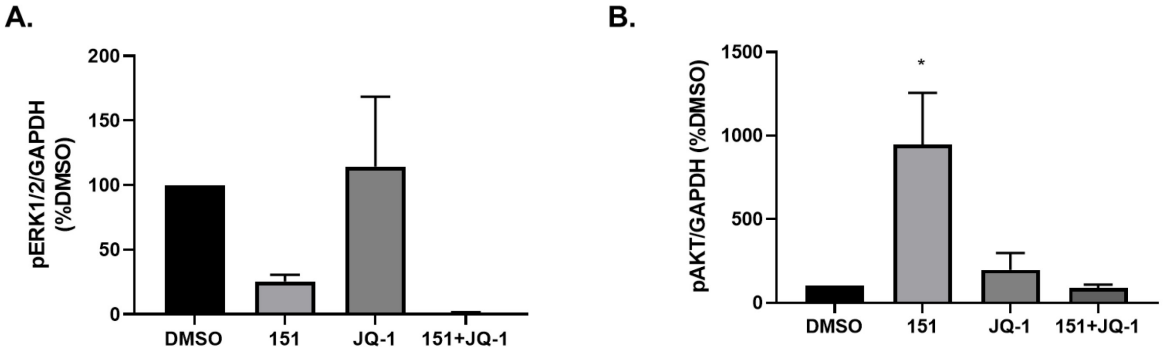

Figure 5.5: JQ-1 decreases AKT activation induced by SC-1-151 treatment in MDA-MB-231 cells. MDA-MB-231 cells were treated with 1 μM SC-1-151 and 300 nM JQ-1 alone and in combination for 5 days. ERK1/2 and AKT activation was examined by western blotting. Data were analyzed by One-way ANOVA with Bonferroni post-hoc correction.

5.3.4 SC-1-151 and LBH-589 cotreatment does not synergistically reduce cell viability in TNBC and TAMR MCF-7 cells.

MDA-MB-231, BT-549, and TAMR MCF-7 cells were treated with increasing concentrations of SC-1-151, LBH-589, and 1:1 combination of the two drugs for 72 hours. Our data suggest that LBH-589 or SC-1-151 treatment alone inhibited cell viability in breast cancer cell lines. SC-1-151+LBH-589 cotreatment did not produce a synergistic reduction in cell viability in TNBC cells (Figure 5.6). The lack of synergy may be due to a maximal decrease in cell viability following LBH-589 treatment alone.

We also examined ERK1/2 and AKT activation after treatment with 100nM LBH-589 or 1 μM SC-1-151 alone and in combination. LBH-589 produced a compensatory increase in ERK1/2 activation. This increase in ERK1/2 activation was inhibited by SC-1-151. Both SC-1-151 and LBH-589 treatment alone produced a 10-fold increase in AKT activation, which may explain why there was no synergy with this combination (Figure 5.7).

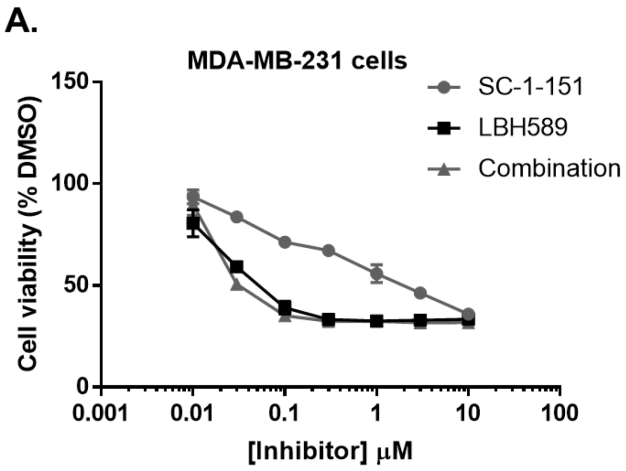

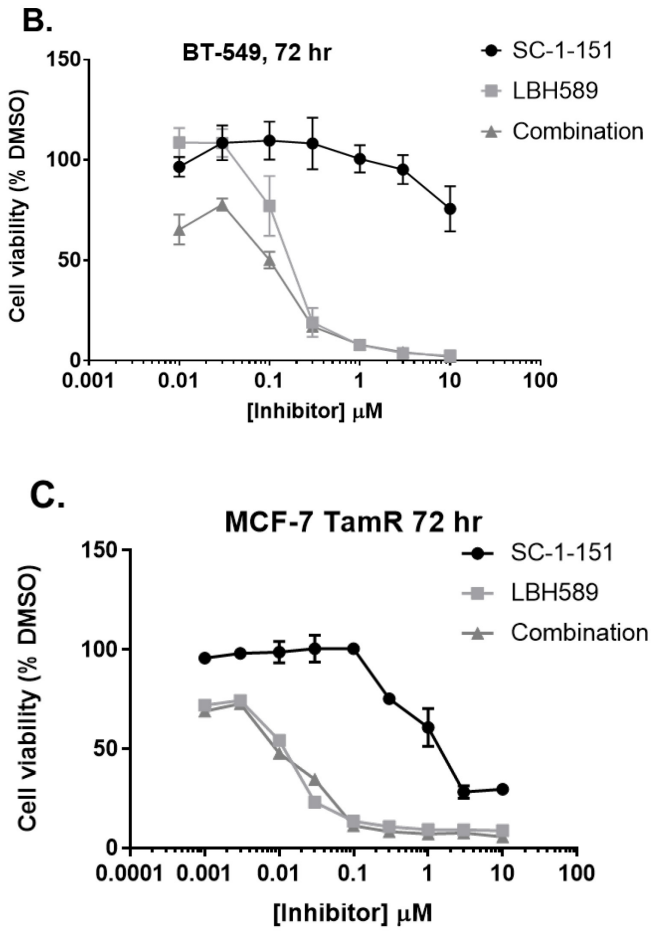

Figure 5.6: SC-1-151 + LBH589 modestly synergize to decrease cell viability in BT-549 cells. (A) MDA-MB-231, **(B)** BT-549, **(C)** MCF-7 TAMR cells were treated with drugs alone and in combination for 72 hours. Cell viability was determined using MTT assay.

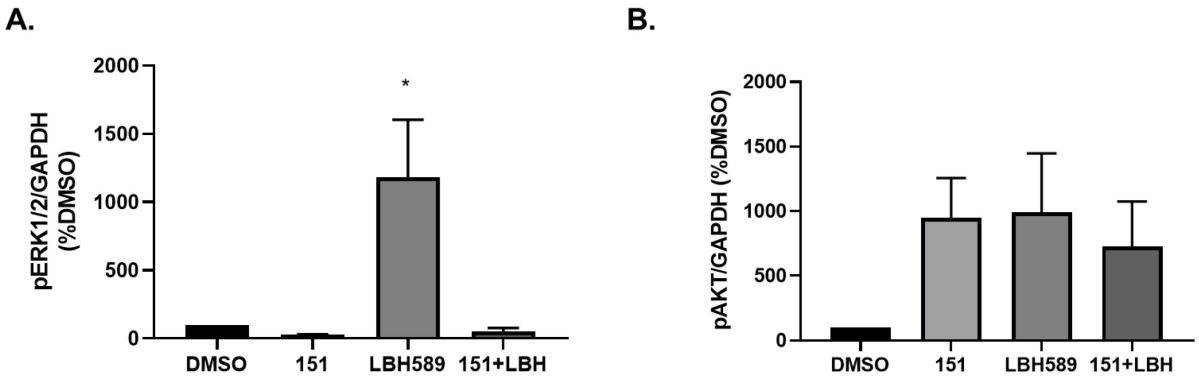

Figure 5.7: SC-1-151 and LBH-589 activate AKT in MDA-MB-231 cells. MDA-MB-231 cells were treated with SC-1-151 and LBH-589 alone and together to examine kinase activation after 5 days of treatment.

5.3.5 Effect of SC-1-151+Palbociclib on cell proliferation in TAMR MCF-7 cells.

Recent studies have shown that MEK inhibition is important for enhanced efficacy of CDK4/6 inhibitors in various cancer models.[131] TAMR MCF-7 cells were treated with SC-1-151 and palbociclib alone and in combination at 0.1 or 1 μM concentration. Palbociclib significantly decreased cell proliferation at 0.1 and 1 μM concentrations, while SC-1-151 decreased cell proliferation only at the 1 μM concentration. In the combination groups, the decrease in cell proliferation was mainly mediated by palbociclib (Figure 5.8).

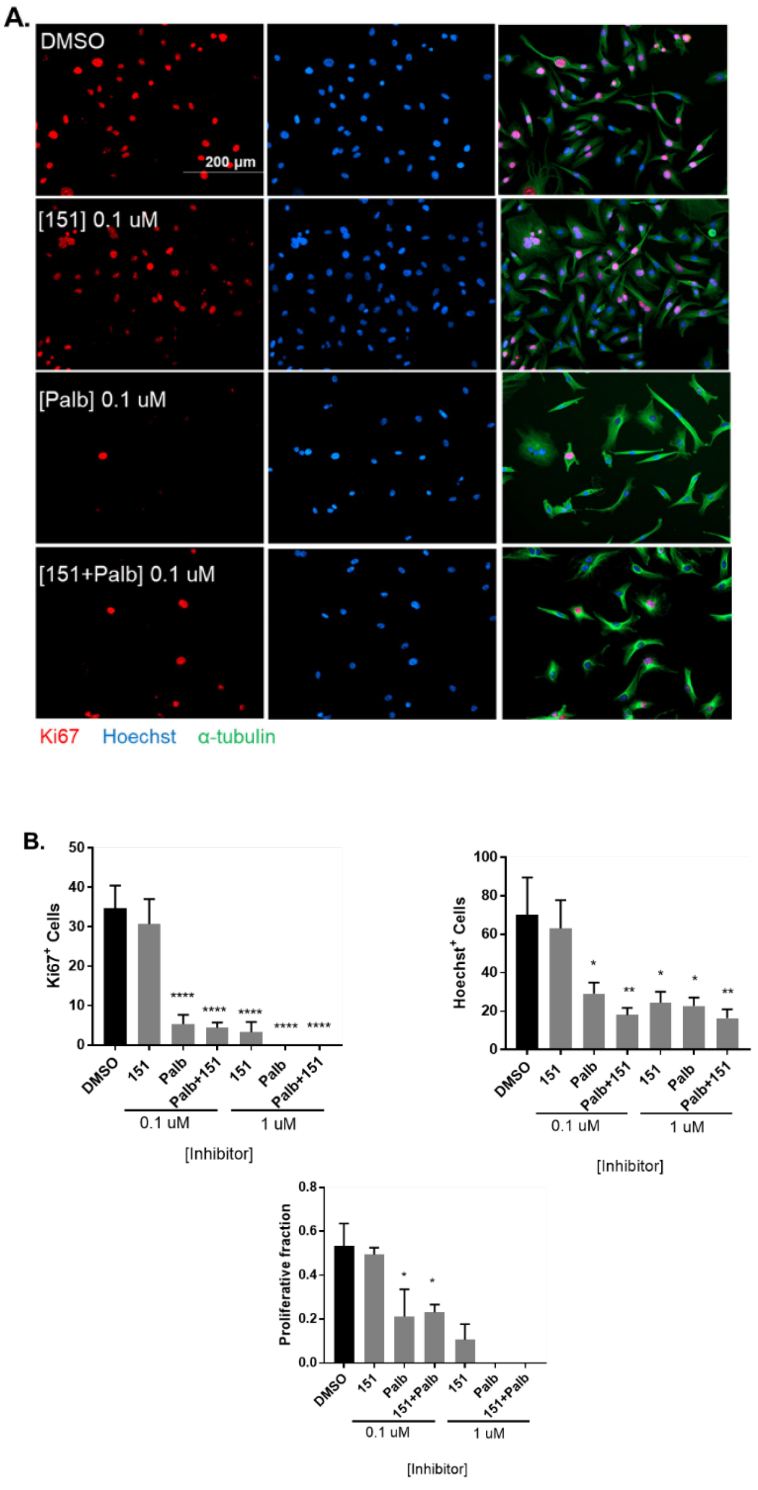

Figure 5.8: Effect of SC-1-151 in combination with Palbociclib on cell proliferation in TAMR MCF-7 cells.

Since the reduction in cell proliferation in 1:1 SC-1-151:Palb combination groups was dominated by palb, we examined the effect of a larger ratio of SC-1-151 to Palbociclib (10:1 combination ratio). SC-1-151 (1uM) and Palbociclib (0.1uM) synergistically decreased cell proliferation in wildtype MCF-7 cells (Figure 5.9A); however, the reduction in cell proliferation in TAMR MCF-7 cells was mainly mediated by SC-1-151. While Palbociclib alone significantly decreased cell proliferation, there was no further reduction in the combination group (Figure 5.9 B).

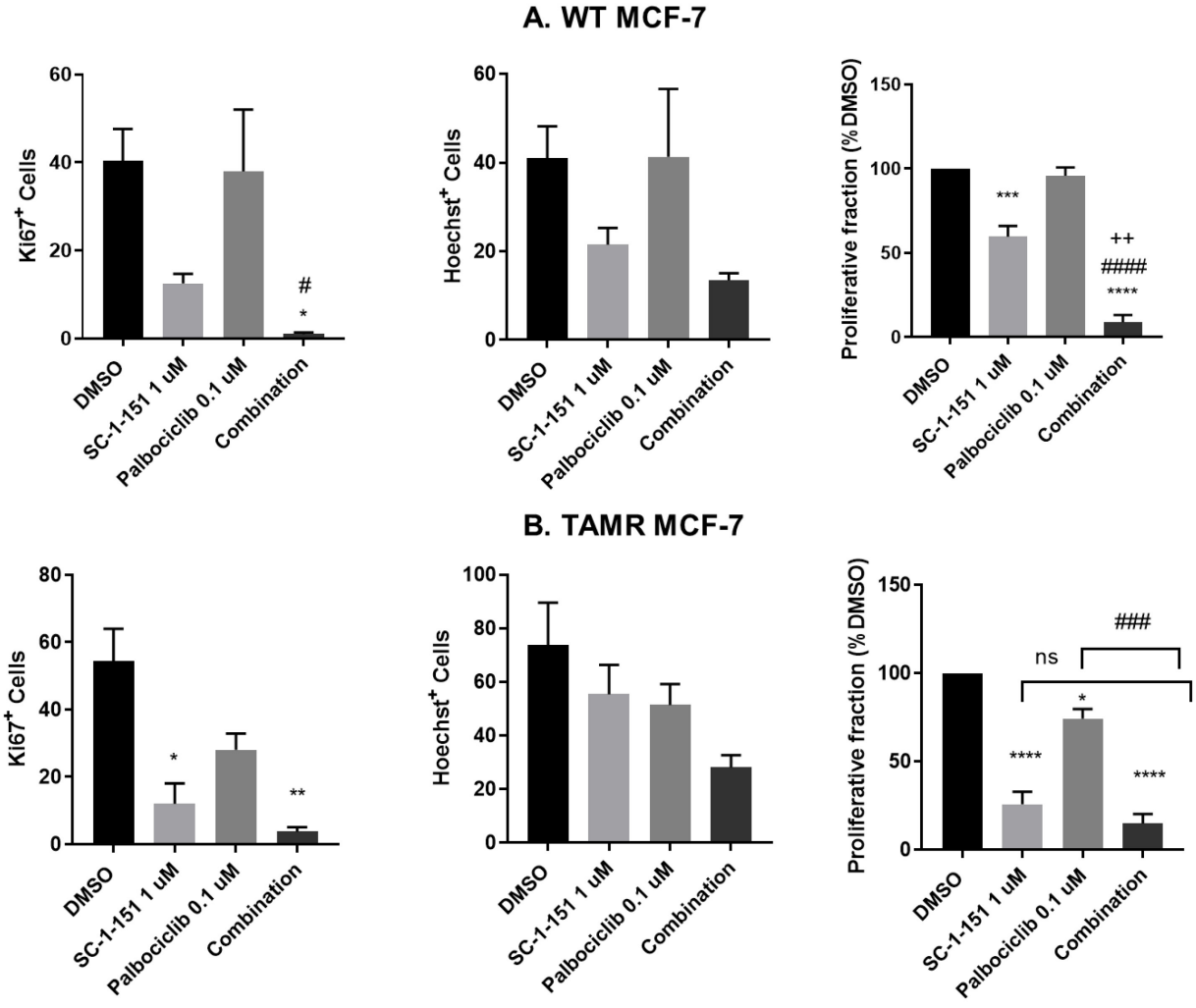

Figure 5.9: SC-1-151 and Palbociclib synergistically decrease cell proliferation in (A) WT-MCF-7 cells but not in (B) TAMR-MCF-7 cells.

5.3.6 Inhibition of MEK1/2, MEK5, and PI3K pathways decreases nuclear ERK5 expression or activation and decreases spheroid viability in breast cancer cells.

Treatment with the AKT inhibitor ipatasertib alone, did not decrease spheroid viability in MDA-MB-231 and TAMR MCF-7 cells. However, the effect of ipatasertib on cell viability was potentiated by MEK inhibitors in these cells (Figure 5.10 A, C). Ipatasertib alone decreased spheroid formation in BT-549 and TU-BcX-4IC cells and there was a synergistic effect when these cells were treated with ipatasertib in combination with the MEK inhibitors (Figure 5.10B, D).

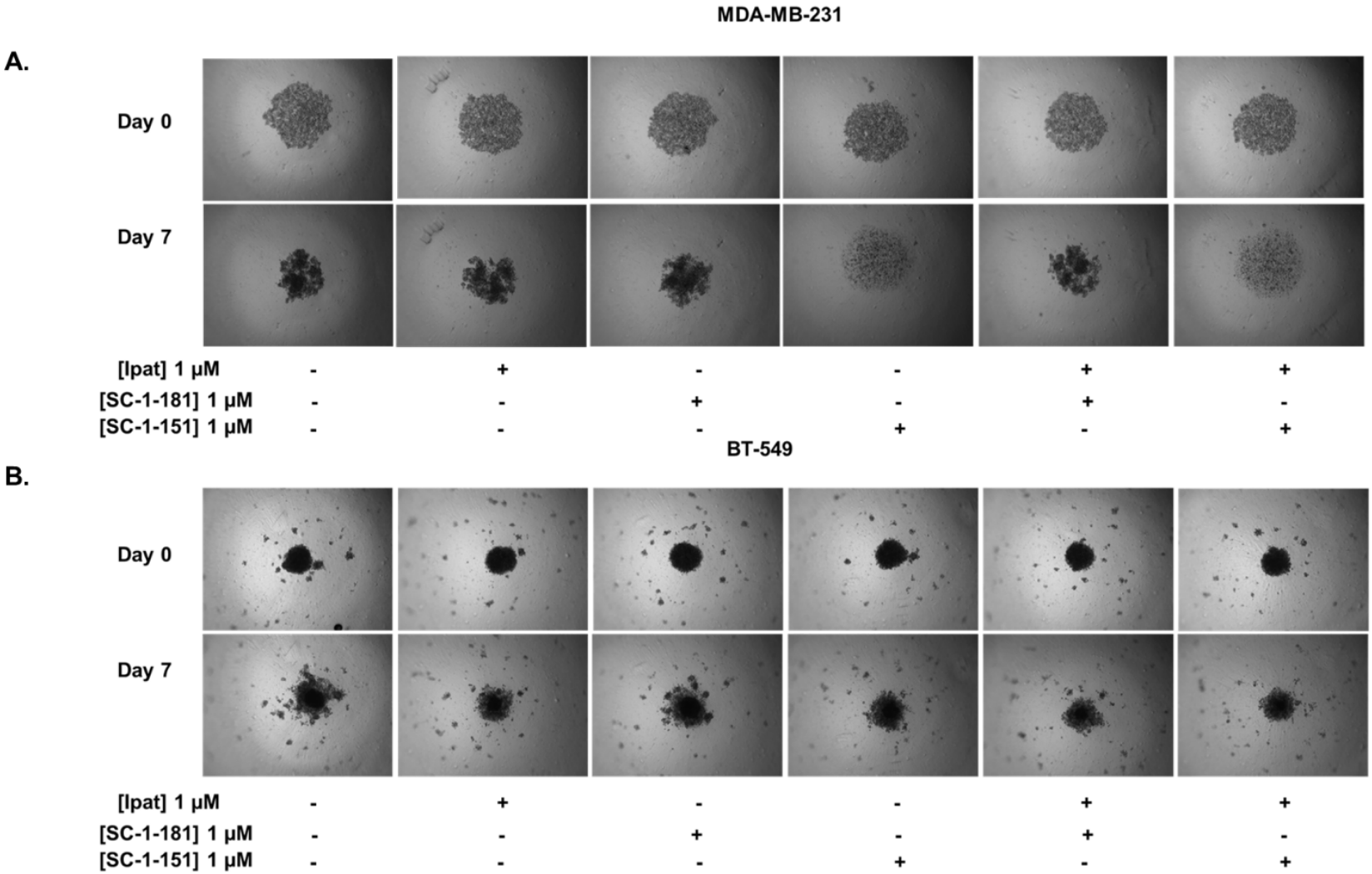
A.
MDA-MB-231
Day 0
Day 7
[Ipat] 1 μM - + - - + +
[SC-1-181] 1 μM - - + - + -
[SC-1-151] 1 μM - - - + - +
B.
BT-549
Day 0
Day 7
[Ipat] 1 μM - + - - + +
[SC-1-181] 1 μM - - + - + -
[SC-1-151] 1 μM - - - + - +

C.

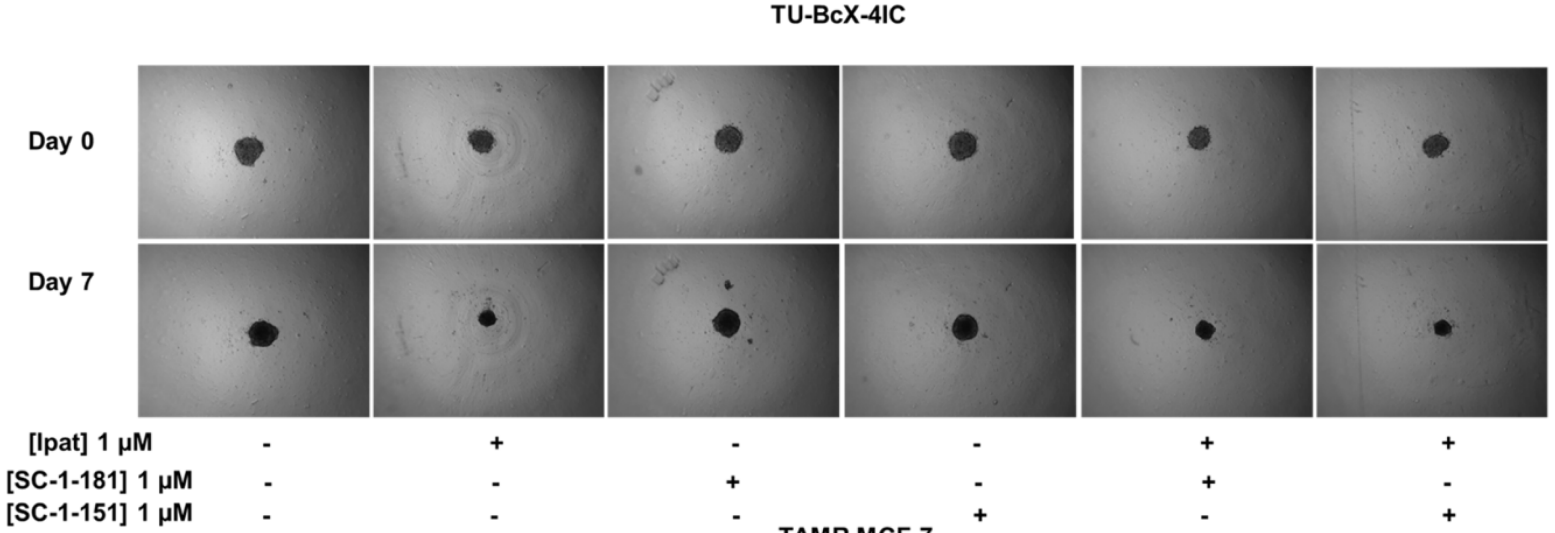
TU-BcX-4IC
Day 0
Day 7
[Ipat] 1 μM - + - - + +
[SC-1-181] 1 μM - - + - + -
[SC-1-151] 1 μM - - - + - +

D.

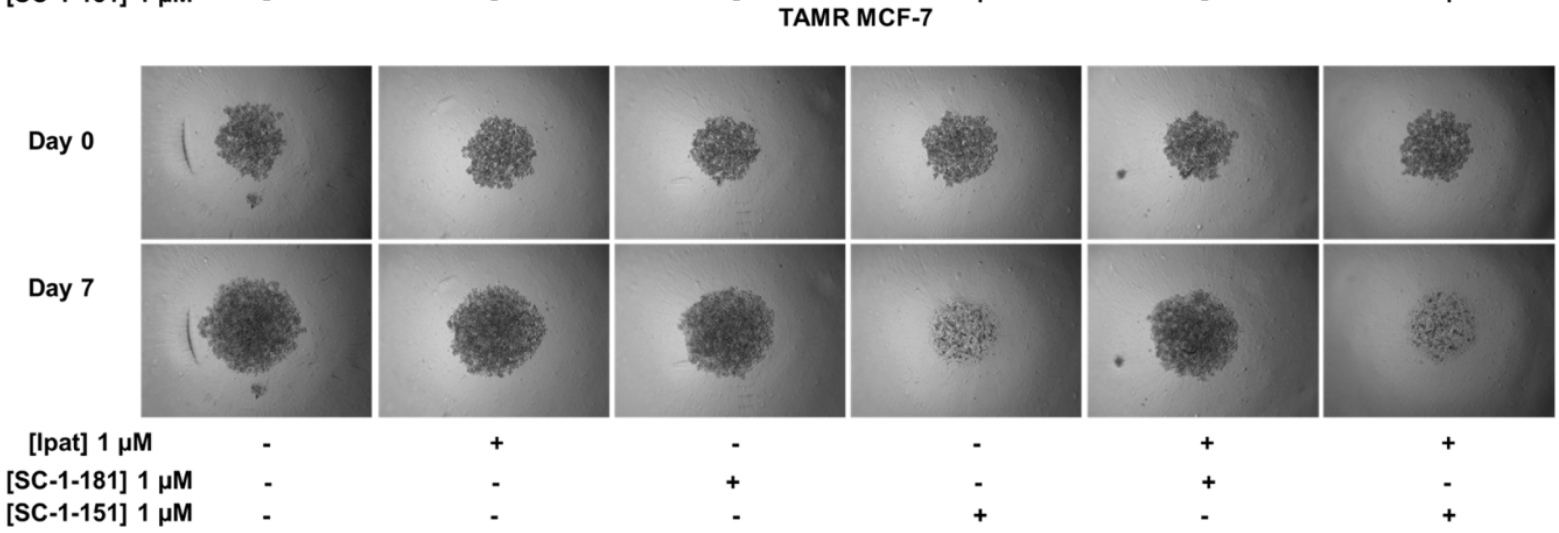
TAMR MCF-7
Day 0
Day 7
[Ipat] 1 μM - + - - + +
[SC-1-181] 1 μM - - + - + -
[SC-1-151] 1 μM - - - + - +

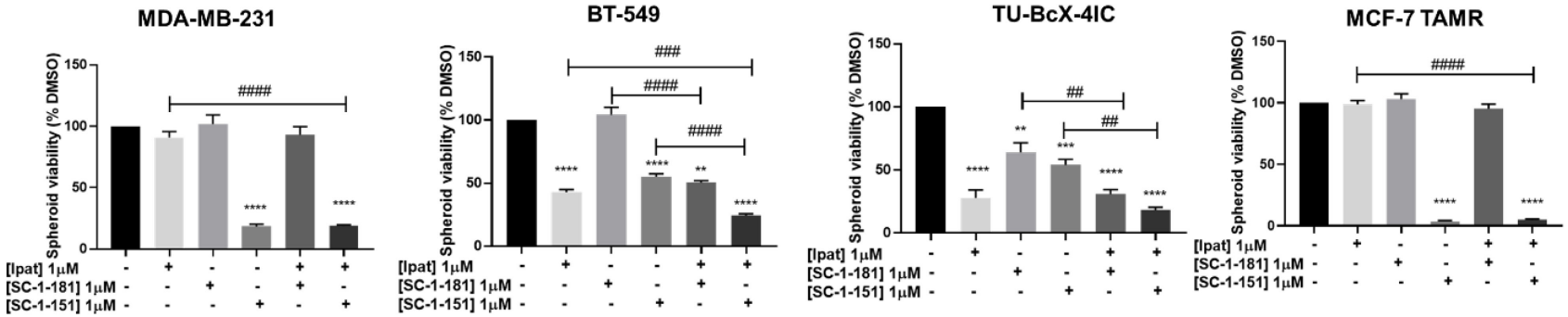

Figure 5.10: Effect of SC-1-151 or SC-1-181 in combination with ipatasertib on spheroid viability in diverse breast cancer subtypes. Effect of SC-1-151 (dual MEK1/2 and MEK5 inhibitor) or SC-1-181 (MEK5 inhibitor) alone and in combination with ipatasertib was evaluated on spheroid viability in (E) MDA-MB-231, (F) BT-549, (G) TU-BcX-4IC and (H) TAMR MCF-7 cells. Spheroid viability was assessed on day 7 after treatment. Data indicate ± SEM of experiments run in triplicate *p<0.05; **p<0.01; ***p<0.001; ****p<0.0001 *vs* DMSO control group, ##p<0.01; ###p<0.001; ####p<0.0001 *vs* individual drug determined by one-way ANOVA with the Bonferroni post hoc test.

Our findings suggest that alternative mechanisms may underlie the activation and nuclear translocation of ERK5 in BT-549 cells because treatment with ERK5 inhibitor XMD8-92 or MEK1/2 inhibitor trametinib did not decrease nuclear ERK5 activation in BT-549 cells. This may also explain why trametinib only induced a partial MET and XMD did not induce a MET in BT-549 cells. We hypothesized that nuclear ERK5 may be responsible for increasing the transcription of genes involved in EMT and spheroid formation. To understand the differences in response to Ipat+181 or Ipat+151 treatment in different breast cancer subtypes, MDA-MB-231 (responsive to MEK1/2 and MEK5 inhibition) and BT-549 cells (responsive to MEK1/2, MEK5, and AKT inhibition) were treated with ipatasertib alone and in combination with SC-1-181 or SC-1-151 for 72 hours and nuclear extracts were collected to examine ERK5 activity and expression of a MEF2 family member MEF2C, a downstream target of ERK5 signaling. MEF2C levels in the nucleus are representative of ERK5 activity.[134]

In MDA-MB-231 cells, SC-1-151, like trametinib (Chapter 4), decreased nuclear ERK5. SC-1-151 and Ipat+SC-1-151 combination groups produced a maximum decrease in nuclear ERK5 and MEF2C expression. SC-1-181 or Ipatasertib alone or in combination did not decrease nuclear ERK5 activation, expression. Ipat+SC-1-151 group produced a maximum decrease in MEF2C expression (Figure 5.11A). In BT-549 cells, ipatasertib modestly decreased ERK5 activation and SC-1-181 modestly decreased MEF2C expression. Surprisingly, ipatasertib in combination with SC-1-181 or SC-1-151 produced a maximum decrease in nuclear ERK5 and MEF2C expression (Figure 5.11B).

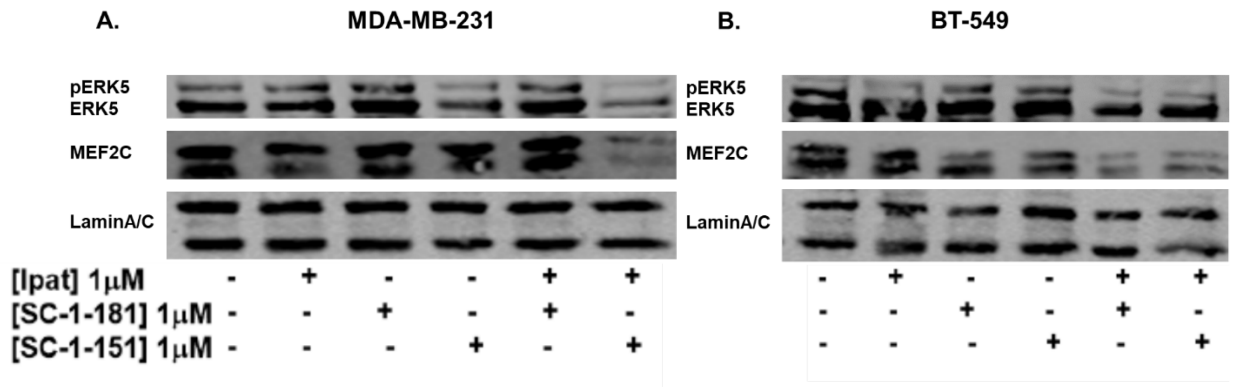

Figure 5.11: Inhibition of MAPK and PI3K pathways decreases nuclear ERK5 and MEF2C in TNBC cells. (A) MDA-MB-231 **(B)** BT-549 cells were treated with AKT inhibitor ipatasertib alone and in combination with SC-1-181 of SC-1-151 for 72 hours. Nuclear extracts were prepared as per the standard protocol.

5.4 Discussion:

In this chapter, we further characterized the effects of SC1-151 on TNBC and TAMR viability, examined the effects of SC-1-151 alone and in combination with a BRD4, HDAC, or cell cycle inhibitor on breast cancer cell viability and proliferation, and examined the effect of the inhibitors on ERK1/2 and AKT pathway activation. SC-1-151 decreased cell viability in MDA-MB-231, TAMR MCF-7, and WT MCF-7 cells. In contrast, SC-1-151 did not decrease cell viability in BT-549. MDA-MB-231 cells have a mutation in the RAF gene which leads to aberrant MEK activity. This may explain why these cells were more sensitive than BT-549 cells to the toxic effects of the dual ERK1/2 and ERK5 pathway inhibitor SC-1-151. The decrease in cell viability following SC-1-151 treatment in wildtype and TAMR MCF-7 cells suggests that tamoxifen-resistance does not affect the cell viability response to dual MEK1/2 and MEK5 inhibition. SC-1-151 did not inhibit cell viability in ERK5-KO MDA-MB-231 cell. This may indicate that inhibition either ERK1/2 or ERK5 pathway may be sufficient to decrease cell viability in MDA-MB-231 cells and perhaps ERK1/2 does not fully compensate for the loss of ERK5 in MDA-MB-231 cells.

In the current study, inhibition of MEK1/2/5 and BRD4 with SC-1-151 and JQ-1, respectively, produces a synergistic effect on cell viability in TNBC and TAMR breast cancer cells. This synergy may be a result of inhibition of shared downstream targets. ETS1/2 is an important downstream target of the ERK1/2 pathway. ETS1/2-mediated gene transcription is also mediated by bromodomain 4 (Figure 5.12). Moreover, we found that a compensatory increase in AKT activation by SC-1-151 was inhibited by JQ-1, which may also explain the observed synergy. Although pharmacological inhibitors with dual ERK5/BRD4 activity are known to decrease cell proliferation in cancer, ours is the first study to report a synergistic effect on cell viability with inhibition of the ERK5 and BRD4 pathways.[119]

The effects of histone deacetylase inhibitors on tumor progression are being recently studied in metastatic breast cancers.[135] Phase-III clinical trial with HDACi in breast cancer has shown promising results. HDAC inhibitors have been shown to synergize with MAPK inhibitors to inhibit cell viability and stemness in medulloblastomas.[136] However, we did not observe synergy between MAPK and HDAC inhibitors in TNBC and TAMR breast cancer. The increase in AKT activation by SC-1-151 (dual MEK1/2 and MEK5 inhibitor) and LBH-589 may be responsible for lack of synergistic response in the combination group. LBH-589 (HDAC inhibitor) alone may have decreased cell viability to its maximum. In future, more combination ratios will be utilized to evaluate the effect on cell viability as well as other functional assays representative of EMT. MDA-MB-231 cells have a mutation in the RAF gene which leads to aberrant MAPK activity. This may explain why these cells were more sensitive to the toxic effects of the dual ERK1/2 and ERK5 pathway inhibitor SC-1-151. Overall, the results from our study

highlights the relevance of targeting MAPK pathway in combination with BET or HDAC inhibitors to target cell viability and proliferation in breast cancer.

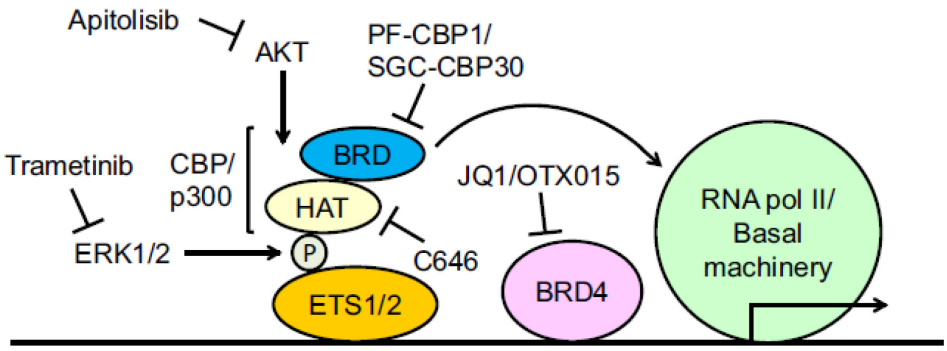

Figure 5.12: Coregulation of ETS1/2-mediated response by MEK1/2 and bromodomain pathways.[129]

Cyclin-dependent kinases play a critical role in regulating the cell cycle and are relevant targets in cancer. Activation of cyclinD1 levels by upstream mitogenic factors and activation of RAS-RAF-MEK-ERK can promote cellular progression to the S phase and compensate for inhibition of the cell cycle by CDK4/6 inhibitors.[130] To explore a possible synergistic effect of MAPK and cell cycle inhibition, we examined proliferation in WT and TAMR MCF-7 cells following treatment with SC-1-151 or Palbociclib, the CDK4/6 inhibitor, alone and in combination. In the SC-1-151 and palbociclib combination, the reduction in cell proliferation was mediated by either palbociclib in 1:1 combination or SC-1-151 in 10:1 combination group. Future studies will be performed to utilize more combination ratios and to examine synergy.

We found that dual ERK1/2 and ERK5 inhibition was sufficient to inhibit spheroid viability in MDA-MB-231 and TAMR MCF-7 cells but further inhibition of AKT was necessary further inhibit spheroid formation in BT-549 and TU-BcX-4IC cells. This

difference may be because SC-1-151, inhibits both ERK1/2 and ERK5 activation by EGF in MDA-MB-231 and TAMR MCF-7 cells, but only inhibits the ERK1/2 activation in BT-549 cells. We found that dual ERK1/2 and ERK5 inhibition was sufficient to decrease spheroid formation in MDA-MB-231 and TAMR-MCF-7 cells whereas additional inhibition of AKT was necessary further inhibit spheroid formation in BT-549 and TU-BcX-4IC cells.

As discussed in the previous chapter, trametinib, a MEK1/2 inhibitor or XMD8-92, an ERK5 inhibitor did not reduce nuclear ERK5 in BT-549 cells meaning alternative pathways may regulate ERK5 nuclear localization in BT-549 cells. Since crosstalk between ERK5 and AKT pathways has been noted and BT-549 cells have a PTEN mutation, we examined whether inhibition of AKT would reduce nuclear ERK5 activity. ERK5 activation and MEF2C expression were examined after treating MDA-MB-231 and BT-549 cells with ipatasertib alone and in combination with SC-1-181 or SC-1-151. Overall, our data suggest that MEK1/2, MEK5, and AKT pathways play an important role in regulating nuclear ERK5 activity. Decrease in nuclear ERK5 activity may be one of the reasons behind observed synergy between MAPK and AKT inhibitors.

Chapter 6: Effect of MAPK or PI3K pathway inhibition on low-dose chemotherapeutic sensitivity in triple-negative breast cancer

6.1 Introduction

Doxorubicin, paclitaxel, and carboplatin are the chemotherapeutic drugs that remain the mainstay treatment for TNBC patients.[137] Unfortunately, TNBCs become resistant to most chemotherapeutic drugs. Drug resistance and off-target toxicity are major problems associated with administration of high doses of chemotherapeutic agents in the clinic. Inherent and acquired mechanisms of drug resistance include dependence of tumors on alternative/novel mutations, increase in drug efflux transporters, and compensatory activation of kinase pathways, which can prolong the survival of cancer cells.

ERK5 overexpression is associated with poor overall survival in breast cancer patients after treatment with chemotherapeutic drugs (Figure 6.1).[30] ERK5 inhibition is known to reverse doxorubicin resistance via p53 upregulation in lung and ovarian cancers.[138] AKT activation is known to mediate resistance to doxorubicin by downregulated PTEN expression in ER-positive breast cancer.[139] Moreover, downregulation of ETS-1, a target of ERK1/2 was found to enhance cisplatin and doxorubicin toxicity in breast cancer.[18] In ovarian cancer, ERK1/2 activation following cisplatin treatment has been shown to mediate resistance to cisplatin.[140] Moreover, ERK1/2 and AKT pathways are known to mediate chemoresistance in cancer via upregulation of multi-drug transporter proteins.[141-142] The goal of this research is to examine the effects of chemotherapeutic drugs at low doses on kinase activation and cell

viability in combination with known MAPK pathway inhibitors XMD8-92, trametinib, and ipatasertib.

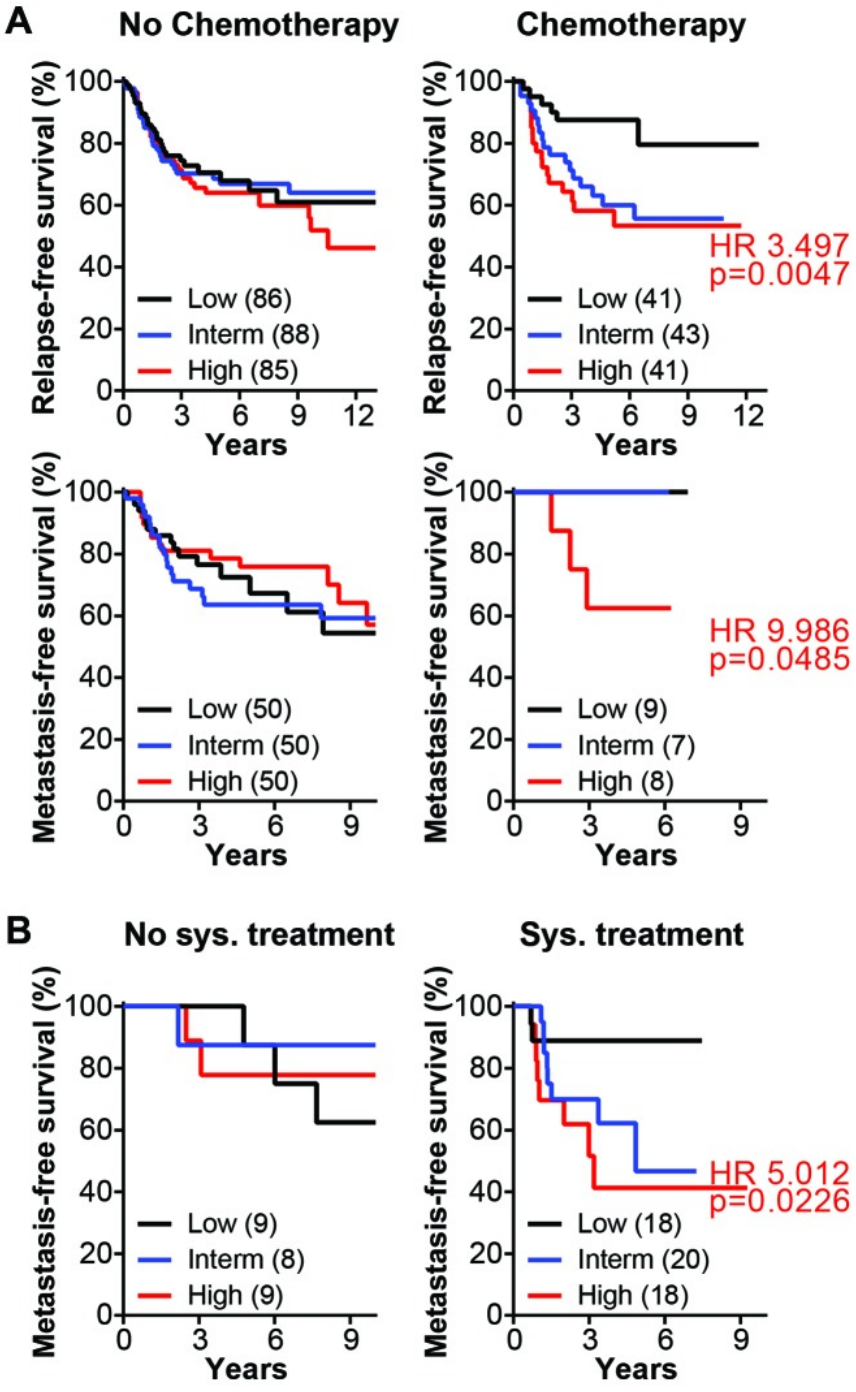

Figure 6.1: Poor overall survival after systemic treatment is associated with MEK5-ERK5 overexpression in TNBC patients.[30]

6.2 Hypothesis

Chemotherapeutic drugs will enhance sensitivity of MAPK or PI3K pathway inhibitors at low doses in triple-negative breast cancer cells.

6.3 Results

6.3.1 Effect of chemotherapeutic drugs doxorubicin, paclitaxel, and carboplatin on cell viability in TNBC

Concentration-response studies revealed differential responses of MDA-MB-231 and BT-549 cells to different chemotherapeutic drugs (Figure 6.2). These studies were performed to identify low doses at which the chemotherapeutic drug produced no effect on cell viability. Cells are resistant to the toxic effects of the drugs at low doses and the goal of our research is to examine whether combination of low-dose kinase inhibitors with low-dose chemotherapeutic drugs synergistically inhibit cell viability.

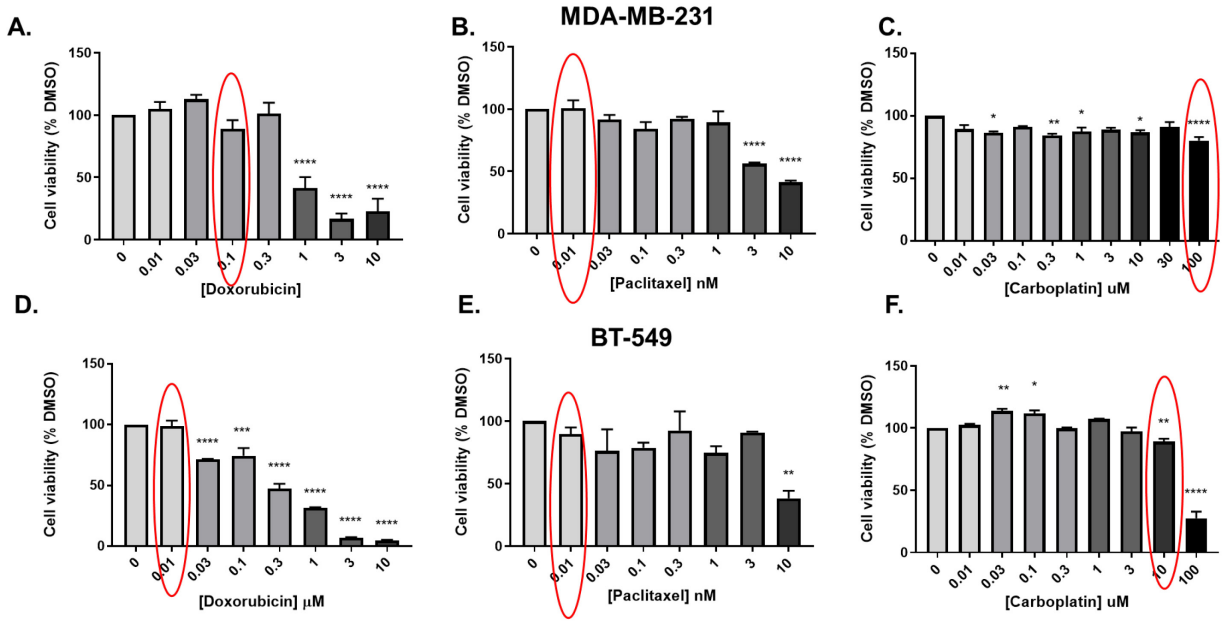

Figure 6.2: Cell viability response to doxorubicin, paclitaxel, and carboplatin in (A-C) MDA-MB-231 and **(D-F)** BT-549 cells.

Drug	MDA-MB-231	BT-549
Doxorubicin	100 nM	10 nM
Paclitaxel	100 pM	100 pM
Carboplatin	100 μM	10 μM

Table 6.1: Concentration at which the drug alone did not decrease cell viability. MTT-assay was performed to examine the effect of increasing concentrations of doxorubicin, paclitaxel, and carboplatin in MDA-MB-231 and BT-549 cells. The maximum concentration to produce no significant reduction in cell viability was selected and these concentrations are summarized in the table.

6.3.2 Cotreatment with low doses of kinase inhibitors and doxorubicin produces toxicity in both MDA-MB-231 and BT-549 cells.

MDA-MB-231 and BT-549 cells were treated with increasing concentrations (0.01, 0.03, 0.1, 0.3, and 1 μM) of the ERK5 inhibitor XMD8-92, the MEK1/2 inhibitor trametinib, and the AKT inhibitor ipatasertib. These doses of inhibitors did not decrease TNBC cell viability (Figure 6.3). DMSO or low-dose doxorubicin were added to TNBCs treated with the various doses of kinase inhibitors (Table 6.1). After 72 hours of treatment, MTT assay was performed to assess cell viability. Cotreatment with low dose of doxorubicin sensitized MDA-MB-231 and BT-549 cells to low doses of XMD8-92 (Figure 6.3 A, D). Trametinib and ipatasertib alone decreased MDA-MB-231 cell viability even at low doses. Doxorubicin did not enhance the toxicity of either kinase inhibitor (Figure 6.3C). In BT-549 cells, trametinib and ipatasertib did not produce decreases in cell viability on their

own. However, in combination with low dose doxorubicin both trametinib and ipatasertib significantly decreased in cell viability in BT-549 cells (Figure 6.3F).

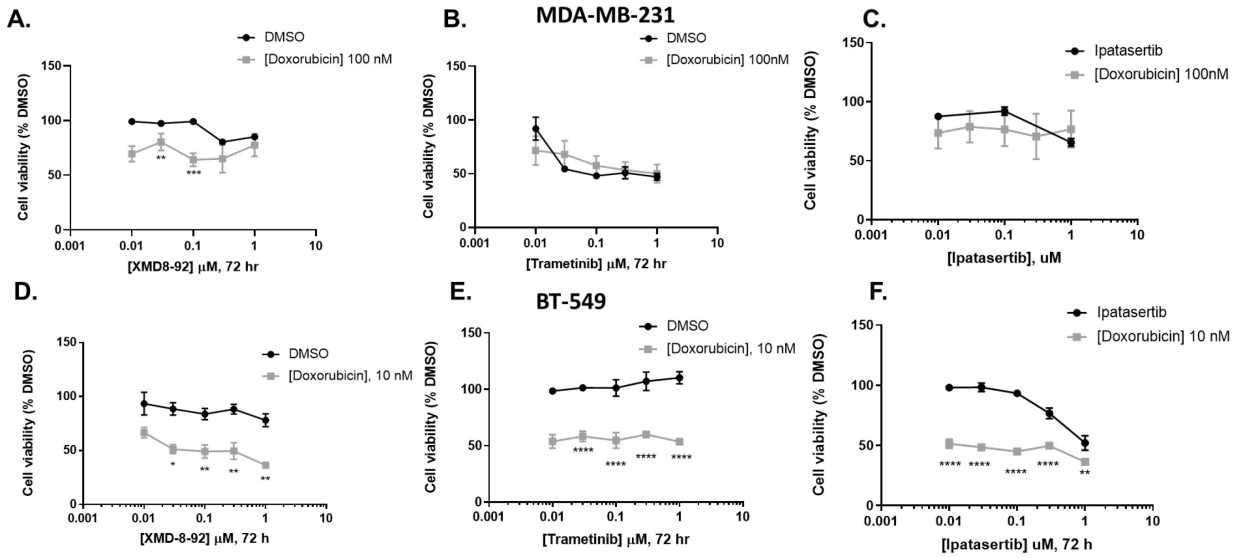

Figure 6.3: Effect of doxorubicin in combination with kinase inhibitors at 72 hours. Data represent the ± SEM of three independent experiments as a percentage of untreated DMSO control group. *p<0.05; **p<0.01; ***p<0.001; ****p<0.0001 combination vs. drug alone determined by two-way ANOVA with the Bonferroni *post hoc* test.

6.3.3 Single pathway kinase inhibitors do not enhance paclitaxel or carboplatin sensitivity in TNBC cells:

Similar as described above, TNBC cells were treated with paclitaxel or carboplatin in combination with kinase inhibitors. With the exception of potentiation at low doses of XMD8-92 in MD-MB-231 cells, cotreatment with paclitaxel or carboplatin and the kinase inhibitors did not significantly decrease cell viability (Figure 6.4 and 6.5). Interestingly, there was an antagonistic interaction between trametinib and paclitaxel or carboplatin because combination with paclitaxel or carboplatin reduced the ability of trametinib to decrease cell viability in MDA-MB-231 cells.

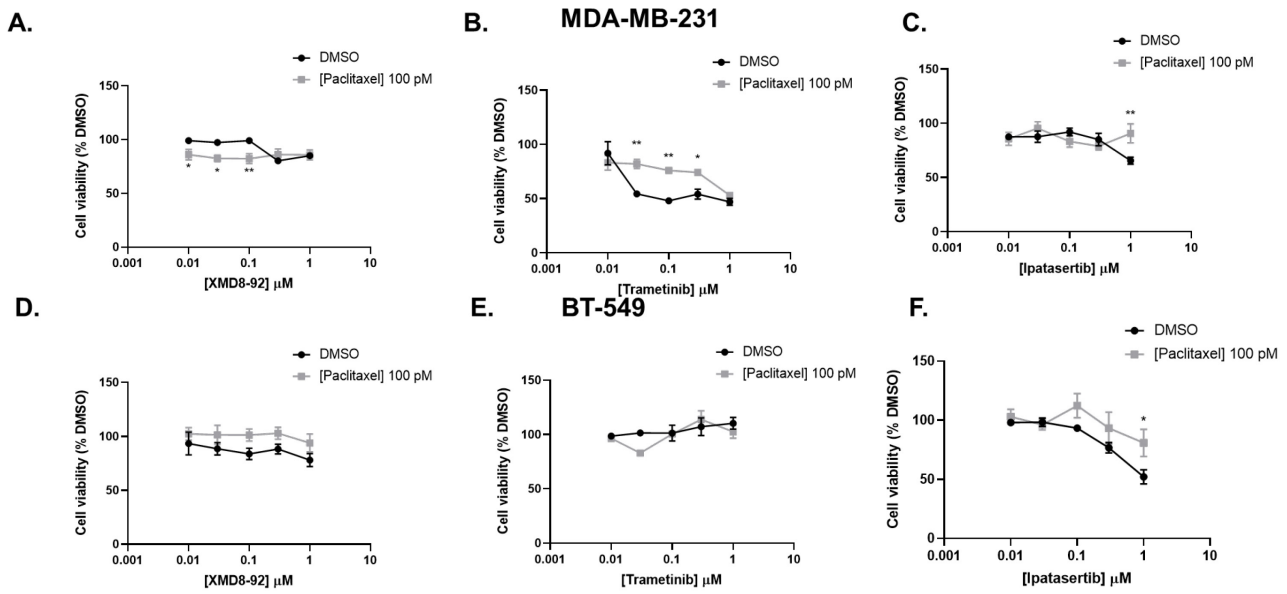

Figure 6.4: Effect of paclitaxel in combination with kinase inhibitors at 72 hours. Data represent the ± SEM of three independent experiments as a percentage of untreated DMSO control group. *p<0.05; **p<0.01 combination vs. drug alone determined by two-way ANOVA with the Bonferroni *post hoc* test.

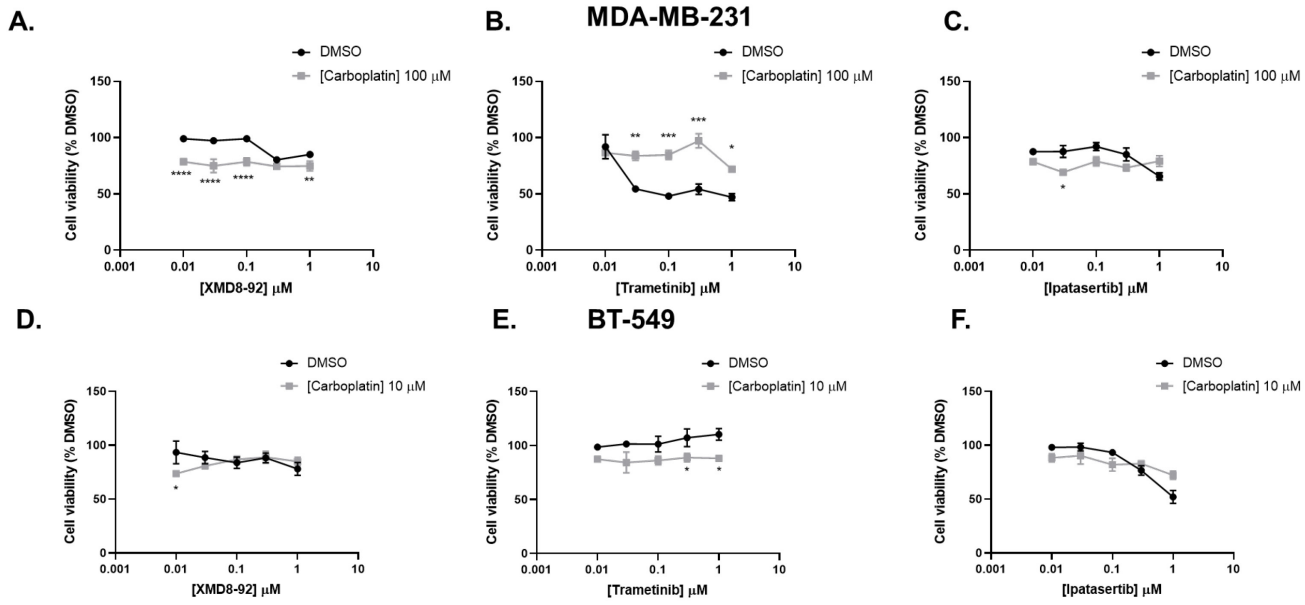

Figure 6.5: Effect of carboplatin in combination with kinase inhibitors at 72 hours. Data represent the ± SEM of three independent experiments as a percentage of untreated

DMSO control group. *p<0.05; **p<0.01; ***p<0.001; ****p<0.0001 combination vs. drug alone determined by two-way ANOVA with the Bonferroni *post hoc* test.

The drug efflux transporters, MDR1 and MRP1, are major drivers of chemotherapeutic resistance in several cancers. Inhibition of ERK5 signaling was shown to inhibit the activity of MDR1, which, in turn, increased the influx of doxorubicin into breast and lung cancer cells.[143] Therefore, we hypothesized that MAPK inhibitors will decrease MDR1 and MRP1 expression to increase the efficacy of low dose chemotherapeutics. Surprisingly, XMD8-92 and trametinib increased MDR1 and MRP1 expression in MDA-MB-231cells (Figure 6.6). In contrast, trametinib decreased MRP1 expression in BT-549 cells (Figure 6.6D). Ipatasertib did not alter MDR1 or MRP1 expression in either TNBC cell line.

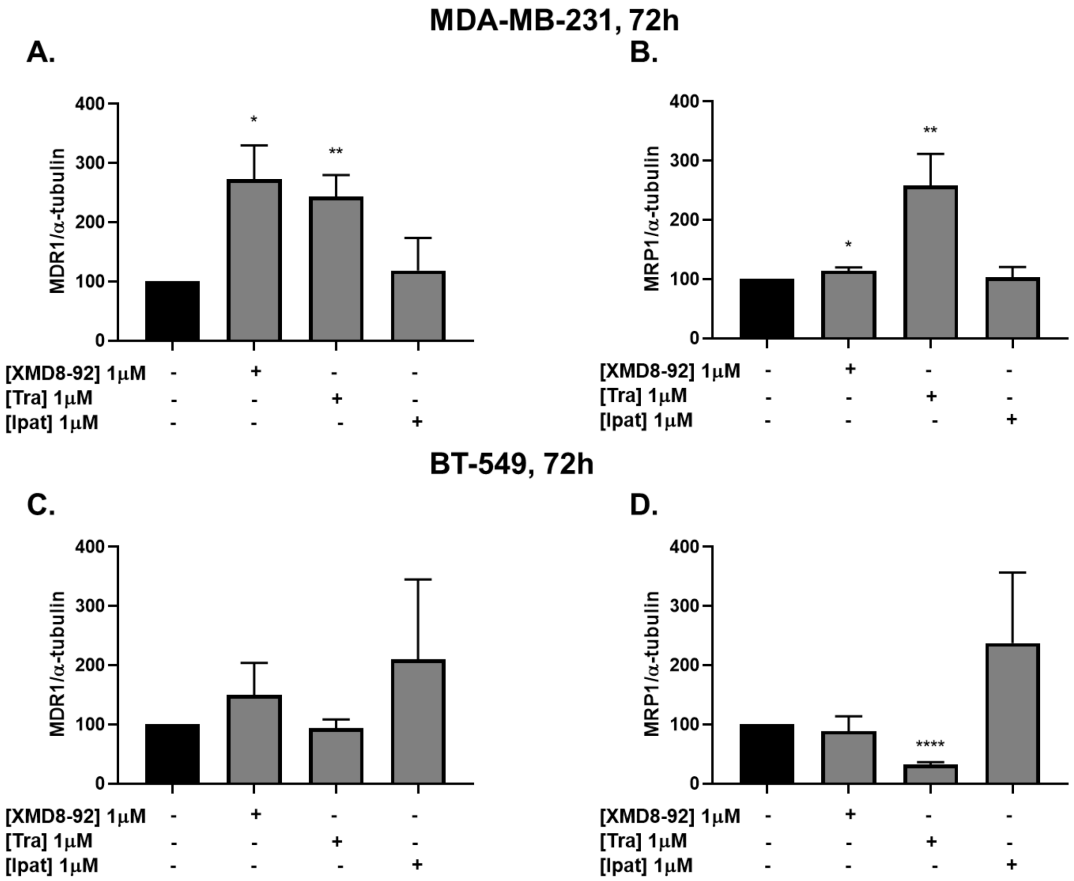

Figure 6.6 XMD8-92 and trametinib modulate the expression of drug efflux transporters in TNBC cells. Trametinib and XMD8-92 increase (A) MDR1 and (B) MRP1 expression in MDA-MB-231 cells, while trametinib decreases MRP1 expression in (C-D) BT-549 cells.

6.4 Discussion

In this study we evaluated whether low-dose chemotherapeutic drugs could enhance the efficacy of kinase inhibitors on cell viability in TNBC. MDA-MB-231 cells were less sensitive to toxic effects of doxorubicin and carboplatin compared to BT-549 cells. One of the reasons accounting for the difference could be the anatomical origin of the two models. MDA-MB-231 cells are derived from metastatic pleural effusions whereas BT-549 cells are derived from primary breast tumor. Since MDA-MB-231 cells are derived

from a metastatic site, these cells may be more aggressive and resistant to the toxic effects of chemotherapy.

Trametinib was found to have an antagonistic interaction with paclitaxel and carboplatin in MDA-MB-231 cells. Doxorubicin, paclitaxel, and carboplatin are known chemotherapeutic substrates for MDR1 and/or MRP1, respectively.[144] One of the possible mechanisms is upregulation of the drug efflux transporters MDR1 and MRP1 by trametinib. Since trametinib decreased MRP1 expression in BT-549 cells, this may be one possible mechanism for increase in sensitivity to cotreatment with doxorubicin or carboplatin and trametinib in BT-549 cells.

Ipatasertib combined with the chemotherapeutic drugs was not effective at decreasing cell viability in TNBC cells. Ipatasertib did not alter the expression of the efflux transporters in either cell line. One of the reasons why cotreatment with ipatasertib with doxorubicin, paclitaxel, or cisplatin did not induce cell death may be that there are compensatory increases in alternative pathways, including the MEK5-ERK5 pathway following AKT inhibition by ipatasertib. In fact, dual ERK5 and AKT inhibition has been shown to increase paclitaxel sensitivity in TNBC.[145] In the next chapter, we examine the effect of dual MEK5/PI3K inhibitors on the sensitivity of chemotherapeutic drugs in TNBC.

In conclusion, our combination data suggest that kinase inhibitors could be combined with chemotherapeutic drugs at low doses. Most chemotherapeutic drugs and kinase inhibitors are administered to the patients at the maximum tolerated dose. We have shown that same effect at higher doses of single drug could be recapitulated at lower doses of chemotherapeutic drug and kinase inhibitor. This approach could be beneficial to prevent collateral toxicity in healthy tissues.

Chapter 7: Evaluation of novel dual MEK5/PI3K quinazoline inhibitors in TNBC

7.1 Introduction

Triple negative breast cancer (TNBC) is in dire need for alternative therapies. Patients with TNBC expressing increased MEK5 display reduced relapse-free survival and increased mortality.[146] MEK5 is a serine/threonine protein kinase in the three-tiered mitogen activated protein kinase (MAPK) cascade that proceeds from external growth receptor signaling to ultimately mediate cell growth, invasion, and metastasis. Although inhibiting MEK5/ERK5 would seem to be an ideal strategy for TNBC therapies, suppression of the MEK5/ERK5 pathway causes a compensatory increase in the activity of the well-known oncogene AKT. Dual inhibition of ERK5 and AKT pathways using known pharmacological inhibitors has been shown to decrease cell viability and decrease off-target toxicity.[147] Therefore, we developed novel small molecule dual ERK5/AKT inhibitors in collaboration with the Flaherty lab to target TNBCs.

Our approach was to canvas the literature for known MEK5 inhibitors. The Binding Database identified a compound (Figure 7.1) from the Craig Thomas lab with off-target MEK5 inhibition (MEK5 IC_{50}=20 μM). The Thomas lab forwarded a sample of the compound while we conducted a re-synthesis. MEK5 inhibition in our cellular inhibition of was identical for each compound preparation. Subsequent analog synthesis from the lead compound and testing has generated over 70 compounds. These compounds were initially tested for MEK1,2 and 5 inhibition at a single dose of 10 μM as well as for alterations of pAKT, an indicator of AKT pathway activation.

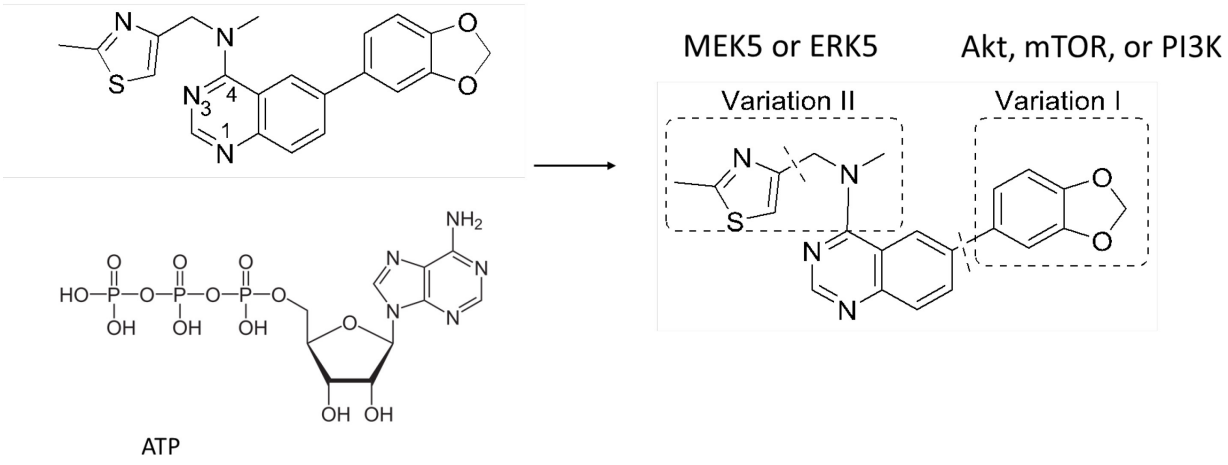

Figure 7.1: Compound from Rosenthal and colleagues.

Selected compounds from the quinazoline series identified compounds were inhibitors of the AKT pathway at the level of PI3K. Additionally, two of the selected compounds, SP-1-90 and SP-1-177 displayed both PI3K isoform selectivity and MEK5 inhibition. The cellular IC50 values were determined for SP-1-90 and SP-1-177. Moreover, the lead compounds were evaluated for their effects on cell viability and chemotherapeutic sensitivity in MDA-MB-231 and BT-549 cells.

7.2 Hypothesis

Chemotherapeutic drugs will enhance the effect of dual MEK5/PI3K inhibitors on cell viability in triple-negative breast cancer cells.

7.3 Results

7.3.1 Identification of quinazolines as dual ERK5/AKT inhibitors

MDA-MB-231 cells (500,000 cells/well) were cultured in a 6-well plate for 24 hours. To examine kinase activity or inhibition, the cells were serum-starved for 18-24 hours.

The quinazoline inhibitors (10 μM concentration) were added for 30 minutes prior to EGF (100ng/ml) stimulation for 15 minutes. Cell lysates were collected and examined for phospho- and total ERK5, ERK1/2, and AKT kinases using standard western blot procedure. Selected compounds were tested for EGFR activation to rule out off-target effects since the quinazoline core is conserved in several EGFR inhibitors. Substitution of hydrogen in K37 with a methyl group diminished EGFR activity while gaining ERK5 selectivity (Figure 7.2). The structures and results are summarized in appendix C.

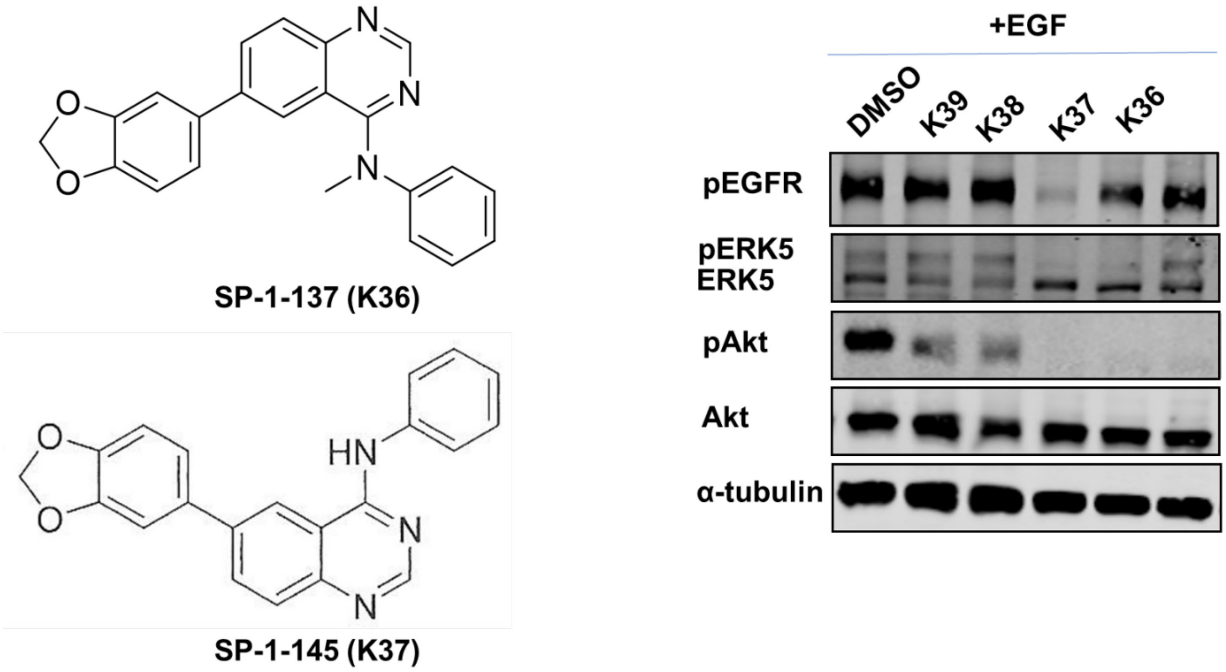

Figure 7.2. Structures and kinase activity data for quinazoline series. K36 was re-synthesis of the Rosenthal compound and used as a positive control to inhibit ERK5.

7.3.2 Potency of lead compounds

Inhibitors SP-1-190 (K33) and SP-1-182 (K46) were selected based on their kinase inhibition profiles (selective ERK5 and AKT inhibition). These compounds were further

evaluated to determine their IC_{50} values for ERK5, AKT, and cell viability inhibition (Figure 7.3).

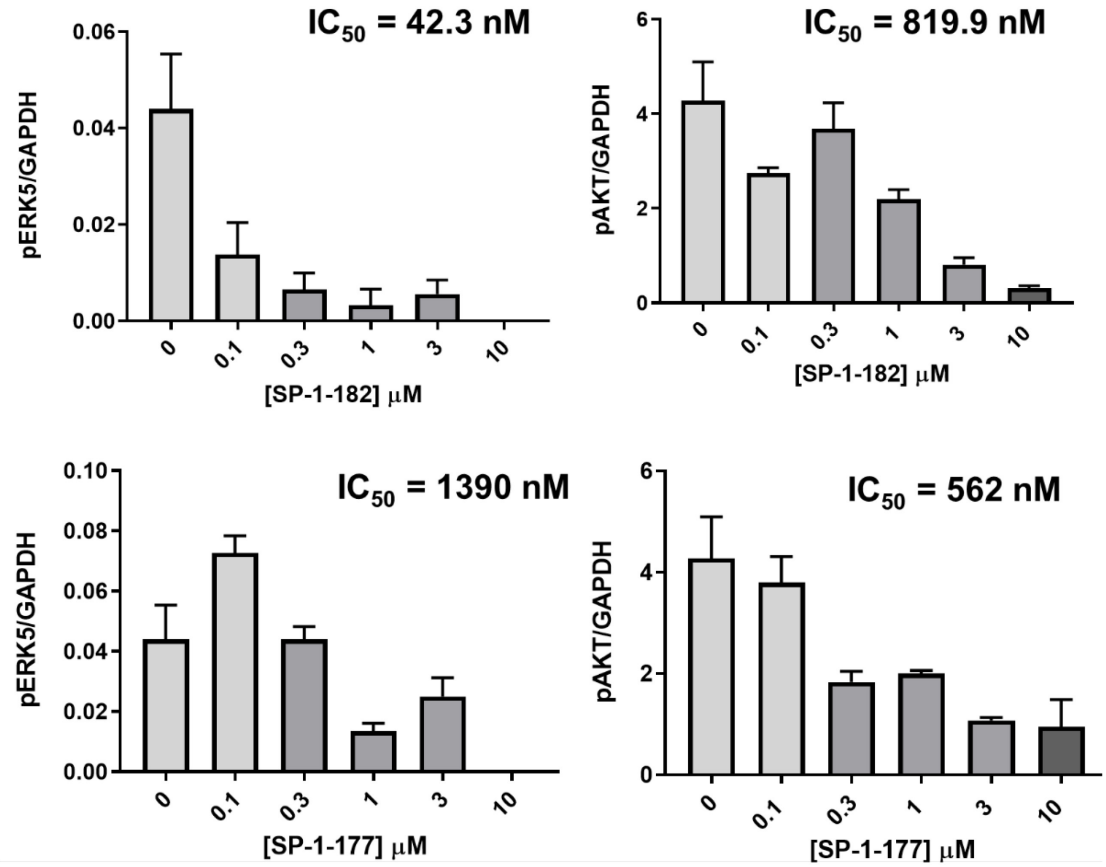

Figure 7.3 SP-1-177 and SP-1-182 are potent dual MEK5/PI3K inhibitors.

7.3.3 Doxorubicin enhances sensitivity of SP-1-177 in MDA-MB-231 cells

The lead compounds from diphenylamine (SC-1-181), thiophene (MG-5-5), and quinazoline (SP-1-77 and SP-1-182) series were combined with low-dose chemotherapeutic drugs paclitaxel, doxorubicin, and carboplatin to examine synergy in MDA-MB-231 and BT-549 cells. We found that SP-1-177, a dual MEK5/AKT inhibitor enhanced doxorubicin sensitivity in MDA-MB-231 cells (Figure 7.2.2). While SP-1-171

alone significantly decreased cell viability in BT-549 cells, there was no further reduction in cell viability observed in combination with chemotherapeutic drugs. SC-1-181 and SP-1-90 enhanced doxorubicin sensitivity in BT-549 cells.

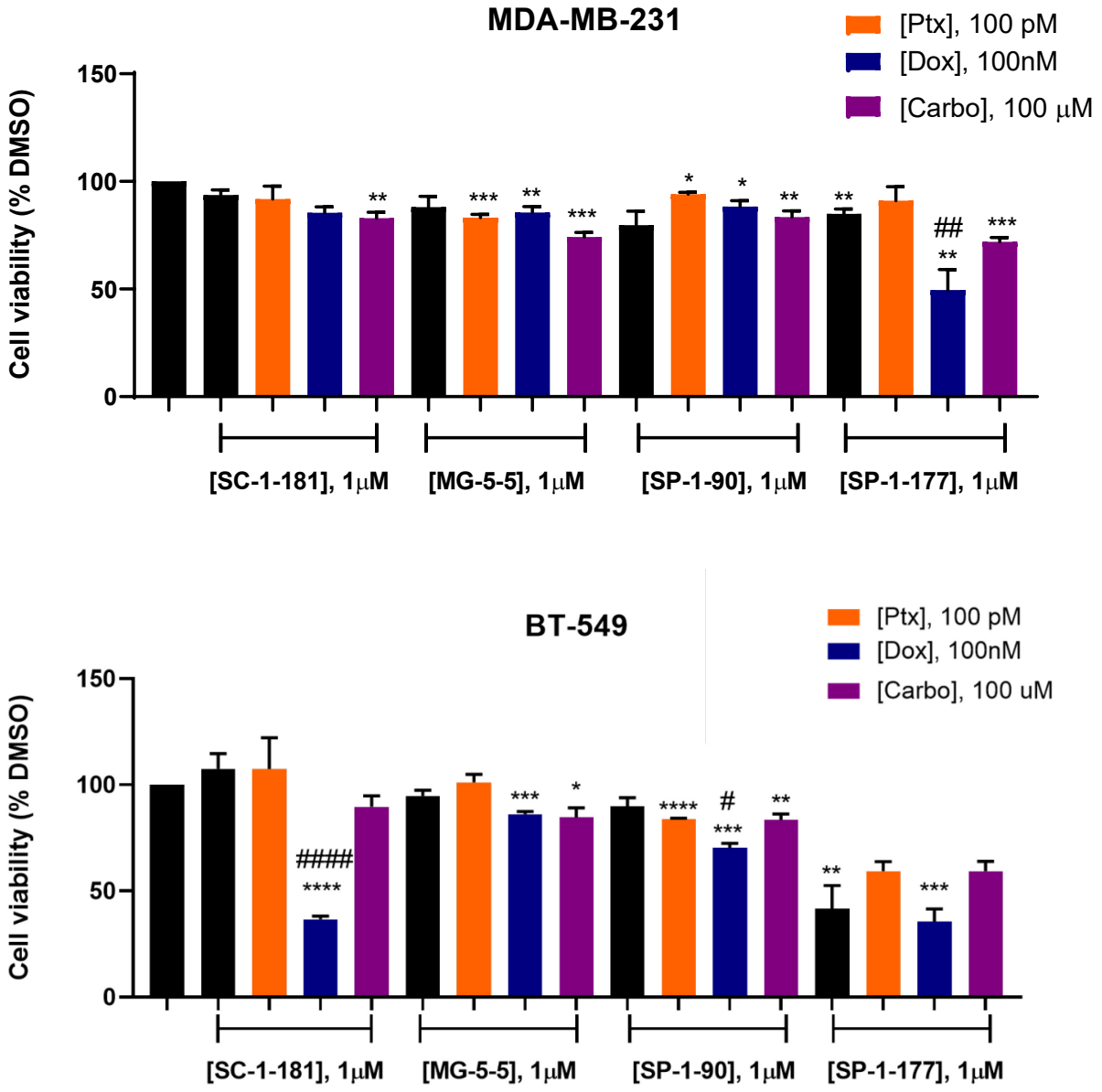

Figure 7.4: Effect of novel MAPK inhibitors in combination with chemotherapeutic agents on cell viability. (A) MDA-MB-231 and **(B)** BT-549 cells were treated with 1μM novel inhibitor in the presence of DMSO or low-dose paclitaxel, doxorubicin, and carboplatin for 72 hours. MTT assay was performed to assess cell viability. Data represent the +/- SEM of three different experiments determined by one-way ANOVA with

the Bonferroni post hoc test. *p<0.05; **P<0.01; ***P<0.001; ****P<0.0001 vs DMSO; #P<0.05, ##P<0.01; ####P<0.0001; vs individual drug determined by one-way ANOVA with the Bonferroni post hoc test.

7.4 Discussion

Due to crosstalk between the ERK5 and AKT pathways, it is important to develop dual targeting agents to simultaneously target both the pathways. In the current chapter, through structure-activity relationships studies, novel MEK5/PI3K inhibitors were identified and characterized for their selective activity against ERK5 and AKT, the downstream substrates of MEK5 and PI3K, respectively. In the previous chapter, we observed synergy with single agent kinase inhibitors in combination with chemotherapeutic drugs. Addition of a pan-PI3K inhibitor GD-0941 to docetaxel showed synergy in mouse xenograft models.[148] Clinically, BMK120, a pan-PI3K inhibitor and paclitaxel combination reversed paclitaxel drug resistance in patients with advanced solid tumors.[149] Paclitaxel was found to enhance cytotoxicity by ipatasertib and XMD8-92 combination in MDA-MB-231 cells.[145] The effect of chemotherapeutic drugs on cytotoxic effects of dual MEK5 and PI3K inhibitors in TNBC is currently unknown. In this study, we combined the chemotherapeutic drugs with lead MEK5 inhibitors or dual PI3K inhibitors from the diphenylamine,[83] thiophene,[150] and quinazolines at low doses and examined their effect of on cell viability.

While doxorubicin did not sensitize the effect of MEK5 inhibitor SC-1-181 on cell viability, doxorubicin significantly enhanced the sensitivity of MDA-MB-231 cells to a dual MEK5/PI3K inhibitor SP-1-177. SP-1-177 produced a greater reduction in cell viability compared to SP-1-90 in BT-549 cells. There was no further reduction after addition of

chemotherapeutic drugs in BT-549 cells. In this study, the chemotherapeutic drugs and kinase inhibitors were added simultaneously. Sequence of drug administration could alter cellular response.[151] Future studies focus on examining the effect of sequential addition of drugs on cell viability.

Chapter 8: Dual inhibition of MEK5 and MEK1/2 or PI3K pathways decreases cell viability, proliferation, migration, and stemness, and induces mesenchymal to epithelial transition in glioblastoma multiforme

8.1 Introduction

Glioblastoma multiforme (GBM) is a very aggressive form of cancer with median survival of only 14-15 months despite standard therapy consisting of surgery, adjuvant radiation, and chemotherapy. Infiltration into surrounding tissue decreases the success of surgical removal of the tumor and further increases the rate of recurrence.[152-153] Hyperactivation of PI3K and MAPK pathways is a frequent event in most GBM cases. Moreover, the mesenchymal subtype of GBM is driven by activation of the ERK1/2 pathway.[154] Figure 8.1 summarizes the tumorigenic effects regulated by ERK1/2 pathway in glioblastoma.

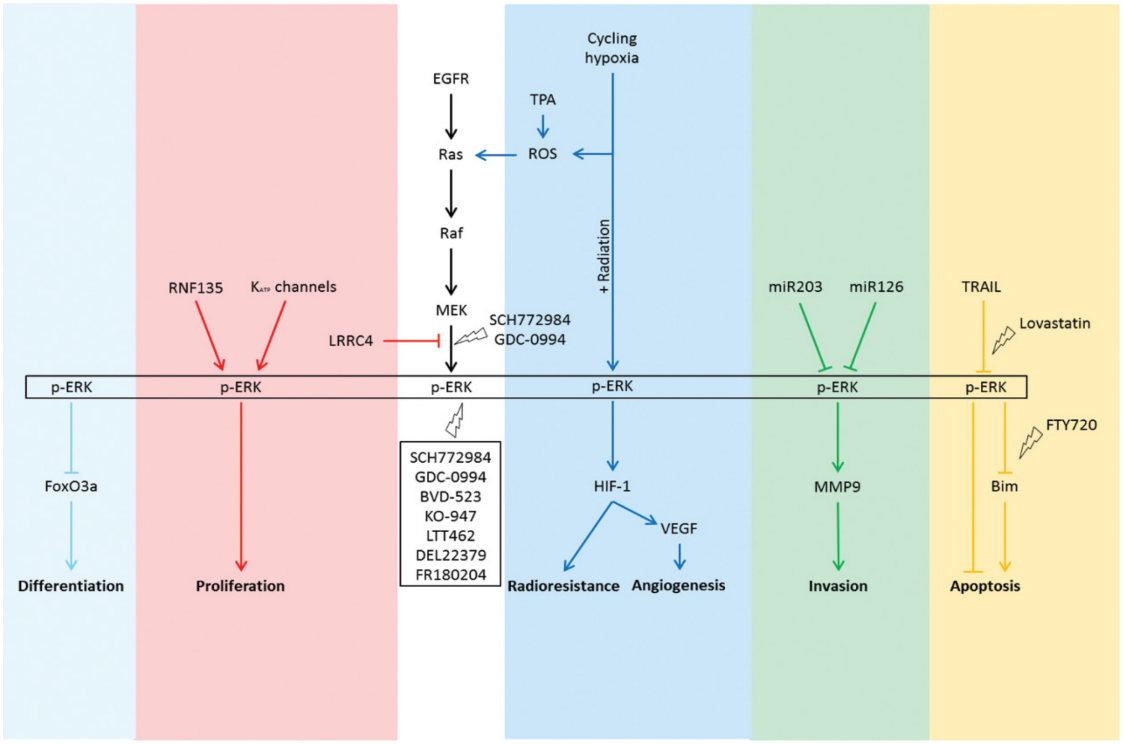

Figure 8.1: ERK pathway in GBM.[154]

The goals of the current research are to identify therapeutic targets and interventions for the treatment of glioblastoma multiforme, which has the worst prognosis and decreased overall survival compared to other brain cancers. There are no current therapies that are effective to treat patients with GBM. There is an urgent need to identify relevant targets that can be inhibited therapeutically to improve prognosis of GBM patients. MAPK and PI3K pathways are recently identified to promote GBM progression.[155] We first utilized a bioinformatics approach to compare genes downstream of MAPK and PI3K pathways and those involved EMT and proliferation in healthy versus GBM tumor samples using publicly available datasets. The MAPK7 gene codes for the newest member of the MAPK pathway, extracellular signal-regulated kinase ERK5, and is significantly upregulated in GBM tumor samples compared to healthy control. GBM tumor samples were enriched in EMT markers and genes involved in cell proliferation, which are known downstream targets of MAPK and PI3K pathways.

Activation of AKT is an important event in GBM progression due to mutation in PTEN or PI3K. One of the limitations of PI3K pathway inhibitors is compensatory increases in alternative pathways, including the MEK5-ERK5 pathway.[145] This necessitates the development of novel and relevant combination strategies to target GBM. We have previously shown that dual inhibition of AKT and ERK5 or triple inhibition of AKT, ERK5, and BRD4 is a relevant strategy to target triple-negative breast cancer (TNBC).[145] Moreover, the crosstalk between ERK5 and AKT pathways has been previously noted in neuroblastomas.[39] Therefore, we evaluated the effect of dual inhibition of ERK5 and AKT pathways on cell viability, proliferation, and migration in GBM. MYC is

a major oncogenic driver in GBM, which was found to be upregulated and positively correlated with MAPK7 in GBM patient samples. Bromodomain inhibitors were developed with a rationale to target the MYC oncogene in cancer.[156] Therefore, a dual MEK5/PI3K inhibitor J19 (MG-3-81)[150] was used alone and in combination with CPI-203, a BRD4 inhibitor. We also examined the effects of previously reported novel inhibitors of MEK5 or MEK1/2 pathways, which reversed the mesenchymal phenotype of TNBC[157] on EMT in GBM.

8.2 Hypothesis

Dual inhibition of the MEK5 and MEK1/2 or PI3K pathways will induce MET and decrease cell viability, proliferation, migration, and colony formation in PTEN mutant GBM cells with a mesenchymal phenotype.

8.3 Results

8.3.1 MAPK7 gene expression is significantly upregulated in GBM tumor samples compared to healthy groups

Glioblastoma multiforme (GBM) was identified to have the worst prognosis among other forms of cancers that originate in the brain (Figure 8.2A). MAPK7 gene, which codes for protein ERK5 was found to be significantly upregulated in GBM tumor samples compared to healthy group (Figure 8.2B). In contrast, MAPK1 and MAPK3 genes were significantly downregulated in GBM vs. healthy group. Epithelial cell markers CDH1 and keratin 1 (KRT1) were significantly downregulated, whereas tight junction protein (TJP1) gene expression did not decrease in GBM versus healthy group. Mesenchymal cell marker vimentin (VIM) and stem cell marker PROM1 were significantly upregulated. As

expected, genes involved in cell proliferation KI67, CCND1, and PCNA were significantly upregulated in GBM versus healthy group. Upstream regulator of MAPK pathway, EGFR was significantly upregulated while there was no increase in PIK3CA gene; however, there was a significant decrease in PTEN gene, which inhibits AKT activation by dephosphorylation. There was a significant increase in AKT1 and AKT2 and decrease in AKT3 gene expression (Figure 8.2B).

8.3.2 MAPK7 gene expression positively correlates with the EMT markers in GBM tumors

ERK5 is known to antagonize the decrease in MYC induced by KRAS suppression, indicating that ERK5 may be upstream of MYC.[53] Interestingly, there was a significant positive correlation between MAPK7 and MYC in GBM. To understand whether ERK5 regulates genes involved in EMT and stemness, MAPK7 gene expression was correlated to stem cell markers PROM1 (gene that codes for CD133), NOTCH1, epithelial cell marker CDH1 (gene that codes for E-cadherin), and mesenchymal markers VIM and ZEB1. MAPK7 gene expression negatively correlated with CDH1 (Figure 8.2D) and positively correlated with stemness markers PROM1 and NOTCH1 (Figure 8.2E, H) and mesenchymal markers VIM and ZEB1 (Figure 8.2F, G), suggesting a role for ERK5 in mediating EMT and stemness in GBM.

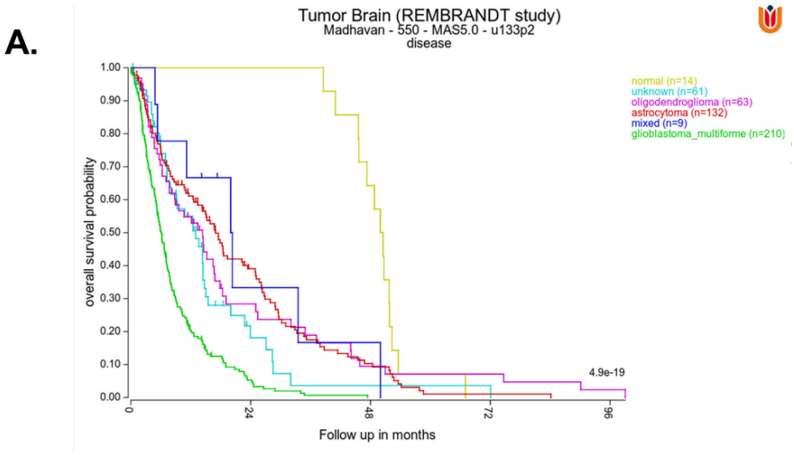
A.
Tumor Brain (REMBRANDT study)
Madhavan - 550 - MAS5.0 - u133p2
disease
normal (n=14)
unknown (n=61)
oligodendroglioma (n=63)
astrocytoma (n=132)
mixed (n=9)
glioblastoma_multiforme (n=210)
overall survival probability
4.9e-19
Follow up in months

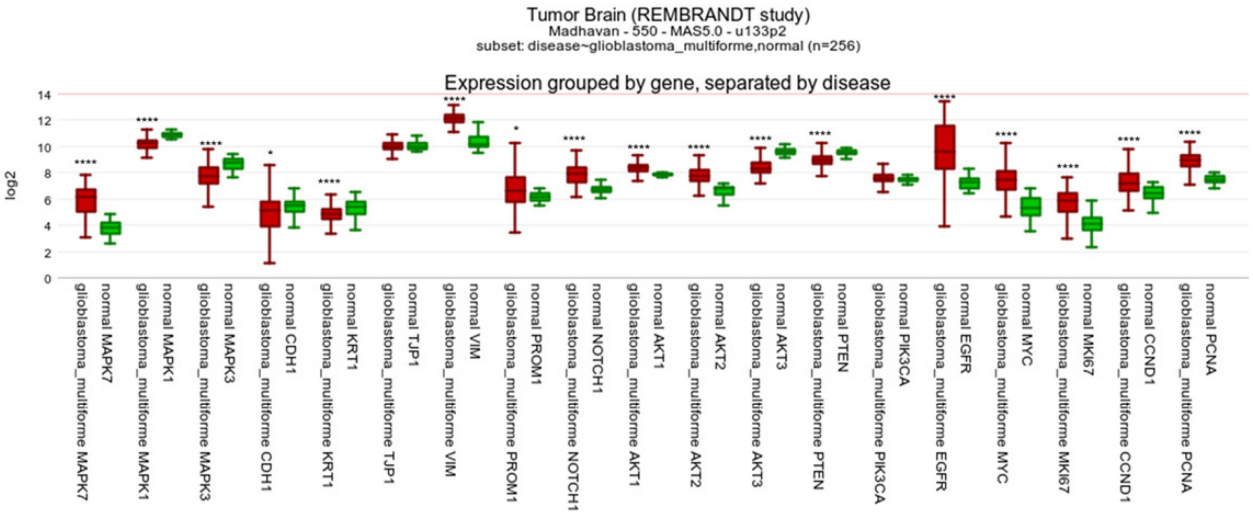
Tumor Brain (REMBRANDT study)
Madhavan - 550 - MAS5.0 - u133p2
subset: disease~glioblastoma_multiforme,normal (n=256)
Expression grouped by gene, separated by disease
log2
glioblastoma_multiforme MAPK7
normal MAPK7
glioblastoma_multiforme MAPK1
normal MAPK1
glioblastoma_multiforme MAPK3
normal MAPK3
glioblastoma_multiforme CDH1
normal CDH1
glioblastoma_multiforme KRT1
normal KRT1
glioblastoma_multiforme TJP1
normal TJP1
glioblastoma_multiforme VIM
normal VIM
glioblastoma_multiforme PROM1
normal PROM1
glioblastoma_multiforme NOTCH1
normal NOTCH1
glioblastoma_multiforme AKT1
normal AKT1
glioblastoma_multiforme AKT2
normal AKT2
glioblastoma_multiforme AKT3
normal AKT3
glioblastoma_multiforme PTEN
normal PTEN
glioblastoma_multiforme PIK3CA
normal PIK3CA
glioblastoma_multiforme EGFR
normal EGFR
glioblastoma_multiforme MYC
normal MYC
glioblastoma_multiforme MKI67
normal MKI67
glioblastoma_multiforme CCND1
normal CCND1
glioblastoma_multiforme PCNA
normal PCNA

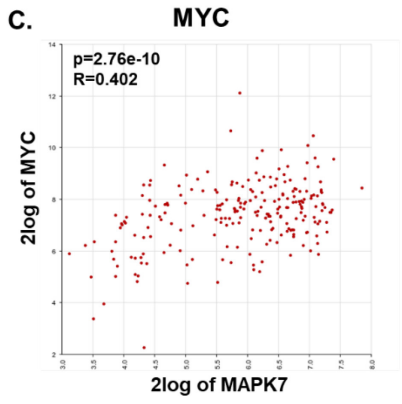
C.
MYC
p=2.76e-10
R=0.402
2log of MYC
2log of MAPK7

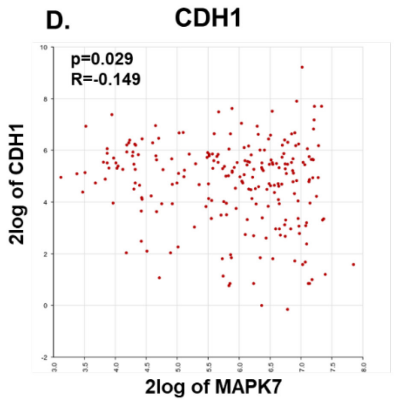
D.
CDH1
p=0.029
R=-0.149
2log of CDH1
2log of MAPK7

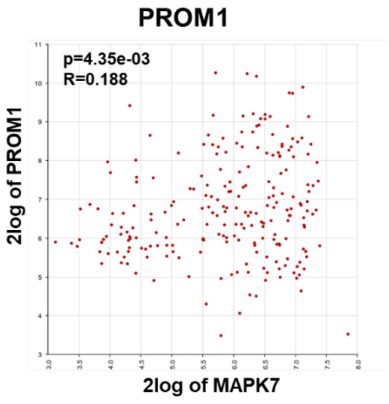
E.
PROM1
p=4.35e-03
R=0.188
2log of PROM1
2log of MAPK7

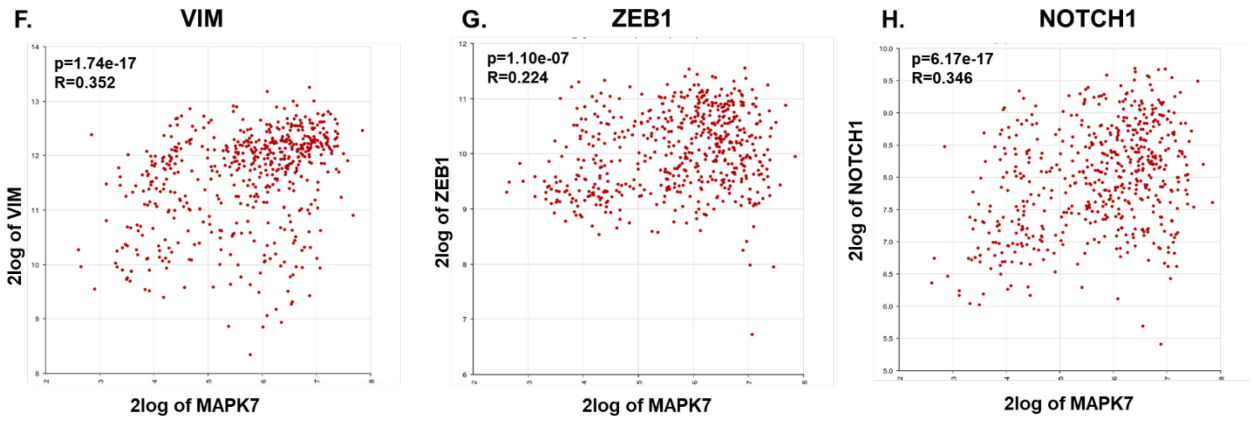

Figure 8.2. Comparison of genes downstream of MAPK and PI3K pathways in tumors derived from GBM patients versus healthy groups. (A) Kaplan-Meier survival analysis in different subtypes of brain cancer **(B)** Gene expression analyses in healthy tissues versus GBM patient samples. Gene correlation between MAPK7 and **(C)** PROM1 **(D)** CDH1, **(E)** MYC **(F)** VIM, **(G)** ZEB1, or **(H)** NOTCH1. Data were plotted using R2: Genomics analysis and visualization platform (https://hgserver1.amc.nl/cgi-bin/r2/main.cgi). Datasets were exported from Tumor Brain (REMBRANDT study) - Madhavan - 550 - MAS5.0 - u133p2.

8.3.3 MAPK1, MAPK7, AKT1, and AKT2 gene expression is associated with poor patient survival in GBM

Kaplan Meier survival analysis was performed to examine the association of MAPK and PI3K pathways on overall survival in GBM using publicly available datasets. High MAPK1 (gene that codes for ERK2), MAPK7 (gene that codes for ERK5), AKT1 and AKT2 expression was associated with worse patient outcome whereas high MAPK3 (gene that codes for ERK1) and AKT3 expression was associated with better patient outcome (Figure 8.3). Overall, these data suggest that ERK5 and AKT1 and 2 are important targets in GBM.

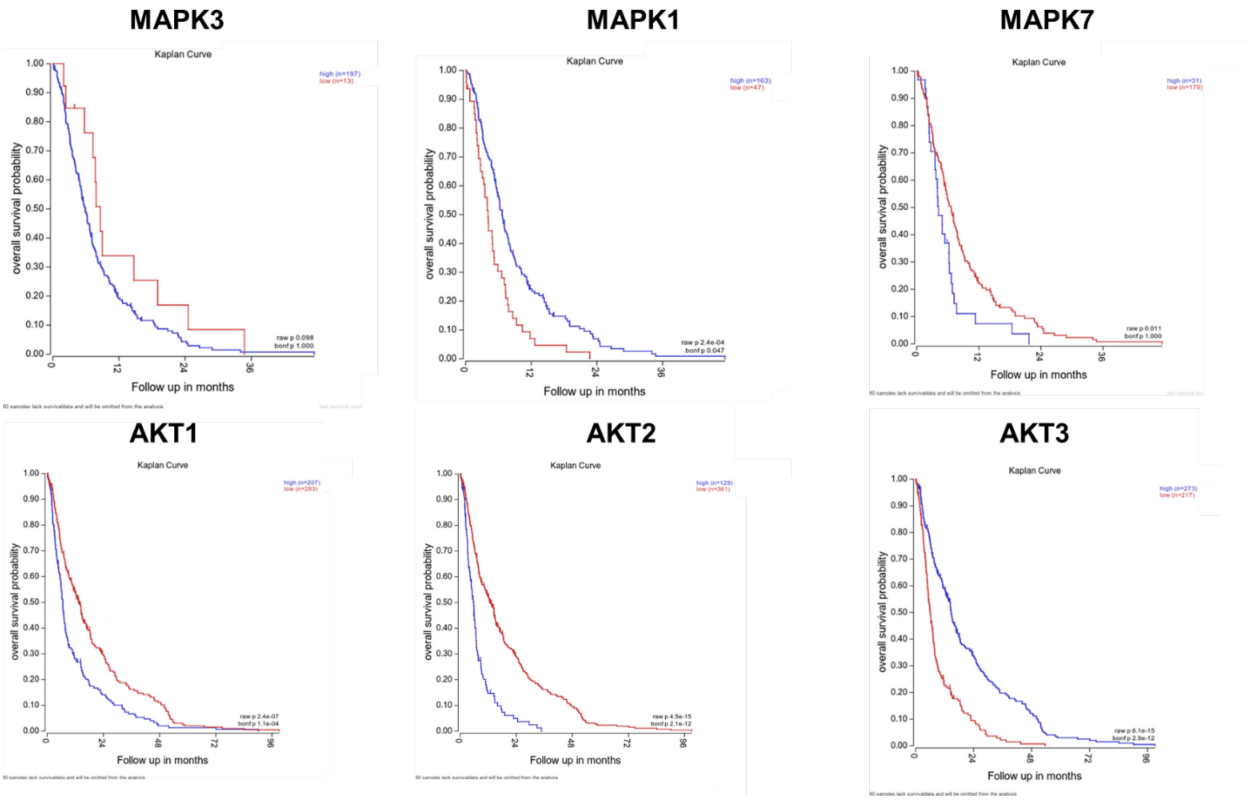

Figure 8.3. MAPK3, MAPK1, and MAPK7 expression correlates with poor patient survival in GBM. Disease free survival was analyzed using R2: Genomics analysis and visualization platform (https://hgserver1.amc.nl/cgi-bin/r2/main.cgi). Datasets were exported from Tumor Brain (REMBRANDT study) - Madhavan - 550 - MAS5.0 - u133p2.

8.3.4 Dual inhibition of ERK5 and AKT pathways synergistically reduces cell viability in GBM

U87MG cells are PTEN mutant and may rely on the AKT pathway for survival and proliferation. Since crosstalk between AKT and ERK5 may exist, the effects of ipatasertib, an AKT inhibitor and XMD8-92, an ERK5 inhibitor alone and in combination were examined on kinase activation, cell viability, and migration. To determine the specificity of kinase inhibitors, U87MG cells were serum starved for 18 hours after 24 hours of cell seeding and treated with kinase inhibitors for 30 minutes. Cells were stimulated with EGF

for 15 minutes. Cell lysates were collected and examined for ERK1/2, ERK5, and AKT activation. As expected, XMD8-92 and XMD8-92+ipatasertib groups decreased ERK5 activation with no effect on AKT or ERK1/2 activation. Ipatasertib targets the ATP-site and keeps AKT in its active form and decreases downstream signaling by AKT. This may explain while there was no decrease in AKT activation, there was still a decrease in cell viability after treatment with ipatasertib. Ipatasertib modestly increased ERK5 activation (Figure 8.4A). Neither of the inhibitors altered ERK1/2 activity. Targeting AKT alone led to compensatory increase in ERK5 activation, which was inhibited in the Ipat+XMD8-92 group compared to control (Figure 8.4A).

While both ipatasertib and XMD8-92 were effective at decreasing cell viability in a concentration-dependent manner (Figure 8.4B-C), combination of ipatasertib with XMD8-92 produced a greater reduction in cell viability. 1:3 combination of ipatasertib and XMD8-92 was more effective than 1:1 ratio at increasing the fraction affected as calculated by using CompuSyn software (Figure 8.4D). While ipat or XMD8-92 did not decrease cell migration alone, the combination significantly decreased cell migration in U87MG cells.

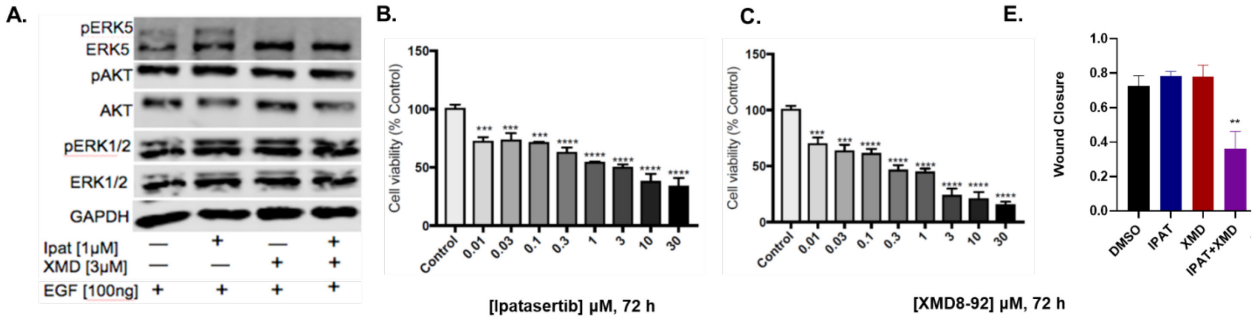

D.

Cell line	Combination (Ipat+XMD)	Fraction affected (Fa)	Combination index (CI)	Synergy designation
U87	0.1, 0.1	0.614	0.134	Strong synergy
	0.3, 0.3	0.571	0.699	Strong synergy
	1, 1	0.543	3.311	Antagonism
	3, 3	0.79	0.285	Strong synergy
	0.1, 0.3	0.571	0.667	Synergy
	1, 3	**0.815**	**0.171**	**Strong synergy**

Figure 8.4. Dual ERK5 and AKT decreases cell viability and migration in U87MG GBM cells. (A) Western blot analysis of ERK5, ERK1/2, and AKT activation by EGF in U87MG cells (B) Cells were treated with XMD8-92 and ipatasertib at increasing concentrations for 72 hours. Data represent the ± SEM of three different experiments for each inhibitor compared to DMSO control. *p<0.05; **p<0.01; ***p<0.001; ****p<0.0001 *vs* DMSO control group determined by one-way ANOVA with the Bonferroni post hoc test. (C) Combination index table for synergy determination. (D) Effect of ipatasertib and XMD8-92 at 1 and 3 μM concentration, respectively on cell migration in U87MG cells. Scratches were made after 24 hours of cell seeding (0h) and cells were treated with the kinase inhibitors for 24 hours. Cells were imaged at the time of scratch (0 h) and after 24 hours from the time of scratch (20X magnification). (Synergy data: Dr. Thomas Wright)

Ipat+XMD combination did not significantly decrease the proliferative fraction (Figure 8.5),

indicating that alternative pathways may regulate cell proliferation in GBM.

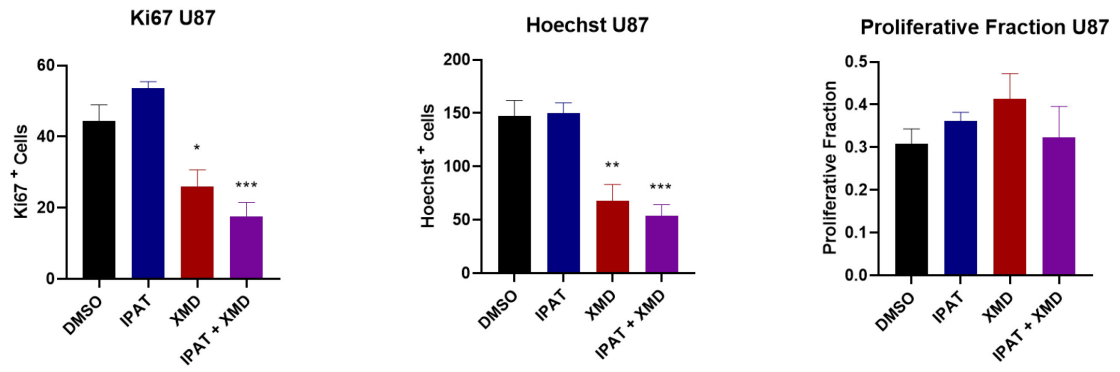

Figure 8.5: Ipat+XMD combination does not decrease proliferative fraction in U87MG cells. (Katie Anna). Cells were treated with indicated inhibitors for 72 hours (20X magnification). Proliferative fraction was evaluated as the number of Ki67 positive cells divided by the number of Hoechst positive cells. Data represent the ± SEM of three different experiments. *p<0.05; **p<0.01; ***p<0.001 *vs.* DMSO control group determined by one-way ANOVA with the Bonferroni post hoc test.

8.3.5 Dual PI3K/MEK5 inhibitor+CPI203 combination significantly decrease cell proliferation via p21 restoration in GBM

BRD4 regulates cell cycle progression via upregulation of c-Myc and cyclinD1, which are also downstream targets of MAPK pathways. Several dual PI3K/MEK5 thiophene analogs were developed as novel therapeutic interventions to target cancer. In this study, we examined the effect of novel dual MEK5/PI3K inhibitor J19 (MG-3-81) in combination with BRD4 inhibitor CPI-203 on cell proliferation. Ipatasertib, J19 (MG-3-81), or CPI-203 alone did not significantly decrease the proliferative fraction as determined by taking the ratio of $Ki67^+$ cells to $Hoechst^+$ cells. While ipatasertib did not potentiate the effect of CPI203 on cell proliferation, J19 (MG-3-81)+CPI-203 combination significantly decreased proliferative fraction to a greater extent compared to either drug alone (Figure 8.6A). The decrease in cell proliferation correlated with an increase in p21, a cell cycle inhibitor (Figure 8.6B).

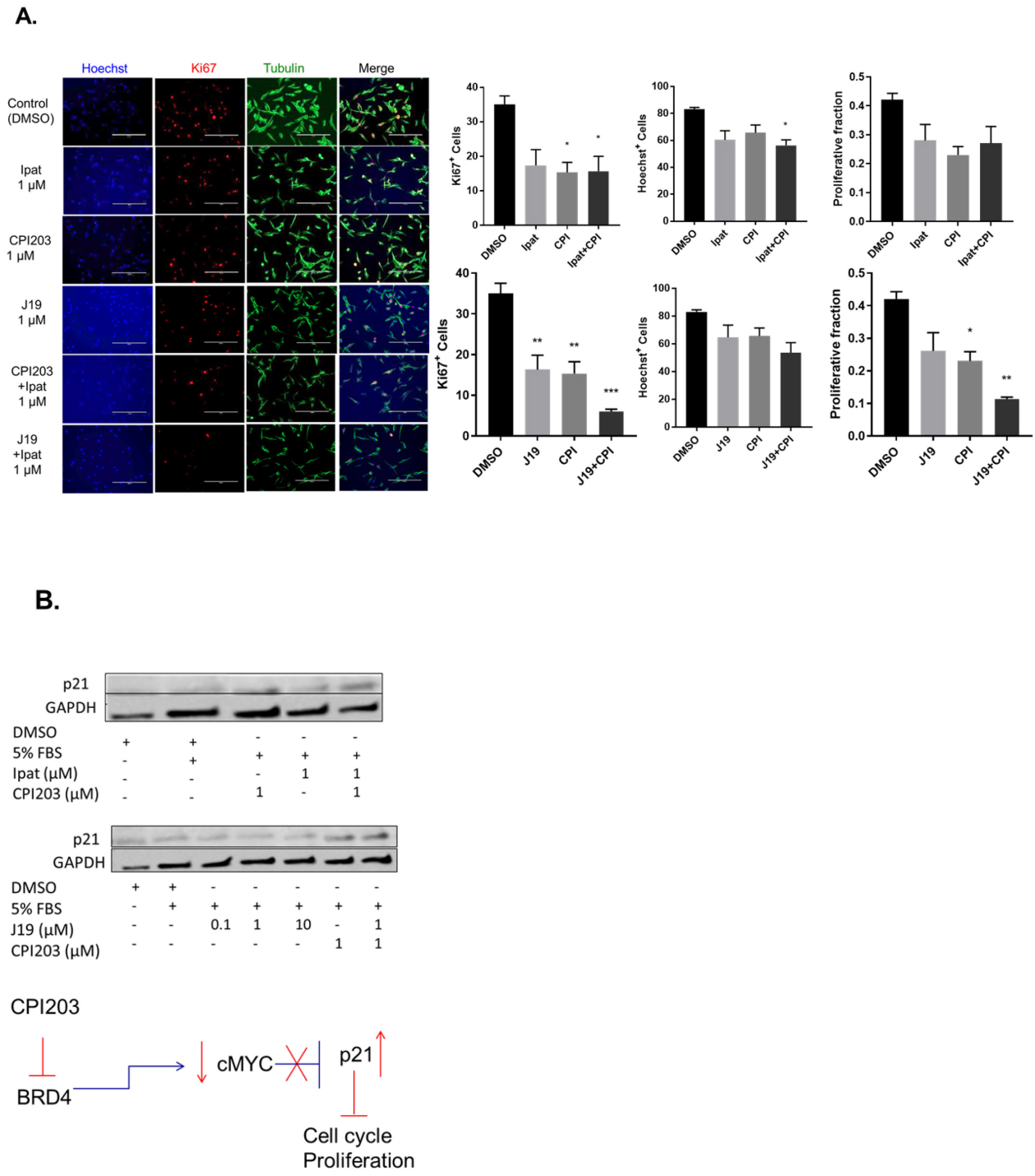

Figure 8.6. Effect of ipatasertib and J19 (MG-3-81) alone and in combination with CPI-203 on cell proliferation and p21 expression in U87MG cells. (A) Cells were treated with indicated inhibitors for 72 hours (20X magnification). Proliferative fraction was evaluated as the number of Ki67 positive cells divided by the number of Hoechst positive cells. Data represent the ± SEM of three different experiments. *p<0.05; **p<0.01;

***p<0.001 *vs.* DMSO control group determined by one-way ANOVA with the Bonferroni post hoc test. (Seraina Schottland).

8.3.6 Dual MEK1/2 and MEK5 inhibitor(s) and LBH589 (HDAC inhibitor) induce MET in U87MG glioblastoma cells.

Reversing EMT is an emerging approach to target cancer. We have previously shown that pharmacological inhibitors of MEK1/2 and MEK5 pathways reversed EMT in triple-negative breast cancer.[157] U87MG cells were treated with novel MEK1/2 inhibitor (SC-1-122), MEK5 inhibitor (SC-1-181), dual MEK1/2 and MEK5 inhibitor (SC-1-151), LBH589, trametinib, or XMD8-92 for 72 hours. The phenotypic switch from mesenchymal to epithelial was most prominent in SC-1-151, trametinib, and LBH-589-treated groups (Figure 8.7A-B). We hypothesized that targeting the AKT pathway may be a relevant strategy to reverse EMT; however, ipatasertib, J19 (MG3-81), or CPI-203 did not reverse EMT in these cells (Figure 8.7A). Therefore, the ERK1/2 and ERK5 pathways may play a larger role in the EMT than the AKT pathway.

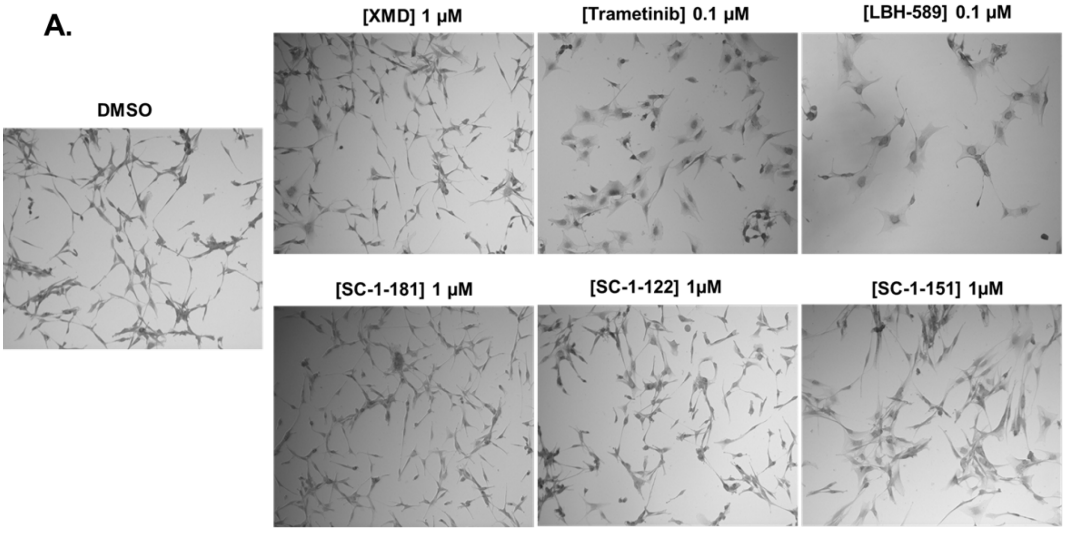

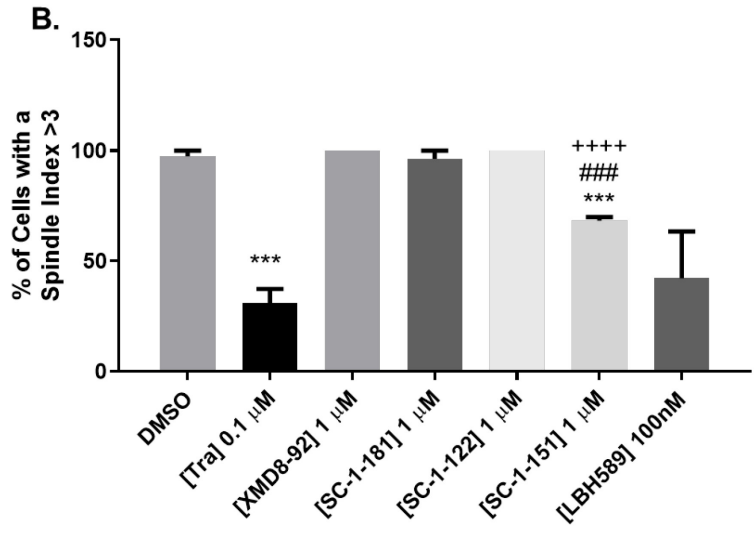

Figure 8.7: Effect of novel and known MAPK inhibitors on MET in U87MG cells. (A) U87MG cells were treated with MAPK inhibitors for 72 hours and stained with crystal violet after 72 hours of treatment. **(B)** Cell morphology was quantified by morphometric analysis 10X (Jordan Martin).

8.3.7 Trametinib decreases ERK5 activation, cell viability, migration, and colony formation in GBM

Since trametinib was most effective at reversing EMT, we further characterized its effects on kinase activation by EGF to determine its specificity, and cell viability, migration, and colony formation assays. U87MG cells were serum starved for 18 hrs and treated with trametinib at 0.1 and 1 μM concentrations for 30 minutes. Cells were then stimulated with EGF for 15 minutes. Lysates were collected and examined for ERK5, ERK1/2, and AKT activation. As expected, trametinib decreased ERK1/2 activation by EGF. Surprisingly, trametinib also inhibited ERK5 activation by EGF (Figure 8.8A). MTT, migration, and colony formation assays were performed to examine the effects of trametinib on U87 cells in 2D and 3D cultures. Trametinib modestly decreased cell

viability at 10 μM concentration (Figure 8.8B) and significantly inhibited cell migration and colony formation, consistent with its effect on MET in U87MG cells (Figure 8.8C-D).

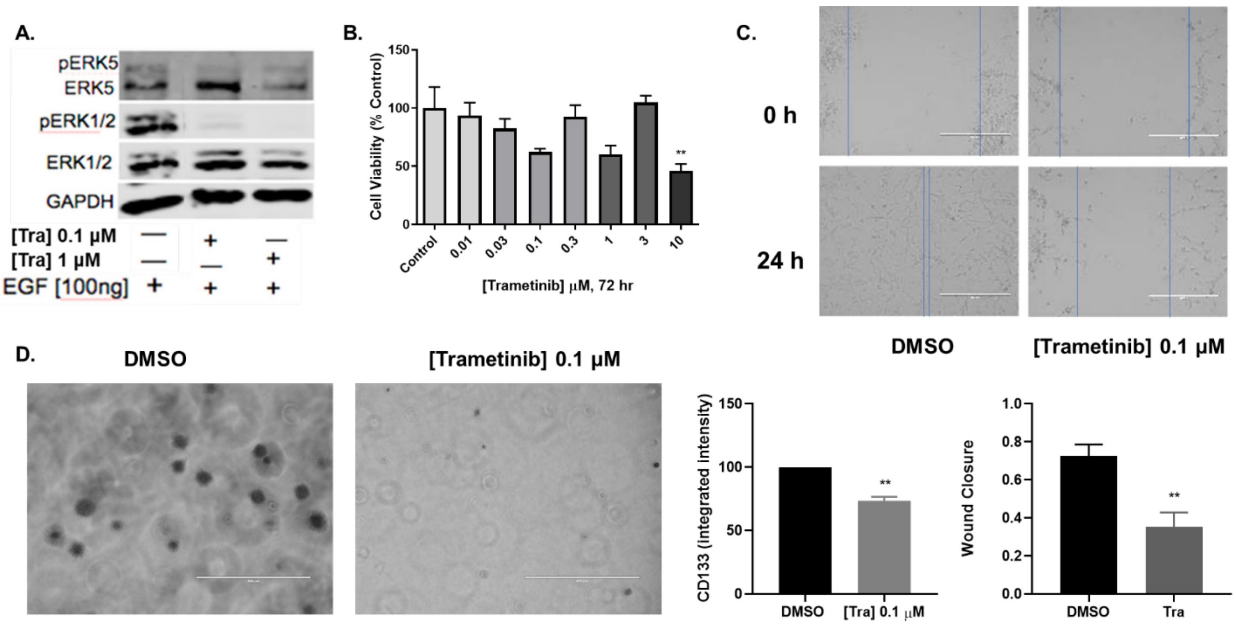

Figure 8.8. Trametinib decreases ERK5 activation, cell viability, migration, and colony formation in U87MG cells. (A) ERK5 and ERK1/2 activation (B) cell viability (C) migration (D) colony formation and CD133 expression in U87MG GBM cells. **p<0.01 *vs* control group determined by Student's t-test.

8.4 Discussion

Glioblastoma multiforme is an aggressive disease with limited therapeutic options. ERK1/2, ERK5, and AKT pathways are important targets in glioblastoma. However, the crosstalk between ERK5 and AKT and effects of MAPK inhibitors on proliferation, EMT, and stemness in glioblastoma are not well-understood. Therefore, we examined the effect of novel and known MAPK pathway inhibitors in combination with PI3K pathway inhibitor(s) on viability, migration, EMT, and stemness in U87 GBM cells.

Recent studies suggest that ERK5 expression and activation are crucial events in regulating EMT in several cancers[90, 105] and targeting the MAPK pathways has been shown to reverse EMT in breast cancer.[157-158] One goal of this research was to identify pathways that were significantly upregulated in GBM compared to healthy controls, so as to therapeutically target the aberrant pathways. Recent evidence suggests that EGFR, PI3K, and PTEN mutations[159] are common oncogenic drivers in GBM, making GBM a relevant disease model to study ERK1/2, ERK5, and AKT protein kinases as relevant drug targets in GBM. From our research, using publicly available datasets from Gusev et al.,[160] we examined specific components of MAPK and PI3K pathways, which were upregulated in GBM versus healthy control.

MAPK7 was found to be significantly upregulated in GBM versus healthy control. Therefore, we correlated MAPK7 gene expression to EMT and proliferation markers. There was a significant increase in the upstream regulator of MAPK pathways, epidermal growth factor receptor (EGFR), in agreement with previous reports.[161]

PTEN deletion is a common event in GBM.[159] Since PTEN expression was significantly downregulated in GBM versus healthy control, AKT may be a relevant target in GBM. Moreover, high AKT1 and AKT2 expression was associated with worse patient outcome. Since high MAPK3 and AKT3 gene expression correlated with better patient outcome, it may be important to develop isoform-specific pharmacological inhibitors of ERK1, AKT1, or AKT2, which spare ERK2 or AKT3 activity. Isoform-specificity of inhibitors are currently being investigated in our laboratory and others.[162] Data suggest it may be important to determine which tumor subtypes may benefit most from isoform-specific compounds.

While we obtained information about putative drug targets by utilizing a bioinformatics approach, these observations do not provide insights into whether there is a subsequent increase in protein expression or activation in different components of the MAPK and PI3K pathways. Therefore, we utilized an in vitro approach to inhibit these pathways using known and novel inhibitors of the MAPK and PI3K pathways to examine their effect on kinase activation, proliferation, EMT, and stemness. To understand whether targeting ERK5, ERK1/2, and/or PI3K pathways was promising in GBM, we utilized PTEN-mutant U87MG cells with moderate EGFR expression and a mesenchymal phenotype.[163-164] In addition to genes involved in the regulation of proteins that promote EMT, cell proliferation genes downstream of MAPK, AKT, and bromodomain pathways were significantly enriched in GBM tumors compared to healthy control. Compensatory activation of the AKT or BET proteins may reactivate MAPK-mediated proliferation in cancer cells.[129] Therefore, combination strategies were designed to target both MAPK and bromodomain proteins in U87MG cells. Similar to our findings in breast cancer, dual ERK5 and AKT inhibition significantly decreased cell viability and migration in U87MG cells. Novel dual PI3K/MEK5 inhibitor J19 (MG-3-81) was more effective in combination with BRD4 inhibitor CPI-203 to decrease cell proliferation compared to AKT inhibitor ipatasertib. Our data suggest that this decrease in cell proliferation was mediated at least in part via p21 restoration.

U87MG cells were especially susceptible to dual targeting of ERK1/2 and ERK5 pathways since treatment with dual MEK1/2 and MEK5 inhibitor significantly decreased the percentage of cells with SI>3 when compared with DMSO control or inhibition ofMEK1/2 or MEK5 alone (SC-1-122 or SC-1-181, respectively). Although MAPK7 gene

expression significantly correlated with mesenchymal markers ZEB1, vimentin, and inversely correlated with epithelial marker E-cadherin, MEK5 inhibitor SC-1-181 did not reverse EMT in U87MG cells. This may be because ERK1/2 pathway is still active. Trametinib, a MEK1/2 inhibitor reversed EMT in U87MG cells. To our knowledge, this is the first study to show the effect of MEK1/2 inhibition on reversal of EMT in glioblastoma. A previous study has reported that downregulation of ERK5 by microRNA-200 suppressed EMT in GBM.[44] This may indicate that total ERK5 expression, rather than its activation may be a driver of EMT in GBM. Trametinib decreased total ERK5 expression even at short time points (Figure 8.8A), which may indicate that inhibition and decrease in total ERK5 expression may be necessary for full effect of trametinib on MET in U87MG cells. LBH589, a histone deacetylase inhibitor was used as a positive control since it known to reverse EMT in some cancers.[165] The possible reasons why ERK5 inhibition alone did not reverse EMT may be because total ERK5 expression may regulate transcription of genes in the nucleus even in the absence of phosphorylated ERK5 in the cytosol.[166]

MEK1/2 inhibitor trametinib decreased ERK1/2 and ERK5 activation in response to EGF. ERK1/2 and ERK5 pathways share ~50% sequence homology at the N-terminal domain.[167] Trametinib-mediated decrease in ERK5 activation may be mediated via MEK1/2 inhibition. Trametinib decreased viability, migration, and colony formation in U87MG cells, indicating that dual MEK1/2 and MEK5 inhibition is a relevant strategy to target EMT in GBM. Overall, our data suggest that ERK1/2 and ERK5 are relevant targets to reverse the EMT and ERK5 and AKT are relevant targets to decrease cell viability and proliferation in glioblastoma cells with a mesenchymal phenotype (Figure 8.9). In

conclusion, this is the first study to examine the effects of pharmacological inhibition of MEK5 and MEK1/2 or PI3K pathways on cell proliferation, migration, stemness, and EMT in GBM.

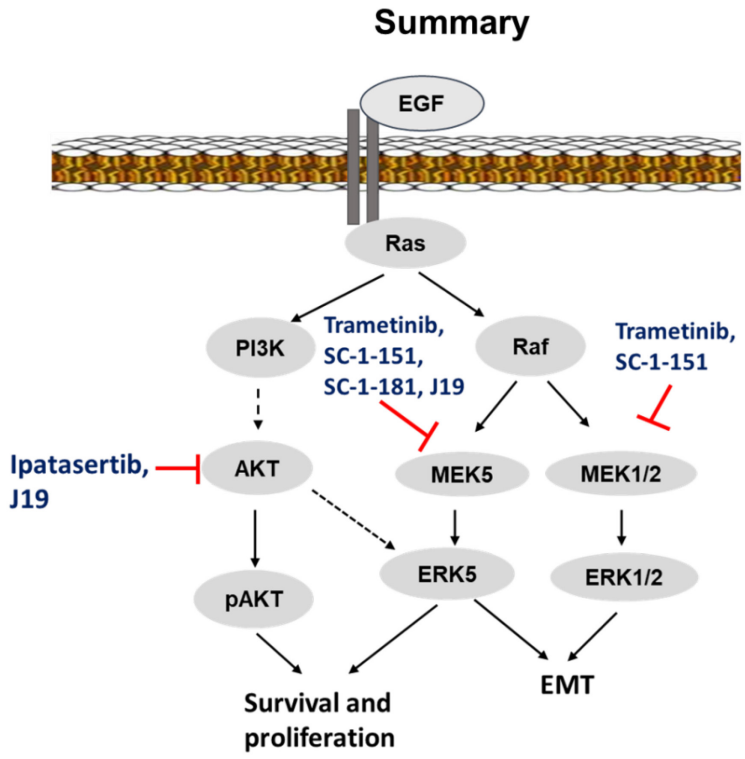

Figure 8.9: Regulation of cell viability, EMT, and stemness via the MAPK and PI3K pathways in GBM.

Chapter 9: Marine cyanobacteria inhibit cell viability and enhance chemotherapeutic sensitivity in triple-negative breast cancer

9.1 Introduction

TNBCs are in dire need for alternative therapies. There is also an urgent need to identify novel targets to develop treatment options, which can selectively target cancer cells. A recent review of the literature[168] has identified a number of marine cyanobacterial peptide and peptide-containing natural compounds that display antitumor cytotoxicity. Sigma-2 receptors was identified as transmembrane protein 97.[169] In this chapter, we will discuss the effects of novel marine peptides, veraguamide M and N, that are putative ligands for sigma-2 receptors, which are overexpressed in TNBCs and promote tumorigenesis. Moreover, sigma 2 receptor ligands have been shown to be toxic in neuroblastoma, and mouse breast cancer cell lines.[170-171] Sigma 2 receptor selective compounds have also been reported to decrease MCF-7 and doxorubicin-resistance MCF7 breast cancer cell proliferation and enhance the sensitivity of MCF-7 cells to doxorubicin[21,22]. Currently, there is only one study that examines the synergistic effects of sigma 2 receptor ligands with PARP inhibitors in MDA-MB-231 TNBC cells and one other study that examines synergy with taxol and a cytotoxic payload delivered to TNBC cells via conjugation to a sigma 2 receptor ligand[23]. In this study, we examined the expression of TMEM97, a gene that codes for sigma 2 receptors, in breast cancer subtypes. Next, we examined the effect of novel sigma 2 ligands on cell viability and chemotherapeutic sensitivity in triple-negative breast cancer cells.

9.2 Hypothesis

Chemotherapeutic drugs will enhance cytotoxic effects of novel sigma 2 receptor ligands in triple-negative breast cancer cells.

9.3 Results

9.3.1 High expression of TMEM97 in diverse breast cancer subtypes is associated with poor overall survival

Bioinformatic analyses of publicly available datasets from Bertucci and colleagues[109] was performed to determine the expression of TMEM97 in diverse breast cancer subtypes. TMEM97 expression was higher in luminal a, luminal b, erbb2, and basal like cancers compared to normal (Figure 9.1A). Higher expression of TMEM97 also decreased disease free survival as compared to breast cancer patients with low tumore expression of TMEM97.

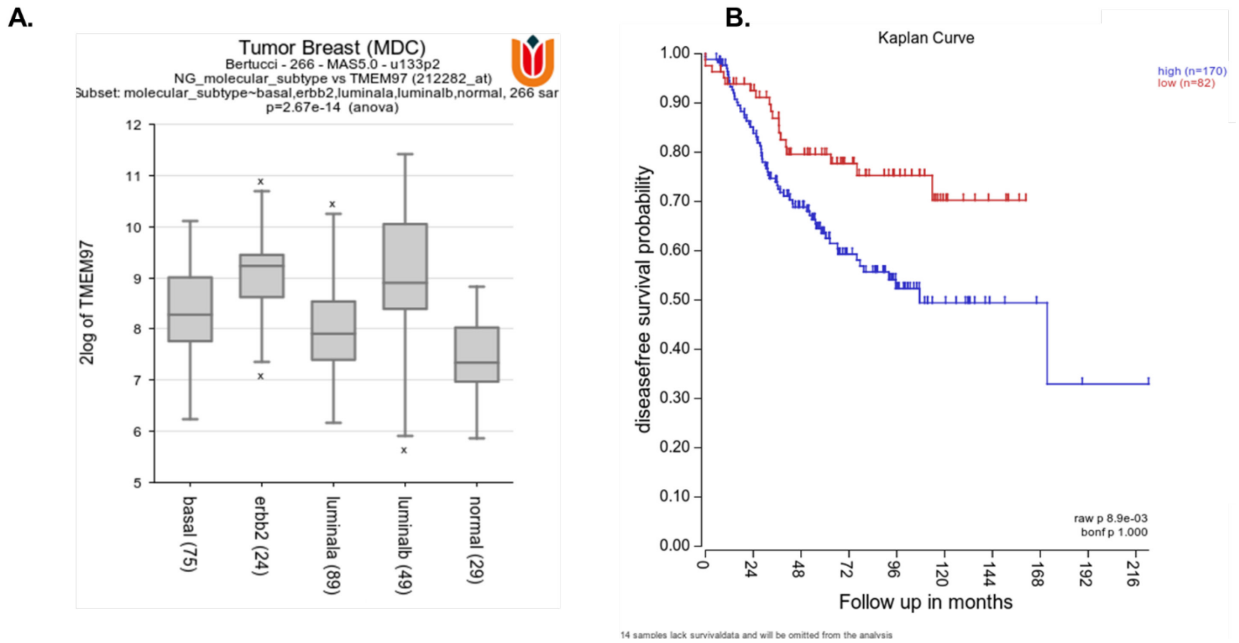

Figure 9.1: TMEM97 is overexpressed in cancer versus healthy groups and high TMEM97 expression correlates with poor overall survival in breast cancer patients. **(A)** TMEM97 is overexpressed in cancer versus healthy control **(B)** High TMEM97 expression correlates with poor patient survival in breast cancer. Disease free survival was analyzed using R2: Genomics analysis and visualization platform (https://hgserver1.amc.nl/cgi-bin/r2/main.cgi). Datasets were exported from Tumor Breast (MDC) Bertucci - 266 - MAS5.0 - u133p2.

9.3.2 Marine cyanobacteria inhibit viability in MDA-MB-231 cells

MDA-MB-231 cells were treated with marine cyanobacteria fractions at 0.1, 1, and 10 ug/ml concentrations for 72 hours. MTT assay was performed to determine cell viability. Fractions B, C, D, E, and F significantly decreased cell viability (Figure 9.2). Barbamide was extracted from fraction F to determine its effect on cell viability. Barbamide produced a significant decrease in cell viability in MDA-MB-231 and BT-549 cells (Figure 9.2).

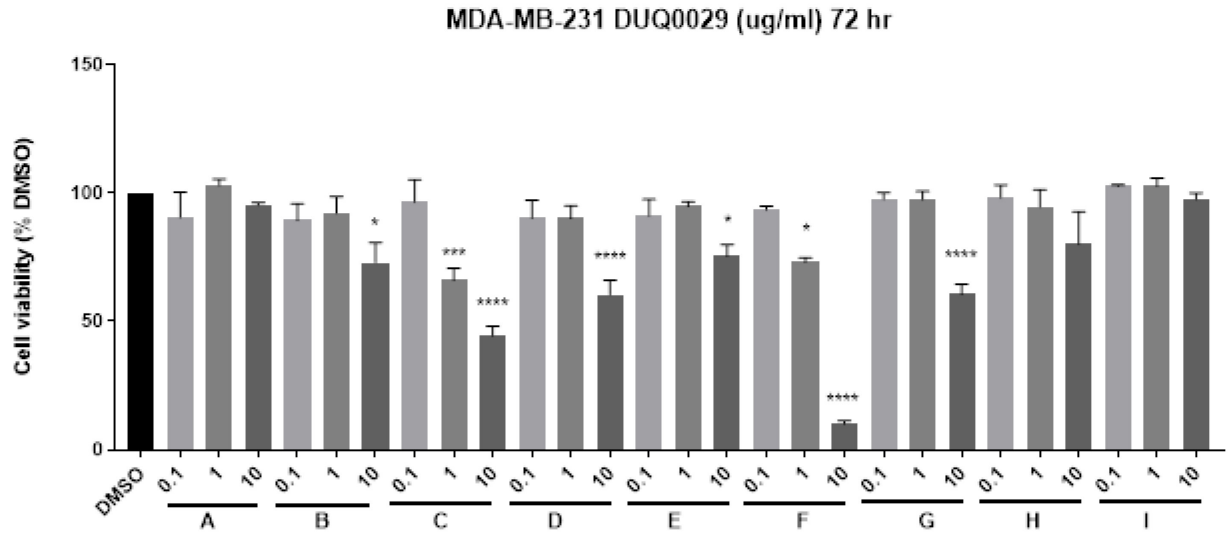

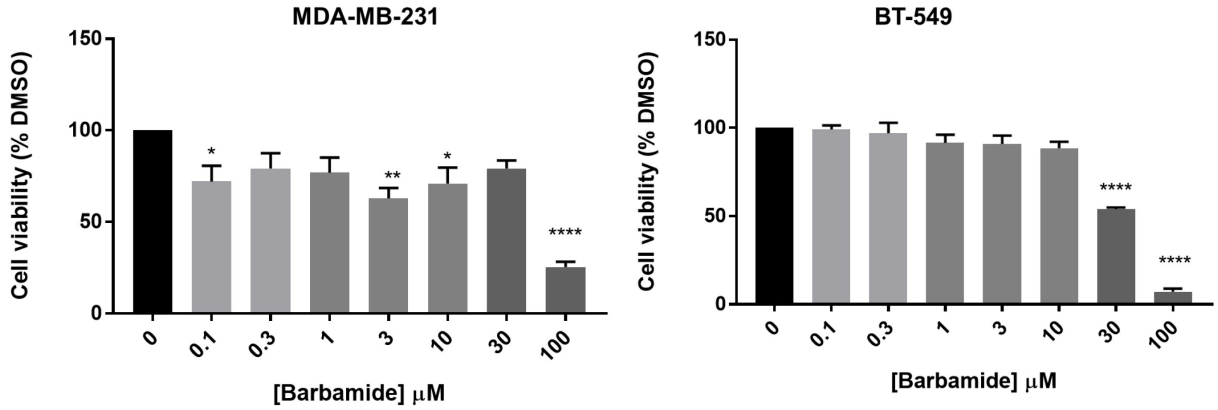

Figure 9.2: Barbamide produced a concentration-dependent decrease in cell viability in MDA-MB-231 cells after 72 hours of treatment. Data represent the ± SEM of three different experiments. *p<0.05; **p<0.01; ****p<0.0001 *vs* control group determined by one-way ANOVA with the Bonferroni post hoc test.

9.3.3 Effect of marine cyanobacteria in combination with chemotherapy on TNBC cell viability

Sigma 2 receptor ligands have been shown to synergize with doxorubicin to inhibit cell growth in MCF-7 cells.[172] However, studies of synergy of sigma 2 ligands with doxorubicin, paclitaxel, and cisplatin in TNBC have not been done. Therefore, we combined two natural sigma 2 receptor ligands veraguamide and barbamide with chemotherapeutics, doxorubicin, paclitaxel, and carboplatin at low doses. The toxic effect of veraguamide was enhanced by doxorubicin and carboplatin in MDA-MB-231 and BT-549 cells. The toxic effects of barbamide was enhanced by doxorubicin and carboplatin in BT-549 cells (Figure 9.3 and Figure 9.4).

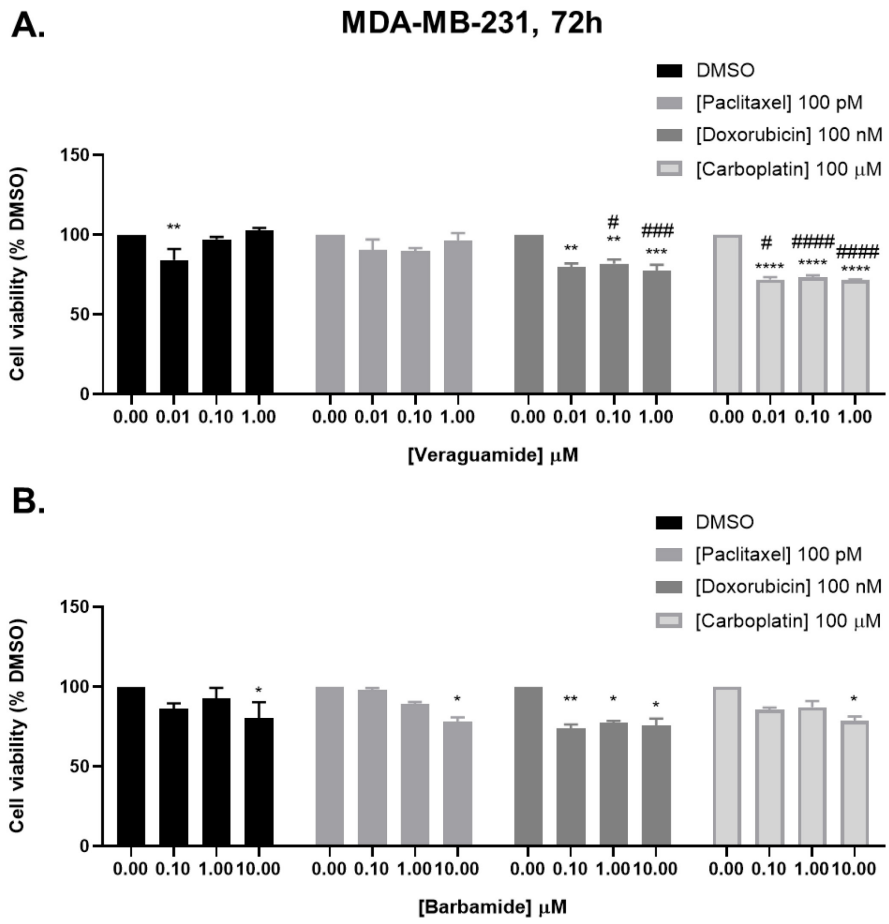

Figure 9.3: Effect of (A) veraguamide and (B) barbamide on chemotherapeutic sensitivity in MDA-MB-231 cells. Data represent the ± SEM of three different experiments. *p<0.05; **p<0.01; ***p<0.001; ****p<0.0001 *vs* control group #p<0.05; ###p<0.001; ####p<0.0001 *vs* chemotherapeutic drug alone determined by one-way ANOVA with the Bonferroni post hoc test.

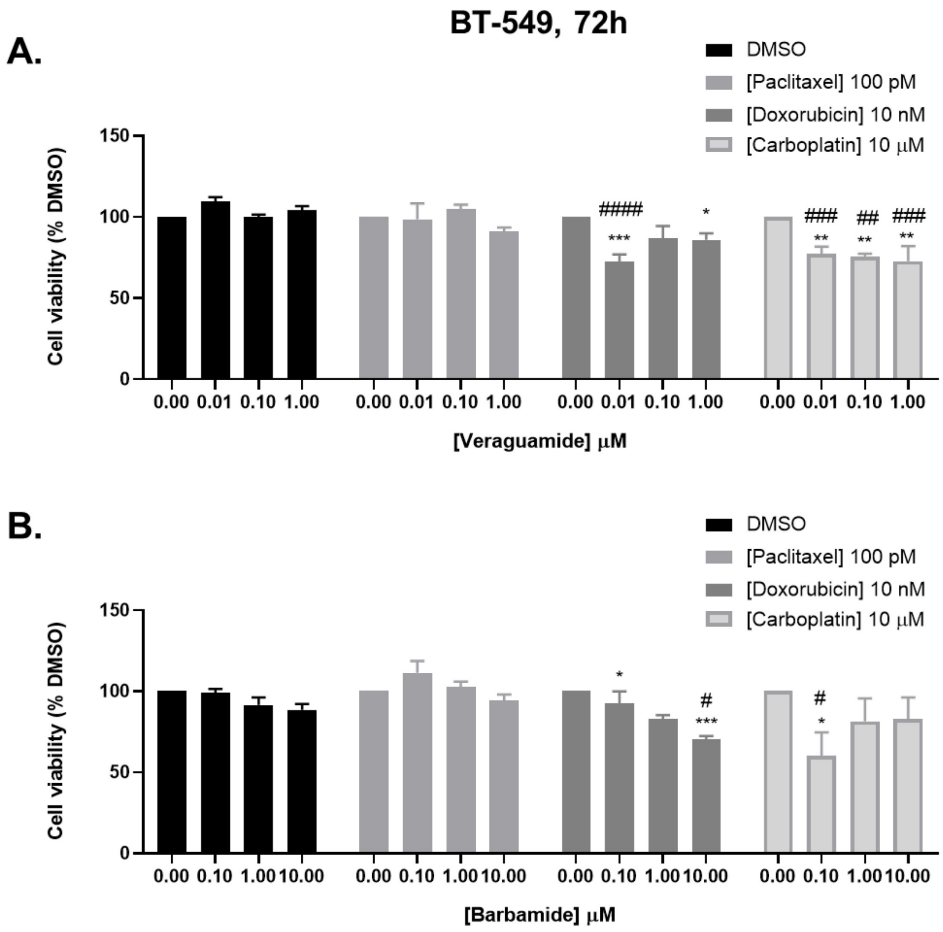

Figure 9.4: Effect of (A) veraguamide and (B) barbamide on chemotherapeutic sensitivity in BT-549 cells. Data represent the ± SEM of three different experiments. *p<0.05; **p<0.01; ***p<0.001 *vs* control group #p<0.05; ##p<0.01; ###p<0.001; ####p<0.0001 *vs* chemotherapeutic drug alone determined by one-way ANOVA with the Bonferroni post hoc test.

9.4 Discussion

Novel cyanobacterial compounds have been identified as sigma 2 receptor ligands. From the initial screen of cyanobacterial fractions, barbamide was isolated from fraction F. Veraguamide and barbamide were used at low doses in combination with chemotherapeutic drugs. There was a modest increase in cytotoxicity of veraguamide and barbamide by carboplatin and doxorubicin. In future, more potent analogs of

barbamide will be synthesized as putative sigma 2 receptor ligands as alternative therapies for diverse breast cancer subtypes. Since natural compounds may be well-tolerated, future studies will examine the effect of low-dose chemotherapeutic drug in combination with higher doses of sigma 2 receptor ligands.

Chapter 10: Conclusion and future directions

Cancer metastasis accounts for 90% cancer related deaths. EMT is the first step in cancer metastases cascade and there are no therapeutic agents, which are known to reverse EMT in aggressive cancer cells with a mesenchymal phenotype. ERK1/2 and ERK5 pathways are known to induce EMT in several cancers; however, the effect of inhibition of the ERK1/2 and ERK5 pathways on the reverse of EMT is not well-understood in cancer. In our research, we utilized bioinformatics, drug discovery, and in vitro approaches to develop strategies to reverse EMT and attenuate tumor forming and metastatic abilities of breast and brain cancers.

Epigenetic pathways and crosstalk with the PI3K pathway may lower the efficacy of ERK1/2 or ERK5 inhibitors on cell viability. Therefore, we designed combination strategies to simultaneously target MAPK and PI3K pathways to target cell viability in triple-negative breast cancer. Development of chemotherapeutic drug resistance is another major problem associated with cancer. Emerging evidence suggests a role of MAPK pathway in mediating chemo-resistance in cancer. Therefore, we developed rational combination strategies to treat cancer cells with a combination of low-dose kinase inhibitors and chemotherapeutic drugs and examined their effect on cell viability. The idea is to utilize low doses of drugs in combination to achieve the same effect as high doses of drugs alone to prevent collateral toxicity. In future, it would be worth assessing whether treating cells with low-dose kinase inhibitors would prevent chemoresistance or treatment of cells that have developed resistance to chemotherapeutic drugs with kinase inhibitors could induce cell death.

In conclusion, we have reported for the first time the effect MAPK pathway inhibition on mesenchymal to epithelial transition, the reverse of EMT, nuclear localization of ERK5 and ERK1/2, and crosstalk with the PI3K-AKT pathway in regulation of EMT and chemotherapeutic sensitivity in breast cancer and glioblastoma models, which have a mesenchymal phenotype.

Appendix A

List of publications

1) **Bhatt, A. B.**; Wright, T. D.; Barnes, V.; Chakrabarty, S.; Matossian, M. D.; Lexner, E.; Ucar, D. A.; Miele, L.; Flaherty, P. T.; Burow, M. E.; Cavanaugh, J. E., Diverse and converging roles of ERK1/2 and ERK5 pathways on mesenchymal to epithelial transition in breast cancer. Translational Oncology 2021, 14 (6), 101046.
2) **Bhatt AB**, Patel S, Matossian MD, Ucar DA, Miele L, Burow ME, Flaherty PT, Cavanaugh JE. Molecular Mechanisms of Epithelial to Mesenchymal Transition Regulated by ERK5 Signaling. Biomolecules. 2021 Jan 29;11(2):183. doi: 10.3390/biom11020183. PMID: 33572742.
3) **Bhatt AB,** Gupta M, Hoang VT, Chakrabarty S, Wright TD, Elliot S, Chopra IK, Monlish D, Anna K, Burow ME, Cavanaugh JE, Flaherty PT. Novel Diphenylamine Analogs Induce Mesenchymal to Epithelial Transition in Triple Negative Breast Cancer. Front Oncol. 2019 Jul 30;9:672. doi: 10.3389/fonc.2019.00672. PMID: 31417863; PMCID: PMC6682674.
4) Wright TD, Raybuck C, **Bhatt A**, Monlish D, Chakrabarty S, Wendekier K, Gartland N, Gupta M, Burow ME, Flaherty PT, Cavanaugh JE. Pharmacological inhibition of the MEK5/ERK5 and PI3K/Akt signaling pathways synergistically reduces viability in triple-negative breast cancer. J Cell Biochem. 2020 Feb;121(2):1156-1168. doi: 10.1002/jcb.29350. Epub 2019 Aug 28. PMID: 31464004; PMCID: PMC6923606.

5) Hoang VT, Matossian MD, Ucar DA, Elliott S, La J, Wright MK, Burks HE, Perles A, Hossain F, King CT, Browning VE, Bursavich J, Fang F, Del Valle L, **Bhatt AB**, Cavanaugh JE, Flaherty PT, Anbalagan M, Rowan BG, Bratton MR, Nephew KP, Miele L, Collins-Burow BM, Martin EC, Burow ME. ERK5 Is Required for Tumor Growth and Maintenance Through Regulation of the Extracellular Matrix in Triple Negative Breast Cancer. Front Oncol. 2020 Aug 3;10:1164. doi: 10.3389/fonc.2020.01164. PMID: 32850332; PMCID: PMC7416559.

6) **Bhatt AB**, Anna K, Schottland S, Martin J, Wright TD, Gupta M, Matossian MD, Ucar DA, Chakrabarty S, Barnes V, Patel S, Miele L, Burow ME, Flaherty PT, Cavanaugh JE. Dual inhibition of MEK5 and MEK1/2 or PI3K pathways decreases cell viability, proliferation, migration, and stemness, and induces mesenchymal to epithelial transition in glioblastoma multiforme. Biochemistry and Pharmacology. 2021. In press.

Appendix B Antibody inventory

Cancer research

Primary antibody

Category	Antibody	Isotype	Molecular weight (kDa)	#Catalog number	Application
Kinase	ERK5	R	115	3372	WB IP
	pERK5 (Thr218/Tyr20)	R	115	3371	WB
	ERK1/2 (p44/42)	M	44, 42	4695	WB IP IHC
	pERK1/2 (phospho-p44/42)	R	44, 42	9101	WB IP IF F
	AKT (Ser 173)	R	60	9272	WB IP IHC
	p-AKT	M	60	4051	WB IP
EMT	E-Cadherin	R	135	3195	WB IHC IF F
	N-Cadherin	R	140	13116	WB IP IHC IF
	Vimentin	R	57	5741	WB IHC IF F
	ZO-1	R	220	5406	WB IP
	Snail	R	29	3879	WB IP
	Slug	R	30	9585	WB IP
	TCF8/ZEB1	R	200	3396	WB IP
	Claudin-1	R	10	13255	WB IP IHC
Miscellaneous	pS6 (Ribosomal protein)	R	32		WB IHC IF F
	Ki67 (cell proliferation marker)	R			IHC
	SOX2 (stem cell biomarker)	R	39	AB5603	WB IHC IF
Loading control	α-tubulin	M	52	3873	WB IHC IF
	GAPDH	R	37	97166	WB

Secondary antibody

Reference no.	Lot no.	Host species	Reactivity species	Fluorophore/conjugate	Application
92668021	C50618-03	G	R	IRDye 680LT	WB ICW
92632210	C30701-01	G	M	IRDye 800CW	WB ICW
A21429	1371057	G	R	Alexa Fluor 555	IF F IHC
A11001	1298479	G	M	Alexa Fluor 488	IF F IHC

Appendix C Structures and data for novel quinazolines and thiophenes.

Cavanaugh lab label	Flaherty lab label	Structure	ERK1/2 % inhibition	SEM	ERK5 % inhibition	SEM	AKT %inhibition	EGFR %inhibition
K1	AJM-1-137	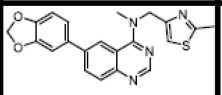	43.04		38.1		96.824	17.28
K4	AJM-1-143	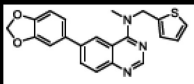	22.46		2.41			
K5	SP-1-5	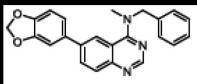	35.5	8.9	88	4.7		
K7	AJM-1-159	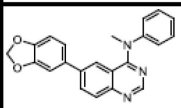	22.1	7.4	100	0		
K36	SP-1-137	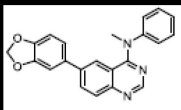	27.48		65.96		96.824	17.28
K37	SP-1-145	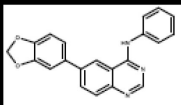	68.82		81.34		98.321	87.61
K42	SP-1-176	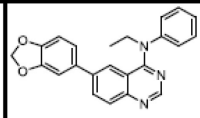	29.7		60.6		81.4	
K2	AJM-1-141	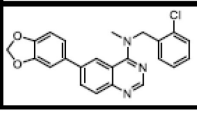	21.28		12.9			

K40	SP-1-168	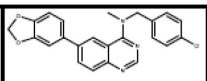	18.3		0		71.7	
K3	AJM-1-142	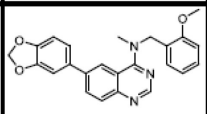	5.19		18.44			
K29	SP-1-71	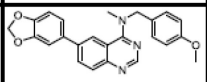	0	3.5	57	15.93		
K28	SP-1_67	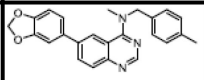	0	17.44	0	11.02		
K8	AJM-1-158	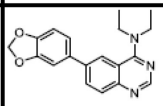	0	32.1	23.6	17.3		
K10	AJM-1-157	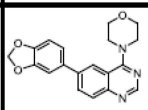	11.7	14.1	20.6	9.3	79.28	

K24	SP-1-57	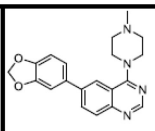	0	38	47	5.5		
K6	AJM-1-173	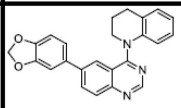	6.7	14.9	45.9	0.6		
K9	AJM-1-151	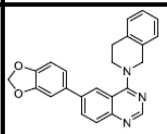	10.2	18.9	12.9	17.1		
K23	SP-1-25	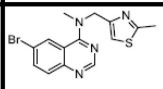	0	27.8	58.6	21.7	64.1	
K19	SP-1-31	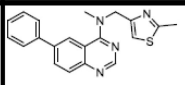	32.6	3.4	72	4.3		
K26	SP-1-55	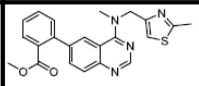	0	35.6	45.6	0.7		
K22	SP-1-41	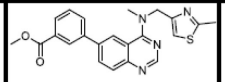	18.6	18.9	57.8	14.5		
K20	SP-1-36	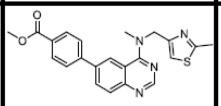	26.3	16.1	65.3	0		

K25	SP-1-58	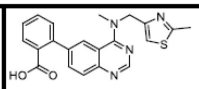	0	40.2	53	9.1		
K27	SP-1-43	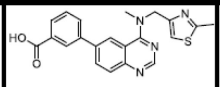	0	32.3	22.8	17.8	0	
K21	SP-1-38	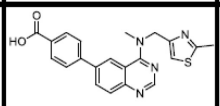	4.7	19.6	30.4	18		
K30	SP-1-77	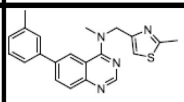	0	1	3	30		
K31	SP-1-86	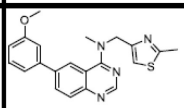	0		0			
K32	SP-1-88	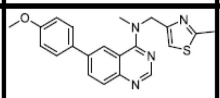	0	27	22.67	33		
K33	SP-1-90	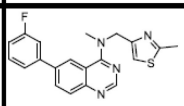	0		90		83.56	
K35	SP-1-106	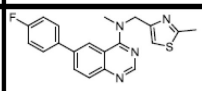	21.99		50		95.072	0
K34	SP-1-102	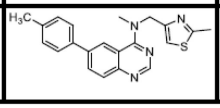	0		53		77.36	

K41	SP-1-153	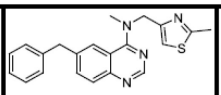	24.9		52.7			
K43	SP-1-148	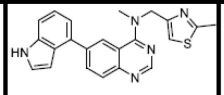	34.4		17.6		98.5	
K44	SP-1-177	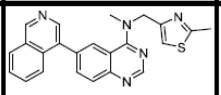	14.5		86		95.6	
K45	SP-1-187	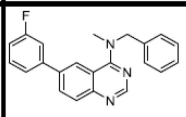	37.8		85.7		88.1	
K46	SP-1-182	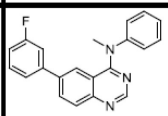	34.8		100		82.9	

Cavanaugh lab	Flaherty lab	Structure	p/tERK1/2	SEM	p/tERK5	SEM	p/tAKT	SEM	pEGFR
K13	MG-3-108	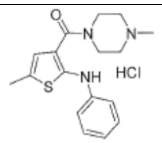	0	17.7	41.1	9.8			
K15	MG-3-104	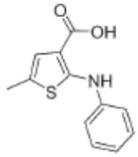	0	9.9	41.4	5.8			
K16	MG-3-110	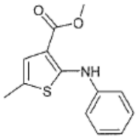	0	2.7	35.8	6.9			
K18	MG-3-96	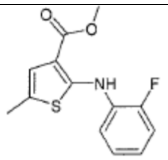	0	18	43.7	15.7			
K38	MG-4-24	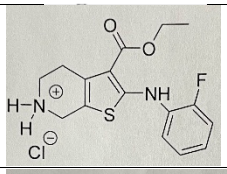	34.96	0.5	0	10.7	0	9.7	0
K39	MG-4-32	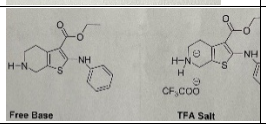	43.64	13.1	0	3.4	0	3.2	0

Appendix D KEGG analysis of pathways upregulated in glioblastoma multiforme

Goal: To identify pathways that are upregulated in GBM.

Method: KEGG pathway analysis was performed to examine the pathways that are upregulated in GBM tumor samples compared to non-tumor controls.

Result: MAPK signaling pathway and genes involved in regulation of the actin cytoskeleton were among the top fifteen categories of significantly upregulated genes. These findings suggest that MAPK pathway is an important target in GBM. The signaling is also outlined below.

Tumor Brain (REMBRANDT study) - Madhavan - 550 - MAS5.0 - u133p2 public
disease~glioblastoma_multiforme,normal 256 of 550 samples, transform_log2
Grouping variable: disease
present calls >=1, selected genes (6968)

3298 combinations meet your criteria
2114 combinations did not meet T-test **p<0.0001** as R and **1** as minimal # of PresentCalls
Date of data procurement: 2-14-2021

Links	Group	In_Set	Total	Percentage	p-value
-	All	3298	5412	60.9%	-
R K A	Axon_guidance	98	121	81.0%	**6.1e-06**
R K A	Retrograde_endocannabinoid_signaling	74	89	83.1%	**1.8e-05**
R K A	Spliceosome	91	119	76.5%	**5.2e-04**
R K A	Glutamatergic_synapse	82	106	77.4%	**5.3e-04**
R K A	Nicotine_addiction	29	32	90.6%	**5.8e-04**
R K A	GABAergic_synapse	61	77	79.2%	**1.0e-03**
R K A	Synaptic_vesicle_cycle	47	58	81.0%	**1.7e-03**
R K A	Long_term_potentiation	49	61	80.3%	**1.9e-03**
R K A	**MAPK_signaling_pathway**	161	227	70.9%	**2.0e-03**
R K A	Circadian_entrainment	63	83	75.9%	**5.2e-03**
R K A	Serotonergic_synapse	67	89	75.3%	**5.5e-03**
R K A	**Regulation_of_actin_cytoskeleton**	133	189	70.4%	**7.9e-03**
R K A	Pancreatic_cancer	50	65	76.9%	**8.3e-03**
R K A	Lysosome	81	111	73.0%	**9.4e-03**
R K A	N_Glycan_biosynthesis	37	47	78.7%	0.01
R K A	Amphetamine_addiction	46	60	76.7%	0.01
R K A	Colorectal_cancer	46	60	76.7%	0.01

RKA	Endometrial_cancer	39	51	76.5%	0.02
RKA	Oxytocin_signaling_pathway	97	138	70.3%	0.02
RKA	MicroRNAs_in_cancer	104	149	69.8%	0.03
RKA	Morphine_addiction	59	81	72.8%	0.03
RKA	Progesterone_mediated_oocyte_maturation	59	81	72.8%	0.03
RKA	Shigellosis	44	59	74.6%	0.03
RKA	Ribosome	76	107	71.0%	0.03
RKA	Vibrio_cholerae_infection	33	43	76.7%	0.03
RKA	DNA_replication	28	36	77.8%	0.04
RKA	ErbB_signaling_pathway	61	85	71.8%	0.04
RKA	Glycosaminoglycan_degradation	13	15	86.7%	0.04
RKA	Arginine_and_proline_metabolism	32	42	76.2%	0.04
RKA	Platelet_activation	76	108	70.4%	0.04
RKA	Mismatch_repair	18	22	81.8%	0.04
RKA	Lysine_degradation	36	48	75.0%	0.05
RKA	Cholinergic_synapse	70	99	70.7%	0.05
RKA	Focal_adhesion	129	190	67.9%	0.05
RKA	Dopaminergic_synapse	81	116	69.8%	0.05
RKA	Protein_processing_in_endoplasmic_reticulum	105	153	68.6%	0.05
RKA	Bladder_cancer	29	38	76.3%	0.05
RKA	Wnt_signaling_pathway	86	124	69.4%	0.05

Kyoto Encyclopedia of Genes and Genomes analysis of pathways regulating GBM progression.

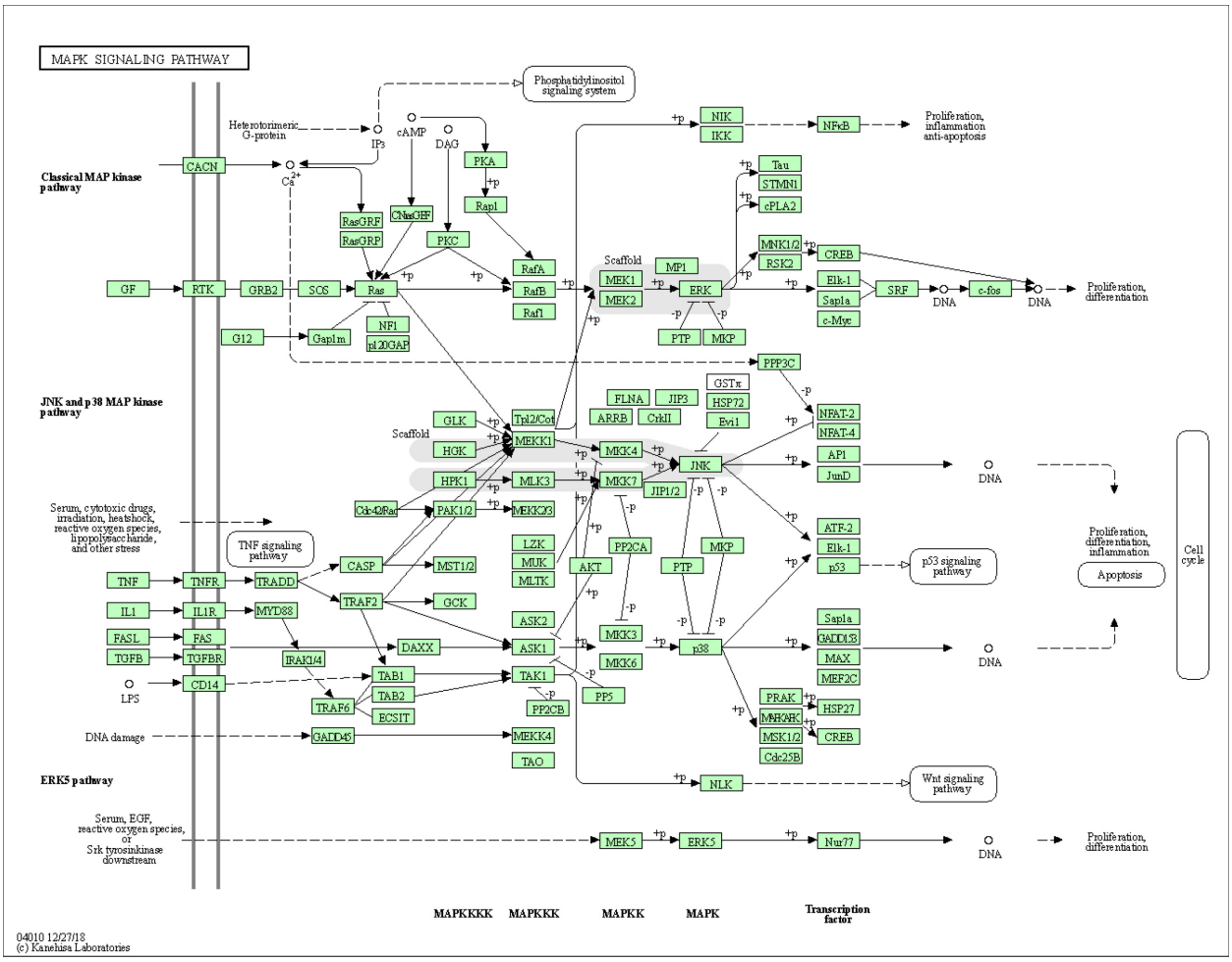
MAPK SIGNALING PATHWAY
Classical MAP kinase pathway
JNK and p38 MAP kinase pathway
ERK5 pathway
Phosphatidylinositol signaling system
Heterotorimeric G-protein
IP3
cAMP
DAG
PKA
Rap1
RasGRP
CNadGEF
PKC
CACN
Ca2+
GF
RTK
GRB2
SOS
Ras
RafA
RafB
Raf1
G12
Gaplm
NF1
p120GAP
Scaffold
MP1
MEK1
MEK2
ERK
PTP
MKP
NIK
IKK
NFkB
Proliferation, inflammation anti-apoptosis
Tau
STMN1
cPLA2
MNK1/2
RSK2
CREB
Elk-1
Sap1a
c-Myc
SRF
c-fos
DNA
Proliferation, differentiation
PPP3C
GSTπ
FLNA
JIP3
HSP72
ARRB
CrkII
Evi1
NFAT-2
NFAT-4
AP1
JunD
GLK
HGK
Tpl2/Cot
MEKK1
HPK1
MLK3
MEKK3
Cdc42/Rac
PAK1/2
MKK4
MKK7
JNK
JIP1/2
Serum, cytotoxic drugs, irradiation, heatshock, reactive oxygen species, lipopolysaccharide, and other stress
TNF signaling pathway
TNF
TNFR
TRADD
CASP
MST1/2
TRAF2
GCK
IL1
IL1R
MYD88
FASL
FAS
TGFB
TGFBR
DAXX
IRAK1/4
LPS
CD14
TAB1
TAB2
TRAF6
ECSIT
DNA damage
GADD45
MEKK4
TAO
LZK
MUK
MLTK
ASK2
ASK1
TAK1
PP2CB
AKT
PP2CA
PP5
MKP
MKK3
MKK6
p38
ATF-2
Elk-1
p53
p53 signaling pathway
Sap1a
GADD153
MAX
MEF2C
PRAK
HSP27
MAPKAPK
MSK1/2
CREB
Cdc25B
Proliferation, differentiation, inflammation
Apoptosis
Cell cycle
NLK
Wnt signaling pathway
Serum, EGF, reactive oxygen species, or Src tyrosinkinase downstream
MEK5
ERK5
Nur77
MAPKKKK
MAPKKK
MAPKK
MAPK
Transcription factor
04010 12/27/18
(c) Kanehisa Laboratories

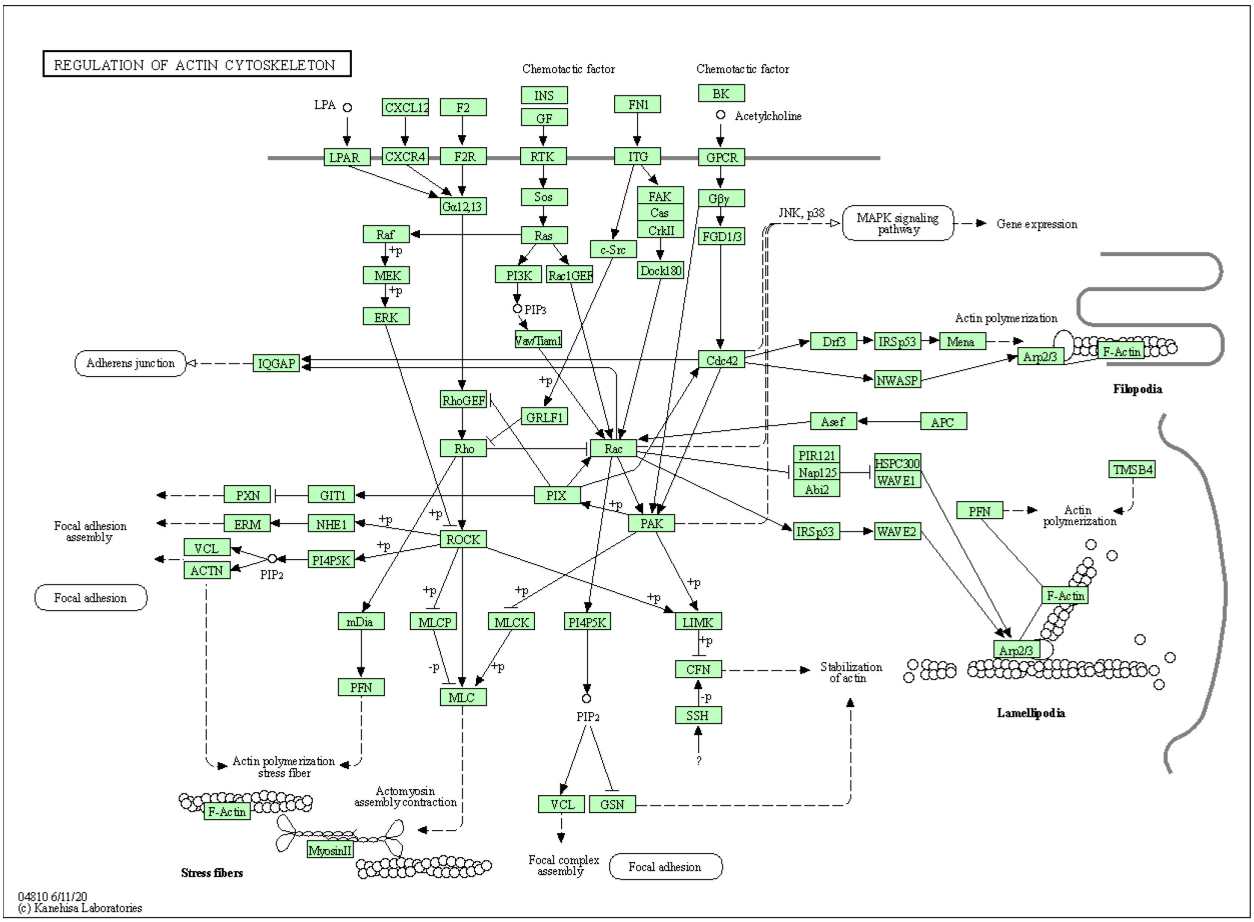

Signaling pathways mediating tumorigenesis in GBM.

Appendix E: Supporting Figures

Hypothesis: Novel diphenylamine compounds will induce MET in TAMR MCF-7 cells.

Method: TAMR MCF-7 cells were treated with diphenylamine compounds for 5 days. The cells were fixed and stained with crystal violet dye and pictures were taken using EVOS.

Result: Compounds reverse EMT in TAMR MCF-7 cells. The SAR obtained in MDA-MB-231 cells was consistent across another model of breast cancer with a mesenchymal phenotype.

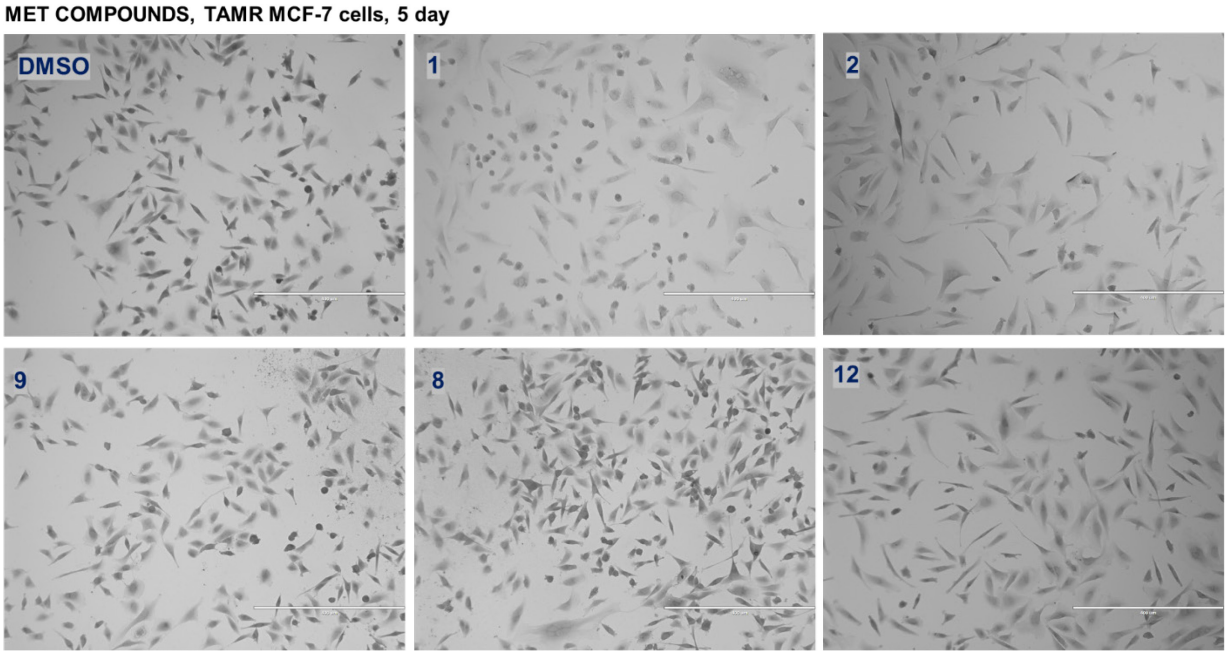

Consistent with MDA-MB-231 cells, treatment with compounds 1, 2, and 9 induced an MET in TAMR MCF-7 cells as examined by crystal violet staining of cells after treatment with 1 uM compounds for 5 days.

Goal: To examine the effect of diphenylamine analogs on AKT activation in MDA-MB-231 cells.

Method: MDA-MB-231 cells were treated with diphenylamine compounds for 5 days. Cell lysates were collected and examined for ERK1/2 and AKT activation via western blotting.

Result: Compounds that inhibited ERK1/2 activation produced a compensatory activation in the AKT pathway, consistent with previous studies.

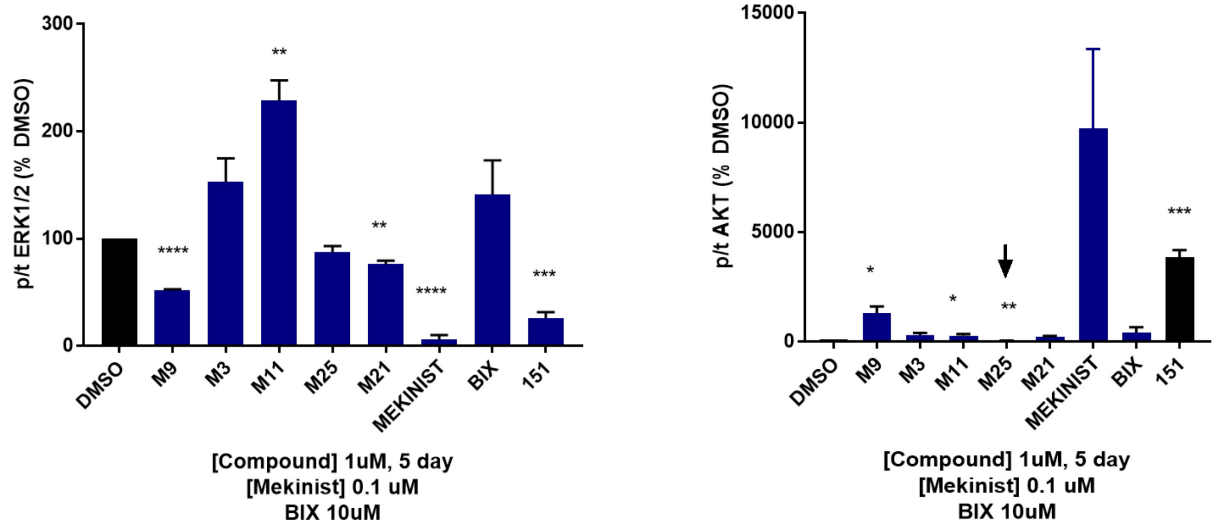

Novel diphenylamine analogs and MEK1/2 or MEK5 inhibitors that inhibit MEK1/2 pathway produced a compensatory increase in AKT pathway.

Hypothesis: Dual inhibition of ERK1/2 and ERK5 pathways will induce a MET in MDA-MB-231 cells.

Method: MDA-MB-231 cells were treated with MEK1/2 inhibitor UO126 and ERK5 inhibitor AX15836 alone and in combination for 5 days. The cells were fixed and stained with crystal violet dye and pictures were taken using EVOS. Cell lysates were collected to examine E-cadherin protein expression. To determine kinase activation, MDA-MB-231 cells were serum starved after 24 hours of plating. Inhibitors were added for 30 minutes followed by 15 minutes of EGF stimulation.

Result: UO126 alone and in combination with AX15826 induces a mesenchymal to epithelial transition in MDA-MB-231 cells as determined by cell morphology and increase in E-cadherin expression. Moreover, treatment with UO126 and AX15836 significantly decreased ERK5 activation by EGF. ERK5 inhibitor AX15836 also inhibited ERK1/2, which was not anticipated and requires further validation.

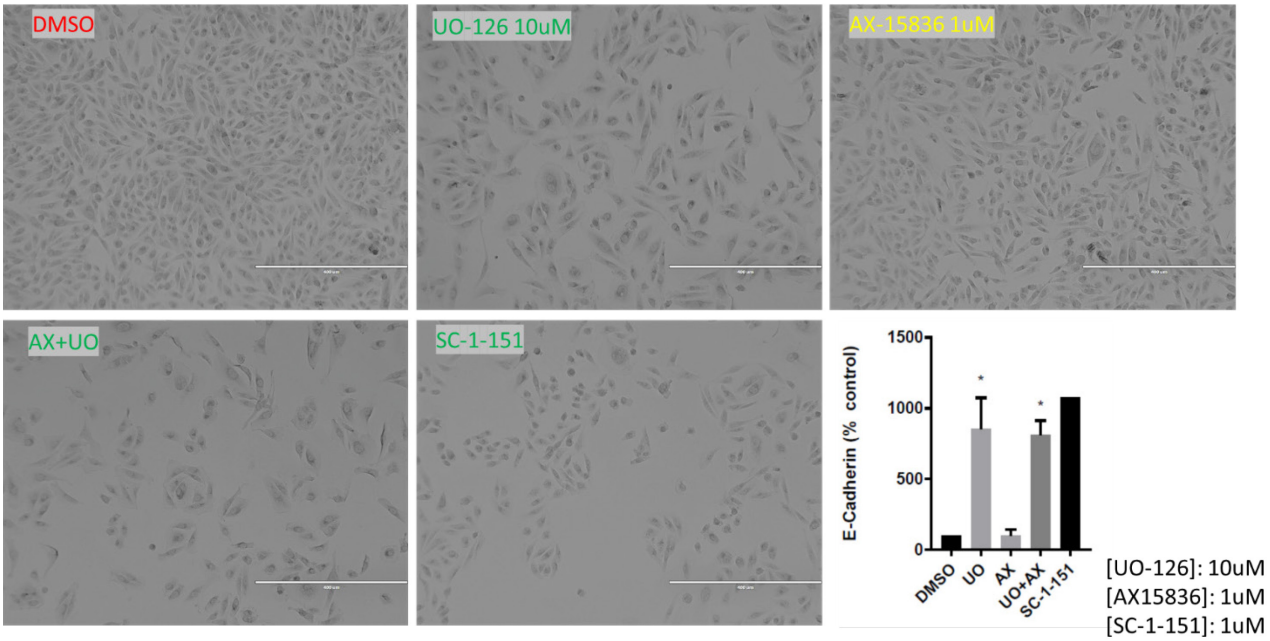

Compound 1 (SC-1-151) – like effects on cell morphology and E-cadherin protein expression could be recapitulated by addition of combination of ERK1/2 inhibitor UO-126 and ERK5 inhibitor AX15836.

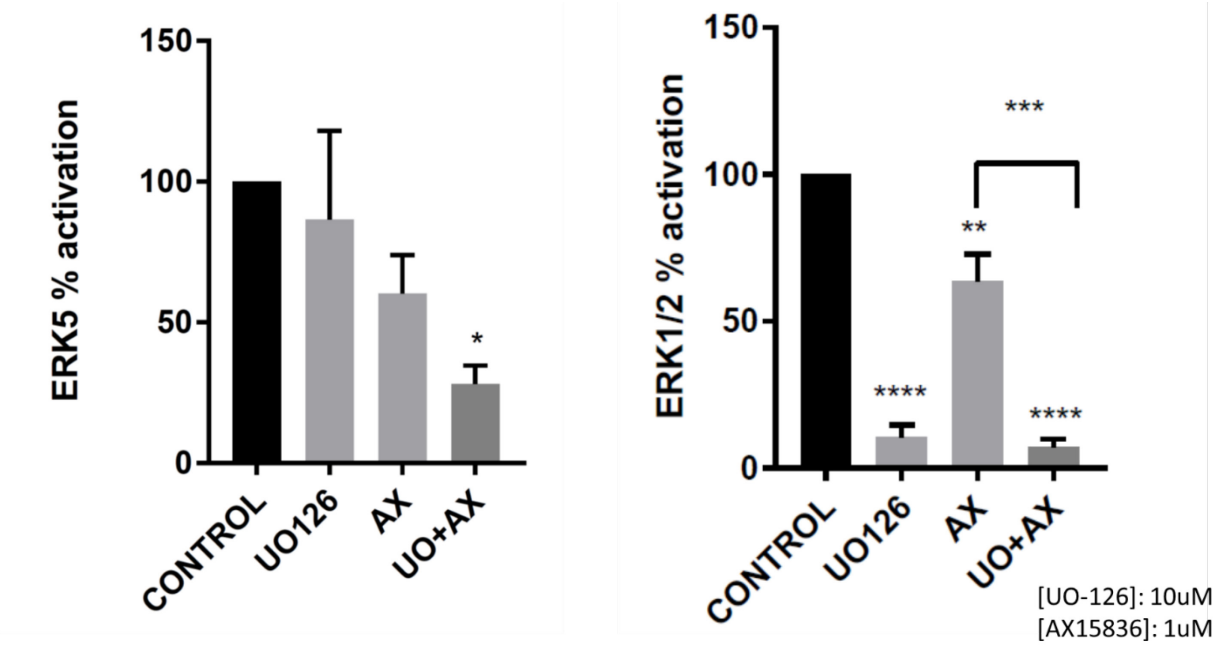

UO+AX combination significantly decreased ERK5 activation by EGF. Moreover, AX15836 significantly decreased ERK1/2 activation by EGF.

Hypothesis: Sequential addition of chemotherapeutic drugs after cells undergo MET will be beneficial to enhance chemosensitivity in TNBC cells.

Method: MDA-MB-231 and BT-549 cells were treated with trametinib, XMD8-92, or combination of Tra+XMD for 48 hours followed by chemotherapeutic drugs for 24 hours. At 72 hours from initial treatment, MTT assay was performed to evaluate cell viability.

Result: Our data indicate that prior treatment with kinase inhibitors does not sensitize the cells (which are in the process of undergoing MET at this stage) to chemotherapeutic drugs paclitaxel, doxorubicin, or carboplatin. Control (Con.) , [Tra] low = 0.01, mid= 0.1, high=1 uM; [XMD] low = 0.1, mid= 1, high= 10 uM; [Tra], [XMD]: low = 0.01, 0.1), Med= 0.1, 1, High= 1, 10. This may be because of increase in drug efflux transporters after treatment with kinase inhibitors.

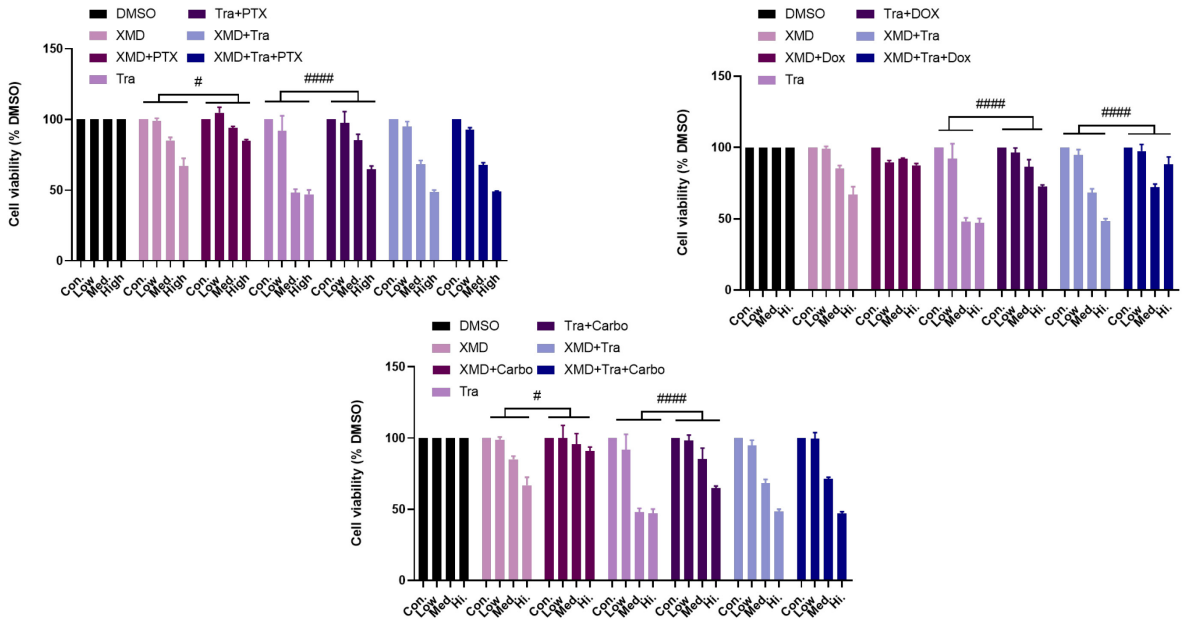

Sequential chemotherapeutic drug treatment did not synergize with MAPK inhibitors in MDA-MB-231 cells.

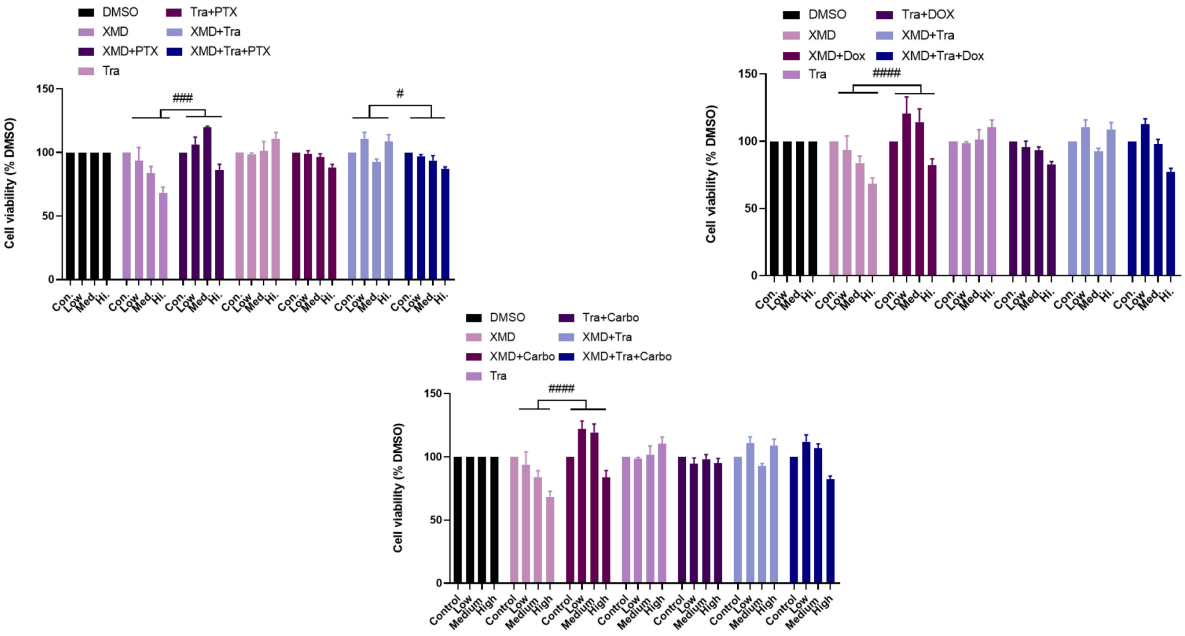

Sequential chemotherapeutic drug treatment did not synergize with MAPK inhibitors in BT-549 cells.

Copyright

Chapter 11: References

1. Siegel, R. L.; Miller, K. D.; Jemal, A., Cancer statistics, 2020. *CA: A Cancer Journal for Clinicians* **2020,** *70* (1), 7-30.

2. Hanahan, D.; Weinberg, R. A., The Hallmarks of Cancer. *Cell* **2000,** *100* (1), 57-70.

3. Hanahan, D.; Weinberg, Robert A., Hallmarks of Cancer: The Next Generation. *Cell* **2011,** *144* (5), 646-674.

4. Davidson, N. E., Diseases of the Breast Jay R. Harris, Marc E. Lippman, Monica Morrow, Samuel Hellman, eds. Philadelphia: Lippincott-Raven, 1996. 1047 pp., illus. $169. ISBN 0-397-51470-0. *JNCI: Journal of the National Cancer Institute* **1997,** *89* (1), 85-85.

5. Oka, H.; Shiozaki, H.; Kobayashi, K.; Inoue, M.; Tahara, H.; Kobayashi, T.; Takatsuka, Y.; Matsuyoshi, N.; Hirano, S.; Takeichi, M.; et al., Expression of E-cadherin cell adhesion molecules in human breast cancer tissues and its relationship to metastasis. *Cancer research* **1993,** *53* (7), 1696-701.

6. Moll, R.; Mitze, M.; Frixen, U. H.; Birchmeier, W., Differential loss of E-cadherin expression in infiltrating ductal and lobular breast carcinomas. *The American journal of pathology* **1993,** *143* (6), 1731-42.

7. Weinberg, R. A., *The Biology of Cancer*. Garland Science: 2014.

8. Roche, J., The Epithelial-to-Mesenchymal Transition in Cancer. *Cancers (Basel)* **2018,** *10* (2), 52.

9. Aroeira, L. S.; Aguilera, A.; Sánchez-Tomero, J. A.; Bajo, M. A.; del Peso, G.; Jiménez-Heffernan, J. A.; Selgas, R.; López-Cabrera, M., Epithelial to Mesenchymal Transition and Peritoneal Membrane Failure in Peritoneal Dialysis Patients: Pathologic Significance and Potential Therapeutic Interventions. *Journal of the American Society of Nephrology* **2007,** *18* (7), 2004.

10. Canel, M.; Serrels, A.; Frame, M. C.; Brunton, V. G., E-cadherin–integrin crosstalk in cancer invasion and metastasis. *Journal of Cell Science* **2013,** *126* (2), 393.

11. Suarez-Carmona, M.; Lesage, J.; Cataldo, D.; Gilles, C., EMT and inflammation: inseparable actors of cancer progression. *Mol Oncol* **2017,** *11* (7), 805-823.

12. Chen, L.; Heymach, J. V.; Qin, F. X.-F.; Gibbons, D. L., The mutually regulatory loop of epithelial-mesenchymal transition and immunosuppression in cancer progression. *Oncoimmunology* **2015,** *4* (5), e1002731-e1002731.

13. Chen, L.; Gibbons, D. L.; Goswami, S.; Cortez, M. A.; Ahn, Y. H.; Byers, L. A.; Zhang, X.; Yi, X.; Dwyer, D.; Lin, W.; Diao, L.; Wang, J.; Roybal, J.; Patel, M.; Ungewiss, C.; Peng, D.; Antonia, S.; Mediavilla-Varela, M.; Robertson, G.; Suraokar, M.; Welsh, J. W.; Erez, B.; Wistuba, II; Chen, L.; Peng, D.; Wang, S.; Ullrich, S. E.; Heymach, J. V.; Kurie, J. M.; Qin, F. X., Metastasis is regulated via microRNA-200/ZEB1 axis control of tumour cell PD-L1 expression and intratumoral immunosuppression. *Nature communications* **2014,** *5*, 5241.

14. Genna, A.; Vanwynsberghe, A. M.; Villard, A. V.; Pottier, C.; Ancel, J.; Polette, M.; Gilles, C., EMT-Associated Heterogeneity in Circulating Tumor Cells: Sticky Friends on the Road to Metastasis. *Cancers* **2020,** *12* (6).

15. Shibue, T.; Weinberg, R. A., EMT, CSCs, and drug resistance: the mechanistic link and clinical implications. *Nat Rev Clin Oncol* **2017,** *14* (10), 611-629.

16. Olea-Flores, M.; Zuniga-Eulogio, M. D.; Mendoza-Catalan, M. A.; Rodriguez-Ruiz, H. A.; Castaneda-Saucedo, E.; Ortuno-Pineda, C.; Padilla-Benavides, T.; Navarro-Tito, N., Extracellular-Signal Regulated Kinase: A Central Molecule Driving Epithelial-Mesenchymal Transition in Cancer. *Int J Mol Sci* **2019,** *20* (12).

17. Cobb, M. H.; Boulton, T. G.; Robbins, D. J., Extracellular signal-regulated kinases: ERKs in progress. *Cell regulation* **1991,** *2* (12), 965-78.

18. Sinh, N. D.; Endo, K.; Miyazawa, K.; Saitoh, M., Ets1 and ESE1 reciprocally regulate expression of ZEB1/ZEB2, dependent on ERK1/2 activity, in breast cancer cells. *Cancer science* **2017,** *108* (5), 952-960.

19. Warn-Cramer, B. J.; Lampe, P. D.; Kurata, W. E.; Kanemitsu, M. Y.; Loo, L. W.; Eckhart, W.; Lau, A. F., Characterization of the mitogen-activated protein kinase phosphorylation sites on the connexin-43 gap junction protein. *The Journal of biological chemistry* **1996,** *271* (7), 3779-86.

20. Yoon, S.; Seger, R., The extracellular signal-regulated kinase: multiple substrates regulate diverse cellular functions. *Growth factors (Chur, Switzerland)* **2006,** *24* (1), 21-44.

21. Carlson, S. M.; Chouinard, C. R.; Labadorf, A.; Lam, C. J.; Schmelzle, K.; Fraenkel, E.; White, F. M., Large-scale discovery of ERK2 substrates identifies ERK-mediated transcriptional regulation by ETV3. *Science signaling* **2011,** *4* (196), rs11.

22. Yang, L.; Zheng, L.; Chng, W. J.; Ding, J. L., Comprehensive Analysis of ERK1/2 Substrates for Potential Combination Immunotherapies. *Trends in pharmacological sciences* **2019,** *40* (11), 897-910.

23. Hoang, V. T.; Yan, T. J.; Cavanaugh, J. E.; Flaherty, P. T.; Beckman, B. S.; Burow, M. E., Oncogenic signaling of MEK5-ERK5. *Cancer Lett* **2017,** *392*, 51-59.

24. Schweppe, R. E.; Cheung, T. H.; Ahn, N. G., Global gene expression analysis of ERK5 and ERK1/2 signaling reveals a role for HIF-1 in ERK5-mediated responses. *The Journal of biological chemistry* **2006,** *281* (30), 20993-21003.

25. Nithianandarajah-Jones, G. N.; Wilm, B.; Goldring, C. E.; Müller, J.; Cross, M. J., ERK5: structure, regulation and function. *Cellular signalling* **2012,** *24* (11), 2187-96.

26. Akshita B. Bhatt, T. D. W., Van Barnes, Suravi Chakrabarty, Margarite D. Matossian, Erin Lexner, Deniz A. Ucar, Lucio Miele, Patrick T. Flaherty, Matthew E. Burow, Jane E. Cavanaugh Diverse and converging roles of ERK1/2 and ERK5 pathways on mesenchymal to epithelial transition in breast cancer.

27. Wang, H.; Dai, Y. Y.; Zhang, W. Q.; Hsu, P. C.; Yang, Y. L.; Wang, Y. C.; Chan, G.; Au, A.; Xu, Z. D.; Jiang, S. J.; Wang, W.; Jablons, D. M.; You, L., DCLK1 is correlated with MET and ERK5 expression, and associated with prognosis in malignant pleural mesothelioma. *International journal of oncology* **2017,** *51* (1), 91-103.

28. Mehta, P. B.; Jenkins, B. L.; McCarthy, L.; Thilak, L.; Robson, C. N.; Neal, D. E.; Leung, H. Y., MEK5 overexpression is associated with metastatic prostate cancer, and stimulates proliferation, MMP-9 expression and invasion. *Oncogene* **2003,** *22* (9), 1381-9.

29. Wrobel, K.; Zhao, Y. C.; Kulkoyluoglu, E.; Chen, K. L. A.; Hieronymi, K.; Holloway, J.; Li, S.; Ray, T.; Ray, P. S.; Landesman, Y.; Lipka, A. E.; Smith, R. L.; Madak-Erdogan, Z., ERα-XPO1 Cross Talk Controls Tamoxifen Sensitivity in Tumors by Altering ERK5 Cellular Localization. *Molecular Endocrinology* **2016,** *30* (10), 1029-1045.

30. Miranda, M.; Rozali, E.; Khanna, K. K.; Al-Ejeh, F., MEK5-ERK5 pathway associates with poor survival of breast cancer patients after systemic treatments. *Oncoscience* **2015,** *2* (2), 99-101.

31. Zhuang, K.; Zhang, J.; Xiong, M.; Wang, X.; Luo, X.; Han, L.; Meng, Y.; Zhang, Y.; Liao, W.; Liu, S., CDK5 functions as a tumor promoter in human colorectal cancer via modulating the ERK5-AP-1 axis. *Cell death & disease* **2016,** *7* (10), e2415-e2415.

32. Tesser-Gamba, F.; Lopes, L. J.; Petrilli, A. S.; Toledo, S. R., MAPK7 gene controls proliferation, migration and cell invasion in osteosarcoma. *Molecular carcinogenesis* **2016,** *55* (11), 1700-1713.

33. Dong, X.; Lv, B.; Li, Y.; Cheng, Q.; Su, C.; Yin, G., MiR-143 regulates the proliferation and migration of osteosarcoma cells through targeting MAPK7. *Archives of biochemistry and biophysics* **2017,** *630*, 47-53.

34. Granados-Jaén, A.; Angulo-Ibáñez, M.; Rovira-Clavé, X.; Gamez, C. P.; Soriano, F. X.; Reina, M.; Espel, E., Absence of ERK5/MAPK7 delays tumorigenesis in Atm-/- mice. *Oncotarget* **2016,** *7* (46), 74435-74447.

35. Holderfield, M.; Deuker, M. M.; McCormick, F.; McMahon, M., Targeting RAF kinases for cancer therapy: BRAF-mutated melanoma and beyond. *Nat Rev Cancer* **2014,** *14* (7), 455-467.

36. Lin, K.; Baritaki, S.; Militello, L.; Malaponte, G.; Bevelacqua, Y.; Bonavida, B., The Role of B-RAF Mutations in Melanoma and the Induction of EMT via Dysregulation of the NF-κB/Snail/RKIP/PTEN Circuit. *Genes Cancer* **2010,** *1* (5), 409-420.

37. Wright, T. D.; Raybuck, C.; Bhatt, A.; Monlish, D.; Chakrabarty, S.; Wendekier, K.; Gartland, N.; Gupta, M.; Burow, M. E.; Flaherty, P. T.; Cavanaugh, J. E., Pharmacological inhibition of the MEK5/ERK5 and PI3K/Akt signaling pathways synergistically reduces viability in triple-negative breast cancer. *Journal of cellular biochemistry* **2019**.

38. Ramos-Nino, M. E.; Blumen, S. R.; Sabo-Attwood, T.; Pass, H.; Carbone, M.; Testa, J. R.; Altomare, D. A.; Mossman, B. T., HGF mediates cell proliferation of human mesothelioma cells through a PI3K/MEK5/Fra-1 pathway. *American journal of respiratory cell and molecular biology* **2008,** *38* (2), 209-17.

39. Umapathy, G.; El Wakil, A.; Witek, B.; Chesler, L.; Danielson, L.; Deng, X.; Gray, N. S.; Johansson, M.; Kvarnbrink, S.; Ruuth, K.; Schonherr, C.; Palmer, R. H.; Hallberg, B., The kinase ALK stimulates the kinase ERK5 to promote the expression of the oncogene MYCN in neuroblastoma. *Science signaling* **2014,** *7* (349), ra102.

40. Castro, N. E.; Lange, C. A., Breast tumor kinase and extracellular signal-regulated kinase 5 mediate Met receptor signaling to cell migration in breast cancer cells. *Breast cancer research : BCR* **2010,** *12* (4), R60-R60.

41. Tsioumpekou, M.; Papadopoulos, N.; Burovic, F.; Heldin, C. H.; Lennartsson, J., Platelet-derived growth factor (PDGF)-induced activation of Erk5 MAP-kinase is dependent on Mekk2, Mek1/2, PKC and PI3-kinase, and affects BMP signaling. *Cellular signalling* **2016,** *28* (9), 1422-31.

42. Carvajal-Vergara, X.; Tabera, S.; Montero, J. C.; Esparís-Ogando, A.; López-Pérez, R.; Mateo, G.; Gutiérrez, N.; Parmo-Cabañas, M.; Teixidó, J. n.; San Miguel, J. s. F.; Pandiella, A., Multifunctional role of Erk5 in multiple myeloma. *Blood* **2005,** *105* (11), 4492-4499.

43. Zhai, L.; Ma, C.; Li, W.; Yang, S.; Liu, Z., miR-143 suppresses epithelial-mesenchymal transition and inhibits tumor growth of breast cancer through down-regulation of ERK5. *Molecular carcinogenesis* **2016,** *55* (12), 1990-2000.

44. Wu, J.; Cui, H.; Zhu, Z.; Wang, L., MicroRNA-200b-3p suppresses epithelial-mesenchymal transition and inhibits tumor growth of glioma through down-regulation of ERK5. *Biochemical and biophysical research communications* **2016,** *478* (3), 1158-64.

45. Eberhard, J.; Gaber, A.; Wangefjord, S.; Nodin, B.; Uhlén, M.; Ericson Lindquist, K.; Jirström, K., A cohort study of the prognostic and treatment predictive value of SATB2 expression in colorectal cancer. *Br J Cancer* **2012,** *106* (5), 931-8.

46. Wang, S.; Zhou, J.; Wang, X. Y.; Hao, J. M.; Chen, J. Z.; Zhang, X. M.; Jin, H.; Liu, L.; Zhang, Y. F.; Liu, J.; Ding, Y. Q.; Li, J. M., Down-regulated expression of SATB2 is associated with metastasis and poor prognosis in colorectal cancer. *The Journal of pathology* **2009,** *219* (1), 114-22.

47. Gu, J.; Wang, G.; Liu, H.; Xiong, C., SATB2 targeted by methylated miR-34c-5p suppresses proliferation and metastasis attenuating the epithelial-mesenchymal transition in colorectal cancer. *Cell Proliferation* **2018,** *51* (4), e12455.

48. Mansour, M. A.; Hyodo, T.; Ito, S.; Kurita, K.; Kokuryo, T.; Uehara, K.; Nagino, M.; Takahashi, M.; Hamaguchi, M.; Senga, T., SATB2 suppresses the progression of colorectal cancer cells via inactivation of MEK5/ERK5 signaling. *The FEBS journal* **2015,** *282* (8), 1394-405.

49. Arias-González, L.; Moreno-Gimeno, I.; del Campo, A. R.; Leticia, S.-O.; Valero, M. L.; Esparís-Ogando, A.; de la Cruz-Morcillo, M. Á.; Melgar-Rojas, P.; García-Cano, J.; Cimas, F. J.; Hidalgo, M. J. R.; Prado, A.; Callejas-Valera, J. L.; Nam-Cha, S. H.; Giménez-Bachs, J. M.; Salinas-Sánchez, A. S.; Pandiella, A.; del Peso, L.; Prieto, R. S., ERK5/BMK1 Is a Novel Target

of the Tumor Suppressor VHL: Implication in Clear Cell Renal Carcinoma. *Neoplasia* **2013,** *15* (6), 649-IN17.

50. Cowey, C. L.; Rathmell, W. K., VHL gene mutations in renal cell carcinoma: role as a biomarker of disease outcome and drug efficacy. *Curr Oncol Rep* **2009,** *11* (2), 94-101.

51. Bhatt, A. B.; Gupta, M.; Hoang, V. T.; Chakrabarty, S.; Wright, T. D.; Elliot, S.; Chopra, I. K.; Monlish, D.; Anna, K.; Burow, M. E.; Cavanaugh, J. E.; Flaherty, P. T., Novel Diphenylamine Analogs Induce Mesenchymal to Epithelial Transition in Triple Negative Breast Cancer. *Frontiers in oncology* **2019,** *9*, 672.

52. de Jong, P. R.; Taniguchi, K.; Harris, A. R.; Bertin, S.; Takahashi, N.; Duong, J.; Campos, A. D.; Powis, G.; Corr, M.; Karin, M.; Raz, E., ERK5 signalling rescues intestinal epithelial turnover and tumour cell proliferation upon ERK1/2 abrogation. *Nature Communications* **2016,** *7* (1), 11551.

53. Vaseva, A. V.; Blake, D. R.; Gilbert, T. S. K.; Ng, S.; Hostetter, G.; Azam, S. H.; Ozkan-Dagliyan, I.; Gautam, P.; Bryant, K. L.; Pearce, K. H.; Herring, L. E.; Han, H.; Graves, L. M.; Witkiewicz, A. K.; Knudsen, E. S.; Pecot, C. V.; Rashid, N.; Houghton, P. J.; Wennerberg, K.; Cox, A. D.; Der, C. J., KRAS Suppression-Induced Degradation of MYC Is Antagonized by a MEK5-ERK5 Compensatory Mechanism. *Cancer Cell* **2018,** *34* (5), 807-822.e7.

54. Song, C.; Wang, L.; Xu, Q.; Wang, K.; Xie, D.; Yu, Z.; Jiang, K.; Liao, L.; Yates, J. R.; Lee, J.-D.; Yang, Q., Targeting BMK1 Impairs the Drug Resistance to Combined Inhibition of BRAF and MEK1/2 in Melanoma. *Scientific reports* **2017,** *7*, 46244-46244.

55. Benito-Jardon, L.; Diaz-Martinez, M.; Arellano-Sanchez, N.; Vaquero-Morales, P.; Esparis-Ogando, A.; Teixido, J., Resistance to MAPK Inhibitors in Melanoma Involves Activation of the IGF1R-MEK5-Erk5 Pathway. *Cancer research* **2019,** *79* (9), 2244-2256.

56. Wang, X.; Pesakhov, S.; Harrison, J. S.; Kafka, M.; Danilenko, M.; Studzinski, G. P., The MAPK ERK5, but not ERK1/2, inhibits the progression of monocytic phenotype to the functioning macrophage. *Experimental cell research* **2015,** *330* (1), 199-211.

57. Adam, C.; Fusi, L.; Weiss, N.; Goller, S. G.; Meder, K.; Frings, V. G.; Kneitz, H.; Goebeler, M.; Houben, R.; Schrama, D.; Schmidt, M., Efficient Suppression of NRAS-Driven Melanoma by Co-inhibition of ERK1/2 and ERK5 MAPK Pathways. *Journal of Investigative Dermatology* **2020**.

58. Tusa, I.; Gagliardi, S.; Tubita, A.; Pandolfi, S.; Urso, C.; Borgognoni, L.; Wang, J.; Deng, X.; Gray, N. S.; Stecca, B.; Rovida, E., ERK5 is activated by oncogenic BRAF and promotes melanoma growth. *Oncogene* **2018,** *37* (19), 2601-2614.

59. Honda, T.; Obara, Y.; Yamauchi, A.; Couvillon, A. D.; Mason, J. J.; Ishii, K.; Nakahata, N., Phosphorylation of ERK5 on Thr732 is associated with ERK5 nuclear localization and ERK5-dependent transcription. *PloS one* **2015,** *10* (2), e0117914-e0117914.

60. Honda T, O. Y., Yamauchi A, Couvillon AD, Mason JJ, Ishii K, Nakahata N, Phosphorylation of ERK5 on Thr732 Is Associated with ERK5 Nuclear Localization and ERK5-Dependent Transcription. *PLoS ONE 10(2): e0117914* **2015**.

61. Mendoza, M. C.; Er, E. E.; Blenis, J., The Ras-ERK and PI3K-mTOR pathways: cross-talk and compensation. *Trends Biochem Sci* **2011,** *36* (6), 320-8.

62. Yu, J.; Zhang, Y.; McIlroy, J.; Rordorf-Nikolic, T.; Orr, G. A.; Backer, J. M., Regulation of the p85/p110 phosphatidylinositol 3'-kinase: stabilization and inhibition of the p110alpha catalytic subunit by the p85 regulatory subunit. *Molecular and cellular biology* **1998,** *18* (3), 1379-87.

63. Rameh, L. E.; Cantley, L. C., The role of phosphoinositide 3-kinase lipid products in cell function. *The Journal of biological chemistry* **1999,** *274* (13), 8347-50.

64. Wymann, M. P.; Pirola, L., Structure and function of phosphoinositide 3-kinases. *Biochimica et biophysica acta* **1998,** *1436* (1-2), 127-50.

65. Fruman, D. A.; Snapper, S. B.; Yballe, C. M.; Davidson, L.; Yu, J. Y.; Alt, F. W.; Cantley, L. C., Impaired B Cell Development and Proliferation in Absence of Phosphoinositide 3-Kinase p85α. *Science* **1999,** *283* (5400), 393-397.

66. Songyang, Z.; Shoelson, S. E.; McGlade, J.; Olivier, P.; Pawson, T.; Bustelo, X. R.; Barbacid, M.; Sabe, H.; Hanafusa, H.; Yi, T.; et al., Specific motifs recognized by the SH2 domains

of Csk, 3BP2, fps/fes, GRB-2, HCP, SHC, Syk, and Vav. *Molecular and cellular biology* **1994,** *14* (4), 2777-85.

67. Mayer, B. J.; Gupta, R., Functions of SH2 and SH3 domains. *Current topics in microbiology and immunology* **1998,** *228*, 1-22.

68. Stauffer, F.; Holzer, P.; García-Echeverría, C., Blocking the PI3K/PKB pathway in tumor cells. *Current medicinal chemistry. Anti-cancer agents* **2005,** *5* (5), 449-62.

69. Jia, S.; Roberts, T. M.; Zhao, J. J., Should individual PI3 kinase isoforms be targeted in cancer? *Current opinion in cell biology* **2009,** *21* (2), 199-208.

70. Vivanco, I.; Sawyers, C. L., The phosphatidylinositol 3-Kinase AKT pathway in human cancer. *Nature reviews. Cancer* **2002,** *2* (7), 489-501.

71. Vivanco, I.; Sawyers, C. L., The phosphatidylinositol 3-Kinase–AKT pathway in human cancer. *Nature Reviews Cancer* **2002,** *2* (7), 489-501.

72. Bi, L.; Okabe, I.; Bernard, D. J.; Nussbaum, R. L., Early embryonic lethality in mice deficient in the p110beta catalytic subunit of PI 3-kinase. *Mammalian genome : official journal of the International Mammalian Genome Society* **2002,** *13* (3), 169-72.

73. Foukas, L. C.; Claret, M.; Pearce, W.; Okkenhaug, K.; Meek, S.; Peskett, E.; Sancho, S.; Smith, A. J.; Withers, D. J.; Vanhaesebroeck, B., Critical role for the p110alpha phosphoinositide-3-OH kinase in growth and metabolic regulation. *Nature* **2006,** *441* (7091), 366-70.

74. Ciraolo, E.; Iezzi, M.; Marone, R.; Marengo, S.; Curcio, C.; Costa, C.; Azzolino, O.; Gonella, C.; Rubinetto, C.; Wu, H.; Dastrù, W.; Martin, E. L.; Silengo, L.; Altruda, F.; Turco, E.; Lanzetti, L.; Musiani, P.; Rückle, T.; Rommel, C.; Backer, J. M.; Forni, G.; Wymann, M. P.; Hirsch, E., Phosphoinositide 3-kinase p110beta activity: key role in metabolism and mammary gland cancer but not development. *Science signaling* **2008,** *1* (36), ra3.

75. Jackson, S. P.; Schoenwaelder, S. M.; Goncalves, I.; Nesbitt, W. S.; Yap, C. L.; Wright, C. E.; Kenche, V.; Anderson, K. E.; Dopheide, S. M.; Yuan, Y.; Sturgeon, S. A.; Prabaharan, H.; Thompson, P. E.; Smith, G. D.; Shepherd, P. R.; Daniele, N.; Kulkarni, S.; Abbott, B.; Saylik, D.;

Jones, C.; Lu, L.; Giuliano, S.; Hughan, S. C.; Angus, J. A.; Robertson, A. D.; Salem, H. H., PI 3-kinase p110beta: a new target for antithrombotic therapy. *Nature medicine* **2005,** *11* (5), 507-14.

76. Torbett, N. E.; Luna-Moran, A.; Knight, Z. A.; Houk, A.; Moasser, M.; Weiss, W.; Shokat, K. M.; Stokoe, D., A chemical screen in diverse breast cancer cell lines reveals genetic enhancers and suppressors of sensitivity to PI3K isoform-selective inhibition. *The Biochemical journal* **2008,** *415* (1), 97-110.

77. Oda, K.; Okada, J.; Timmerman, L.; Rodriguez-Viciana, P.; Stokoe, D.; Shoji, K.; Taketani, Y.; Kuramoto, H.; Knight, Z. A.; Shokat, K. M.; McCormick, F., PIK3CA Cooperates with Other Phosphatidylinositol 3′-Kinase Pathway Mutations to Effect Oncogenic Transformation. *Cancer research* **2008,** *68* (19), 8127-8136.

78. Jia, S.; Liu, Z.; Zhang, S.; Liu, P.; Zhang, L.; Lee, S. H.; Zhang, J.; Signoretti, S.; Loda, M.; Roberts, T. M.; Zhao, J. J., Essential roles of PI(3)K-p110beta in cell growth, metabolism and tumorigenesis. *Nature* **2008,** *454* (7205), 776-9.

79. Fan, Q. W.; Knight, Z. A.; Goldenberg, D. D.; Yu, W.; Mostov, K. E.; Stokoe, D.; Shokat, K. M.; Weiss, W. A., A dual PI3 kinase/mTOR inhibitor reveals emergent efficacy in glioma. *Cancer cell* **2006,** *9* (5), 341-9.

80. Thiery, J. P.; Sleeman, J. P., Complex networks orchestrate epithelial-mesenchymal transitions. *Nature reviews. Molecular cell biology* **2006,** *7* (2), 131-42.

81. Barros, J. C.; Marshall, C. J., Activation of either ERK1/2 or ERK5 MAP kinase pathways can lead to disruption of the actin cytoskeleton. *J Cell Sci* **2005,** *118* (Pt 8), 1663-71.

82. Pavan, S.; Meyer-Schaller, N.; Diepenbruck, M.; Kalathur, R. K. R.; Saxena, M.; Christofori, G., A kinome-wide high-content siRNA screen identifies MEK5–ERK5 signaling as critical for breast cancer cell EMT and metastasis. *Oncogene* **2018,** *37* (31), 4197-4213.

83. Chakrabarty, S.; Monlish, D. A.; Gupta, M.; Wright, T. D.; Hoang, V. T.; Fedak, M.; Chopra, I.; Flaherty, P. T.; Madura, J.; Mannepelli, S.; Burow, M. E.; Cavanaugh, J. E., Structure activity relationships of anthranilic acid-based compounds on cellular and in vivo mitogen activated

protein kinase-5 signaling pathways. *Bioorganic & medicinal chemistry letters* **2018,** *28* (13), 2294-2301.

84. Koo, V.; El Mekabaty, A.; Hamilton, P.; Maxwell, P.; Sharaf, O.; Diamond, J.; Watson, J.; Williamson, K., Novel in vitro assays for the characterization of EMT in tumourigenesis. *Cellular oncology : the official journal of the International Society for Cellular Oncology* **2010,** *32* (1-2), 67-76.

85. Koo, V.; El Mekabaty, A.; Hamilton, P.; Maxwell, P.; Sharaf, O.; Diamond, J.; Watson, J.; Williamson, K., Novel in vitro assays for the characterization of EMT in tumourigenesis. *Cellular oncology : the official journal of the International Society for Cellular Oncology* **2010,** *32* (1-2), 67-76.

86. Hu, K. H.; Eichorst, J. P.; McGinnis, C. S.; Patterson, D. M.; Chow, E. D.; Kersten, K.; Jameson, S. C.; Gartner, Z. J.; Rao, A. A.; Krummel, M. F., ZipSeq: barcoding for real-time mapping of single cell transcriptomes. *Nature methods* **2020,** *17* (8), 833-843.

87. De Laurentiis, M.; Cianniello, D.; Caputo, R.; Stanzione, B.; Arpino, G.; Cinieri, S.; Lorusso, V.; De Placido, S., Treatment of triple negative breast cancer (TNBC): current options and future perspectives. *Cancer treatment reviews* **2010,** *36 Suppl 3*, S80-6.

88. Chang, M., Tamoxifen resistance in breast cancer. *Biomol Ther (Seoul)* **2012,** *20* (3), 256-267.

89. Hiscox, S.; Jiang, W. G.; Obermeier, K.; Taylor, K.; Morgan, L.; Burmi, R.; Barrow, D.; Nicholson, R. I., Tamoxifen resistance in MCF7 cells promotes EMT-like behaviour and involves modulation of β-catenin phosphorylation. *International journal of cancer* **2006,** *118* (2), 290-301.

90. Bhatt, A. B.; Patel, S.; Matossian, M. D.; Ucar, D. A.; Miele, L.; Burow, M. E.; Flaherty, P. T.; Cavanaugh, J. E., Molecular Mechanisms of Epithelial to Mesenchymal Transition Regulated by ERK5 Signaling. *Biomolecules* **2021,** *11* (2).

91. Benito-Jardón, L.; Díaz-Martínez, M.; Arellano-Sánchez, N.; Vaquero-Morales, P.; Esparís-Ogando, A.; Teixidó, J., Resistance to MAPK Inhibitors in Melanoma Involves Activation of the IGF1R-MEK5-Erk5 Pathway. *Cancer research* **2019,** *79* (9), 2244-2256.

92. Buonato, J. M.; Lazzara, M. J., ERK1/2 blockade prevents epithelial-mesenchymal transition in lung cancer cells and promotes their sensitivity to EGFR inhibition. *Cancer research* **2014,** *74* (1), 309-19.

93. Pasquier, J.; Abu-Kaoud, N.; Al Thani, H.; Rafii, A., Epithelial to Mesenchymal Transition in a Clinical Perspective. *Journal of oncology* **2015,** *2015*, 792182.

94. Kalluri, R.; Weinberg, R. A., The basics of epithelial-mesenchymal transition. *The Journal of clinical investigation* **2009,** *119* (6), 1420-8.

95. Wu, P.; Clausen, M. H.; Nielsen, T. E., Allosteric small-molecule kinase inhibitors. *Pharmacology & therapeutics* **2015,** *156*, 59-68.

96. Wang, R.; Lv, Q.; Meng, W.; Tan, Q.; Zhang, S.; Mo, X.; Yang, X., Comparison of mammosphere formation from breast cancer cell lines and primary breast tumors. *Journal of thoracic disease* **2014,** *6* (6), 829-837.

97. Cao, Z.; Livas, T.; Kyprianou, N., Anoikis and EMT: Lethal "Liaisons" during Cancer Progression. *Crit Rev Oncog* **2016,** *21* (3-4), 155-168.

98. Yuan, J.; Liu, M.; Yang, L.; Tu, G.; Zhu, Q.; Chen, M.; Cheng, H.; Luo, H.; Fu, W.; Li, Z.; Yang, G., Acquisition of epithelial-mesenchymal transition phenotype in the tamoxifen-resistant breast cancer cell: a new role for G protein-coupled estrogen receptor in mediating tamoxifen resistance through cancer-associated fibroblast-derived fibronectin and β1-integrin signaling pathway in tumor cells. *Breast cancer research : BCR* **2015,** *17* (1), 69.

99. Hiscox, S.; Jiang, W. G.; Obermeier, K.; Taylor, K.; Morgan, L.; Burmi, R.; Barrow, D.; Nicholson, R. I., Tamoxifen resistance in MCF7 cells promotes EMT-like behaviour and involves modulation of beta-catenin phosphorylation. *International journal of cancer* **2006,** *118* (2), 290-301.

100. Ribatti, D.; Tamma, R.; Annese, T., Epithelial-Mesenchymal Transition in Cancer: A Historical Overview. *Translational oncology* **2020,** *13* (6), 100773-100773.

101. Chaffer, C. L.; Weinberg, R. A., A perspective on cancer cell metastasis. *Science (New York, N.Y.)* **2011,** *331* (6024), 1559-64.

102. Gee, J. M. W.; Robertson, J. F. R.; Ellis, I. O.; Nicholson, R. I., Phosphorylation of ERK1/2 mitogen-activated protein kinase is associated with poor response to anti-hormonal therapy and decreased patient survival in clinical breast cancer. *International journal of cancer* **2001,** *95* (4), 247-254.

103. Adeyinka, A.; Nui, Y.; Cherlet, T.; Snell, L.; Watson, P. H.; Murphy, L. C., Activated Mitogen-activated Protein Kinase Expression during Human Breast Tumorigenesis and Breast Cancer Progression. *Clinical Cancer Research* **2002,** *8* (6), 1747.

104. Antoon, J. W.; Martin, E. C.; Lai, R.; Salvo, V. A.; Tang, Y.; Nitzchke, A. M.; Elliott, S.; Nam, S. Y.; Xiong, W.; Rhodes, L. V.; Collins-Burow, B.; David, O.; Wang, G.; Shan, B.; Beckman, B. S.; Nephew, K. P.; Burow, M. E., MEK5/ERK5 signaling suppresses estrogen receptor expression and promotes hormone-independent tumorigenesis. *PloS one* **2013,** *8* (8), e69291.

105. Hoang, V. T.; Yan, T. J.; Cavanaugh, J. E.; Flaherty, P. T.; Beckman, B. S.; Burow, M. E., Oncogenic signaling of MEK5-ERK5. *Cancer letters* **2017,** *392*, 51-59.

106. Ali, S.; Rasool, M.; Chaoudhry, H.; N Pushparaj, P.; Jha, P.; Hafiz, A.; Mahfooz, M.; Abdus Sami, G.; Azhar Kamal, M.; Bashir, S.; Ali, A.; Sarwar Jamal, M., Molecular mechanisms and mode of tamoxifen resistance in breast cancer. *Bioinformation* **2016,** *12* (3), 135-139.

107. Shin, S.; Dimitri, C. A.; Yoon, S.-O.; Dowdle, W.; Blenis, J., ERK2 but not ERK1 induces epithelial-to-mesenchymal transformation via DEF motif-dependent signaling events. *Molecular cell* **2010,** *38* (1), 114-127.

108. Barros, J. C.; Marshall, C. J., Activation of either ERK1/2 or ERK5 MAP kinase pathways can lead to disruption of the actin cytoskeleton. *Journal of Cell Science* **2005,** *118* (8), 1663.

109. Bertucci, F.; Ueno, N. T.; Finetti, P.; Vermeulen, P.; Lucci, A.; Robertson, F. M.; Marsan, M.; Iwamoto, T.; Krishnamurthy, S.; Masuda, H.; Van Dam, P.; Woodward, W. A.; Cristofanilli, M.; Reuben, J. M.; Dirix, L.; Viens, P.; Symmans, W. F.; Birnbaum, D.; Van Laere, S. J., Gene expression profiles of inflammatory breast cancer: correlation with response to neoadjuvant chemotherapy and metastasis-free survival. *Annals of oncology : official journal of the European Society for Medical Oncology* **2014,** *25* (2), 358-65.

110. Purrington, K. S.; Knight, J., 3rd; Dyson, G.; Ali-Fehmi, R.; Schwartz, A. G.; Boerner, J. L.; Bandyopadhyay, S., CLCA2 expression is associated with survival among African American women with triple negative breast cancer. *PloS one* **2020,** *15* (4), e0231712.

111. Saitoh, M., Involvement of partial EMT in cancer progression. *Journal of biochemistry* **2018,** *164* (4), 257-264.

112. Mani, S. A.; Guo, W.; Liao, M. J.; Eaton, E. N.; Ayyanan, A.; Zhou, A. Y.; Brooks, M.; Reinhard, F.; Zhang, C. C.; Shipitsin, M.; Campbell, L. L.; Polyak, K.; Brisken, C.; Yang, J.; Weinberg, R. A., The epithelial-mesenchymal transition generates cells with properties of stem cells. *Cell* **2008,** *133* (4), 704-15.

113. Buschbeck, M.; Ullrich, A., The unique C-terminal tail of the mitogen-activated protein kinase ERK5 regulates its activation and nuclear shuttling. *The Journal of biological chemistry* **2005,** *280* (4), 2659-67.

114. Gomez, N.; Erazo, T.; Lizcano, J. M., ERK5 and Cell Proliferation: Nuclear Localization Is What Matters. *Front Cell Dev Biol* **2016,** *4*, 105.

115. Buonato, J. M.; Lazzara, M. J., ERK1/2 Blockade Prevents Epithelial–Mesenchymal Transition in Lung Cancer Cells and Promotes Their Sensitivity to EGFR Inhibition. *Cancer Research* **2014,** *74* (1), 309.

116. Smith, B. N.; Burton, L. J.; Henderson, V.; Randle, D. D.; Morton, D. J.; Smith, B. A.; Taliaferro-Smith, L.; Nagappan, P.; Yates, C.; Zayzafoon, M.; Chung, L. W.; Odero-Marah, V. A.,

Snail promotes epithelial mesenchymal transition in breast cancer cells in part via activation of nuclear ERK2. *PloS one* **2014,** *9* (8), e104987.

117. Pavan, S.; Meyer-Schaller, N.; Diepenbruck, M.; Kalathur, R. K. R.; Saxena, M.; Christofori, G., A kinome-wide high-content siRNA screen identifies MEK5-ERK5 signaling as critical for breast cancer cell EMT and metastasis. *Oncogene* **2018,** *37* (31), 4197-4213.

118. Nishimoto, S.; Nishida, E., MAPK signalling: ERK5 versus ERK1/2. *EMBO Rep* **2006,** *7* (8), 782-786.

119. Lin, E. C. K.; Amantea, C. M.; Nomanbhoy, T. K.; Weissig, H.; Ishiyama, J.; Hu, Y.; Sidique, S.; Li, B.; Kozarich, J. W.; Rosenblum, J. S., ERK5 kinase activity is dispensable for cellular immune response and proliferation. *Proceedings of the National Academy of Sciences* **2016,** *113* (42), 11865.

120. Lochhead, P. A.; Tucker, J. A.; Tatum, N. J.; Wang, J.; Oxley, D.; Kidger, A. M.; Johnson, V. P.; Cassidy, M. A.; Gray, N. S.; Noble, M. E. M.; Cook, S. J., Paradoxical activation of the protein kinase-transcription factor ERK5 by ERK5 kinase inhibitors. *Nature Communications* **2020,** *11* (1), 1383.

121. Javaid, S.; Zhang, J.; Smolen, G. A.; Yu, M.; Wittner, B. S.; Singh, A.; Arora, K. S.; Madden, M. W.; Desai, R.; Zubrowski, M. J.; Schott, B. J.; Ting, D. T.; Stott, S. L.; Toner, M.; Maheswaran, S.; Shioda, T.; Ramaswamy, S.; Haber, D. A., MAPK7 Regulates EMT Features and Modulates the Generation of CTCs. *Molecular cancer research : MCR* **2015,** *13* (5), 934-43.

122. Hoang, V. T.; Matossian, M. D.; Ucar, D. A.; Elliott, S.; La, J.; Wright, M. K.; Burks, H. E.; Perles, A.; Hossain, F.; King, C. T.; Browning, V. E.; Bursavich, J.; Fang, F.; Del Valle, L.; Bhatt, A. B.; Cavanaugh, J. E.; Flaherty, P. T.; Anbalagan, M.; Rowan, B. G.; Bratton, M. R.; Nephew, K. P.; Miele, L.; Collins-Burow, B. M.; Martin, E. C.; Burow, M. E., ERK5 Is Required for Tumor Growth and Maintenance Through Regulation of the Extracellular Matrix in Triple Negative Breast Cancer. *Frontiers in oncology* **2020,** *10*, 1164-1164.

123. Razavi, P.; Chang, M. T.; Xu, G.; Bandlamudi, C.; Ross, D. S.; Vasan, N.; Cai, Y.; Bielski, C. M.; Donoghue, M. T. A.; Jonsson, P.; Penson, A.; Shen, R.; Pareja, F.; Kundra, R.; Middha, S.; Cheng, M. L.; Zehir, A.; Kandoth, C.; Patel, R.; Huberman, K.; Smyth, L. M.; Jhaveri, K.; Modi, S.; Traina, T. A.; Dang, C.; Zhang, W.; Weigelt, B.; Li, B. T.; Ladanyi, M.; Hyman, D. M.; Schultz, N.; Robson, M. E.; Hudis, C.; Brogi, E.; Viale, A.; Norton, L.; Dickler, M. N.; Berger, M. F.; Iacobuzio-Donahue, C. A.; Chandarlapaty, S.; Scaltriti, M.; Reis-Filho, J. S.; Solit, D. B.; Taylor, B. S.; Baselga, J., The Genomic Landscape of Endocrine-Resistant Advanced Breast Cancers. *Cancer cell* **2018,** *34* (3), 427-438.e6.

124. Caunt, C. J.; Sale, M. J.; Smith, P. D.; Cook, S. J., MEK1 and MEK2 inhibitors and cancer therapy: the long and winding road. *Nature reviews. Cancer* **2015,** *15* (10), 577-92.

125. Murphy, T.; Hori, S.; Sewell, J.; Gnanapragasam, V. J., Expression and functional role of negative signalling regulators in tumour development and progression. *International journal of cancer* **2010,** *127* (11), 2491-9.

126. Andrieu, G.; Tran, A. H.; Strissel, K. J.; Denis, G. V., BRD4 Regulates Breast Cancer Dissemination through Jagged1/Notch1 Signaling. *Cancer research* **2016,** *76* (22), 6555-6567.

127. Lombard, D. B.; Cierpicki, T.; Grembecka, J., Combined MAPK Pathway and HDAC Inhibition Breaks Melanoma. *Cancer Discovery* **2019,** *9* (4), 469.

128. Corno, C.; Arrighetti, N.; Ciusani, E.; Corna, E.; Carenini, N.; Zaffaroni, N.; Gatti, L.; Perego, P., Synergistic Interaction of Histone Deacetylase 6- and MEK-Inhibitors in Castration-Resistant Prostate Cancer Cells. *Front Cell Dev Biol* **2020,** *8*, 610-610.

129. Tetsu, O.; McCormick, F., ETS-targeted therapy: can it substitute for MEK inhibitors? *Clinical and Translational Medicine* **2017,** *6* (1), 16.

130. Niu, Y.; Xu, J.; Sun, T., Cyclin-Dependent Kinases 4/6 Inhibitors in Breast Cancer: Current Status, Resistance, and Combination Strategies. *J Cancer* **2019,** *10* (22), 5504-5517.

131. Fang, Z.; Jung, K. H.; Lee, J. E.; Cho, J.; Lim, J. H.; Hong, S.-S., MEK blockade overcomes the limited activity of palbociclib in head and neck cancer. *Translational Oncology* **2020,** *13* (11), 100833.

132. Mendoza, M. C.; Er, E. E.; Blenis, J., The Ras-ERK and PI3K-mTOR pathways: cross-talk and compensation. *Trends Biochem Sci* **2011,** *36* (6), 320-328.

133. Qiu, H.; Li, J.; Clark, L. H.; Jackson, A. L.; Zhang, L.; Guo, H.; Kilgore, J. E.; Gehrig, P. A.; Zhou, C.; Bae-Jump, V. L., JQ1 suppresses tumor growth via PTEN/PI3K/AKT pathway in endometrial cancer. *Oncotarget* **2016,** *7* (41), 66809-66821.

134. Kasler, H. G.; Victoria, J.; Duramad, O.; Winoto, A., ERK5 is a novel type of mitogen-activated protein kinase containing a transcriptional activation domain. *Molecular and cellular biology* **2000,** *20* (22), 8382-8389.

135. Zucchetti, B.; Shimada, A. K.; Katz, A.; Curigliano, G., The role of histone deacetylase inhibitors in metastatic breast cancer. *The Breast* **2019,** *43*, 130-134.

136. da Cunha Jaeger, M.; Ghisleni, E. C.; Cardoso, P. S.; Siniglaglia, M.; Falcon, T.; Brunetto, A. T.; Brunetto, A. L.; de Farias, C. B.; Taylor, M. D.; Nör, C.; Ramaswamy, V.; Roesler, R., HDAC and MAPK/ERK Inhibitors Cooperate To Reduce Viability and Stemness in Medulloblastoma. *Journal of molecular neuroscience : MN* **2020,** *70* (6), 981-992.

137. Gupta, G. K.; Collier, A. L.; Lee, D.; Hoefer, R. A.; Zheleva, V.; Siewertsz van Reesema, L. L.; Tang-Tan, A. M.; Guye, M. L.; Chang, D. Z.; Winston, J. S.; Samli, B.; Jansen, R. J.; Petricoin, E. F.; Goetz, M. P.; Bear, H. D.; Tang, A. H., Perspectives on Triple-Negative Breast Cancer: Current Treatment Strategies, Unmet Needs, and Potential Targets for Future Therapies. *Cancers* **2020,** *12* (9).

138. Yang, Q.; Liao, L.; Deng, X.; Chen, R.; Gray, N. S.; Yates, J. R., 3rd; Lee, J. D., BMK1 is involved in the regulation of p53 through disrupting the PML-MDM2 interaction. *Oncogene* **2013,** *32* (26), 3156-3164.

139. Liu, T.; Guo, J.; Zhang, X., MiR-202-5p/PTEN mediates doxorubicin-resistance of breast cancer cells via PI3K/Akt signaling pathway. *Cancer biology & therapy* **2019,** *20* (7), 989-998.

140. Kielbik, M.; Krzyzanowski, D.; Pawlik, B.; Klink, M., Cisplatin-induced ERK1/2 activity promotes G1 to S phase progression which leads to chemoresistance of ovarian cancer cells. *Oncotarget* **2018,** *9* (28), 19847-19860.

141. Yang, J. M.; Vassil, A. D.; Hait, W. N., Activation of phospholipase C induces the expression of the multidrug resistance (MDR1) gene through the Raf-MAPK pathway. *Molecular pharmacology* **2001,** *60* (4), 674-80.

142. Pick, A.; Wiese, M., Tyrosine kinase inhibitors influence ABCG2 expression in EGFR-positive MDCK BCRP cells via the PI3K/Akt signaling pathway. *ChemMedChem* **2012,** *7* (4), 650-62.

143. Wang, F.; Li, D.; Zheng, Z.; Kin Wah To, K.; Chen, Z.; Zhong, M.; Su, X.; Chen, L.; Fu, L., Reversal of ABCB1-related multidrug resistance by ERK5-IN-1. *Journal of Experimental & Clinical Cancer Research* **2020,** *39* (1), 50.

144. Pan, S. T.; Li, Z. L.; He, Z. X.; Qiu, J. X.; Zhou, S. F., Molecular mechanisms for tumour resistance to chemotherapy. *Clinical and experimental pharmacology & physiology* **2016,** *43* (8), 723-37.

145. Wright, T. D.; Raybuck, C.; Bhatt, A.; Monlish, D.; Chakrabarty, S.; Wendekier, K.; Gartland, N.; Gupta, M.; Burow, M. E.; Flaherty, P. T.; Cavanaugh, J. E., Pharmacological inhibition of the MEK5/ERK5 and PI3K/Akt signaling pathways synergistically reduces viability in triple-negative breast cancer. *Journal of cellular biochemistry* **2020,** *121* (2), 1156-1168.

146. Simoes, A. E. S.; Rodrigues, C. M. P.; Borralho, P. M., The MEK5/ERK5 signalling pathway in cancer: a promising novel therapeutic target. *Drug Discov Today* **2016**.

147. Wright, T. D.; Raybuck, C.; Bhatt, A.; Monlish, D.; Chakrabarty, S.; Wendekier, K.; Gartland, N.; Gupta, M.; Burow, M. E.; Flaherty, P. T.; Cavanaugh, J. E., Pharmacological

inhibition of the MEK5/ERK5 and PI3K/Akt signaling pathways synergistically reduces viability in triple-negative breast cancer. *J. Cell. Biochem.* **2020,** *121* (2), 1156-1168.

148. Wallin, J. J.; Guan, J.; Prior, W. W.; Lee, L. B.; Berry, L.; Belmont, L. D.; Koeppen, H.; Belvin, M.; Friedman, L. S.; Sampath, D., GDC-0941, a novel class I selective PI3K inhibitor, enhances the efficacy of docetaxel in human breast cancer models by increasing cell death in vitro and in vivo. *Clinical cancer research : an official journal of the American Association for Cancer Research* **2012,** *18* (14), 3901-11.

149. Dirix, L.; Schuler, M.; Machiels, J.; Hess, D.; Awada, A.; Steeghs, N.; Paz-Ares, L.; von Moos, R.; Rabault, B.; Rodon, J., Phase IB Dose-Escalation Study of BEZ235 or BKM120 in Combination with Paclitaxel (PTX) in Patients With Advanced Solid Tumors. *Annals of Oncology* **2012,** *23*, ix157-ix158.

150. Gupta, M.; Shah, D.; Flaherty, P.; Wright, T.; Bhatt, A.; Cavanaugh, J. In *Selective allosteric inhibition of MEK5: novel target for cancer therapeutics*, ABSTRACTS OF PAPERS OF THE AMERICAN CHEMICAL SOCIETY, AMER CHEMICAL SOC 1155 16TH ST, NW, WASHINGTON, DC 20036 USA: 2018.

151. Kano, Y.; Tanaka, M.; Akutsu, M.; Mori, K.; Yazawa, Y.; Mano, H.; Furukawa, Y., Schedule-dependent synergism and antagonism between pemetrexed and docetaxel in human lung cancer cell lines in vitro. *Cancer chemotherapy and pharmacology* **2009,** *64* (6), 1129-37.

152. Tran, B.; Rosenthal, M. A., Survival comparison between glioblastoma multiforme and other incurable cancers. *Journal of clinical neuroscience : official journal of the Neurosurgical Society of Australasia* **2010,** *17* (4), 417-21.

153. Stupp, R.; Mason, W. P.; van den Bent, M. J.; Weller, M.; Fisher, B.; Taphoorn, M. J.; Belanger, K.; Brandes, A. A.; Marosi, C.; Bogdahn, U.; Curschmann, J.; Janzer, R. C.; Ludwin, S. K.; Gorlia, T.; Allgeier, A.; Lacombe, D.; Cairncross, J. G.; Eisenhauer, E.; Mirimanoff, R. O., Radiotherapy plus concomitant and adjuvant temozolomide for glioblastoma. *The New England journal of medicine* **2005,** *352* (10), 987-96.

154. Hannen, R.; Hauswald, M.; Bartsch, J. W., A Rationale for Targeting Extracellular Regulated Kinases ERK1 and ERK2 in Glioblastoma. *Journal of Neuropathology & Experimental Neurology* **2017,** *76* (10), 838-847.

155. Finch, A.; Solomou, G.; Wykes, V.; Pohl, U.; Bardella, C.; Watts, C., Advances in Research of Adult Gliomas. *Int J Mol Sci* **2021,** *22* (2), 924.

156. Delmore, J. E.; Issa, G. C.; Lemieux, M. E.; Rahl, P. B.; Shi, J.; Jacobs, H. M.; Kastritis, E.; Gilpatrick, T.; Paranal, R. M.; Qi, J.; Chesi, M.; Schinzel, A. C.; McKeown, M. R.; Heffernan, T. P.; Vakoc, C. R.; Bergsagel, P. L.; Ghobrial, I. M.; Richardson, P. G.; Young, R. A.; Hahn, W. C.; Anderson, K. C.; Kung, A. L.; Bradner, J. E.; Mitsiades, C. S., BET bromodomain inhibition as a therapeutic strategy to target c-Myc. *Cell* **2011,** *146* (6), 904-17.

157. Bhatt, A. B.; Gupta, M.; Hoang, V. T.; Chakrabarty, S.; Wright, T. D.; Elliot, S.; Chopra, I. K.; Monlish, D.; Anna, K.; Burow, M. E.; Cavanaugh, J. E.; Flaherty, P. T., Novel Diphenylamine Analogs Induce Mesenchymal to Epithelial Transition in Triple Negative Breast Cancer. *Frontiers in Oncology* **2019,** *9* (672).

158. Hoang, V. T.; Matossian, M. D.; Ucar, D. A.; Elliott, S.; La, J.; Wright, M. K.; Burks, H. E.; Perles, A.; Hossain, F.; King, C. T.; Browning, V. E.; Bursavich, J.; Fang, F.; Del Valle, L.; Bhatt, A. B.; Cavanaugh, J. E.; Flaherty, P. T.; Anbalagan, M.; Rowan, B. G.; Bratton, M. R.; Nephew, K. P.; Miele, L.; Collins-Burow, B. M.; Martin, E. C.; Burow, M. E., ERK5 Is Required for Tumor Growth and Maintenance Through Regulation of the Extracellular Matrix in Triple Negative Breast Cancer. *Frontiers in Oncology* **2020,** *10* (1164).

159. Brennan, C. W.; Verhaak, R. G.; McKenna, A.; Campos, B.; Noushmehr, H.; Salama, S. R.; Zheng, S.; Chakravarty, D.; Sanborn, J. Z.; Berman, S. H.; Beroukhim, R.; Bernard, B.; Wu, C. J.; Genovese, G.; Shmulevich, I.; Barnholtz-Sloan, J.; Zou, L.; Vegesna, R.; Shukla, S. A.; Ciriello, G.; Yung, W. K.; Zhang, W.; Sougnez, C.; Mikkelsen, T.; Aldape, K.; Bigner, D. D.; Van Meir, E. G.; Prados, M.; Sloan, A.; Black, K. L.; Eschbacher, J.; Finocchiaro, G.; Friedman, W.; Andrews, D. W.; Guha, A.; Iacocca, M.; O'Neill, B. P.; Foltz, G.; Myers, J.; Weisenberger, D. J.;

Penny, R.; Kucherlapati, R.; Perou, C. M.; Hayes, D. N.; Gibbs, R.; Marra, M.; Mills, G. B.; Lander, E.; Spellman, P.; Wilson, R.; Sander, C.; Weinstein, J.; Meyerson, M.; Gabriel, S.; Laird, P. W.; Haussler, D.; Getz, G.; Chin, L., The somatic genomic landscape of glioblastoma. *Cell* **2013,** *155* (2), 462-77.

160. Gusev, Y.; Bhuvaneshwar, K.; Song, L.; Zenklusen, J.-C.; Fine, H.; Madhavan, S., The REMBRANDT study, a large collection of genomic data from brain cancer patients. *Scientific Data* **2018,** *5* (1), 180158.

161. An, Z.; Aksoy, O.; Zheng, T.; Fan, Q.-W.; Weiss, W. A., Epidermal growth factor receptor and EGFRvIII in glioblastoma: signaling pathways and targeted therapies. *Oncogene* **2018,** *37* (12), 1561-1575.

162. Thorpe, L. M.; Yuzugullu, H.; Zhao, J. J., PI3K in cancer: divergent roles of isoforms, modes of activation and therapeutic targeting. *Nat Rev Cancer* **2015,** *15* (1), 7-24.

163. Diaz Miqueli, A.; Rolff, J.; Lemm, M.; Fichtner, I.; Perez, R.; Montero, E., Radiosensitisation of U87MG brain tumours by anti-epidermal growth factor receptor monoclonal antibodies. *British Journal of Cancer* **2009,** *100* (6), 950-958.

164. Pore, N.; Liu, S.; Haas-Kogan, D. A.; O'Rourke, D. M.; Maity, A., PTEN mutation and epidermal growth factor receptor activation regulate vascular endothelial growth factor (VEGF) mRNA expression in human glioblastoma cells by transactivating the proximal VEGF promoter. *Cancer research* **2003,** *63* (1), 236-41.

165. Matossian, M. D.; Burks, H. E.; Elliott, S.; Hoang, V. T.; Bowles, A. C.; Sabol, R. A.; Bunnell, B. A.; Martin, E. C.; Burow, M. E.; Collins-Burow, B. M., Panobinostat suppresses the mesenchymal phenotype in a novel claudin-low triple negative patient-derived breast cancer model. *Oncoscience* **2018,** *5* (3-4), 99-108.

166. Tubita, A.; Lombardi, Z.; Tusa, I.; Dello Sbarba, P.; Rovida, E., Beyond Kinase Activity: ERK5 Nucleo-Cytoplasmic Shuttling as a Novel Target for Anticancer Therapy. *Int J Mol Sci* **2020,** *21* (3), 938.

167. Cargnello, M.; Roux, P. P., Activation and function of the MAPKs and their substrates, the MAPK-activated protein kinases. *Microbiol Mol Biol Rev* **2011,** *75* (1), 50-83.

168. Mi, Y.; Zhang, J.; He, S.; Yan, X., New Peptides Isolated from Marine Cyanobacteria, an Overview over the Past Decade. *Marine drugs* **2017,** *15* (5).

169. Zeng, C.; Weng, C.-C.; Schneider, M. E.; Puentes, L.; Riad, A.; Xu, K.; Makvandi, M.; Jin, L.; Hawkins, W. G.; Mach, R. H., TMEM97 and PGRMC1 do not mediate sigma-2 ligand-induced cell death. *Cell Death Discovery* **2019,** *5* (1), 58.

170. Liu, C.-C.; Yu, C.-F.; Wang, S.-C.; Li, H.-Y.; Lin, C.-M.; Wang, H.-H.; Abate, C.; Chiang, C.-S., Sigma-2 receptor/TMEM97 agonist PB221 as an alternative drug for brain tumor. *BMC Cancer* **2019,** *19* (1), 473.

171. Cantonero, C.; Camello, P. J.; Abate, C.; Berardi, F.; Salido, G. M.; Rosado, J. A.; Redondo, P. C., NO1, a New Sigma 2 Receptor/TMEM97 Fluorescent Ligand, Downregulates SOCE and Promotes Apoptosis in the Triple Negative Breast Cancer Cell Lines. *Cancers* **2020,** *12* (2), 257.

172. Crawford, K. W.; Bowen, W. D., Sigma-2 Receptor Agonists Activate a Novel Apoptotic Pathway and Potentiate Antineoplastic Drugs in Breast Tumor Cell Lines. *Cancer research* **2002,** *62* (1), 313.